The effects of anthropogenic disturbance on ecosystem structure and function in Coastal Plain streams in the southeastern United States

by

Samuel Lawrence Bickley

A dissertation submitted to the Graduate Faculty of
Auburn University
in partial fulfillment of the
requirements for the Degree of
Doctor of Philosophy

Auburn, Alabama
December 10, 2022

Keywords: salinity, urbanization, ecosystem metabolism, restoration, tidal creek, headwaters, *Fundulus grandis*

Approved by

Christopher J. Anderson, Chair, Professor, College of Forestry, Wildlife, and Environment, Auburn University
Latif Kalin, Professor, College of Forestry, Wildlife, and Environment, Auburn University
Natalie A. Griffiths, Research Staff, Environmental Sciences Division, Oak Ridge National Laboratory
Brian S. Helms, Professor, Department of Biological and Environmental Sciences, Troy University

Abstract

Widespread development fueled by economic growth continues to stress aquatic resources. The world continues to both urbanize and deal with the effects of climate change. In the Southeastern United States, more frequent and intense rainfall events, coupled with increased runoff from urban areas, threaten headwater and coastal aquatic ecosystems. This research assesses how headwater ecosystems respond to restoration intended to reduce the effects of watershed disturbance, and to understand how tidal creek ecosystems respond to coastal watershed development. In my first study, I found that coarse woody debris dam restorations were not effective 14-15 years after restoration at increasing ecosystem functional rates and did not reduce total suspended solids or nutrient concentrations. Further, the effects of watershed disturbance were still apparent following restoration. In my second study, I found that coastal watershed development led to increased salinity variability in tidal creeks associated with freshwater runoff, and that this reduced ecosystem respiration. In my third study, I found that salinity variability led to lower abundance of a tidal creek fish, *Fundulus grandis*, but that abundance increased with mean site salinity. I found that salinity at a subset of my study sites decreased between 2012 and 2020, and this likely drove the observed decrease in *F. grandis* abundance between 2012 and 2020. In my fourth study, I found that *F. grandis* diets were broad and appear to be robust to changes in the watershed. Taken together, my research highlights that 1) restoration is likely to be insufficient if disturbance in the watershed is not addressed, 2) even low levels of disturbance can lead to detectable changes in ecosystem function, and 3) changes in climate and land use are leading to reduced *F. grandis* abundance, with implications for energy transfer from tidal creeks.

Acknowledgements

I would like to thank Seonju, Sora, and Charles for their love and support over the last five years. Without their support I would not have returned to school and this dissertation would not exist. My time in graduate school was overshadowed, like everything else, by the COVID-19 pandemic. During this scary time, Seonju and I homeschooled our children, while she worked, and I plugged away at my research. Spending more time with my family made me realize what it is I want out of life, and that is more time with them. While I conducted the research in this dissertation, I watched as my children grew into kind, caring, adventurous, funny, curious, and strong kids who put up with me being out in the field more than they'd have liked. Thank you to Seonju for being a constant source of support, helping me think through and live what I want my life and my science to look like. Late night conversations with you over the last 25 years have shaped, and continue to shape, the man I am today.

Thank you to my advisor Chris Anderson, who introduced me to the wonderful of tidal creeks and salt marshes and supported my research and helped me craft research questions with real-world application. I would also like to acknowledge his understanding as I precariously balanced family, research, and the COVID-19 pandemic. I would like to thank Brian Helms for being my introduction to stream ecology research, his guidance and humor and, teaching me about cigar box guitars. I would like to thank Natalie Griffiths for introducing me to the wild and wonderful world of stream metabolism. Thank you to Latif Kalin for introducing me to hydrology and the physical forces undergirding aquatic ecosystems. In addition to providing invaluable research and scientific advice, I'd like to thank my committee for being people I genuinely enjoy intellectually engaging with.

Thank you to Audrey Grindle for helping me navigate the Byzantine world of graduate studies and being the person I'd frantically email at 8:00 pm when I realized I'd forgotten some very important form. The College of Forestry, Wildlife, and Environment would not be able to operate without you. Thank you to James Fukai for helping me navigate a myriad of technical problems during my time at Auburn. Thank you to Todd Steury for his help in understanding the intricacies of mixed effects models and responding to reviewers in the publication for the second chapter of this dissertation.

Thank you to all the people who helped me in the field collecting data, carrying backpacks, driving boats, backing up trailers, and giving me a place to sleep, including Dan Isenberg, Kaelyn Fogelman, Frank D'Alonzo, Anthony Roney, Clara Zubrik, and the wonderful folks at Weeks Bay National Estuarine Reserve. Thank you to Dan Morris for helping me dissect and bomb fish.

Thank you to my union comrades in United Campus Workers Local 3965 who are continuing the work of building graduate worker power at Auburn University. Solidarity!

Thank you to Amy Gill for being my mentor at the USGS and teaching me about the wild world of water quality sampling.

And thank you to all my friends in Virginia Scientist-Community Interface (V-SCI) who showed me how to make my science work for people and communities, and who ultimately helped me understand that science is messy, fun, and important. My work with V-SCI was profoundly important for me personally and integral in helping me to develop my approach to scientific research. I am deeply indebted to y'all.

Table of Contents

List of Tables

List of Figures

List of abbreviations

ANOVA	analysis of variance
CN	curve number
CPUE	catch per unit effort
CWD	coarse woody debris
DO	dissolved oxygen
DOC	dissolved organic carbon
EPA	Environmental Protection Agency
ER	ecosystem respiration
ET	evapotranspiration
FBMI	Fort Benning Military Installation
GOM	Gulf of Mexico
GPP	gross primary production
IS	impervious surface
LMM	linear mixed-effects model
MinP	mineralized phosphorus
NEM	net ecosystem metabolism
NH_4^+	ammonium
NLCD	National Landcover Dataset
NO_3^-	nitrate
NRCS	Natural Resources Conservation Service
POST-LT	long-term 14-15 year post-restoration period
POST-ST	short-term 1-3 year post-restoration period
PRE	pre-restoration period
SRP	soluble reactive phosphorous
Sw	spiraling length
SWAT	Soil and Water Assessment Tool
TSS	total suspended solids
U	areal uptake rate
UN	United Nations
USDA	United States Department of Agriculture
USGS	United States Geological Survey
vf	uptake velocity

Chapter 1: Introduction

Threats to water

Water has always provided sustenance to humans. However, as societies have grown, economic development has stressed aquatic resources to a point that habitats and ecosystem functions have been lost or disturbed over time (Webster et al. 1992, Vorosmarty 2000, Walsh et al. 2005c). Economic development associated with the current economic system takes many forms and can include large-scale agriculture, industry, transportation, and overall urbanization of the landscape. The United Nations (UN) estimate that two-thirds of the human population will live in cities by 2050 (United Nations 2019), further straining water resources during a time of wide-spread ecological and climate change.

Urbanization within a watershed can lead to significant changes in the hydrological regime, and represents a major disturbance to aquatic ecosystems (Webster et al. 1992, Stepenuck et al. 2002, Walsh et al. 2005c, Nagy et al. 2011b). As watersheds urbanize, hard, impervious surfaces such as roads, parking lots, and buildings made of concrete and asphalt spread, hinder the infiltration of precipitation into soils and quickly convey sediment, nutrient, and heavy metal-laden runoff across this hardened landscape to stormwater systems, ditches, and streams, leading to significant physical, chemical, and biological changes to urban streams (Walsh et al. 2005c, Shuster et al. 2005). Runoff from impervious surfaces also enters nearby streams with increased energy, which can lead to greater stream channel erosion and widening rates (Hawley et al. 2020), and increased runoff volume also leads to the higher peak flows and increased variability in stream flows (Dunne and Leopold 1978, Cheng et al. 2010, Roodsari and

Chandler 2017). The suite of changes within streams associated with watershed urbanization is known as the "urban stream syndrome" (Walsh et al. 2005c).

The urban stream syndrome framework has been applied to different stream types and regions (Morgan and Cushman 2005, Epstein et al. 2016, Lisi et al. 2018, McPhillips et al. 2019, Hawley et al. 2020, Alvareda et al. 2020), but has mostly been limited to freshwater systems. It is not known whether this framework applies to coastal watersheds, and tidal creeks in particular. It can be expected that coastal watersheds would function similarly to low-gradient, upland watersheds, but that the dynamic freshwater-saltwater environment that is characteristic of tidal creeks might differentially interact with urbanization stressors and result in different ecosystem process responses than in freshwater systems. For example, it has long been understood that salinity structures estuarine ecosystems (Pritchard 1952) and that estuarine ecosystems experience natural fluctuations in salinity associated with tidal exchange. However, in coastal watersheds with greater coverage of impervious surfaces than less-developed watersheds, increased freshwater runoff can lead to an increased frequency and magnitude of salinity fluctuations in tidal creeks (Lerberg et al. 2000, Holland et al. 2004, Sanger et al. 2008, Wedge and Anderson 2017). This change to the salinity regime in tidal creeks likely represents a significant disturbance affecting both the structure and function of these ecosystems. In addition to land use changes leading to changes in salinity regime, climate change, which is widely understood to be a threat to water resources around the world (Barnett et al. 2004, Piao et al. 2010, Sowers et al. 2011, Mall et al. 2022), is leading to increased precipitation (Sinha et al. 2017, Armal et al. 2018), which in turn could lead to greater freshwater runoff and reduced salinities in lower-order tidal creeks.

Role of monitoring and restoration in low-order aquatic ecosystems

Because of the disproportionate impact of ecosystem functions associated with lower-order streams (Peterson et al. 2001), it is vitally important to understand how these smaller systems respond to both climate and land use change. Ecosystem monitoring is important to understand how these ecosystems currently function, understanding how they may change in the future, and understanding how the effects of disturbance on these systems can be ameliorated. Historically, ecosystem monitoring has focused on ecosystem structure and used measures such as water quality, community structure, species diversity, and habitat structure (Pereira et al. 2013, Sparrow et al. 2020). However, techniques measuring ecosystem function (primary production, respiration, nutrient cycling) have become more widespread and accessible. Further, ecosystem functional measures have been repeatedly shown to be responsive to watershed disturbance (Bernot et al. 2006, Young et al. 2008b, Flores et al. 2011b, Arango et al. 2015b, Roberts et al. 2021, Bickley et al. 2021). Taken together, ecosystem monitoring that utilizes both ecosystem structure and functional metrics provides a more holistic understanding of ecosystem-level changes taking place in response to climate and land use change, but also in response to restoration of those ecosystems.

For example, stream restoration of low-order, headwater streams (Fig. 1-2) is an expensive undertaking and one that is rarely monitored to ensure the restorations are actually effective over time (Palmer et al. 2005, Bernhardt 2005). The Environmental Protection Agency (EPA) has previously estimated that 50% of wadeable streams in the United States are in poor biological condition (EPA 2016), indicating the wide potential for future restoration projects.

However, important questions remain about the overall effectiveness of stream restoration techniques such as coarse woody debris addition (Fig. 1-3) and whether they are a wise use of resources.

In addition to low-order streams being subjected to watershed disturbance, coastal watersheds are particularly vulnerable to degradation. Nearly one-third of the global human population lives within 100 km of a coast (Gittman et al. 2016), a trend also observed in the United States, where nearly 16 million people live in coastal counties along the Gulf of Mexico (GOM; U.S. Census 2017). Tidal creeks and salt marshes (Fig. 1-2) have been identified as sentinel habitats (Sanger et al. 2011), which means these systems show signs of the effects of watershed disturbance before other aquatic ecosystems, and are therefore important ecosystems to monitor to understand how they respond to climate and land use change. One way to assess changes to tidal creek ecosystems is through the study of the Gulf killifish (*Fundulus grandis*; Fig. 1-4), which are a common fish found in tidal creek ecosystems in the Gulf coast and are easily captured using minnow traps (Fig. 1-5).

Purpose of this study

The purpose of my research was to examine how low-order coastal streams respond to land use change, disturbance, and restoration in the Coastal Plain in Alabama, Florida, and Georgia, USA. I performed four research projects, with the first being a long-term assessment of stream restoration at a military installation in western Georgia, USA. The objectives of this study were to evaluate whether 1) ecosystem respiration and nutrient uptake rates were still elevated 14-15 years following restoration, 2) gross primary production rates increased over this period of

time, and 3) total suspended solid and nutrient concentrations were reduced following restoration.

Second, I evaluated how salinity regime and stream metabolism responded to development in mesohaline tidal creeks along the northern GOM in Alabama and west Florida. The objectives for this study were to evaluate 1) the role of increased freshwater runoff associated with watershed development on tidal creek salinity regime, and 2) whether development and altered salinity regime led to changes in gross primary production and ecosystem respiration.

Third, I evaluated how the abundance of *Fundulus grandis*, a dominant salt marsh resident fish species, responded to development and potential changes in salinity regime. The objectives for this study were to 1) compare *F. grandis* abundance from 2019-2020 to 2012-2013, and 2) whether abundance responded to watershed development and changes in salinity regime.

Fourth, I examined how *F. grandis* diets and condition responded to watershed development. The objective for this study was to understand how 1) development structures *F. grandis* diets and 2) diet and environmental conditions affect *F. grandis* body condition.

Literature cited

Alvareda, E., C. Lucas, M. Paradiso, A. Piperno, P. Gamazo, V. Erasun, P. Russo, A. Saracho, R. Banega, G. Sapriza, and F. T. de Mello. 2020. Water quality evaluation of two urban streams in Northwest Uruguay: Are national regulations for urban stream quality sufficient? Environmental Monitoring and Assessment 192:661.

Arango, C. P., P. W. James, and K. B. Hatch. 2015. Rapid ecosystem response to restoration in an urban stream. Hydrobiologia 749:197–211.

Armal, S., N. Devineni, and R. Khanbilvardi. 2018. Trends in Extreme Rainfall Frequency in the Contiguous United States: Attribution to Climate Change and Climate Variability Modes. Journal of Climate 31:369–385.

Barnett, T., R. Malone, W. Pennell, D. Stammer, B. Semtner, and W. Washington. 2004. The Effects of Climate Change on Water Resources in the West: Introduction and Overview. Climatic Change 62:1–11.

Bernhardt, E. S. 2005. ECOLOGY: Synthesizing U.S. River Restoration Efforts. Science 308:636–637.

Bernot, M. J., J. L. Tank, T. V. Royer, and M. B. David. 2006. Nutrient uptake in streams draining agricultural catchments of the midwestern United States. Freshwater Biology 51:499–509.

Bickley, S. L., B. S. Helms, D. Isenberg, J. W. Feminella, B. J. Roberts, and N. A. Griffiths. 2021. Lack of long-term effect of coarse woody debris dam restoration on ecosystem functioning and water quality in Coastal Plain streams. Freshwater Science 40:593–607.

Cheng, S., C. Lee, and J. Lee. 2010. Effects of Urbanization Factors on Model Parameters. Water Resources Management 24:775–794.

Dunne, T., and L. B. Leopold. 1978. Water in environmental planning. , 1st edition. W. H. Freeman and Company, New York, NY.

Epstein, D. M., J. E. Kelso, and M. A. Baker. 2016. Beyond the urban stream syndrome: Organic matter budget for diagnostics and restoration of an impaired urban river. Urban Ecosystems 19:1623–1643.

Flores, L., A. Larrañaga, J. Díez, and A. Elosegi. 2011. Experimental wood addition in streams: Effects on organic matter storage and breakdown: Effects of wood addition on organic matter. Freshwater Biology 56:2156–2167.

Gittman, R. K., S. B. Scyphers, C. S. Smith, I. P. Neylan, and J. H. Grabowski. 2016. Ecological Consequences of Shoreline Hardening: A Meta-Analysis. BioScience 66:763–773.

Hawley, R. J., K. R. MacMannis, M. S. Wooten, E. V. Fet, and N. L. Korth. 2020. Suburban stream erosion rates in northern Kentucky exceed reference channels by an order of magnitude and follow predictable trajectories of channel evolution. Geomorphology 352:106998.

Holland, A. F., D. M. Sanger, C. P. Gawle, S. B. Lerberg, M. S. Santiago, G. H. M. Riekerk, L. E. Zimmerman, and G. I. Scott. 2004. Linkages between tidal creek ecosystems and the landscape and demographic attributes of their watersheds. Journal of Experimental Marine Biology and Ecology 298:151–178.

Lerberg, S. B., A. F. Holland, and D. M. Sanger. 2000. Responses of tidal creek macrobenthic communities to the effects of watershed development. Estuaries 23:838–853.

Lisi, P. J., E. S. Childress, R. B. Gagne, E. F. Hain, B. A. Lamphere, R. P. Walter, J. D. Hogan, J. F. Gilliam, M. J. Blum, and P. B. McIntyre. 2018. Overcoming urban stream

syndrome: Trophic flexibility confers resilience in a Hawaiian stream fish. Freshwater Biology 63:492–502.
Mall, R. K., A. Gupta, R. Singh, and R. S. Singh. 2022. Water resources and climate change: An Indian perspective. 18.
McPhillips, L. E., S. R. Earl, R. L. Hale, and N. B. Grimm. 2019. Urbanization in Arid Central Arizona Watersheds Results in Decreased Stream Flashiness. Water Resources Research 55:9436–9453.
Morgan, R. P., and S. F. Cushman. 2005. Urbanization effects stream fish assemblages in Maryland, USA. Journal of the North American Benthological Society 24:643–655.
Nagy, R. C., B. G. Lockaby, L. Kalin, and C. Anderson. 2011. Effects of urbanization on stream hydrology and water quality: The Florida Gulf Coast: URBANIZATION EFFECTS ON WATER RESOURCES. Hydrological Processes 26:2019–2030.
Palmer, M. A., E. S. Bernhardt, J. D. Allan, P. S. Lake, G. Alexander, S. Brooks, J. Carr, S. Clayton, C. N. Dahm, J. Follstad Shah, D. L. Galat, S. G. Loss, P. Goodwin, D. D. Hart, B. Hassett, R. Jenkinson, G. M. Kondolf, R. Lave, J. L. Meyer, T. K. O'Donnell, L. Pagano, and E. Sudduth. 2005. Standards for ecologically successful river restoration: Ecological success in river restoration. Journal of Applied Ecology 42:208–217.
Pereira, H. M., S. Ferrier, M. Walters, G. N. Geller, R. H. G. Jongman, R. J. Scholes, M. W. Bruford, N. Brummitt, S. H. M. Butchart, A. C. Cardoso, N. C. Coops, E. Dulloo, D. P. Faith, J. Freyhof, R. D. Gregory, C. Heip, R. Höft, G. Hurtt, W. Jetz, D. S. Karp, M. A. McGeoch, D. Obura, Y. Onoda, N. Pettorelli, B. Reyers, R. Sayre, J. P. W. Scharlemann, S. N. Stuart, E. Turak, M. Walpole, and M. Wegmann. 2013. Essential Biodiversity Variables. Science 339:277–278.
Peterson, B. J., W. M. Wollheim, P. J. Mulholland, J. R. Webster, J. L. Meyer, J. L. Tank, E. Martí, W. B. Bowden, H. M. Valett, A. E. Hershey, W. H. McDowell, W. K. Dodds, S. K. Hamilton, S. Gregory, and D. D. Morrall. 2001. Control of Nitrogen Export from Watersheds by Headwater Streams. Science 292:86–90.
Piao, S., P. Ciais, Y. Huang, Z. Shen, S. Peng, J. Li, L. Zhou, H. Liu, Y. Ma, Y. Ding, P. Friedlingstein, C. Liu, K. Tan, Y. Yu, T. Zhang, and J. Fang. 2010. The impacts of climate change on water resources and agriculture in China. Nature 467:43–51.
Pritchard, D. W. 1952. Salinity distribution and circulation in the Chesapeake Bay estuarine system. Journal of Marine Research 11:106–123.
Roberts, B. J., N. A. Griffiths, J. N. Houser, and P. J. Mulholland. 2021. Response of Stream Metabolism to Coarse Woody Debris Additions Along a Catchment Disturbance Gradient. Ecosystems.
Roodsari, B. K., and D. G. Chandler. 2017. Distribution of surface imperviousness in small urban catchments predicts runoff peak flows and stream flashiness. Hydrological Processes 31:2990–3002.
Sanger, D., D. Bergquist, A. Blair, G. Riekerk, E. Wirth, L. Webster, J. Felber, T. Washburn, and A. F. Holland. 2011. Gulf of Mexico Tidal Creeks Serve as Sentinel Habitats for Assessing the Impact of Coastal Development on Ecosystem Health. Page 76. NOS NCCOS 136.
Sanger, D., A. Blair, G. DiDonato, T. Washburn, S. Jones, R. Chapman, D. Bergquist, G. Riekerk, E. Wirth, J. Stewart, D. White, L. Vandiver, S. White, and D. Whitall. 2008. Support for Integrated Ecosystem Assessments of NOAA's National Estuarine Research Reserves System (NERRS), Volume One. The Impacts of Coastal Development on the

Ecology and Human Well-Being of Tidal Creek Ecosystems of the U.S. Southeast. NOAA Technical Memorandum I:88.
Shuster, W. D., J. Bonta, H. Thurston, E. Warnemuende, and D. R. Smith. 2005. Impacts of impervious surface on watershed hydrology: A review. Urban Water Journal 2:263–275.
Sinha, E., A. M. Michalak, and V. Balaji. 2017. Eutrophication will increase during the 21st century as a result of precipitation changes. Science 357:405–408.
Sowers, J., A. Vengosh, and E. Weinthal. 2011. Climate change, water resources, and the politics of adaptation in the Middle East and North Africa. Climatic Change 104:599–627.
Sparrow, B. D., W. Edwards, S. E. M. Munroe, G. M. Wardle, G. R. Guerin, J.-F. Bastin, B. Morris, R. Christensen, S. Phinn, and A. J. Lowe. 2020. Effective ecosystem monitoring requires a multi-scaled approach(1).pdf. Biological Reviews 1706–1719.
Stepenuck, K. F., R. L. Crunkilton, and L. Wang. 2002. Impacts of urban landuse on macroinvertebrate communities in southeastern Wisconsin streams. Journal of the American Water Resources Association 38:1041–1051.
United Nations, Department of Economic and Social Affairs, Population Division. 2019. World urbanization prospects: The 2018 revision. United Nations, New York.
United States Environmental Protection Agency. 2016. National rivers and streams assessment 2008–2009: A collaborative survey. United States Environmental Protection Agency,Office of Water and Office of Research and Development, Washington, D. C. (Available from: https://www.epa.gov/sites/default/files/2016-03/documents/nrsa_0809_march_2_final.pdf)
Vorosmarty, C. J. 2000. Global Water Resources: Vulnerability from Climate Change and Population Growth. Science 289:284–288.
Walsh, C. J., A. H. Roy, J. W. Feminella, P. D. Cottingham, P. M. Groffman, and R. P. Morgan. 2005. The urban stream syndrome: Current knowledge and the search for a cure. Journal of the North American Benthological Society 24:706–723.
Webster, J. R., E. F. Benfield, J. L. Meyer, W. T. Swank, and J. B. Wallace. 1992. Catchment Disturbance and Stream Response: An Overview of Stream Research at Coweeta Hydrologic Laboratory. River Conservation and Management 23.
Wedge, M., and C. J. Anderson. 2017. Urban Land use Affects Resident Fish Communities and Associated Salt Marsh Habitat in Alabama and West Florida, USA. Wetlands 37:715–727.
Young, R. G., C. D. Matthaei, and C. R. Townsend. 2008. Organic matter breakdown and ecosystem metabolism: Functional indicators for assessing river ecosystem health. Journal of the North American Benthological Society 27:605–625.

Figure 1-1. Photograph of the tidal creek and fringing salt marsh at Long Bayou, Baldwin County, Alabama. Photograph by Sam Bickley.

Figure 1-2. Photograph of a low-order tributary to Sally Branch, Fort Benning Military Installation, Georgia. Photograph by Sam Bickley.

Figure 1-3. Coarse woody debris dam installed in 2003, picture taken in 2018. Rebar stakes attach the two logs in the foreground to the streambed.

Figure 1-4. Photograph of the Gulf killifish (*Fundulus grandis*), a ubiquitous fish species in the Cyprinidae family, and a dominant resident fish species in tidal creeks and salt marshes. Photograph by Sam Bickley.

Figure 1-5. Minnow traps deployed along the marsh edge at falling tide to capture *Fundulus grandis*. Photograph by Madeline Wedge.

Chapter 2: Lack of long-term effect of coarse woody debris dam restoration on ecosystem functioning and water quality in Coastal Plain streams

Abstract

Coarse woody debris (CWD) addition is a restoration technique that has been used to reduce effects of landscape disturbance on instream habitat. However, efficacy of this technique for improving ecosystem condition is not well established, in part because monitoring designed to evaluate long-term efficacy is rare. We assessed the effectiveness of CWD additions in disturbed Coastal Plain streams at Fort Benning Military Installation, Georgia, USA, 14 y after initial restoration. In October 2003, 4 disturbed streams received CWD additions (restored streams), and 4 streams were left as unrestored controls. Pre-restoration (2001–2003) and post-restoration (2003–2006) monitoring of nutrient uptake, stream metabolism, and water-quality variables revealed 1) minimal change in water-quality variables, 2) increased stream metabolism and nutrient-uptake rates immediately following restoration, and 3) decreased metabolism and uptake over the remainder of the 3-y post-restoration period. We returned to these streams in 2017 and 2018, measured the same variables, and found minimal long-term effects of restoration on water quality, nutrient uptake, and whole-stream metabolism indicators; however, streamwater pH decreased in all streams 14 y after restoration, and there was a weak treatment × period interaction, indicating that CWD additions may decrease pH in the long term. Further, we found few relationships between watershed disturbance and water-quality variables and ecosystem function metrics, although some relationships were apparent during certain seasons and years. Our study is one of the few that have assessed the long-term effects of CWD additions, or any

other stream-restoration technique, on ecosystem function. These long-term assessments may be necessary to determine if restorations are a good use of limited resources.

Introduction

Lotic ecosystems sustain human societies and support a diverse array of habitats and biota, yet continued population growth and economic development have strained water resources and disturbed watersheds, leading to degraded instream habitat and altered ecosystem function (Webster et al. 1992, Vörösmarty et al. 2000, Walsh et al. 2005). In the United States (US) alone, close to 50% of streams are in poor biological condition (USEPA 2016). Stream restoration projects attempt to minimize the impacts of anthropogenic disturbances; however, these projects are expensive, and post-restoration monitoring rarely takes place over the long term (Bernhardt et al. 2005). Without effective long-term monitoring, it is difficult to determine the degree to which post-restoration success can be sustained.

Many post-restoration monitoring efforts evaluate effects immediately after restoration (mean monitoring period = 3.4 y), and few studies are designed to examine effects at or beyond 10 y (Roni et al. 2008). Moreover, ecosystem-level monitoring is generally focused on structural changes (e.g., fish abundance or habitat heterogeneity), whereas ecosystem functional measures are rarely assessed (Lake et al. 2007, Rubin et al. 2017), despite widespread recognition that ecosystem process rates are indicative of stream health (Young et al. 2008) and can signal a response to human disturbance. Thus, long-term post-restoration monitoring efforts coupling multiple structural and functional measurements can be highly effective at informing practitioners of sustained success (or lack thereof) of stream restorations (Bunn and Davies 2000, Palmer et al. 2005, Riipinen et al. 2009).

Coarse woody debris (CWD) addition is a low-cost restoration technique in streams (Roberts et al. 2007, Howson et al. 2012, Arango et al. 2015, Keys et al. 2018) that can decrease water velocity, increase organic-matter retention, and create habitat for benthic organisms (Benke and Wallace 2003, Flores et al. 2011, Osei et al. 2015). Addition of CWD dams can also increase hydrodynamic complexity by increasing transient storage, thereby increasing nutrient uptake and stream-metabolism rates (Roberts et al. 2007, Arango et al. 2015). However, efficacy of CWD additions can be mixed and site specific (Hoellein et al. 2011). Flores et al. (2011) found that benthic organic matter increased in experimentally restored (vs unrestored) reaches receiving CWD additions, but leaf-litter decomposition rates did not increase. Further, effects of CWD additions are transitory because of wood decay, erosion (Chen et al. 2005), and the dynamic nature of stream ecosystems. It may, therefore, take a long period after CWD restoration before ecosystem changes occur, or effects will diminish over time, indicating the need for long-term assessment of their use as an effective restoration technique (Chen et al. 2005, Entrekin et al. 2008, Roni et al. 2008).

At Fort Benning Military Installation (FBMI), Georgia, USA, streams and their watersheds have been affected by various disturbances over time. Historical (pre-1942) agricultural disturbance influenced instream water quality and increased rates of sediment flux and channel erosion (Cavalcanti and Lockaby 2005, Lockaby et al. 2005, Mulholland et al. 2007, Maloney et al. 2008). Contemporary (post-1942) disturbance associated with military training, such as ground-disturbing tracked-vehicle maneuvers, has decreased nutrient-uptake and stream-metabolism rates, increased concentrations of total suspended solids (TSS), and decreased CWD abundance in some streams (Houser et al. 2005, 2006, Maloney et al. 2005, Roberts et al. 2007).

However, other systems within FBMI have been less affected by historical and contemporary disturbance because of local topography or position in the landscape. The strongly contrasting levels of landscape disturbance and instream CWD levels across watersheds at FBMI represented an opportunity to evaluate the long-term efficacy of instream CWD dam additions to mitigate the effects of upland disturbance.

In 2001, an experimental study involving pre- and post-restoration monitoring was conducted in 8 streams along an upland disturbance gradient at FBMI (Houser et al. 2005, 2006, Maloney et al. 2005). After 3 y of pre-treatment monitoring, CWD dams were added to 4 of these streams, with 4 other streams left as unrestored controls (Mulholland et al. 2007, Roberts et al. 2007). Post-restoration monitoring from 2003 to 2006 found increased transient storage and ammonium (NH_4^+) uptake in restored streams within 1 mo of restoration (Roberts et al. 2007), increased ecosystem respiration (ER) rates in restored streams for the first 2 y after restoration, and increased rates of gross primary productivity (GPP) in restored streams in winter and spring of the 2nd y after restoration (Roberts et al. 2021); however, there was no change in water-quality variables (TSS and nutrient concentrations) (Mulholland et al. 2007).

It is possible that some structural and functional variables may respond more slowly to CWD additions, thus necessitating longer-term measurements. Therefore, in 2017, we revisited the same streams 14 y after CWD additions and remeasured ecosystem structure (as water-quality variables) and function (as whole-stream metabolism and nutrient uptake). We predicted that, if CWD additions resulted in sustainable (i.e., long-term) improvements in ecosystem processes, 1) NH_4^+ uptake and ER rates would remain elevated, 2) GPP rates would increase, and

3) TSS and nutrient concentrations would decrease, compared with shorter-term post-restoration conditions. We also investigated whether upland disturbance remained an important driver of instream structure and ecosystem processes.

METHODS

To assess the efficacy of CWD additions on ecosystem structure and function, we conducted a before–after control–impact field experiment by adding CWD to 4 of 8 headwater streams. Measurements occurred across 3 periods: pre-restoration (2001–2003), post-restoration (2003–2006), and long-term post-restoration (2017–2018). For simplicity, we use the following notation to refer to the 3 different periods of measurement: PRE for the pre-restoration period, POST-ST for the short-term 1- to 3-y post-restoration period, and POST-LT for the long-term 14- to 15-y post-restoration period. Only 7/8 original streams were included in the present study (Table 2-1) because watershed disturbance at 1 unrestored stream (Bonham Creek tributary 2) increased from 3.2 to 11.2% following the 2004 creation of a multipurpose training-range complex (Mulholland et al. 2009).

Study site

FBMI, located near Columbus, Georgia, USA (Fig. 2-1), is in the Southeastern Plains Environmental Protection Agency (EPA) Level III ecoregion, with the study streams located within the Sand Hills and Southern Hilly Gulf Coastal Plain EPA Level IV ecoregions. Physiographic characteristics of these ecoregions include rolling hills, streams with greater slope than those in lower-elevation Coastal Plain regions, and underlying low-nutrient sand and clay-

loam soils (Griffith et al. 2001). Restored stream watershed area ranged from 33 to 369 ha, and unrestored stream watershed area ranged from 100 to 215 ha. All streams drained into Upatoi Creek, a large tributary of the Chattahoochee River.

Riparian canopy in the study streams during summer was high (usually >90%; Maloney et al. 2005) and dominated by black tupelo (*Nyssa sylvatica*), with other common riparian species including wax myrtle (*Myrica cerifera*), yellow poplar (*Liriodendron tulipifera*), sweetgum (*Liquidambar styraciflua*), sweetbay (*Magnolia virginiana*), American holly (*Ilex opaca*), red maple (*Acer rubrum*), and flowering dogwood (*Cornus florida*) (Cavalcanti and Lockaby 2005).

Some streams were affected by military-training activities, including tracked-vehicle and infantry maneuvers. Landscape disturbance in FBMI watersheds, as indicated by barren land and unpaved road cover, ranged from 4.6 to 13.7% (generated from 0.5-m resolution digital orthophotography from 1999) (Maloney et al. 2005). Both restored and unrestored streams had similar ranges of watershed disturbance (Table 2-1).

Experimental design

Pre-restoration monitoring at eight 1st- and 2nd-order FBMI streams occurred in July 2001 through October 2003 (water-quality variables, *n*/stream = 13–17; Maloney et al. 2005, Houser et al. 2006), July 2001 through August 2003 (stream metabolism, *n*/stream = 9; Houser et al. 2005), and during October 2003 (nutrient uptake, *n*/stream = 1; Roberts et al. 2007) (Fig. 2-S1).

In October 2003, CWD dams were installed at 4 of 8 streams, with the other 4 streams serving as unrestored controls. CWD additions included the construction of 10 z-shaped debris dams installed every ~10 m along a 100 to 150-m stream reach, resulting in an increase of 3.1 to 5.2% CWD areal coverage in restored streams (Roberts et al. 2007). High sedimentation rates caused substantial burial of CWD dams in the 2 most heavily disturbed restored streams (Sally Branch 3 and Little Pine Knot), which necessitated adding 10 more CWD dams in each of these streams in November 2004, creating CWD dams every 5 m within these study reaches (Mulholland et al. 2007).

Post-restoration measurements were made at all streams during November 2003 through November 2006 (water-quality variables, *n*/stream = 18–37), November 2003 through October 2005 (nutrient uptake, *n*/stream = 5), and January 2004 through November 2006 (stream metabolism, *n*/stream = 12) (Fig. 2-S1).

In the present study, we revisited these streams and took measurements of water-quality variables (*n*/stream = 11–19) during May 2017 through December 2018 and measurements of nutrient uptake (*n*/stream = 5) and stream metabolism (*n*/stream = 5) during June 2017 through December 2018 (Fig. 2-S1).

Coarse woody debris surveys

We quantified instream CWD at each stream during POST-LT using a modified transect method (Wallace and Benke 1984, Maloney et al. 2005). We divided each study reach into 15 equidistant transects, at which we recorded wetted width and bank width. At each transect, we

counted and measured the length and width of any CWD with a diameter ≥2.5 cm located up to 10 cm deep in the sediment and within 0.5 m upstream and downstream of each transect. We expressed CWD data as m^2 CWD/m^2 stream bed and as a total percentage of the streambed area.

We used linear mixed-effects models (LMM; Harrison et al. 2018) to assess the difference in areal CWD between restored and unrestored streams. The response variable was areal CWD as a total percentage of streambed area, restoration treatment (restored, unrestored) was a fixed effect, and stream was a random effect. For these LMM models, and all others used in our study, we generated residual plots to assess linearity and Q-Q plots to examine the data distribution. Some data exhibited heteroscedasticity and non-normal distributions, so we chose LMMs because they generate estimates that are robust to violations of the standard model assumptions (Schielzeth et al. 2020).

We used R statistical software (version 3.3.3; R Project for Statistical Computing, Vienna, Austria) and the *nlme* package (Pinheiro et al. 2017) for all LMM analyses. We used the *car* package (Fox and Weisberg 2019) to analyze fixed effects on response variables, which generated a type-II analysis of variance (ANOVA) table for each LMM, and we then used the partial likelihood ratio test (Fox and Weisberg 2019) to generate *p*-values. We used the *emmeans* package (Lenth et al. 2019) to calculate estimated marginal means for factors in LMMs and to conduct post-hoc Tukey's honestly significant difference pairwise tests comparing these factors.

Water-quality sampling

We measured multiple water-quality variables at each stream monthly during POST-LT, although military-training activities sometimes led to site restrictions that resulted in longer sampling intervals (Fig. 2-S1). Sampling and analysis of water-quality variables during PRE and POST-ST followed methods of Houser et al. (2006). During POST-LT, we measured streamwater temperature, pH, and specific conductance using a YSI model 556 meter (Yellow Springs Instruments, Yellow Springs, Ohio) and took water-column grab samples at base flow for additional analyses. Water samples were collected in a 60-mL acid-washed syringe, filtered through a 25-mm glass fiber filter (0.7-µm nominal retention), and stored in acid-washed 60-mL high-density polyethylene (HDPE) bottles for NH_4^+, NO_x-N, and soluble reactive phosphorus (SRP) analyses and in 40-mL ashed amber glass vials for analysis of dissolved organic carbon (DOC). Unfiltered water samples for TSS were collected in rinsed 1000-mL HDPE bottles. We placed all grab samples on ice in the field until returning them to the laboratory. We froze (–20°*C)* nutrient samples, preserved (with 2 drops of 6N HCl) and refrigerated (4°*C)* DOC samples, and refrigerated (4°C) TSS samples until analyzed (Houser et al. 2006).

In the laboratory, we analyzed samples for concentrations of nutrients, DOC, and TSS. Specifically, we analyzed NH_4^+ with the phenol hypochlorite method, NO_x-N (NO_3-N + NO_2-N; most NO_x is as NO_3^- and will be referred to as thus henceforth) with the cadmium reduction method, and SRP with the molybdate blue method (APHA 2005) on an AA3 autoanalyzer (SEAL Analytical Limited, Southampton, United Kingdom). We analyzed DOC with the high-temperature combustion catalytic oxidation method (Standard Method 5310 B; APHA 2005) on a Shimadzu TOC-L CSH/CSN analyzer (Kyoto, Japan). For TSS, we filtered a known volume of water through an ashed, pre-weighed, 45-mm glass fiber filter and then oven dried the filter for

48 h at 60°C. After drying, we reweighed samples and calculated TSS (mg/L) (Houser et al. 2006).

We used LMMs to assess the effects of CWD additions on water-quality variables among restored and unrestored streams and across all 3 restoration periods (PRE, POST-ST, POST-LT). For each water-quality variable, a separate LMM was created with that variable as the response variable. Fixed effects were treatment, period of restoration, season, and all interactions between them. To evaluate the random effect of stream, season was nested within period, which was nested within stream. We corrected *p*-values for multiple comparisons using the Benjamini–Hochberg method (Jafari and Ansari-Pour 2019). To evaluate the effect of period on variables, we ran an additional LMM for each water-quality variable with only period as a fixed effect. Additional models were used to analyze water-quality variable response to CWD during POST-LT only. For each of these LMMs, the response variable was a water-quality variable, the fixed effects were treatment and season, and stream was a random effect.

NH_4^+ uptake

We measured NH_4^+-uptake rates once in each of 5 seasons (summer 2017, autumn 2017, spring 2018, summer 2018, and autumn 2018) using short-term (1–2-h) NH_4^+Cl and NaCl solution (injectate) injections in reaches ranging in length from 65 to 120 m (Stream Solute Workshop 1990, Roberts et al. 2007). Reach lengths matched those of the original study, as did the overall approach to measuring uptake (Roberts et al. 2007). We made measurements in each season in all streams within a 1- to 2-wk period depending on site access. Prior to each nutrient

release, we measured background specific conductance and collected 2 replicate filtered-water samples, to be analyzed for background NH_4^+ concentrations, at 4 equidistant transects along each study reach. We added the injectate solution into the stream at a constant rate using a metered pump (Fluid Metering Incorporated, Syosset, New York), raising specific conductance and the NH_4^+ concentration of stream water. As the injectate was added, we recorded the change in specific conductance at the downstream end of the reach until there was no change in specific conductance over 20 min. We then remeasured specific conductance and collected replicate filtered-water samples at the same 4 transects. We placed filtered-water samples on ice in the field and then froze (*–20°C)* them in the laboratory until analyzed. Following the injectate release, we measured wetted width every ~2 m throughout the study reach to determine mean wetted width. We calculated NH_4^+ uptake length (S_w) as the decline in NH_4^+ concentration along each study reach relative to changes of the conservative tracer (NaCl, measured as specific conductance) and fit to a 1st-order decay function (Stream Solute Workshop 1990, Tank et al. 2006). From uptake length, we calculated uptake velocity (v_f) and uptake rate (U) according to methods in the Stream Solute Workshop (1990). We only analyzed v_f and U in this study because of the predominant influence of discharge on S_w.

NH_4^+ uptake was always measured in autumn of each year during each restoration period but not always in other seasons. For example, during PRE, NH_4^+ uptake was only measured in autumn, so we could only compare uptake rates for spring and summer between POST-ST and POST-LT. Site access constraints imposed by military-training schedules occurred during POST-LT, so we made seasonal NH_4^+-uptake measurements during late autumn 2017 and early winter 2018. These measurements took place within 2 wk of each other, so we considered both as

autumn measurements. Thus, we could not compare NH_4^+-uptake rates for winter between POST-ST and POST-LT.

We expected NH_4^+-uptake metrics to differ seasonally (Roberts et al. 2007, 2021), so we analyzed each metric separately by season (spring, summer, autumn). Specifically, for each NH_4^+-uptake metric in each season, we created a separate LMM with that metric as a response variable. Fixed effects were treatment, period, and all interaction between them, and stream was a random effect. Additional models were used to analyze differences in NH_4^+ uptake among seasons (response variables were NH_4^+-uptake metrics and the fixed effect was season) and to analyze NH_4^+-uptake responses to CWD treatment across all seasons during POST-LT only (response variables were NH_4^+-uptake metrics, treatment was a fixed effect, and stream was a random effect).

Whole-stream metabolism indicators

We initially estimated whole-stream metabolism during PRE and POST-ST by using a modification of the single-station diel oxygen change method (Odum 1956) and estimated reaeration rates by using propane injections as detailed in Houser et al. (2005). Because of low GPP in the study reaches, contemporary stream metabolism models were unable to accurately estimate reaeration rates and provided unrealistic estimates of GPP and ER. Therefore, during POST-LT, we estimated whole-stream metabolism based on characteristics of the diurnal dissolved oxygen (DO) profile (extreme value method, sensu Wang et al. 2003). Previous work in these study reaches validated this approach and found that GPP was positively correlated with daily amplitude of DO deficit and ER was positively correlated with maximum daily DO deficit

(Mulholland et al. 2005). We recalculated whole-stream metabolism estimates during PRE and POST-ST by using the extreme value method, based on raw DO data used in Houser et al. (2005) and Roberts et al. (2021).

For DO measurements during POST-LT, we deployed a DO sensor (Precision Measurement Engineering, Vista, California) in each stream, which provided 5 seasonal estimates (summer 2017, autumn 2017, spring 2018, summer 2018, and autumn 2018) of whole-stream metabolism indicators. We retrieved DO sensors during the next water-quality sampling event (~1 mo metabolism trials). As done in the prior study, we estimated daily amplitude of the DO deficit (i.e., GPP indicator) and maximum daily DO deficit (i.e., ER indicator) during baseflow conditions, beginning on the 1st full day after DO sensors were deployed and continuing until the last full day before a rain event (Roberts et al. 2021). We used mean values of the amplitude of the DO deficit and the maximum daily DO deficit in each season in analyses.

Whole-stream metabolism was always measured in autumn of each year during each restoration period but not always in other seasons. Similar to NH_4^+ uptake, site access constraints resulted in whole-stream metabolism measurements being made during late autumn 2017 and early winter 2018, but we considered these measurements as autumn measurements. Thus, we could not compare whole-stream metabolism indicators for winter between PRE and POST-LT or between POST-ST and POST-LT.

Similar to NH_4^+ uptake, we expected whole-stream metabolism indicators to differ seasonally (Roberts et al. 2007, 2021), and we therefore analyzed these metrics separately by

season (spring, summer, autumn). Specifically, for each whole-stream metabolism indicator in each season, we created a separate LMM with that indicator as the response variable. Fixed effects were treatment, period, and all interaction between them, and stream was a random effect. Additional models were used to analyze whole-stream metabolism response to CWD treatment across all seasons during POST-LT only. For these LMMs, response variables were whole-stream metabolism indicators, the fixed effect was treatment, and stream was a random effect.

Disturbance analysis

We estimated watershed disturbance, using the same criteria of disturbance as in Maloney et al. (2005), as the percentage of bare ground on slopes >5% summed with the percentage of unpaved road area within the watershed. Whereas Maloney et al. (2005) used digital orthophotography (from July 1999) at a 0.5-m resolution and ground-truthed by FBMI personnel (R. G. Bufford, Installation and Geographic Information and Services, FBMI, personal communication), we used the 30-m resolution 2016 National Land Cover Dataset (NLCD; Yang et al. 2018). Land-cover classification using 2016 NLCD data was done in ArcMap (version 10.7.1; Esri™, Redlands, California). However, we considered the original disturbance data of Maloney et al. (2005) to be more accurate (0.5-m resolution) than the lower-resolution (30-m) NLCD data we generated. We excluded data from stream Bonham Creek (used in the earlier studies by Houser et al. 2005, Maloney et al. 2005, and Roberts et al. 2007) because its floodplain was flatter and broader than other streams, which may have provided increased protection from upland disturbance (see Houser et al. 2005). Thus, our disturbance analysis was limited to data from 6 streams.

We tested the putative relationship between % watershed disturbance, as estimated by both Maloney et al. (2005) and 2016 NLCD data on instream water-quality variables, and ecosystem-function metrics by using simple linear regression. As described above for LMM analyses, we used residual plots and Q-Q plots to assess whether data met the model assumptions. To understand how the effect of disturbance (as estimated by Maloney et al. 2005) changed by restoration period, we ran regressions through the mean value of each water-quality variable and ecosystem-function metric observed for that period. For watershed disturbance estimated from 2016 NLCD data, we ran regressions through the mean value of each water-quality variable and ecosystem-function metric during only POST-LT. We corrected *p*-values for multiple comparisons among variables and periods using the Benjamini–Hochberg method (Jafari and Ansari-Pour 2019). We used SigmaPlot® (version14.0; Systat Software, San Jose, California) to complete linear regressions.

RESULTS

Long-term effects of CWD additions

CWD Areal CWD coverage across all restored and unrestored streams ranged from 15.2 to 36.8% during POST-LT. There was no effect of restoration on areal CWD coverage between restored and unrestored streams during POST-LT ($p = 0.63$, Wald $\chi^2 = 0.23$; Table 2-S1).

Water quality In general, there was high variation in water-quality variables among study streams, although mean values for each stream tended to remain similar over the entire 18-y study period (Fig. 2-2, Table 2-S2). Across both restored and unrestored streams, NO_3^-, NH_4^+, and SRP concentrations were lower in POST-LT than in previous periods (Tables 2-2, 2-S2).

Differences were also observed among periods in particular seasons for pH, DOC, NO_3^-, NH_4^+, and SRP.

Streamwater pH showed strong differences among seasons (ANOVA, $p < 0.01$, Wald $\chi^2 = 34.0$) and periods ($p < 0.01$, Wald $\chi^2 = 61.6$), and there was a strong treatment × period interaction ($p < 0.01$, Wald $\chi^2 = 11.7$; Table 2-S3). Overall, pH values during POST-LT were more variable in each stream and 7.6 and 4.7% lower than during POST-ST and PRE, respectively ($p < 0.01$, Wald $\chi^2 = 30$; Fig. 2-2, Table 2-S4). There were no differences in pH between restored and unrestored streams within seasons during each period (all $p > 0.2$).

Seasonal differences between restoration treatments across periods were also observed for DOC concentrations (treatment × period × season $p = 0.02$; Table 2-S3). In winter, DOC concentrations were 156.3% higher in restored streams during POST-LT than in restored streams during PRE ($p < 0.01$, $t = 7.0$) and 156.1% higher than during POST-ST ($p < 0.01$, $t = 7.3$). This difference was likely driven by high DOC values measured at 2 restored sites following heavy rains (see Discussion for more detail). There were no other differences in DOC during any other season (all $p > 0.19$).

There was no effect of restoration treatment on NO_3^-, NH_4^+, SRP, or TSS concentrations or on specific conductance when analyzed across the 3 time periods, though there were some differences observed across seasons and periods (Table 2-S3). In investigating treatment effects within POST-LT only (Table 2-S5), some differences between restored and unrestored streams emerged. Specifically, TSS concentrations during POST-LT were 192% higher in restored vs

unrestored streams ($p = 0.07$, $t = 2.3$) and DOC concentrations were 175% higher in restored vs unrestored streams in the winter during POST-LT ($p < 0.01$, $t = 5.3$).

NH_4^+ uptake Overall, there was no increase in v_f or U in restored vs unrestored streams over the long-term restoration period (Fig. 2-3A, B). There was no effect of treatment, period, or the treatment × period interaction on U in autumn or summer (all $p > 0.1$; Tables 2-S6, 2-S7), nor was there an effect of period or treatment × period on U in spring (all $p > 0.2$; Table 2-S8). However, there was an effect of treatment on U (ANOVA, $p = 0.05$, Wald $\chi^2 = 3.8$; Table 2-S8) during spring, with U in restored streams being 88% lower than in unrestored streams. There was no effect of treatment or treatment × period during autumn on v_f (Table 2-S7). However, there was an effect of period on v_f in autumn ($p = 0.04$, Wald $\chi^2 = 6.6$; Table 2-S7), with v_f in POST-LT streams being 90% higher than in POST-ST streams ($p < 0.05$, $t = 2.7$). There were effects of treatment ($p < 0.01$, Wald $\chi^2 = 7.0$), period ($p = 0.02$, Wald $\chi^2 = 5.3$), and treatment × period ($p = 0.03$, Wald $\chi^2 = 4.7$) on v_f in spring (Table 2-S8). During spring, v_f was 456% higher in unrestored POST-LT streams than in unrestored POST-ST streams ($p = 0.03$, $t = 3.2$), and v_f in POST-LT restored streams was 84% lower than in unrestored streams during the same period ($p = 0.02$, $t = 3.4$). There was no effect of treatment, period, or treatment × period (ANOVA, all $p > 0.2$; Table 2-S6) on v_f during summer. In addition to variation within each season among restoration periods, v_f and U were variable among streams across all periods (Table 2-S9).

When uptake data were summarized over the entire 18-y period by season, mean U was 33.28 mg N m^{-2} d^{-1} (SE = 5.39) in autumn, 21.12 mg N m^{-2} d^{-1} (5.29) in spring, and 24.33 mg N m^{-2} d^{-1} (11.56) in summer, although there was no difference among seasons ($p = 0.27$, Wald $\chi^2 =$

3.9). Mean v_f over the 18-y period was 0.017 mm/s (SE = 0.003) in autumn, 0.019 mm/s (0.007) in spring, and 0.012 mm/s (0.005) in summer. Similar to U, v_f did not vary by season (p = 0.3, Wald χ^2 = 3.6).

In examining the effect of restoration during POST-LT only, there was no difference in U (p = 0.76, Wald χ^2 = 0.09) or v_f (p = 0.22, Wald χ^2 = 1.5; Table 2-S10) in restored vs unrestored streams.

Whole-stream metabolism indicators There was no increase in maximum daily DO deficit (ER indicator) or daily amplitude of the DO deficit (GPP indicator) in restored vs unrestored streams over the long-term restoration period (Fig. 2-4A, B). Maximum daily DO deficit did not differ by restoration treatment within any season (autumn: ANOVA, p = 0.38, Wald χ^2 = 2.0; spring: p = 0.38, Wald χ^2 = 1.93; summer: p = 0.2, Wald χ^2 = 3.3) over the entire 18-y period (Tables 2-S11-S13). Daily amplitude of the DO deficit also did not vary with restoration treatment during any season (autumn: ANOVA, p = 0.57, Wald χ^2 = 1.13; spring: p = 0.95, Wald χ^2 = 0.10; summer: p = 0.69, Wald χ^2 = 0.73) over the entire 18-y period (Tables 2-S11-S13).

Mean maximum daily DO deficit over the entire 18-y period was 1.4 mg/L (SE = 0.04) in the autumn, 0.99 mg/L (0.04) in winter, 1.17 mg/L (0.04) in spring, and 1.15 mg/L (0.04) in summer. Daily amplitude of the DO deficit over the entire 18-y period was 0.40 mg/L (SE = 0.03) in the autumn, 0.43 mg/L (0.03) in winter, 0.48 mg/L (0.03) in spring, and 0.39 mg/L (0.02) in summer. The daily amplitude of the DO deficit during spring was 23% greater than

during summer (p = 0.01, t = 3.04) and 20.8% greater than during autumn (p = 0.09, t = 2.4). Maximum daily DO deficit and daily amplitude of the DO deficit varied among streams across all periods (Table 2-S14), but these indicators did not vary with restoration treatment within any season of POST-LT (all $p > 0.1$, Table 2-S15).

Influence of watershed disturbance on water-quality variables and ecosystem function

There was no relationship between % watershed disturbance, as estimated from the lower-resolution 2016 NLCD data, and any water-quality variable or ecosystem-function metric across the 6 study streams (site Bonham Creek excluded, see Methods; all $p > 0.10$). The following results are for watershed disturbance from higher-resolution imagery as calculated in Maloney et al. (2005).

The relationship between watershed disturbance and water quality varied by period (Figs 5, S2). Watershed disturbance exhibited a positive relationship with TSS during PRE (p = 0.09, r^2 = 0.55) and POST-ST (p = 0.1, r^2 = 0.53) and with NH_4^+ during PRE (p = 0.07, r^2 = 0.60) and POST-LT (p = 0.76, r^2 = 0.2), whereas a negative relationship was observed with DOC during PRE (p = 0.06, r^2 = 0.64) and POST-ST (p = 0.03, r^2 = 0.72) (Fig. 2-S2). There was no relationship between disturbance and pH during PRE or POST-ST, but there was a positive relationship during POST-LT (p = 0.06, r^2 = 0.62) (Fig. 2-5). There was no relationship between watershed disturbance and NO_3^-, SRP, or specific conductance during any period over the entire 18-y study period (Fig. 2-S2).

The relationships between watershed disturbance and NH_4^+ uptake and whole-stream metabolism were variable. There was no relationship between watershed disturbance and *U* during any period (all $p > 0.1$; Table 2-S16), but there were negative relationships between disturbance and v_f during PRE ($p = 0.07$, $r^2 = 0.60$) and POST-ST ($p = 0.08$, $r^2 = 0.59$) but not during POST-LT ($p = 0.83$, $r^2 = 0.01$) (Fig. 2-5). There was no relationship between disturbance and daily amplitude of the DO deficit during any period (all $p > 0.14$). There was no relationship between disturbance and maximum daily DO deficit during PRE ($p = 0.14$, $r^2 = 0.47$), a negative relationship during POST-ST ($p = 0.10$, $r^2 = 0.53$), and no relationship during POST-LT ($p = 0.60$, $r^2 = 0.08$) (Fig. 2-5).

Overall, the responses of water-quality variables and ecosystem functions to watershed-scale disturbance were limited when the responses were averaged across seasons for each period, although there were responses in some seasons and years (Tables 2-S16-S18). For example, there were strong positive relationships between disturbance and TSS during spring 2018 and between disturbance and daily amplitude of the DO deficit during summer 2017 (Tables 2-S17, 2-S18).

DISCUSSION

In this study, we quantified the long-term effects of CWD dams in restored, low-gradient streams at Fort Benning Military Installation in the southeastern US. We found minimal pronounced, long-term effects of CWD additions on water-quality variables and instream ecosystem functions (Table 2-3), although there were some differences among streams and across restoration periods. These findings suggest that CWD additions may have minimal long-term effects on ecosystem function in sandy-bottom, Coastal Plain streams.

Limited long-term effect of CWD additions on water quality and ecosystem function

Studies evaluating water-quality responses to instream restoration, and to CWD additions in particular, are extremely limited. A review of 345 stream-restoration studies (Roni et al. 2008) revealed only 33 studies that assessed water-quality responses to different restoration techniques (road improvements, riparian rehabilitation, floodplain connectivity, nutrient additions, and instream-habitat improvement), only 1 of which examined the effects of rock, wood, or log additions on water quality. The dearth of water-quality-response studies suggests that our study is among the few to investigate water-quality responses to CWD additions and, especially, to evaluate long-term (>10-y) responses.

Whereas some restoration techniques appear to improve water quality by decreasing nutrient and TSS concentrations and export (Lowrance 1997, Palmer et al. 2014, Mrozińska et al. 2018), our results suggest that CWD additions in the absence of a watershed-scale restoration are not effective at improving water quality over the long term (nor the short term; Mulholland et al. 2007). This limited response may be related to the already low nutrient concentrations in these streams (Table 2-2; Houser et al. 2006), which would limit the ability of CWD dams to reduce concentrations further. Additionally, CWD dams may not be a suitable restoration technique to reduce TSS concentrations in low-gradient, Coastal Plain streams because they may create meandering flow paths that concentrate flow into stream banks, leading to erosion and channel widening (Davis and Gregory 1994, Gurnell et al. 1995).

Despite early work in these streams reporting NH_4^+ uptake rates increasing immediately after CWD additions (Roberts et al. 2007), there was no longer-term effect of additions on uptake 14 y following restoration. Instead, our analysis of the longer dataset revealed that elevated uptake rates returned to pre-restoration levels after only 1 y post-restoration. The lack of long-term effect of CWD additions on NH_4^+-uptake rates also may explain why nutrient concentrations did not decrease over POST-ST and POST-LT. Such short-term restoration responses are similar to those of Arango et al. (2015), who found that large wood additions and channel redesign in an open-canopy urban stream elevated NH_4^+-uptake rates for only 35 d. Increased algal biomass and nutrient demand following restoration led to the immediate post-restoration increase in nutrient-uptake rates, with the subsequent decrease in uptake coinciding with algal senescence (Arango et al. 2015). In our closed-canopy study streams, the immediate post-restoration increases in U and v_f likely occurred because of increased heterotrophic microbial demand (Roberts et al. 2007), but we did not quantify algal biomass.

Our finding of no long-term effect of CWD additions on NH_4^+ uptake supports other studies that evaluated different restoration techniques over the long and short term. Restored urban streams in Maryland, USA, that combined stormwater ponds and floodplain-connectivity methods had similar nutrient-uptake metrics, but lower water velocities, compared with non-restored sites 6 y after restoration (Klocker et al. 2009). Klocker et al. (2009) suggested this pattern occurred because nutrient loads were greater than biotic demand and that stream restoration techniques could not address watershed nutrient loading. Likewise, channelized Kentucky, USA, streams restored by creating meanders, pools, and riffles showed only marginally increased NH_4^+-uptake velocity 2 y following restoration, which may have been

partially attributable to increased autotrophic demand following relocation of the stream channel to an open-canopy floodplain (Bukaveckas 2007). Our study was much longer than either of these studies, and our restoration technique was different, but taken together, all found no long-term effect of restoration on NH_4^+ uptake.

Surprisingly, few studies have assessed responses of whole-stream metabolism to CWD additions, even though metabolism may be sensitive to CWD abundance and its effects on respiration (Houser et al. 2005). ER rates in restored streams during POST-ST were higher than in unrestored streams for the first 2 y after CWD additions, but these rates decreased in the 3rd y (Roberts et al. 2021). However, our examination of long-term responses found no differences in the maximum daily DO deficit (ER indicator) of restored vs unrestored streams during POST-LT. Our long-term study is one of the few to examine the influence of CWD additions on ecosystem function, but our finding of no effect is similar to studies of short and intermediate length that reported limited responses to restoration (Larson et al. 2001, Palmer et al. 2010, Langford et al. 2012).

Effects of spatial and temporal variation on restoration efficacy

A factor likely contributing to the minimal long-term restoration effect we observed in FBMI streams was sedimentation and burial of CWD additions after high-flow events. For example, suitable habitat for microbes responsible for heterotrophic respiration may be buried by sand, which is a substrate less suitable for microbial growth (Entrekin et al. 2008, Hoellein et al. 2011). In the original study, CWD additions in streams draining 2 of the most heavily disturbed watersheds (Sally Branch 4 and Little Pine Knot) were substantially buried within the 1st y after

restoration, necessitating supplemental CWD additions during POST-ST (in autumn 2004; Mulholland et al. 2007). Burial of CWD associated with watershed disturbance likely contributed to the negative correlation between CWD abundance and disturbance (Maloney et al. 2005).

Despite being able to visually locate the CWD dams in restored streams 14 y after CWD additions, there was no difference in CWD areal coverage between restored and unrestored streams during the POST-LT period (Table 2-S1). This result suggests that CWD burial likely remained an issue in these streams over the entire restoration study. CWD burial during POST-LT was likely, given that 2016 saw both historically high and low flows at a US Geological Survey (USGS) gage downstream of our watersheds (USGS station 02341800, Upatoi Creek near Columbus, Georgia). Because of the highly variable nature of sediment dynamics in these sandy-bottom streams, continuous monitoring of stream restoration projects may be necessary for better tracking and separation of restoration effects from natural year-to-year variation. Limited maintenance of CWD dams can further hinder stream restorations from remaining effective over long periods (Moore and Rutherfurd 2017); thus, regular augmentation and assessment of CWD abundance may be necessary to retain adequate instream CWD to sustain ecosystem function in these dynamic Coastal Plain streams.

Individual streams respond differently to restoration, in part because of nuanced variability in stream features and environmental conditions. For example, in this study, NH_4^+ concentrations in summer in unrestored streams were lower during POST-LT than during POST-ST and PRE, but this pattern appeared to be driven primarily by lower concentrations in 1 of the 3 unrestored streams (Sally Branch 4), rather than being a consistent response across all 3

unrestored streams. Further, Michigan streams receiving gravel and boulder additions in 1 reach and no addition in another showed increased nutrient uptake and ER rate at only 1 of 3 restored streams (Hoellein et al. 2011). However, the differential response Hoellein et al. (2011) observed resulted from the addition of favorable algal-colonization substrates (gravel, boulders) to a stream bed with a greater % of sand than the other 2 streams, allowing for a greater response over the non-restored reach. Because it is often difficult to ensure that all streams being compared in a restoration assessment have a similar baseline of physical and chemical characteristics (Townsend et al. 2004), it is important to examine the factors that drive differential restoration responses among multiple streams. Our 7 study streams were chosen as part of a larger project that examined whether restoration could ameliorate the impacts of upland disturbance on stream ecosystem structure and function (Houser et al. 2005, 2006, Maloney et al. 2005, Mulholland et al. 2007, Roberts et al. 2007) and were never intended to serve as replicates. These streams exhibited a wide range of physical and chemical properties (Tables 2-1, 2-S9), despite being within 18 km of one another, further highlighting the difficulty in finding streams with a comparable environmental baseline when conducting an experimental assessment of restoration.

In our study, accounting for seasonal variation in water-quality variables over the 3 study periods (PRE, POST-ST, POST-LT) was important when assessing overall effects of restoration. Both NO_3^- (restored) and NH_4^+ (unrestored streams) concentrations were lower during summer POST-LT than in earlier summer periods, suggesting a decrease in different N forms in POST-LT during summer, irrespective of restoration. Additionally, there was an interaction between treatment and period for streamwater pH. Specifically, streamwater pH was lower in all streams

during POST-LT compared with earlier periods (Fig. 2-2) and lower than in previous studies in these and other FBMI streams (Bhat et al. 2006). We conclude that this treatment × period interaction resulted from lower pH measures during the POST-LT period in certain seasons and that this interaction was driven largely by differences among periods rather than restoration treatment. Although low, pH in our study streams was similar to other blackwater Coastal Plain streams in other regions (Zampella et al. 2007). Similarly, SRP concentrations also were lower in certain seasons during POST-LT, although these decreases may not necessarily be ecologically significant (e.g., a 50% decrease in SRP concentration of 3 µg/L).

One possible explanation for the lower pH and nutrient concentrations during POST-LT is that all 7 streams experienced a decrease in watershed disturbance and nonpoint-source inputs independent of CWD additions. This hypothesis is supported by the positive relationship between pH and disturbance observed in earlier studies (Houser et al. 2006) and during POST-LT in our study (Fig. 2-5). Houser et al. (2006) observed Ca^{2+} to be positively correlated with % sandy loam and pH and negatively correlated with % loamy sand and suggested that the relationship between pH and disturbance was an interaction between soil characteristics and disturbance effects.

Houser et al. (2006) also observed a negative correlation between silica and disturbance, suggesting that decreased disturbance may be associated with changes in sediment sources. For our study streams, a decrease in system-wide disturbance may have resulted in decreased sedimentation from more Ca^{2+}-rich soils and an increase in sedimentation from sandy, silica-rich soils. However, we did not analyze water samples for Ca^{2+} or silica. Further studies examining

the effects of changes in disturbance regimes on water-quality variables in these systems are needed.

Because of limited site access at FBMI, sampling sometimes occurred during non-baseflow conditions. Two very high DOC concentrations measured at 2 restored streams (Little Pine Knot and King's Mill) on the same day (15 February 2018) likely led to the differences observed in DOC concentration between restoration periods and between restored and unrestored streams during the POST-LT winter season. The observed high DOC concentrations were likely due to heavy rain on 11 February 2018, which produced 37.8 mm of precipitation, as measured at a nearby USGS gage (0241800 Upatoi Creek near Columbus, Georgia). Discharges measured on 15 February were in the 46^{th}- (Little Pine Knot) and 98^{th}- (King's Mill) percentile classes for all measured discharges at each respective stream. This aspect of our results highlights the complexity in interpreting stream ecosystem responses to restoration among changing environmental conditions in both the short and long term.

Seasonality in ecosystem functions was minimal, with differences mainly driven by low ecosystem metabolism in winter. This observation was surprising not only because we expected GPP, ER, and NH_4^+ uptake to vary seasonally with changes in temperature, light availability, and leaf-litter input but also because seasonality of GPP and ER was previously observed in these study streams (Houser et al. 2005, Roberts et al. 2021). Minimal seasonality may have occurred because the extreme value method we used is not a perfect correlate of GPP and ER (Mulholland et al. 2005) and may be less sensitive to seasonality. It may also simply be that, because of site-access limitations, POST-LT measurements of ecosystem function occurred at different times

within each seasonal window compared with previous periods (e.g., late-autumn POST-LT measurements vs mid-autumn POST-ST measurements), which resulted in missing peak litterfall. Similarly, site-access limitations coupled with variation in spring leaf out may have resulted in measurements that occurred at different times relative to spring leaf out during POST-LT. To fully capture both seasonality in the chosen ecosystem-function response metrics and changes in watershed disturbance over time, post-restoration assessment measurements should occur seasonally at regular intervals every 1 to 2 y, with the sampling occurring at the same relative time each season (e.g., prior to leaf out, at peak litterfall).

Disturbance effect

Restored and unrestored streams in this study spanned a gradient of % watershed disturbance, and it is important to understand how the effect of disturbance on response metrics changed over time. Earlier work in the study streams during PRE found that TSS and pH were positively correlated with watershed disturbance, SRP and DOC were negatively correlated with disturbance, and there was no correlation of NO_3^- or NH_4^+ with disturbance (Houser et al. 2006). Additionally, negative relationships were observed between watershed disturbance and ER (but not GPP) during PRE (Houser et al. 2005) and between watershed disturbance and NH_4^+-uptake metrics immediately before (PRE) and immediately after (POST-ST) restoration (Roberts et al. 2007). However, our analysis of these same water-quality variables and ecosystem-function metrics found differing results during these same periods (though our POST-ST period [2003–2006] is different than the immediate post-restoration [~1 mo] period analyzed in Roberts et al. [2007]). The differential responses observed in our disturbance analyses compared with earlier analyses (Houser et al. 2005, 2006, Roberts et al. 2007) could be because of changes in the

mechanism driving disturbance, but the differing responses likely arose from differences in the number of streams used in each analysis. Streams that experienced substantial landscape changes due to military-training activities (Mulholland et al. 2009) between PRE and POST-LT were excluded from our study, which resulted in a different number of streams available for disturbance analysis during each period (PRE = 9, Houser et al. 2005, 2006; POST-ST = 7, Roberts et al. 2007; POST-LT = 6, this study). The differing number of streams among periods may confound our ability to discern any temporal changes in response to disturbance; however, limited responses to disturbance were apparent after 18 y.

Contemporary upland disturbance, primarily stemming from military-training activities at FBMI, did not appear to be a strong driver for most water-quality variables and ecosystem functions in FBMI streams during POST-LT (Fig. 2-5). Even though pH and NH_4^+ concentrations showed a positive relationship with watershed disturbance during POST-LT, variables that were previously related (i.e., TSS, DOC, SRP; Houser et al. 2006) showed no relationships when responses were averaged across seasons within POST-LT. For example, there was a negative relationship between DOC and disturbance during PRE and POST-ST, but that relationship was not apparent during POST-LT. This change in DOC response to disturbance may be due to changes in flow between periods, which resulted in greater DOC input across all streams. There were, however, relationships between these variables when examined by season during POST-LT. For example, there was a negative relationship between disturbance and DOC during autumn 2018 (POST-LT) and a positive relationship between disturbance and TSS during spring 2018 (POST-LT) (Table 2-S17). Additionally, the lack of a strong long-term effect (i.e., during POST-LT) of disturbance on ecosystem-functioning measures that previously were

negatively related to watershed disturbance (Houser et al. 2005, Roberts et al. 2007) is further evidence that any effect of watershed disturbance was minimal over the most recent study period (POST-LT). When relationships were examined by season during POST-LT, the only responses to disturbance were strong positive relationships between disturbance and daily amplitude of the DO deficit during autumn of 2017 (Tables 2-S18).

Land management practices at FBMI have changed since the publication of Maloney et al. (2005) and include revegetation of heavily disturbed areas, improvement of roads, and implementation of best management practices (Fort Benning 2014). These changes in landscape management practices, coupled with the limited relationships between disturbance and water-quality variables and ecosystem-function metrics, suggest that the mechanisms influencing these relationships may have changed and, thus, the effects of watershed disturbance may have diminished system wide.

Broader implications

Our study is one of the few long-term restoration assessments that have captured an initial increase in ecosystem-functioning rates immediately after restoration followed by a return to pre-restoration conditions over time. These results, although limited to Coastal Plain streams, are important to consider because of the large number of high-cost stream restorations being implemented with minimal assessment of efficacy (Bernhardt et al. 2005). Improving ecosystem functioning is rarely a goal of stream restoration, and success should be judged in the context of the stated restoration goals, but our results nonetheless highlight the need for monitoring over a longer period of time. Short-term monitoring alone may indicate restoration success, but long-

term assessments of restoration efficacy that incorporate seasonal and interannual variability may lead to strongly contrasting conclusions.

Literature cited

American Public Health Association (APHA). 2005. Standard methods for the examination of water and wastewater, 21st edition. American Public Health Association, Washington, DC.

Benke, A. C., and B. Wallace. 2003. Influence of wood on invertebrate communities in streams and rivers. Pages 149–177 *in* S. V. Gregory, K. L. Boyer, and A. M. Gurnell (editors). The ecology and management of wood in world rivers. American Fisheries Society, Symposium 37, Bethesda, Maryland.

Bernhardt, E. S., M. A. Palmer, J. D. Allan, G. Alexander, K. Barnas, S. Brooks, J. Carr, S. Clayton, C. Dahm, J. Follstad-Shah, D. Galat, S. Gloss, P. Goodwin, D. Hart, B. Hassett, R. Jenkinson, S. Katz, G. M. Kondolf, P. S. Lake, R. Lave, J. L. Meyer, T. K. O'Donnell, L. Pagano, B. Powell, and O. Sudduth. 2005. Synthesizing U.S. river restoration efforts. Science 308:636–638.

Bhat, S., J. M. Jacobs, K. Hatfield, and J. Prenger. 2006. Relationships between stream water chemistry and military land use in forested watersheds in Fort Benning, Georgia. Ecological Indicators 6:458–466.

Bukaveckas, P. A. 2007. Effects of channel restoration on water velocity, transient storage, and nutrient uptake in a channelized stream. Environmental Science & Technology 41:1570–1576.

Bunn, S., and P. Davies. 2000. Biological processes in running waters and their implications for the assessment of ecological integrity. Hydrobiologia 422:61–70.

Cavalcanti, G. G., and B. G. Lockaby. 2005. Effects of sediment deposition on fine root dynamics in riparian forests. Soil Science Society of America Journal 69:729–737.

Chen, X., X. Wei, and R. Scherer. 2005. Influence of wildfire and harvest on biomass, carbon pool, and decomposition of large woody debris in forested streams of southern interior British Columbia. Forest Ecology and Management 208:101–114.

Entrekin, S. A., J. L. Tank, E. J. Rosi-Marshall, T. J. Hoellein, and G. A. Lamberti. 2008. Responses in organic matter accumulation and processing to an experimental wood addition in three headwater streams. Freshwater Biology 53:1642–1657.

Flores, L., A. Larrañaga, J. Díez, and A. Elosegi. 2011. Experimental wood addition in streams: Effects on organic matter storage and breakdown. Freshwater Biology 56:2156–2167.

Fort Benning. 2014. Integrated natural resources management plan Fort Benning, Georgia. 2014 Revision. Directorate of Public Works, Environmental Management Division, Fort Benning, Georgia. (Available from: https://www.benning.army.mil/Garrison/DPW/EMD/Content/PDF/4 - Fort Benning 2014 INRMP Revision_Final Draft.pdf)

Fox, J., and S. Weisberg. 2019. An R companion to applied regression. 3rd edition. Sage, Thousand Oaks, California.

Griffith, G. E., J. M. Omernik, J. A. Comstock, S. Lawrence, G. Martin, A. Goddard, V. J. Hulcher, and T. Foster. 2001. Ecoregions of Alabama and Georgia. United States Geological Survey, Reston, Virginia. (Available from: http://ecologicalregions.info/data/ga/alga_front.pdf)

Harrison, X. A., L. Donaldson, M. E. Correa-Cano, J. Evans, D. N. Fisher, C. E. D. Goodwin, B. S. Robinson, D. J. Hodgson, and R. Inger. 2018. A brief introduction to mixed effects modelling and multi-model inference in ecology. PeerJ 6:e4794.

Hoellein, T. J., J. L. Tank, S. A. Entrekin, E. J. Rosi-Marshall, M. L. Stephen, and G. A. Lamberti. 2011. Effects of benthic habitat restoration on nutrient uptake and ecosystem

metabolism in three headwater streams. River Research and Applications 7:1451–1461.
Houser, J. N., P. J. Mulholland, and K. O. Maloney. 2005. Catchment disturbance and stream metabolism: Patterns in ecosystem respiration and gross primary production along a gradient of upland soil and vegetation disturbance. Journal of the North American Benthological Society 24:538–552.
Houser, J. N., P. J. Mulholland, and K. O. Maloney. 2006. Upland disturbance affects headwater stream nutrients and suspended sediments during baseflow and stormflow. Journal of Environmental Quality 35:352–365.
Howson, T. J., B. J. Robson, T. G. Matthews, and B. D. Mitchell. 2012. Size and quantity of woody debris affects fish assemblages in a sediment-disturbed lowland river. Ecological Engineering 40:144–152.
Jafari, M., and N. Ansari-Pour. 2019. Why, when and how to adjust your p values? Cell Journal 20:604–607.
Keys, T. A., H. Govenor, C. N. Jones, W. C. Hession, E. T. Hester, and D. T. Scott. 2018. Effects of large wood on floodplain connectivity in a headwater Mid-Atlantic stream. Ecological Engineering 118:134–142.
Klocker, C. A., S. S. Kaushal, P. M. Groffman, P. M. Mayer, and R. P. Morgan. 2009. Nitrogen uptake and denitrification in restored and unrestored streams in urban Maryland, USA. Aquatic Sciences 71:411–424.
Lake, P. S., N. Bond, and P. Reich. 2007. Linking ecological theory with stream restoration. Freshwater Biology 52:597–615.
Langford, T. E. L., J. Langford, and S. J. Hawkins. 2012. Conflicting effects of woody debris on stream fish populations: Implications for management. Freshwater Biology 57:1096–1111.
Larson, M. G., D. B. Booth, and S. A. Morley. 2001. Effectiveness of large woody debris in stream rehabilitation projects in urban basins. Ecological Engineering 18:211–226.
Lenth, R., P. Buerkner, M. Herve, J. Love, H. Riebl, and H. Singmann. 2019. *emmeans*: Estimated marginal means, aka least-squares means. (Available from: https://CRAN.R-project.org/package=emmeans)
Lockaby, B. G., R. Governo, E. Schilling, G. Cavalcanti, and C. Hartsfield. 2005. Effects of sedimentation on soil nutrient dynamics in riparian forests. Wetlands and Aquatic Processes 34:390–396.
Lowrance, R. 1997. Water quality functions of riparian forest buffers in Chesapeake Bay watersheds. Environmental Management 21:687–712.
Maloney, K. O., J. W. Feminella, R. M. Mitchell, S. A. Miller, P. J. Mulholland, and J. N. Houser. 2008. Landuse legacies and small streams: Identifying relationships between historical land use and contemporary stream conditions. Journal of the North American Benthological Society 27:280–294.
Maloney, K. O., P. J. Mulholland, and J. W. Feminella. 2005. Influence of catchment-scale military land use on stream physical and organic matter variables in small Southeastern Plains catchments (USA). Environmental Management 35:677–691.
Moore, H. E., and I. D. Rutherfurd. 2017. Lack of maintenance is a major challenge for stream restoration projects. River Research and Applications 33:1387–1399.
Mrozińska, N., K. Glińska-Lewczuk, P. Burandt, S. Kobus, W. Gotkiewicz, M. Szymańska, M. Bakowska, and K. Obolewski. 2018. Water quality as an indicator of stream restoration effects—A case study of the Kwacza River restoration project. Water 10:1249.
Mulholland, P. J., J. W. Feminella, B. G. Lockaby, and G. L. Hollon. 2007. Riparian ecosystem

management at military installations: Determination of impacts and evaluation of restoration and enhancement strategies. Final Technical Report SI-1186. United States Department of Defense Strategic Environmental Research and Development Program, Alexandria, Virginia. (Available from: https://apps.dtic.mil/sti/pdfs/ADA606739.pdf)

Mulholland, P. J., J. W. Feminella, B. G. Lockaby, and G. L. Hollon. 2009. Final report addendum: Effects of construction of the digital multipurpose range complex (DMPRC) on riparian and stream ecosystems at Fort Benning, Georgia. SERDP Project RC-1186. United States Department of Defense Strategic Environmental Research and Development Program, Alexandria, Virginia. (Available from: https://apps.dtic.mil/sti/pdfs/ADA534277.pdf)

Mulholland, P. J., J. N. Houser, and K. O. Maloney. 2005. Stream diurnal dissolved oxygen profiles as indicators of in-stream metabolism and disturbance effects: Fort Benning as a case study. Ecological Indicators 5:243–252.

Odum, H. T. 1956. Primary Production in Flowing Waters. Limnology and Oceanography 1:102–117.

Osei, N. A., A. M. Gurnell, and G. L. Harvey. 2015. The role of large wood in retaining fine sediment, organic matter and plant propagules in a small, single-thread forest river. Geomorphology 235:77–87.

Palmer, M. A., E. S. Bernhardt, J. D. Allan, P. S. Lake, G. Alexander, S. Brooks, J. Carr, S. Clayton, C. N. Dahm, J. Follstad Shah, D. L. Galat, S. G. Loss, P. Goodwin, D. D. Hart, B. Hassett, R. Jenkinson, G. M. Kondolf, R. Lave, J. L. Meyer, T. K. O'Donnell, L. Pagano, and E. Sudduth. 2005. Standards for ecologically successful river restoration. Journal of Applied Ecology 42:208–217.

Palmer, M. A., S. Filoso, and R. M. Fanelli. 2014. From ecosystems to ecosystem services: Stream restoration as ecological engineering. Ecological Engineering 65:62–70.

Palmer, M. A., H. L. Menninger, and E. Bernhardt. 2010. River restoration, habitat heterogeneity and biodiversity: A failure of theory or practice? Freshwater Biology 55:205–222.

Pinheiro, J., D. Bates, S. DebRoy, D. Sarkar, EISPACK, S. Heisterkamp, B. Van Willigen, J. Ranke, and R Core Team. 2017. *nlme*: linear and nonlinear mixed effects models. (Available from: https://CRAN.R-project.org/package=nlme)

Riipinen, M. P., J. Davy-Bowker, and M. Dobson. 2009. Comparison of structural and functional stream assessment methods to detect changes in riparian vegetation and water pH. Freshwater Biology 54:2127–2138.

Roberts, B. J., N. A. Griffiths, J. N. Houser, and P. J. Mulholland. 2021. Response of stream metabolism to coarse woody debris additions along a catchment disturbance gradient. Ecosystems 2021. (Available from: https://doi.org/10.1007/s10021-021-00687-9)

Roberts, B. J., P. J. Mulholland, and J. N. Houser. 2007. Effects of upland disturbance and instream restoration on hydrodynamics and ammonium uptake in headwater streams. Journal of the North American Benthological Society 26:38–53.

Roni, P., K. Hanson, and T. Beechie. 2008. Global review of the physical and biological effectiveness of stream habitat rehabilitation techniques. North American Journal of Fisheries Management 28:856–890.

Rubin, Z., G. M. Kondolf, and B. Rios-Touma. 2017. Evaluating stream restoration projects: What do we learn from monitoring? Water 9:174.

Schielzeth, H., N. J. Dingemanse, S. Nakagawa, D. F. Westneat, H. Allegue, C. Teplitsky, D. Réale, N. A. Dochtermann, L. Z. Garamszegi, and Y. G. Araya-Ajoy. 2020. Robustness of

linear mixed-effects models to violations of distributional assumptions. Methods in Ecology and Evolution 11:1141–1152.
Stream Solute Workshop. 1990. Concepts and methods for assessing solute dynamics in stream ecosystems. Journal of the North American Benthological Society 9:95–119.
Tank, J. L., M. J. Bernot, and E. J. Rosi-Marshall. 2006. Nitrogen limitation and uptake. Pages 213–238 *in* F. R. Hauer and G. A. Lamberti (editors). Methods in stream ecology. 2nd edition. Academic Press, Cambridge, Massachusetts.
Townsend, C. R., B. J. Downes, K. Peacock, and C. J. Arbuckle. 2004. Scale and the detection of land-use effects on morphology, vegetation and macroinvertebrate communities of grassland streams. Freshwater Biology 49:448–462.
USEPA (United States Environmental Protection Agency). 2016. National rivers and streams assessment 2008–2009: A collaborative survey. EPA/841/R-16/007. United States Enrironmental Protection Agency, Office of Water and Office of Research and Development, Washington, DC. (Available from: https://www.epa.gov/sites/default/files/2016-03/documents/nrsa_0809_march_2_final.pdf)
Vörösmarty, C. J., P. Green, J. Salisbury, and R. B. Lammers. 2000. Global water resources: Vulnerability from climate change and population growth. Science 289:284–288.
Wallace, J. B., and A. C. Benke. 1984. Quantification of wood habitat in subtropical Coastal Plain streams. Canadian Journal of Fisheries and Aquatic Sciences 41:1643–1652.
Walsh, C. J., A. H. Roy, J. W. Feminella, P. D. Cottingham, P. M. Groffman, R. P. Morgan II. 2005. The urban stream syndrome: Current knowledge and the search for a cure. Journal of the North American Benthological Society 24:706–723.
Wang, H., M. Hondzo, C. Xu, V. Poole, and A. Spacie. 2003. Dissolved oxygen dynamics of streams draining an urbanized and an agricultural catchment. Ecological Modelling 160:145–161.
Webster, J. R., S. W. Golladay, E. F. Benfield, J. L. Meyer, W. T. Swank, and J. B. Wallace. 1992. Catchment disturbance and stream response: An overview of stream research at Coweeta Hydrologic Laboratory. Pages 232–253 *in* P. J. Boon, P. Calow, and G. E. Petts (editors). River conservation and management. John Wiley & Sons, West Sussex, United Kingdom.
Yang, L., S. Jin, P. Danielson, C. Homer, L. Gass, S. M. Bender, A. Case, C. Costello, J. Dewitz, J. Fry, M. Funk, B. Granneman, G. C. Likens, M. Rigge, and G. Xian. 2018. A new generation of the United States National Land Cover Database: Requirements, research priorities, design, and implementation strategies. ISPRS Journal of Photogrammetry and Remote Sensing 146:108–123.
Young, R. G., C. D. Matthaei, and C. R. Townsend. 2008. Organic matter breakdown and ecosystem metabolism: Functional indicators for assessing river ecosystem health. Journal of the North American Benthological Society 27:605–625.
Zampella, R. A., K. J. Laidig, and R. L. Lowe. 2007. Distribution of diatoms in relation to land use and pH in blackwater coastal plain streams. Environmental Management 39:369–384.

Table 2-1. Watershed area (ha), disturbance intensity (% watershed; as calculated in Maloney et al. 2005), and Universal Transverse Mercator (UTM) northing and easting coordinates of the 7 study sites at Fort Benning Military Installation, Georgia, USA.

Treatment	Stream	Watershed area (ha)	Disturbance intensity (% watershed)	UTM N	UTM E
Unrestored	Hollis Branch	215	6.6	3583120	717850
	Bonham Creek	210	10.5	3588327	710969
	Sally Branch 4	100	13.7	3584950	716048
Restored	King's Mill	369	4.6	3600135	720598
	Sally Branch 2	123	8.1	3584831	716828
	Sally Branch 3	72	10.5	3584625	716761
	Little Pine Knot	33	11.3	3585421	719223

Table 2-2. Mean (±SE) values of water-quality metrics (total suspended solid [TSS], pH, specific conductance [SC], nitrate [NO_3^-], ammonium [NH_4^+], soluble reactive phosphorus [SRP], and dissolved organic carbon [DOC] concentrations) across treatments (restored and unrestored) in the pre-restoration (PRE), 1- to 3-y post-restoration (POST-ST), and 14-y post-restoration (POST-LT) periods in streams at Fort Benning Military Installation, Georgia, USA. See text for further details.

Treatment	Period	TSS (mg/L)	pH	SC (µS/cm)	NO_3^- (µg N/L)	NH_4^+ (µg N/L)	SRP (µg P/L)	DOC (mg/L)
Restored	PRE	8.07 ± 0.63	5.72 ± 0.06	18.49 ± 0.69	28.84 ± 2.63	10.57 ± 1.06	2.53 ± 0.24	2.39 ± 0.13
	POST-ST	9.12 ± 0.78	5.85 ± 0.08	18.07 ± 0.64	23.71 ± 2.19	11.82 ± 1.05	2.29 ± 0.19	2.19 ± 0.10
	POST-LT	11.6 ± 1.37	5.28 ± 0.11	15.73 ± 0.72	18.48 ± 2.92	11.36 ± 1.28	2.10 ± 0.18	4.91 ± 1.09
Unrestored	PRE	6.46 ± 0.65	5.21 ± 0.07	21.02 ± 0.74	26.97 ± 3.35	17.45 ± 2.00	3.03 ± 0.30	2.12 ± 0.15
	POST-ST	6.58 ± 0.78	5.39 ± 0.06	19.60 ± 0.47	27.61 ± 3.46	17.38 ± 1.73	2.65 ± 0.22	2.29 ± 0.11
	POST-LT	6.24 ± 0.96	5.20 ± 0.13	16.50 ± 0.90	24.55 ± 3.72	9.85 ± 1.31	1.79 ± 0.24	2.83 ± 0.29

Table 2-3. Responses of water quality, NH_4^+ uptake, gross primary productivity (GPP), and ecosystem respiration (ER) to restoration during the 1- to 3-y post-restoration (POST-ST) and 14-y post-restoration (POST-LT) periods and the POST-LT response we predicted before the experiment, all relative to the pre-restoration (PRE) period, for streams at Fort Benning Military Installation, Georgia, USA. The symbol ↑ indicates an increase or improvement in the response metric, and ↔ indicates no change in the response metric relative to PRE.

Response metric	POST-ST	POST-LT	Predicted POST-LT
Water quality	↔	↔	↑
NH_4^+ uptake	↑	↔	↑
GPP	↔	↔	↑
ER	↑	↔	↑

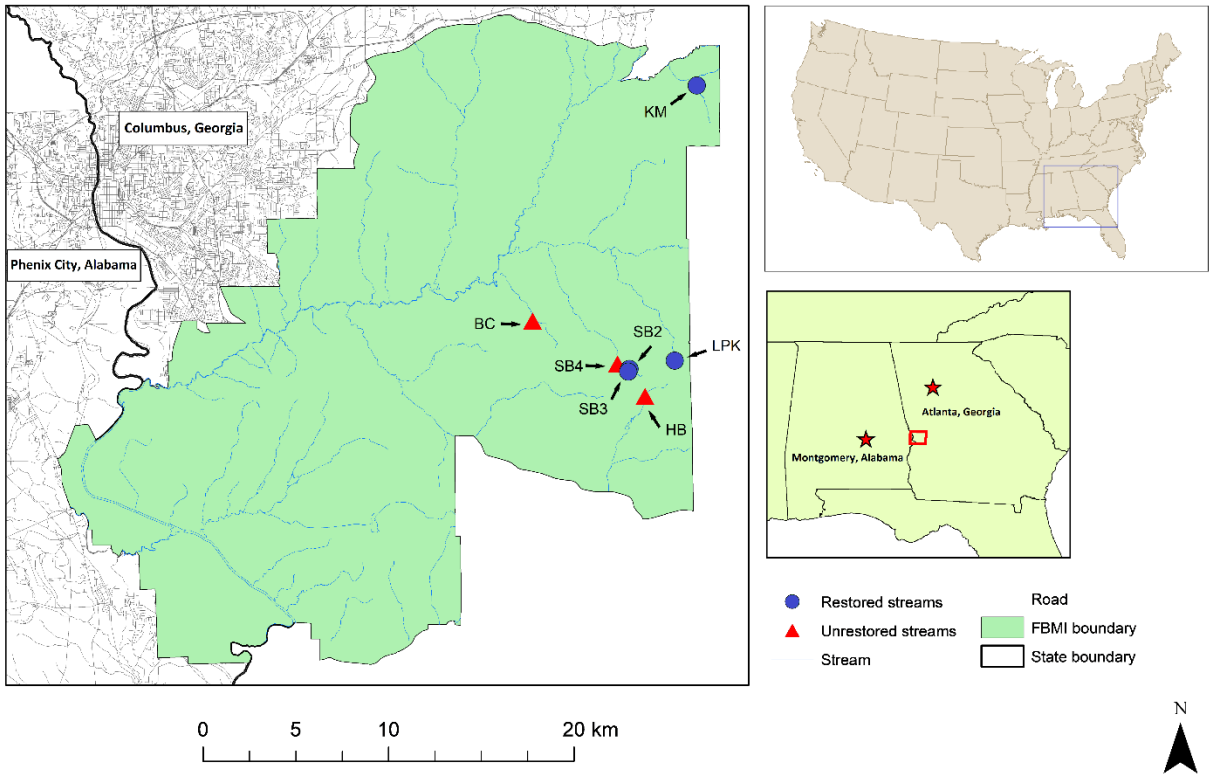

Figure 2-1. Location of Fort Benning Military Installation (FBMI) in Georgia, USA (red rectangle in inset map), and the location of Hollis Branch (HB), Bonham Creek (BC), Sally Branch 4 (SB4), King's Mill (KM), Sally Branch 2 (SB2), Sally Branch 3 (SB3), and Little Pine Knot (LPK) at FBMI (larger map). Blue circles represent restored streams, and red triangles represent unrestored streams. Red stars indicate state capitols. Blue rectangle on inset map indicates the location of study region within the contiguous United States.

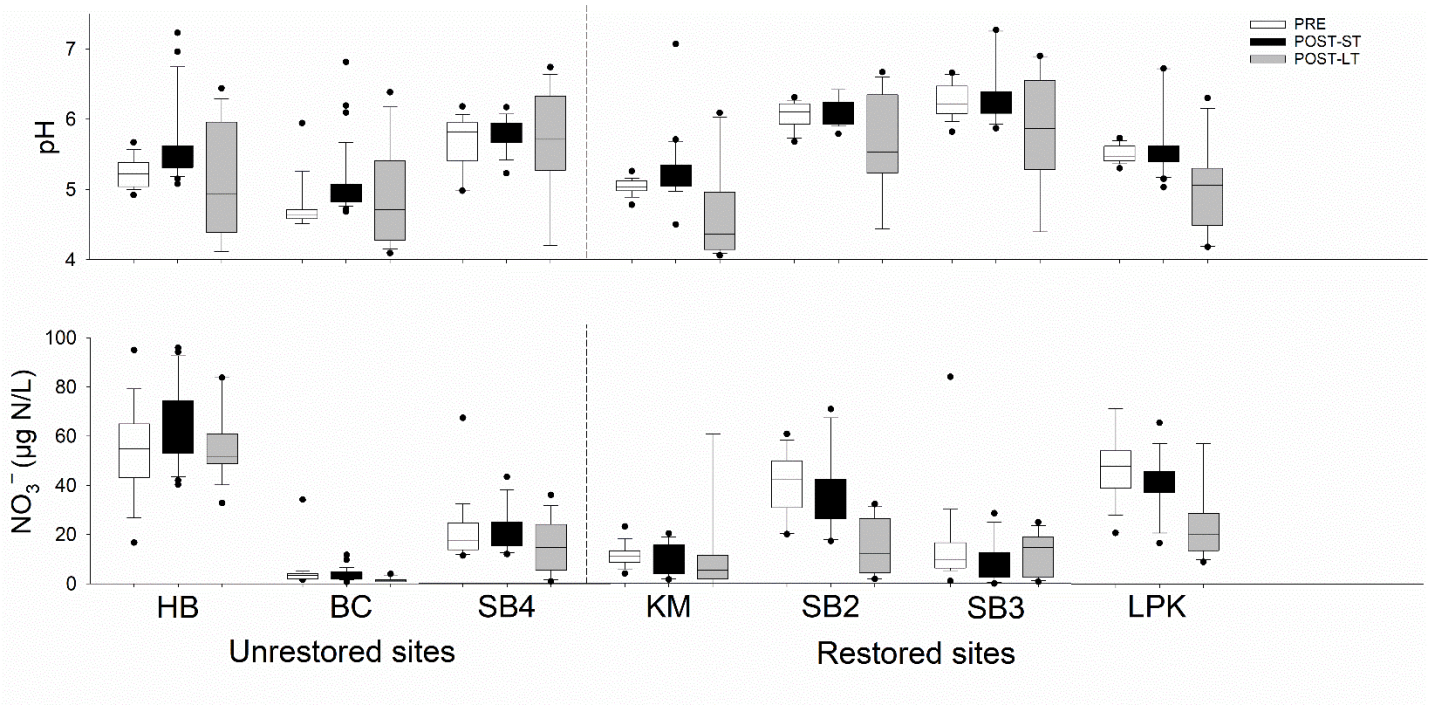

Figure 2-2. Boxplots of water-column pH and nitrate [NO_3^-] concentrations (µg N/L) in unrestored (Hollis Branch [HB], Sally Branch 4 [SB4], Bonham Creek [BC]) and restored (King's Mill [KM], Sally Branch 2 [SB2], Sally Branch 3 [SB3], Little Pine Knot [LPK]) streams at Fort Benning Military Installation in Georgia, USA, across pre-restoration (PRE; white), 1- to 3-y post-restoration (POST-ST; black), and 14-y post-restoration (POST-LT; gray) periods. Dashed vertical lines indicate unrestored (to the left of the line) and restored (to the right of the line) sites. The horizontal line within each box indicates the median, the edges of the boxes indicate the 25th and 75th percentiles, and whiskers represent the 10th and 90th percentiles. Black circles represent outlier datapoints.

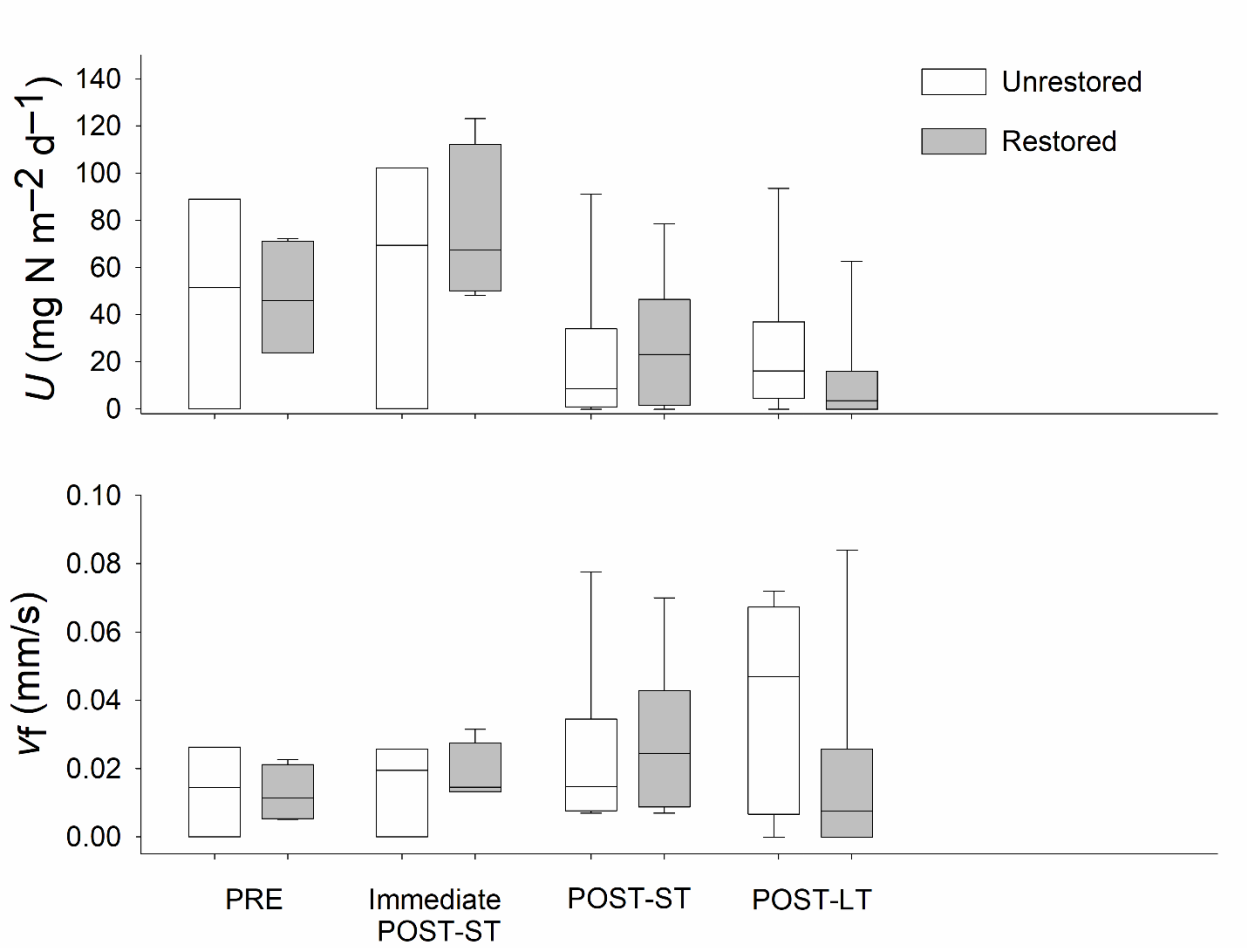

Figure 2-3. Mean (+SE) areal uptake rates (U [mg N m^{-2} d^{-1}]) (A) and uptake velocity (v_f [mm/s]) (B) of ammonium during the autumn immediately before (PRE) and after (immediate POST-ST; Roberts et al. 2007) coarse woody debris additions and during the 1- to 3-y post-restoration (POST-ST) and 14-y post-restoration (POST-LT) periods in restored (white striped) and unrestored (black) streams at Fort Benning Military Installation in Georgia, USA.

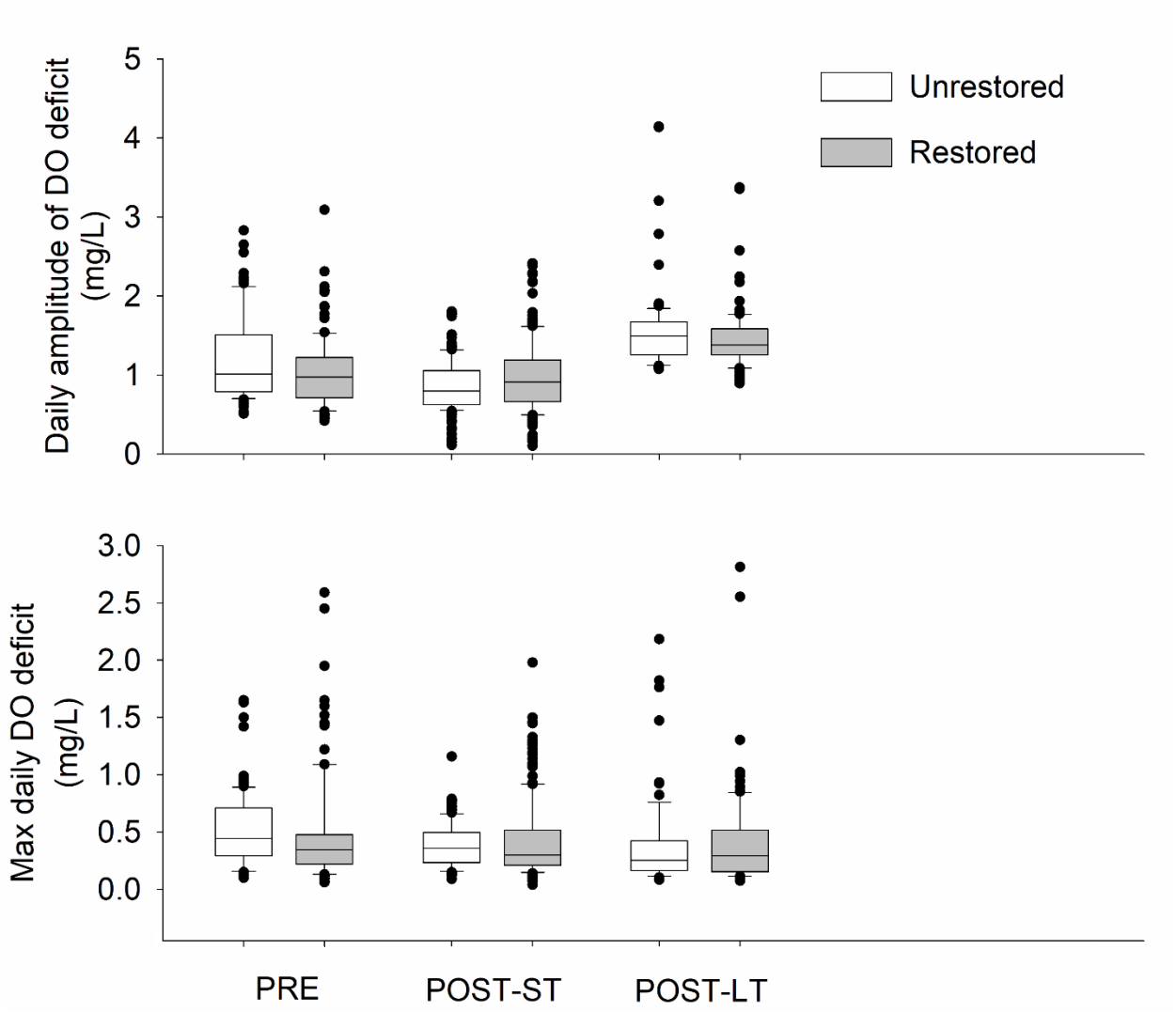

Figure 2-4. Mean (+SE) whole-stream metabolism indicators, daily amplitude of dissolved oxygen (DO) deficit (mg/L) (A) and maximum daily DO deficit (mg/L) (B), across all seasons during the pre-restoration (PRE), 1- to 3-y post-restoration (POST-ST), and 14-y post-restoration (POST-LT) periods in restored (white striped) and unrestored (black) streams at Fort Benning Military Installation in Georgia, USA. Immediate POST-ST data are not available for direct comparison with Fig. 2-3.

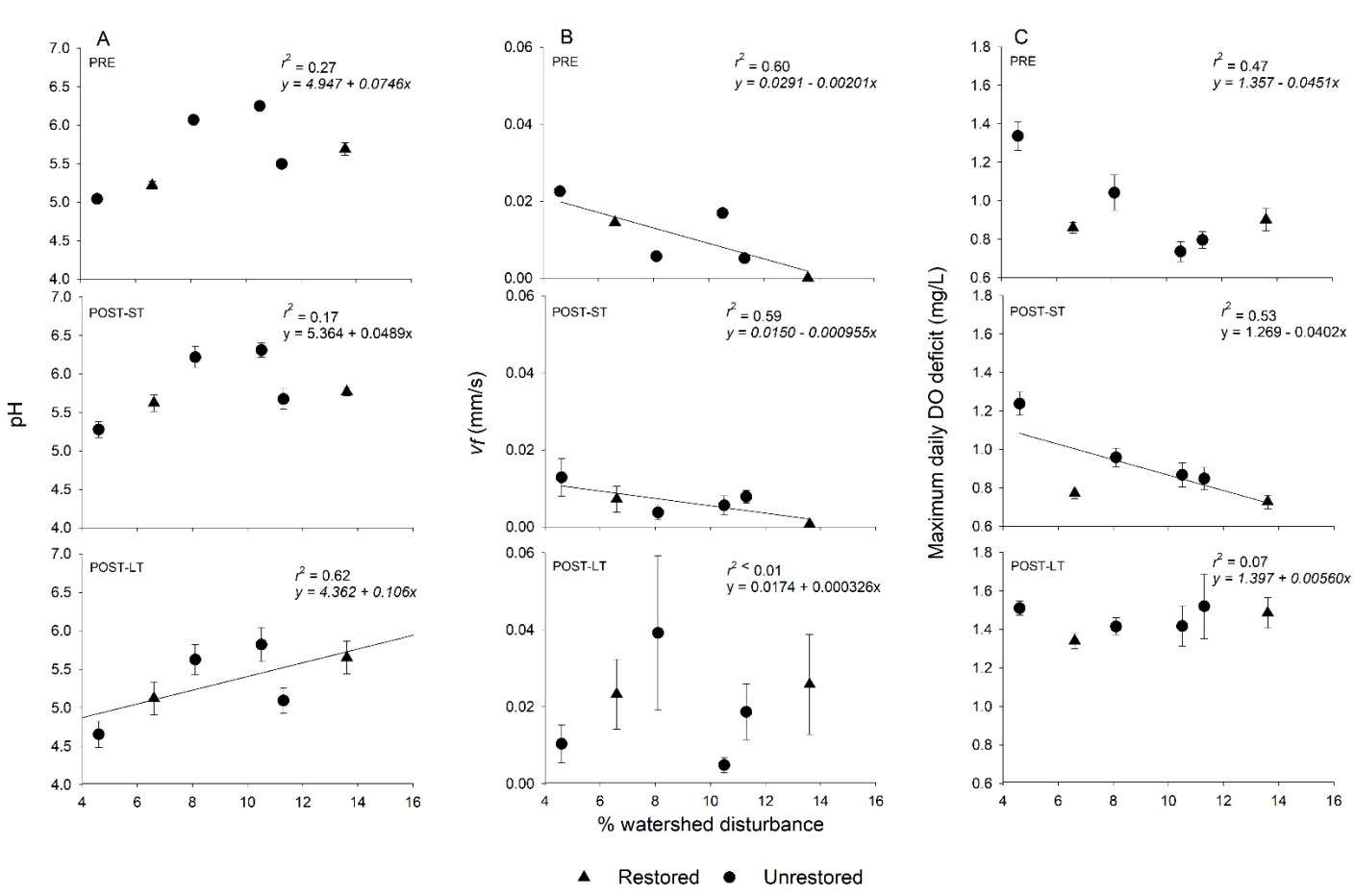

Figure 2-5. Relationships between mean (±SE) pH, ammonium uptake velocity (v_f; mm/s), and maximum daily dissolved oxygen (DO) deficit (mg/L) and % watershed disturbance across all seasons (only autumn data available for v_f and maximum daily DO deficit) in the pre-restoration (PRE; top row), 1- to 3-y post-restoration (POST-ST; middle row), and 14-y post-restoration (POST-LT; bottom row) periods for streams at Fort Benning Military Installation in Georgia, USA. Dashed line indicates positive or negative relationship based on $r^2 > 0.5$.

Chapter 3: Coastal watershed development alters tidal creek salinity and ecosystem metabolism.

Abstract

Much of the development along the northern Gulf of Mexico and many other coastal zones is characterized by the rapid spread of low- to moderate-density suburban land use that may lead to negative effects on coastal waters. One understudied urban impact is increased stormwater runoff to tidal creeks and potential shifts in salinity regime and ecosystem functions. To better understand these linkages, we installed sensors and data loggers in 12 second- and third-order tidal creeks across an urban gradient in Alabama and west Florida, USA, and measured salinity (n=12) and ecosystem metabolism (n=6) for over one year. We found that salinity flashiness (the average relative change per hourly measure, assessed using the Richard-Baker (RB)) index increased with watershed urban land cover and the related runoff curve number (CN). Based on a diel-oxygen approach, all six assessed tidal creeks were strongly heterotrophic throughout the study period and frequently experienced periods of low dissolved oxygen. Although direct associations between urban development and ecosystem metabolism were not detected, we noted that as seasonal RB-index values increased among sites, corresponding measures of gross primary production (GPP) and ecosystem respiration (ER) decreased. Our results suggest that urbanization, even at low- to moderate-levels, is leading to detectable shifts in salinity patterns and metabolic activity of tidal creeks. Because climate change is leading to both more intense storms and rising sea levels, further research is needed to understand how these new stressors will interact with increased salinity variation due to urbanization in tidal creeks.

Introduction

Coastal creeks and fringing salt marshes are important parts of estuaries and have been identified as valuable 'sentinel habitats' that exhibit the effects of disturbance before other ecosystems, and are increasingly vulnerable to degradation as urbanization increases in coastal areas (Wilson and Fischetti 2010, Xian et al. 2012). It is widely understood that urban land use can cause substantial changes in drainage patterns and receiving waters (Walsh et al. 2005). For instance, as watersheds become more urban, impervious surfaces divert more stormwater runoff to drainage systems and waterways (Dunne and Leopold 1978). This increased runoff can alter streams by increasing water yields, hydrologic energy, and stream channel erosion. Most of our understanding related to the urban stream syndrome is derived from inland, freshwater streams (Walsh et al. 2005). In coastal drainages, increased runoff may result in other changes such as increased frequency and magnitude of salinity fluctuations in tidal creeks (Lerberg et al. 2000, Holland et al. 2004, Sanger et al. 2008, Wedge and Anderson 2017). Variation in salinity due to hydrologic alteration can reduce submerged plant biomass due to physiological stress (Montague and Ley 1993). Thus, salinity fluctuation has been suggested as an indicator of hydrological alteration and may contribute to important shifts in aquatic habitat and ecological function (Lerberg et al. 2000, Holland et al. 2004). Increased runoff could also lead to greater benthic and water column primary production rates, an important measure of ecosystem function. Stormwater runoff is often a major source of freshwater and nutrient input to creeks, and even

smaller storms can greatly elevate nutrient concentrations and increase algae production (McDiffett et al. 1989, D. K. Borah et al. 2003, Walsh et al. 2005).

Ecosystem metabolism, as measured using the single-station diel oxygen change method (Odum 1956), is an integrative measure of gross primary production (GPP) and ecosystem respiration (ER) and can be an informative and reliable measure of ecosystem-level changes (Mulholland et al. 2007, Roberts et al. 2007, Young et al. 2008a, Flores et al. 2011a, Arango et al. 2015a, Bernhardt et al. 2018, Bickley et al. 2021). Ecosystem metabolism can also indicate the trophic status of an aquatic ecosystem and whether it is autotrophic (GPP:ER>1) or heterotrophic (GPP:ER<1) and can be expressed as net ecosystem metabolism (NEM), which is the flux of carbon into or out of an ecosystem. Changes in ecosystem trophic status can indicate changes in productivity and shifts in the basal food sources available for consumers. As dissolved oxygen (DO) sensors have become more affordable, estimations of ecosystem metabolism as a measure of ecosystem function have become more readily available.

The ecosystem metabolism of tidal creeks has not been widely studied, but some inferences from the more abundant freshwater literature can be drawn. For instance, allochthonous inputs of organic matter from a forested riparian zone and watershed are considered an important energy source fueling respiration in low-order streams which generally exhibit heterotrophic metabolic regimes (Mulholland et al. 2001, Roberts and Mulholland 2007, Bernot et al. 2010). While ER rates are generally greater than GPP rates in most stream systems (Mulholland et al. 2001), urbanized streams are often more autotrophic, as GPP rates often

increase with urbanization (Iwata et al. 2007, Bernot et al. 2010, Kaushal et al. 2014, Alberts et al. 2017). One reason for this increase in GPP is because the loss of riparian vegetation, common in urban streams, can lead to increased light availability and higher rates of primary production (Mulholland et al. 2001, Bernot et al. 2010, Alberts et al. 2017, Bernhardt et al. 2018, Reisinger et al. 2019). Additionally, increased nutrient inputs (Walsh et al. 2005b) can cause higher rates of GPP and ER in urban streams (Bernot et al. 2010, Alberts et al. 2017). Common sources of nutrients in stormwater include leaky septic tanks/sewer lines, pet waste, runoff from construction sites, excess fertilization, and atmospheric deposition (Bannerman et al. 1993, Carpenter et al. 1998, Hatt et al. 2004). In low-order tidal creeks with forested watersheds, it is likely that organic matter inputs may lead to a more heterotrophic metabolic regime. For example, tidal creeks draining extensive marsh meadows at National Estuarine Research Reserve sites were strongly heterotrophic, and ER was consistently higher than GPP, likely due to extensive organic matter inputs from the marsh itself (Caffrey 2004). This occurs even though tidal creeks are generally unshaded and receive ample sunlight. Moreover, as with freshwater streams, urbanization can result in reduced forest cover in the watershed and increased nutrient loading that may ultimately increase GPP and ER rates.

There is also evidence for potential interactions between salinity and aquatic ecosystem metabolism in estuaries and these interactions may be present in tidal creeks. For example, following the release of freshwater from a eutrophic reservoir into the Youngsan River Estuary in South Korea, salinity dropped from ~30 ppt to ~4 ppt, and there were short-term increases in algal biomass, diversity, community composition, as well as two blooms of red-tide dinoflagellates (Sin and Jeong 2015). As salinity decreases, brackish phytoplankton species can

show reduced growth while the composition of phytoplankton communities can shift from flagellates to other taxa, such as diatoms, green algae, and cyanobacteria that contribute to increased algal biomass (Lionard et al. 2005, Lehman 2007, Quinlan and Phlips 2007). Algae has also increasingly been recognized as a critical component to tidal creek and salt marsh food webs (Kreeger and Newell 2000). Because of the strong correlation between GPP and ER in estuarine systems, any increase in GPP following increased freshwater input will often result in increased ER (Caffrey 2004, Caffrey et al. 2014). It was shown that ER rates were highest in low-salinity areas across three Southeastern United States estuaries, possibly because increased freshwater inputs into estuaries may provide more allochthonous organic matter (Caffrey 2004, Caffrey et al. 2014). Therefore, understanding how land use contributes to possible changes in ecosystem metabolism should be considered when evaluating the effects of watershed urbanization on coastal landscapes.

The goal of this study was to quantify the relationship between salinity and ecosystem metabolism for low-order tidal creeks draining lands representing a gradient of urban development typical for the northern Gulf of Mexico (GOM) region. Using tidal creeks along the Alabama and West Florida, USA, coast, we predicted that the magnitude and frequency of salinity variation would increase with watershed urban cover. Further, we predicted increasing urban land use and associated nutrient and freshwater input would stimulate higher rates of GPP

and ER and this difference would be most pronounced following rain events and during seasons when stormwater input was highest.

Methods

Study sites

This study was conducted in 12 second- and third-order tidal creeks across the northern GOM (Fig. 3-1), with ecosystem metabolism analyzed at a subset of six sites (Table 3-1). Study sites were located near the outlet of each creek draining into a local bay. Sites were initially identified based on the presence of fringing salt marsh dominated by black needlerush (*Juncus roemerianus)* which was considered an indicator of a common salinity range amongst sites. Using the Venice salinity classification system (Reusser and Lee 2011), all of the sites were considered mesohaline (5-18 ppt) but they did experience oligohaline (0-5 ppt) and polyhaline (18-30 ppt) conditions during certain periods. Site selection was also based on creeks with watersheds ranging from primarily forested cover to highly urbanized (Table 3-1) and whether there was nearby boat ramp access. Six study creeks were located in the Wolf-Perdido Bay system in Alabama and west Florida (Fig. 3-1), where urban land cover within each watershed ranged from 0.0-17.6% (based on NLCD 2016) and watershed area ranged from 0.4-8.8 km^2 (Table 3-1). Six sites were in the Escambia-Pensacola-East Bay system in Florida (Fig. 3-1), where urban land cover within each watershed ranged from 8.2-87.5% (based on NLCD 2016) and watershed area ranged from 2.5-46.4 km^2 (Table 3-1). Urban land use within each watershed was typically dominated by low-intensity, suburban residential development (<10% developed). Along the creeks, other urban features commonly included structures like boat docks, piers, and

hardened shoreline structures like bulkheads and riprap. Texar Bayou, located within Pensacola, Florida is a substantially larger waterway that is heavily urbanized and drains a substantial portion of the city center. While Texar Bayou is outside the range of most of the low-intensity development seen along the northern GOM, it was included in the study to extend the urban gradient affecting tidal creeks in the region. Agricultural land cover was also common in the region, particularly within the Wolf-Perdido Bay system, where it ranged from 0.0-46.1% of watersheds (Table 3-1). The NRCS Curve Number (CN) values, which indicates the runoff generating potential of a landscape based on its hydrologic soil group, land cover, and hydrologic conditions (USDA 1986), ranged from 35.0 to 59.6 (Table 3-1).

Sensor deployment and data collection

For each site, water sensors with data loggers were installed within the creek near fringing salt marshes along the edge. In the summer of 2019, sensors were deployed including 1) HOBO U-24-002-C saltwater conductivity sensors (Onset Computer Corporation, Bourne, Massachusetts, USA) that automatically converted conductivity to salinity according to the practical salinity scale (Lewis and Perkin 1981), and also measured temperature and was used to correct DO measurements (see below), and 2) pressure transducers (In-Situ Inc., Fort Collins, Colorado, USA) to quantify water-level fluctuation (m) associated with tides. To measure DO (mg/l), PME miniDOT sensors (Precision Measurement Engineering, Vista, California, USA)

were installed at a subset of six sites extending across the urban gradient. All sensors were programmed to record measurements every 15 minutes.

The DO, salinity, and pressure transducer sensors were placed in a perforated PVC housing and attached to either a fence post driven into the creek bottom or a dock piling already present in the creek. Care was taken to place the sensors close to the surface but below the mean low-tide to ensure that sensors remained submerged most of the time. Sensors were cleaned and data were downloaded every 2 months during the study, with a longer 4-month gap between February 2020-June 2020 and June 2020-October 2020 due to COVID-19 pandemic travel restrictions and tropical storm activity. Sensors were removed from the water in October 2020.

Nutrient load and streamflow predictions

Resources were unavailable to sample and analyze nutrient and sediment concentrations and tidal creek discharge. Therefore, the Soil & Water Assessment Tool (SWAT) (Arnold et al., 1998) was used to estimate the nutrient loading and streamflow at each site. SWAT has been shown to be suitable for complicated geohydrologic conditions found in coastal watersheds (Wu and Xu, 2006; Wang and Kalin, 2011) and has been successfully applied in nearby coastal watersheds (R. Niraula et al. 2011, Wang and Kalin 2011, 2018, Wang et al. 2014, Singh et al. 2015). Model inputs included daily precipitation and min/max temperature, hydrography (USGS 2019), 10-meter DEM (USDA 2016), county-level SSURGO soil (Soil Survey Staff), 2016 land cover data (NLCD, Dewitz 2019). We delineated the watersheds draining to each site using ArcSWAT version 10.4 and divided the project area and study creeks into three discrete model

groups (WEST, MIDDLE, EAST) based on their proximity to each other (Fig. 3-1). For each group model run, study sites were represented by individual subwatershed outlets. Sites grouped in WEST were Graham Creek, Long Bayou, Stone Quarry, and Manuel Bayou. Sites grouped in MIDDLE were Heron Bayou, Bayou Grande, Weakley Bayou, and Texar Bayou. Sites grouped in EAST were Trout Bayou, Indian Bayou, Mulat Bayou, and Robinson Bayou. The SWAT models were run to produce daily measures of flow and nutrient (NO_3^-, NH_4^+, and mineralized P) loads between 2019-2020 using local precipitation and temperature data (PRISM Climate Group 2014). We used SWAT parameters that were previously calibrated and validated for previous work in the nearby Wolf Bay and Magnolia River watersheds of coastal Alabama (Wang and Kalin 2011). For analysis purposes, flow rates were divided by the corresponding watershed areas (m^3 sec^{-1} $m\text{-}^{2}$), and nutrient loads were converted to concentrations by dividing the loads by discharge. Our intention with using SWAT outputs was not to focus on absolute model estimates but to generate relative differences expected between sites based on differences in land use. Although SWAT predicted flows and nutrient loads were not validated due to lack of observed data, the availability of model parameters from previously calibrated SWAT models at nearby watersheds provided reasonable assurance for this study.

Salinity analysis

Before analyzing 15-minute salinity data, large, unexplainable decreases, and sudden increases in salinity between timesteps and other data anomalies in the time-series were removed. To quantify differences in the rate and magnitude of salinity change (i.e., flashiness), we calculated a flashiness index based on the Richard-Baker (RB) index (Baker et al. 2004b).

This modified RB-index was first used by Barksdale et al. (2014) and has since been used in other hydrological studies in the northern GOM (Wedge and Anderson 2017, Rezaeianzadeh et al. 2017). Briefly, the modified RB-index is a measure of the rate of change in salinity in proportion to overall salinity and was calculated as follows:

$$RB = \left(\frac{\sum_{i=1}^{n} |y_i - y_{i-1}|}{\sum_{i=0}^{n} y_i} \right) * 100$$

where y_i is the salinity at the 15-minute timestep i.

For each site, RB-index was calculated for the entire period of record (June 2019-October 2020) and seasonally (spring, summer, autumn, and winter). As a second measure of salinity variability, the amplitude of daily salinity was calculated for each creek as the difference between the highest and lowest salinity measurements in each day using the 15-minute salinity data series. Mean daily amplitude per creek was also calculated for the entire period of record and seasonally. Finally, salinity was averaged per day for each site and used to build 7-day moving average time-series and frequency (seven data points averaged on a daily time step) graphs for each creek during the study period.

Ecosystem metabolism model

For each creek, ecosystem metabolism was estimated using the single station diel-oxygen method (Odum 1956). In lotic, non-tidal systems, it is assumed that observed DO is uniform throughout the study reach, and that changes in DO are related to photosynthesis, respiration, and

gas exchange with the atmosphere. Contemporary stream metabolism models estimate metabolism and gas exchange with the atmosphere in non-tidal, lotic systems. Tidal advection (the movement of parcels of water past a single sensor due to diurnal tides) transports water parcels across various aquatic habitats, each with their own metabolic regimes and DO dynamics (Kemp and Boynton 1980, Caffrey 2003). In tidally influenced systems, the effects of tidal advection potentially outweigh the biological processes that drive DO dynamics, which would violate the assumption that DO is uniform within a reach, and may lead to anomalous estimates of daily metabolism (Odum 1956, Caffrey 2003, Collins et al. 2013).

We used the WtRegDO R package (Beck 2016) to model rates of GPP and ER. We measured DO (mg/l) temperature (°C), and water level (m) at 15-minute time steps. Measured water level (m) was used to convert volumetric DO concentrations to areal rates of (m^2) ecosystem metabolism. Changes in DO dynamics driven by the biological processes of metabolism are largely influenced by solar cycles, and when solar and tidal cycles are correlated, the model may not be able to differentiate between the effects of physical and biological processes and may lead to biased estimates of metabolism (Beck 2016). If needed, the WtRegDO package can use a weighted regression to filter the DO profile and remove tidal influence. However, correlation analysis found that water level and DO at each site were uncorrelated, which indicate that the effects of tidal advection on DO dynamics were minimal (personal

communication, M. Beck, Tampa Bay Estuary Program) and weighted regression was not needed to tidally filter the DO data.

Salinity sensor malfunctions and other issues resulted in some missing salinity data at each site, ranging from 6.7% of the data at Manuel Bayou to 66.7% of the data at Indian Bayou. This resulted in a minimum of 16 days of data at Indian Bayou during winter (2020) and a maximum of 184 days of data at Mulat Bayou during summer (2019 and 2020). Because WtRegDO uses salinity to calculate DO saturation in saline waters, gaps in salinity were filled by direct substitution using the salinity data from the next closest site. Data analysis revealed that DO saturation calculations differed by only 2.8% within a 5-ppt range, suggesting that filling gaps in salinity data resulted in negligible differences in DO saturation calculations. Periods of anomalous DO observations (large, unexplainable jumps in DO between timesteps) were removed from Long Bayou, Manuel Bayou, and Weakley Bayou, likely a result of both biofouling and sediment partially filling the PVC housing between site visits.

Statistical Analyses

We used simple linear regressions to test the effect of watershed urban land cover (%) and runoff CN on salinity RB-index and mean daily amplitude. We assessed the normality of the model variables using probability plots and Anderson-Darling normality tests using Minitab Statistical Software v. 20.3 (“Minitab 17 Statistical Software” 2022). RB-index was log10 transformed to meet linear regression assumptions of normality and mean daily amplitude was untransformed, and both were averaged across the entire study period for each site. Texar Bayou

was considered an outlier in watershed size and urban land cover (Table 3-1) and omitted from linear regression analysis.

To address gaps within our DO dataset and potential lag in responses, we averaged ecosystem metabolism metrics (GPP and ER) by season (summer 2019 and 2020, autumn 2019 and 2020, winter 2019, and spring 2020) for each site. We used a stepwise linear regression process to examine drivers of seasonal ecosystem metabolism across tidal creeks. Response variables were seasonal averages of GPP, ER, and NEM (the difference between GPP and ER). To meet linear regression assumptions of normality, non-normally distributed covariates were log10 transformed (Table 3-2). Predictor variables were seasonally averaged measures and included log10 transformed RB-index of salinity, salinity amplitude, SWAT-derived flow, SWAT-derived nutrient concentrations (NO_3^-, NH_4^+, and mineralized P) and untransformed mean salinity and water temperature (Table 3-2). Because of the small sample size, we used corrected AIC (AIC_c; see Read et al. 2018) to compare linear regression models. We assessed the normality of model variables using probability plots and Anderson-Darling normality tests using Minitab Statistical Software v. 20.3 ("Minitab 17 Statistical Software" 2022). We also used

simple linear regression to examine for potential relationships between seasonal RB-index and temperature on seasonal averages of GPP, ER, and NEM.

Results

Salinity

Mean daily salinity across all 12 sites ranged from 5.5 ± 0.2 ppt (Heron Bayou) to 14.1 ± 0.1 ppt (Stone Quarry Bayou) and fluctuated seasonally throughout the study period (Fig. 3-2). Time series analyses indicated that some sites had greater salinity variability following rain events (> 1 cm precipitation) than other sites, and this was reflected in their RB-index scores. For example, following a rain event, runoff caused water column salinity to decrease more rapidly at Mulat Bayou (mean RB-index: 1.90) compared to Trout Bayou (mean RB-index: 0.40) (Fig. 3-3). Salinity variability based on RB-index varied across all twelve sites and ranged from 0.20 (Stone Quarry Bayou) to 1.90 (Mulat Bayou) throughout the study period (Table 3-3). There was a positive relationship between RB-index and watershed CN ($p = 0.04$, $r^2 = 0.39$) and percent urban cover within tidal creek watersheds ($p = 0.05$, $r^2 = 0.36$) (Fig. 3-4). There was also a range in mean daily salinity amplitude across sites ranging from 0.94 ± 0.04 ppt (Stone Quarry Bayou) to 3.53 ± 0.18 ppt (Bayou Grande) (Table 3-3). There was a weaker positive relationship between mean daily amplitude and watershed CN ($p = 0.23$, $r^2 = 0.15$) and percent urban cover ($p = 0.14$, $r^2 = 0.22$). There was a positive relationship between average salinity amplitude and RB-index among sites ($p < 0.01$, $r^2 = 0.63$).

Mean daily salinity was highest in autumn and lowest in winter, and the range of salinity was most variable across sites during spring (Fig. 3-5). Mulat Bayou experienced lower mean

daily salinity across most seasons, while Long Bayou experienced higher mean daily salinities (Fig. 3-5). Mean daily water temperature was highest in summer and lowest in winter, and values during each season were similar across sites, except for Long Bayou where temperatures were higher (Fig. 3-6).

Temporal and spatial patterns in ecosystem metabolism

Average seasonal rates of GPP ranged from 318 to 92 mmol O_2 $m^{-2}d^{-1}$, -188 to -844 mmol O_2 $m^{-2}d^{-1}$ for ER, and from -96 to -632 mmol O_2 $m^{-2}d^{-1}$ for NEM. Ecosystem metabolism at the six study creeks exhibited strong seasonal trends. Mean seasonal GPP and ER across all sites were highest (more negative for ER) during spring and summer, and lowest (less negative for ER) during winter and autumn (Table 3-4 and Fig. 3-3-7). All sites were net-heterotrophic across all seasons, with NEM rates being highest in spring and autumn, and lowest at all sites except for Weakley Bayou during winter (Table 3-2- 4). GPP was highest at Manuel Bayou (318 mmol O_2 $m^{-2}d^{-1}$ ± 30) and Long Bayou (306 mmol O_2 $m^{-2}d^{-1}$ ± 22) during spring, and lowest at Texar Bayou (92 mmol O_2 $m^{-2}d^{-1}$ ± 8) during winter and Long Bayou (105 mmol O_2 $m^{-2}d^{-1}$ ± 6) during autumn. ER was highest at Manuel Bayou during the spring (844 mmol

O_2 $m^{-2}d^{-1}$ ± 73) and autumn (831 mmol O_2 $m^{-2}d^{-1}$ ± 103), and lowest at Texar Bayou (188 mmol O_2 $m^{-2}d^{-1}$ ± 11) during winter.

Drivers controlling tidal creek ecosystem metabolism

NEM rates were most strongly controlled by a combination of salinity RB-index, mean salinity, and NH_4^+ concentrations (Table 3-2- 5). Linear regression analysis showed a weak negative relationship between GPP and RB-index, but a stronger positive relationship between GPP and temperature (Fig. 3-8). Similarly, there was a negative relationship between ER and both RB-index and temperature (Fig. 3-8).

Discussion

Salinity

In this study, we quantified variation in the salinity regimes of 12 *Juncus*-dominated tidal creeks and ecosystem metabolism at a subset of six *Juncus*-dominated tidal creeks along the northern GOM. As predicted, we found that greater watershed urban development was associated with an increase in the magnitude and frequency of occurrence of salinity fluctuations. This effect was apparent even at the relatively low levels (<10% developed) of watershed development typical of this part of the northern GOM. It has been suggested that the hydrological response in streams to low-density urban land use may be less sensitive in a Coastal Plain watershed because of lower topographical relief and sandier soils (Utz et al. 2011). However, our results suggest that even low levels of development increased stormwater flow and

influenced salinity regimes in these tidal creeks. Others working in this part of the northern GOM have also detected hydrologic, biological, and chemical responses at relatively low urban development. Schneid et al. (2017) found benthic macroinvertebrates and various water quality metrics in non-tidal streams responded to low-level urbanization (1.5 – 10.9% impervious surface cover) within the same area as our study. Likewise, Nagy et al. (2011) detected a positive response in various chemical and hydrologic measures within non-tidal coastal streams draining low-intensity urban lands (0-15% impervious surface cover) in nearby Apalachicola, FL. Collectively, these results suggest that even at the lowest levels of urbanization, detectable alterations to receiving creeks are likely in these low-gradient systems.

Although few studies have measured salinity across an urban gradient, salinity variability has still been identified as a potential disturbance factor in estuarine systems. For example, in tidal creeks along the South Carolina, USA coast, the abundance of pollution-sensitive marine worms decreased when the observed range of salinity and proportion of impervious surfaces in the watershed increased (Lerberg et al. 2000). Similarly, the standard deviation of measured salinity was negatively correlated with seagrass biomass, number of seagrass species present, and macroinvertebrate density in a managed canal system in Florida Bay, USA (Montague and Ley 1993). In larger embayments along the Texas, USA coast, salinity variability was highest in the upper reaches, and lowest near the ocean, and this was negatively correlated with benthic infauna diversity (Van Diggelen and Montagna 2016). The longitudinal pattern of decreasing salinity variation found by Van Diggelen and Montagna (2016) suggests that first-order tidal creeks likely experience greater salinity variation in response to freshwater inflows. In our study, RB-index was responsive to percent urban land cover and watershed CN, and predicted ecosystem

metabolism. Our results, when combined with previous work in the same region (Wedge and Anderson 2017), suggest that not only is RB-index a useful measure of salinity variability, but it is also a potential predictor of biological changes in the water column.

We found that mean salinity was highest in autumn compared to spring and winter due to higher watershed evapotranspiration (ET) and low autumn precipitation (Fig. 3-9) which led to decreased freshwater inflows. The observed seasonal differences in mean daily salinity is not surprising, given that the highest salinities in two northern GOM bays (Weeks Bay and Apalachicola Bay) were observed during autumn (Caffrey et al. 2014), suggesting that salinity in coastal waters in this region is heavily influenced by freshwater inflows. We also detected seasonal patterns in salinity variation as RB-index measures were highest during the winter when precipitation events were more common (Fig. 3-9), which likely increased freshwater runoff in tidal creeks. In addition to increasing urbanization, greater precipitation, and more severe storms associated with climate change in the Southeastern United States is projected (Sinha et al. 2017, Armal et al. 2018), which may further increase the magnitude and frequency of occurrence of salinity variation in coastal waters along the northern GOM.

Temporal and spatial patterns in ecosystem metabolism

Ecosystem metabolism rates exhibited seasonal trends, with GPP and ER rates being highest in the spring and summer and decreasing in the autumn and winter. Both GPP and ER had a positive relationship with temperature, which explains much of the observed seasonality. Observed GPP and ER rates and seasonal trends were similar to those observed in nearby

Magnolia River, a third-order mesohaline tidal creek that drains into Weeks Bay, Alabama (Mortazavi et al. 2012). A strong relationship between GPP and nitrogen load has been observed in other estuaries within the GOM region (Caffrey et al. 2014), and seasonality of water column nutrient concentrations in the Magnolia River was also observed, with both NO_3^- and NH_4^+ concentrations peaking in early spring (Mortazavi et al. 2012). Similarly, our SWAT model estimated nutrient loads were highest during spring (Table 3-6), likely coinciding with maximum flows and fertilizer application to agricultural lands, and potentially stimulating higher GPP and ER rates during spring. This trend was most apparent at Manuel Bayou, which had the largest proportion of its watershed as agriculture, and consistently had the highest rates of ER across all seasons.

To our knowledge, ecosystem metabolism has not been previously estimated in tidal creek ecosystems like those in our study. However, because tidal creeks occur at the interface of both estuaries and freshwater streams, and because estimates of freshwater metabolism rates are widespread (Mulholland et al. 2001, Hall and Beaulieu 2013, Bernhardt et al. 2018, Appling et al. 2018, Reisinger et al. 2019, Bickley et al. 2021), some comparisons contextualizing our results with freshwater ecosystem metabolism can be made. For example, across 365 freshwater rivers and streams in the United States, mean summer (June-August) GPP was 114 mmol O_2 $m^{-2}d^{-1}$ and mean summer ER was -182 mmol O_2 $m^{-2}d^{-1}$ (Appling et al. 2018), while across our study sites the mean summer GPP was 248 mmol O_2 $m^{-2}d^{-1}$, and mean summer ER was -640 mmol O_2 $m^{-2}d^{-1}$. Compared to freshwater streams, tidal creeks receive inputs of organic matter from upstream, lateral inputs from fringing salt marshes, and inputs with tidal inundation (Middelburg and Herman 2007), potentially fueling higher rates of ecosystem respiration. Tidal

creeks also lack a tree canopy that could shade the water column and reduce rates of gross primary production (Hill et al. 1995). The high rates of both GPP and ER at our sites compared to the mean values of freshwater rivers and streams in the United States is not surprising given these differences in physical characteristics between these two types of aquatic ecosystems.

Factors controlling ecosystem metabolism

We found that temperature, mean salinity, salinity RB-index, and NH_4^+ concentrations were the most important factors predicting ecosystem metabolism in our tidal creeks. Because these parameters are often responsive to urbanization, this suggests that ecosystem metabolism may also be influenced by landscape alteration. It is important to consider how ecosystem metabolism may respond to changes in the landscape because the processes of GPP and ER are crucial to providing the energy needed for aquatic food webs (Rosenfeld and Mackay 1987, Marcarelli et al. 2011, Welti et al. 2017) and any changes in these ecosystem functions could result in structural changes to the ecosystem (Ziegler et al. 2021). Further, by understanding the factors that control these functions currently, we may be better able to predict how these sentinel ecosystems will continue to respond to climate change and land use change in the future (Bernhardt et al. 2018). Ecosystem metabolism in both freshwater lakes and streams has been shown to be responsive to changes in the watershed (Houser et al. 2005, Young et al. 2008a, Blaszczak et al. 2019, Bickley et al. 2021). Our findings add mesohaline tidal creeks to that list,

suggesting that ecosystem metabolism is an informative parameter to measure in studies examining the effects of human disturbance and restoration.

All six sites were strongly heterotrophic (ER>GPP) during all seasons and likely rely on inputs of organic matter to fuel ecosystem processes. It is not surprising that these systems were net heterotrophic, as tidal creeks receive inputs of allochthonous organic matter locally from the fringing marsh surface, upland discharge, and tidal inundation (Fagherazzi et al. 2013). Large storm events may be particularly important for moving allochthonous C to tidal creeks and storms have also been shown to provide subsidies of organic matter to salt marshes (Turner et al. 2006). Our study region experienced five large tropical storms during the study period, and while sensor failure resulted in data not being available for all sites following these events, rates of ER increased notably following storm-surges, with no comparatively large increase in GPP (personal observation). The periodic delivery of organic matter to tidal creeks following large storm events likely supplements carbon stocks in tidal creeks to fuel ER throughout the year, providing an important transfer of energy to different trophic levels in adjacent coastal waters (Deegan et al. 2002).

The GPP range during the spring and summer seasons at all six sites was between 179 - 317 mmol O_2 $m^{-2}d^{-1}$, which is similar to the range (130-400 mmol O_2 $m^{-2}d^{-1}$) of summer rates observed in nearby Weeks Bay, AL, Apalachicola Bay, FL, and Grand Bay, MS (Caffrey et al., 2014). Additionally, our highest observed seasonal GPP rate (317 mmol O_2 $m^{-2}d^{-1}$) was slightly higher than the highest monthly GPP rate observed in the nearby Magnolia River of 259 mmol

O_2 $m^{-2}d^{-1}$ (Mortazavi et al. 2012). Seasonal measures of GPP were comparable to rates measured at other estuarine sites along the GOM and the Caribbean, but lower than sites along the Atlantic seaboard (Caffrey et al. 2014). We found that temperature was the strongest factor controlling GPP across all six sites, and GPP increased with temperature. This is similar to other estuaries across the USA, and particularly in the southeast, where temperature also is an important predictor of GPP (Caffrey 2004). While temperature is an important factor in controlling GPP across most ecosystems (Mulholland et al. 2001), it may be particularly important in warmer, temperate, and sub-tropical waters.

ER rates were highest at Manuel Bayou across all seasons, with the biggest seasonal difference in winter and autumn. GPP rates across all sites were within a similar range during spring, summer, and autumn, but variation was more apparent during winter, suggesting that factors besides temperature were important controls on ecosystem metabolism rates. Manuel Bayou saw the highest total N concentrations during winter, likely stimulating higher ER and GPP during that season. Weakley Bayou also exhibited higher rates of ER and NEM during winter compared to other sites and experienced the highest flow rate per area during this season. Flow was an important factor in all but the highest-ranked NEM stepwise regression models. Thus, increased flow rates and associated N export during the winter months are likely the cause of increased ER and NEM in the winter. Watershed runoff and nutrient loading are intrinsically

linked to land cover characteristics within a watershed (Nagy et al. 2011a, 2011b), and these effects may be most pronounced during winter in our six tidal creeks.

Texar Bayou, the most urbanized watershed in our study, had both lower ecosystem metabolism rates and lower RB-index values than expected, and was an outlier that was not included in regression models. Texar Bayou is located near downtown Pensacola, Florida (Fig. 3-1) and likely benefits from more city-wide stormwater infrastructure, such as retention ponds. These features have been shown to ameliorate the negative effects of runoff (Walsh et al. 2005a, Prudencio and Null 2018). Heavy siltation in Texar Bayou due to historic commercial and residential development within the watershed and reduced tidal flushing due to the constriction of the bayou outlet following the construction of a railroad trestle in the late 19th century (Liebens et al. 2006) may lead to increased turbidity, which reduces light availability and subsequently GPP (Murrell et al. 2007, 2018, Mangan et al. 2020). These additional factors highlight that highly urbanized tidal creeks like Texar Bayou are likely subjected to multiple environmental stressors, and it may be difficult to attribute measures of ecosystem function to a small suite of variables.

Conclusion

We examined the effect of development on salinity regime and ecosystem metabolism rates in tidal creek ecosystems in Alabama and West Florida, USA. We found that the RB-index, a measure of salinity variation, increased with watershed development. Tidal creeks in our study were strongly heterotrophic throughout the year, and salinity, the RB-index, temperature, and

NH_4^+ concentrations were major drivers of ecosystem metabolism rates. To our knowledge, this is the first study to measure ecosystem metabolism in small tidal creeks along the northern GOM, and therefore it is hard to contextualize our values, however, our results are within the range of data collected in nearby estuaries (Caffrey et al. 2014) and greater than from larger, freshwater rivers (Appling et al. 2018).

Tidal creek ecosystems have been recognized as "sentinel habitats" (Sanger et al. 2015), which present the effects of disturbance before other ecosystems, so increased long-term monitoring of these systems is needed to further understand how they will respond to future disturbances. We found that relatively low levels of watershed development can lead to changes in the salinity regime, thereby decreasing ecosystem metabolism rates. Understanding how these processes respond to even relatively low levels of development is important for scientists and resource managers to better assess how these systems will continue to respond to climate change. Increased precipitation is likely to lead to greater freshwater runoff and increased salinity variation in tidal creeks while rising sea levels are likely to increase baseline salinity. Future research that examines how these environmental changes interact will be needed to ensure that ecosystem function is maintained in a changing world.

Literature Cited

Alberts, J. M., J. J. Beaulieu, and I. Buffam. 2017. Watershed Land Use and Seasonal Variation Constrain the Influence of Riparian Canopy Cover on Stream Ecosystem Metabolism. Ecosystems 20:553–567.

Appling, A. P., J. S. Read, L. A. Winslow, M. Arroita, E. S. Bernhardt, N. A. Griffiths, R. O. Hall, J. W. Harvey, J. B. Heffernan, E. H. Stanley, E. G. Stets, and C. B. Yackulic. 2018. The metabolic regimes of 356 rivers in the United States. Scientific Data 5:180292.

Arango, C. P., P. W. James, and K. B. Hatch. 2015. Rapid ecosystem response to restoration in an urban stream. Hydrobiologia 749:197–211.

Armal, S., N. Devineni, and R. Khanbilvardi. 2018. Trends in Extreme Rainfall Frequency in the Contiguous United States: Attribution to Climate Change and Climate Variability Modes. Journal of Climate 31:369–385.

Baker, D. B., R. P. Richards, T. T. Loftus, and J. W. Kramer. 2004. A new flashiness index: characteristics and applications to midwestern rivers and streams. Journal of the American Water Resources Association 40:503–522.

Bannerman, R. T., D. W. Owens, R. B. Dodds, and N. J. Hornewer. 1993. Sources of pollutants in Wisconsin stormwater. Water Science and Technology 28:241–259.

Barksdale, W. F., C. J. Anderson, and L. Kalin. 2014. The influence of watershed run-off on the hydrology, forest floor litter and soil carbon of headwater wetlands. Ecohydrology 7:803–814.

Beck, M. W. 2016. SWMPr: An R Package for Retrieving, Organizing, and Analyzing Environmental Data for Estuaries. The R Journal 8:14.

Bernhardt, E. S., J. B. Heffernan, N. B. Grimm, E. H. Stanley, J. W. Harvey, M. Arroita, A. P. Appling, M. J. Cohen, W. H. McDowell, R. O. Hall, J. S. Read, B. J. Roberts, E. G. Stets, and C. B. Yackulic. 2018. The metabolic regimes of flowing waters. Limnology and Oceanography 63:S99–S118.

Bernot, M. J., D. J. Sobota, R. O. Hall, P. J. Mulholland, W. K. Dodds, J. R. Webster, J. L. Tank, L. R. Ashkenas, L. W. Cooper, C. N. Dahm, S. V. Gregory, N. B. Grimm, S. K. Hamilton, S. L. Johnson, W. H. McDowell, J. L. Meyer, B. Peterson, G. C. Poole, H. M. Maurice Valett, C. Arango, J. J. Beaulieu, A. J. Burgin, C. Crenshaw, A. M. Helton, L. Johnson, J. Merriam, B. R. Niederlehner, J. M. O'Brien, J. D. Potter, R. W. Sheibley, S. M. Thomas, and K. Wilson. 2010. Inter-regional comparison of land-use effects on stream metabolism. Freshwater Biology 55:1874–1890.

Bickley, S. L., B. S. Helms, D. Isenberg, J. W. Feminella, B. J. Roberts, and N. A. Griffiths. 2021. Lack of long-term effect of coarse woody debris dam restoration on ecosystem functioning and water quality in Coastal Plain streams. Freshwater Science 40:593–607.

Blaszczak, J. R., J. M. Delesantro, D. L. Urban, M. W. Doyle, and E. S. Bernhardt. 2019. Scoured or suffocated: Urban stream ecosystems oscillate between hydrologic and dissolved oxygen extremes. Limnology and Oceanography 64:877–894.

Caffrey, J. M. 2003. Production, respiration and net ecosystem metabolism in U.S. estuaries. Environmental monitoring and assessment 81:207–19.

Caffrey, J. M. 2004. Factors Controlling Net Ecosystem Metabolism in U. S. Estuaries. Estuaries 27:90–101.

Caffrey, J. M., M. C. Murrell, K. S. Amacker, J. W. Harper, S. Phipps, and M. S. Woodrey. 2014. Seasonal and Inter-annual Patterns in Primary Production, Respiration, and Net

Ecosystem Metabolism in Three Estuaries in the Northeast Gulf of Mexico. Estuaries and Coasts 37:222–241.
Carpenter, S. R., N. F. Caraco, D. L. Correll, R. W. Howarth, A. N. Sharpley, and V. H. Smith. 1998. Carpenter_et_al-1998-Ecological_Applications. Ecology 8:559–568.
Collins, J. R., P. A. Raymond, W. F. Bohlen, and M. M. Howard-Strobel. 2013. Estimates of New and Total Productivity in Central Long Island Sound from In Situ Measurements of Nitrate and Dissolved Oxygen. Estuaries and Coasts 36:74–97.
Deegan, L. A., J. E. Hughes, and R. A. Rountree. 2002. Salt Marsh Ecosystem Support of Marine Transient Species. Pages 333–365 *in* M. P. Weinstein and D. A. Kreeger (editors). Concepts and Controversies in Tidal Marsh Ecology. Kluwer Academic Publishers, Dordrecht.
Dewitz, J. 2019. National Land Cover Database (NLCD) 2016 Products (ver. 2.0, July 2020). United States Geological Survey.
Fagherazzi, S., P. L. Wiberg, S. Temmerman, E. Struyf, Y. Zhao, and P. A. Raymond. 2013. Fluxes of water, sediments, and biogeochemical compounds in salt marshes. Ecological Processes 2:3.
Flores, L., A. Larrañaga, J. Díez, and A. Elosegi. 2011. Experimental wood addition in streams: Effects on organic matter storage and breakdown. Freshwater Biology 56:2156–2167.
Hall, R. O., and J. J. Beaulieu. 2013. Estimating autotrophic respiration in streams using daily metabolism data. Freshwater Science 32:507–516.
Hatt, B. E., T. D. Fletcher, C. J. Walsh, and S. L. Taylor. 2004. The influence of urban density and drainage infrastructure on the concentrations and loads of pollutants in small streams. Environmental Management 34:112–124.
Holland, A. F., D. M. Sanger, C. P. Gawle, S. B. Lerberg, M. S. Santiago, G. H. M. Riekerk, L. E. Zimmerman, and G. I. Scott. 2004. Linkages between tidal creek ecosystems and the landscape and demographic attributes of their watersheds. Journal of Experimental Marine Biology and Ecology 298:151–178.
Houser, J. N., P. J. Mulholland, and K. O. Maloney. 2005. Catchment disturbance and stream metabolism: Patterns in ecosystem respiration and gross primary production along a gradient of upland soil and vegetation disturbance. 24:15.
Kemp, W. M., and W. R. Boynton. 1980. Influence of biological and physical processes on dissolved oxygen dynamics in an estuarine system: Implications for measurement of community metabolism. Estuarine and Coastal Marine Science 11:407–431.
Lehman, P. W. 2007. The influence of phytoplankton community composition on primary productivity along the riverine to freshwater tidal continuum in the San Joaquin River , California The Influence of Phytoplankton Community Composition on Primary Productivity along the Rive. 30:82–93.
Lerberg, S. B., A. F. Holland, and D. M. Sanger. 2000. Responses of tidal creek macrobenthic communities to the effects of watershed development. Estuaries 23:838–853.
Liebens, J., C. J. Mohrherr, K. R. Rao, and C. A. Houser. 2006. Pollution in an Urban Bayou: Magnitude, Spatial Distribution and Origin. Water, Air, and Soil Pollution 174:235–263.
Lionard, M., K. Muylaert, D. Van Gansbeke, and W. Vyverman. 2005. Influence of changes in salinity and light intensity on growth of phytoplankton communities from the Schelde river and estuary (Belgium/The Netherlands). Hydrobiologia 540:105–115.

Mangan, S., A. M. Lohrer, S. F. Thrush, and C. A. Pilditch. 2020. Water Column Turbidity Not Sediment Nutrient Enrichment Moderates Microphytobenthic Primary Production. Journal of Marine Science and Engineering 8:732.

Marcarelli, A. M., C. V. Baxter, M. M. Mineau, and R. O. Hall. 2011. Quantity and quality: Unifying food web and ecosystem perspectives on the role of resource subsidies in freshwaters. Ecology 92:1215–1225.

Minitab 17 Statistical Software. 2022. Minitab, Inc.

Montague, C. L., and J. A. Ley. 1993. A Possible Effect of Salinity Fluctuation on Abundance of Benthic Vegetation and Associated Fauna in Northeastern Florida Bay. Estuaries 16:703–717.

Mortazavi, B., A. A. Riggs, J. M. Caffrey, H. Genet, and S. W. Phipps. 2012. The Contribution of Benthic Nutrient Regeneration to Primary Production in a Shallow Eutrophic Estuary, Weeks Bay, Alabama. Estuaries and Coasts 35:862–877.

Mulholland, P. J., C. S. Fellows, J. L. Tank, N. B. Grimm, J. R. Webster, S. K. Hamilton, E. Martí, L. Ashkenas, W. B. Bowden, W. K. Dodds, W. H. Mcdowell, M. J. Paul, and B. J. Peterson. 2001. Inter-biome comparison of factors controlling stream metabolism. Freshwater Biology 46:1503–1517.

Mulholland, P. J., J. W. Feminella, B. G. Lockaby, and G. L. Hollon. 2007. Riparian ecosystem management at military installations: Determination of impacts and evaluation of restoration and enhancement strategies. Final Technical Report SI-1186. Alexandria, Virginia.

Murrell, M. C., J. M. Caffrey, D. T. Marcovich, M. W. Beck, B. M. Jarvis, and J. D. Hagy. 2018. Seasonal Oxygen Dynamics in a Warm Temperate Estuary: Effects of Hydrologic Variability on Measurements of Primary Production, Respiration, and Net Metabolism. Estuaries and Coasts 41:690–707.

Murrell, M. C., J. D. Hagy, E. M. Lores, and R. M. Greene. 2007. Phytoplankton production and nutrient distributions in a subtropical estuary: Importance of freshwater flow. Estuaries and Coasts 30:390–402.

Nagy, R. C., B. G. Lockaby, B. Helms, L. Kalin, and D. Stoeckel. 2011a. Water Resources and Land Use and Cover in a Humid Region: The Southeastern United States. Journal of Environmental Quality 40:867–878.

Nagy, R. C., B. G. Lockaby, L. Kalin, and C. Anderson. 2011b. Effects of urbanization on stream hydrology and water quality: The Florida Gulf Coast: URBANIZATION EFFECTS ON WATER RESOURCES. Hydrological Processes 26:2019–2030.

Odum, H. T. 1956. Primary Production in Flowing Waters1. Limnology and Oceanography 1:102–117.

PRISM Climate Group. 2014, February 4. Oregon State University. (Available from: https://prism.oregonstate.edu)

Prudencio, L., and S. E. Null. 2018. Stormwater management and ecosystem services: A review. Environmental Research Letters 13:033002.

Quinlan, E. L., and E. J. Phlips. 2007. Phytoplankton assemblages across the marine to low-salinity transition zone in a blackwater dominated estuary. Journal of Plankton Research 29:401–416.

R. Niraula, L. Kalin, R. Wang, and P. Srivastava. 2011. Determining Nutrient and Sediment Critical Source Areas with SWAT: Effect of Lumped Calibration. Transactions of the ASABE 55:137–147.

Reisinger, A. J., T. R. Doody, P. M. Groffman, S. S. Kaushal, and E. J. Rosi. 2019. Seeing the light: Urban stream restoration affects stream metabolism and nitrate uptake via changes in canopy cover. Ecological Applications 29:e01941.

Rezaeianzadeh, M., L. Kalin, and C. J. Anderson. 2017. Wetland Water-Level Prediction Using ANN in Conjunction with Base-Flow Recession Analysis. Journal of Hydrologic Engineering 22:D4015003.

Roberts, B. J., and P. J. Mulholland. 2007. In-stream biotic control on nutrient biogeochemistry in a forested stream, West Fork of Walker Branch. Journal of Geophysical Research: Biogeosciences 112:1–11.

Roberts, B. J., P. J. Mulholland, and J. N. Houser. 2007. Effects of upland disturbance and instream restoration on hydrodynamics and ammonium uptake in headwater streams. Journal of the North American Benthological Society 26:38–53.

Rosenfeld, J. S., and R. J. Mackay. 1987. Assessing the Food Base of Stream Ecosystems: Alternatives to the P/R Ratio. Oikos 50:141.

Sanger, D., A. Blair, G. DiDonato, T. Washburn, S. Jones, R. Chapman, D. Bergquist, G. Riekerk, E. Wirth, J. Stewart, D. White, L. Vandiver, S. White, and D. Whitall. 2008. Support for Integrated Ecosystem Assessments of NOAA's National Estuarine Research Reserves System (NERRS), Volume One. The Impacts of Coastal Development on the Ecology and Human Well-Being of Tidal Creek Ecosystems of the U.S. Southeast. NOAA Technical Memorandum I:88.

Sanger, D., A. Blair, G. DiDonato, T. Washburn, S. Jones, G. Riekerk, E. Wirth, J. Stewart, D. White, L. Vandiver, and A. F. Holland. 2015. Impacts of Coastal Development on the Ecology of Tidal Creek Ecosystems of the US Southeast Including Consequences to Humans. Estuaries and Coasts 38:49–66.

Schneid, B. P., C. J. Anderson, and J. W. Feminella. 2017. The influence of low-intensity watershed development on the hydrology, geomorphology, physicochemistry and macroinvertebrate diversity of small coastal plains streams. Ecological Engineering 108:380–390.

Sin, Y., and B. Jeong. 2015. Short-term variations of phytoplankton communities in response to anthropogenic stressors in a highly altered temperate estuary. Estuarine, Coastal and Shelf Science 156:83–91.

Singh, H. V., L. Kalin, A. Morrison, P. Srivastava, G. Lockaby, and S. Pan. 2015. Post-validation of SWAT model in a coastal watershed for predicting land use/cover change impacts. Hydrology Research 46:837–853.

Sinha, E., A. M. Michalak, and V. Balaji. 2017. Eutrophication will increase during the 21st century as a result of precipitation changes. Science 357:405–408.

Soil Survey Staff. Web Soil Survey. Soil Survey Geographic (SSURGO) Database for Baldwin County, Alabama, and Escambia County and Santa Rosa County, Florida. (Available from: http://websoilsurvey.nrcs.usda.gov)

Taylor, B. W. 2006. Loss of a Harvested Fish Species Disrupts Carbon Flow in a Diverse Tropical River. Science 313:833–836.

Turner, R. E., J. J. Baustian, E. M. Swenson, and J. S. Spicer. 2006. Wetland Sedimentation from Hurricanes Katrina and Rita. Science 314:449–452.

United States Geological Survey. 2019. National Hydrography Dataset Best Resolution (NHD) for Hydrologic Unit (HU) 4—2001. (Available from: https://www.usgs.gov/national-hydrography/access-national-hydrography-products)

USDA. 1986. Urban hydrology for small watersheds. Technical Release TR-55, nited States Department for Agriculture Soil Conservation Service, Washington, D. C.
USDA. 2016. Geospatial Data Gateway. USDA, Natural Resources Conservation Service. (Available from: https://doi.org/10.15482/USDA.ADC/1241880)
Van Diggelen, A. D., and P. A. Montagna. 2016. Is Salinity Variability a Benthic Disturbance in Estuaries? Estuaries and Coasts 39:967–980.
Walsh, C. J., T. D. Fletcher, and A. R. Ladson. 2005a. Stream restoration in urban catchments through redesigning stormwater systems: Looking to the catchment to save the stream. Journal of the North American Benthological Society 24:690–705.
Walsh, C. J., A. H. Roy, J. W. Feminella, P. D. Cottingham, P. M. Groffman, R. P. M. Ii, and R. A. P. M. O. Ii. 2005b. The urban stream syndrome: Current knowledge and the search for a cure. North American Benthological Society 24:706–723.
Wang, R., and L. Kalin. 2011. Modelling effects of land use/cover changes under limited data. Ecohydrology 4:265–276.
Wang, R., and L. Kalin. 2018. Combined and synergistic effects of climate change and urbanization on water quality in the Wolf Bay watershed, southern Alabama. Journal of Environmental Sciences 64:107–121.
Wang, R., L. Kalin, W. Kuang, and H. Tian. 2014. Individual and combined effects of land use/cover and climate change on Wolf Bay watershed streamflow in southern Alabama: Relative impacts of land use/cover and climate change on streamflow. Hydrological Processes 28:5530–5546.
Wedge, M., and C. J. Anderson. 2017. Urban Land use Affects Resident Fish Communities and Associated Salt Marsh Habitat in Alabama and West Florida, USA. Wetlands 37:715–727.
Welti, N., M. Striebel, A. J. Ulseth, W. F. Cross, S. DeVilbiss, P. M. Glibert, L. Guo, A. G. Hirst, J. Hood, J. S. Kominoski, K. L. MacNeill, A. S. Mehring, J. R. Welter, and H. Hillebrand. 2017. Bridging Food Webs, Ecosystem Metabolism, and Biogeochemistry Using Ecological Stoichiometry Theory. Frontiers in Microbiology 8:1298.
Wilson, G. W., and T. R. Fischetti. 2010. Coastline Population Trends in the United States: 1960 to 2008. U. S. Cencus Bureau 1–28.
Xian, G., C. Homer, B. Bunde, P. Danielson, J. Dewitz, J. Fry, and R. Pu. 2012. Quantifying urban land cover change between 2001 and 2006 in the Gulf of Mexico region. Geocarto International 27:479–497.
Young, R. G., C. D. Matthaei, and C. R. Townsend. 2008. Organic matter breakdown and ecosystem metabolism: Functional indicators for assessing river ecosystem health. Journal of the North American Benthological Society 27:605–625.
Ziegler, S. L., R. Baker, S. C. Crosby, D. D. Colombano, M. A. Barbeau, J. Cebrian, R. M. Connolly, L. A. Deegan, B. L. Gilby, D. Mallick, C. W. Martin, J. A. Nelson, J. F. Reinhardt, C. A. Simenstad, N. J. Waltham, T. A. Worthington, and L. P. Rozas. 2021. Geographic Variation in Salt Marsh Structure and Function for Nekton: A Guide to Finding Commonality Across Multiple Scales. Estuaries and Coasts.

Table 3-1. Site watershed area (km^2), average watershed curve number (CN), and land-cover distribution (% of watershed) from 2016 NLCD. Asterisk (*) indicates subset of sites used in tidal creek ecosystem metabolism analysis. Urban is a summation of multiple land cover classes, with development including all levels of development (open, low, medium, high), wetland includes woody and emergent wetlands, and Agric. includes pasture and row crops.

Site	Area (km^2)	CN	Urban (%)	Forest/Herb/ Shrub (%)	Wetland (%)	Agric. (%)	Barren Land & Open Water (%)
Wolf-Perdido Bay							
Stone Quarry (SQ)	0.4	35.00	0.0	93.6	6.4	0.0	0.0
Manuel Bayou (MB)*	6.2	46.21	8.4	38.7	6.2	46.1	0.2
Weakley Bayou (WB)*	6.7	42.71	17.6	25.9	55.2	0.6	0.4
Long Bayou (LB)*	6.8	54.26	3.3	23.3	61.0	11.1	0.4
Graham Creek (GC)	8.8	59.62	8.4	47	21.3	21.0	2.2
Heron Bayou (HB)	13.6	45.92	38.8	10.7	48.1	1.2	0.5
Escambia-Pensacola-East Bay							
Trout Bayou (TB)	2.5	46.36	13.9	10.6	73.5	0.5	1.4
Robinson Pointe (RP)	3.1	49.08	8.2	35.9	37.3	13.4	4.5
Indian Bayou (IB)*	5.1	46.42	12.3	1.9	84.7	0.0	1.0
Mulat Bayou (MU)*	10.3	52.55	24.8	13.9	57.2	2.7	1.2
Bayou Grande (BG)	18.3	45.12	27.6	20.3	47.5	2.2	1.4
Texar Bayou (TX)*	46.4	53.84	87.5	6.8	2.0	0.2	3.1

Table 3-2. Summary of predictor variables used in stepwise regression analyses.

Variable	Description	Abbreviate	Method	Transformation
RB-index of salinity	Index measure of salinity change over time series	RB	Calculated from 15-minute measured salinity	Log10
Mean salinity (ppt)	Mean seasonal salinity	SalMean	Calculated from 15-minute measured salinity	None
Salinity amplitude (ppt)	Mean daily amplitude of salinity	SalAmp	Calculated from 15-minute measured salinity	Log10
Temperature (°C)	Mean seasonal temperature	Temp	Calculated from 15-minute measured temperature	None
Flow (cms)	Area corrected flow	Flow	Derived from SWAT	Log10
NO_3^- (µg/L)	Mean seasonal nitrate concentration	NO_3^-	Derived from SWAT	Log10
NH_4^+ (µg/L)	Mean seasonal ammonium concentration	NH_4^+	Derived from SWAT	Log10
Mineralized-P (µg/L)	Mean seasonal organic mineralized phosphorous concentration	MinP	Derived from SWAT	Log10

Table 3-3. Summary statistics based on mean daily salinity (± standard error), salinity amplitude (daily change in salinity; ppt), RB for the entire study period (June 2019-October 2020) and mean daily temperature (± standard error).

Site	n days of salinity	Mean salinity (ppt)	Salinity Amplitude (ppt)	Salinity RB	n days of temperature	Mean water temperature (°C)
Bayou Grande	307	11.6 (± 0.2)	3.5 (± 0.2)	1.39	489	26.5 (± 0.3)
Graham Creek	383	11.4 (± 0.1)	2.4 (± 0.2)	1.05	500	26.3 (± 0.3)
Heron Bayou	210	5.5 (± 0.2)	1.8 (± 0.1)	1.5	499	24.6 (± 0.3)
Indian Bayou	168	12.4 (± 0.3)	1.4 (± 0.2)	0.58	362	23.9 (± 0.3)
Long Bayou	287	11.8 (± 0.2)	1.6 (± 0.2)	0.84	357	28.1 (± 0.2)
Manuel Bayou	472	10.6 (± 0.1)	1.5 (± 0.0)	0.52	492	25.9 (± 0.3)
Mulat Bayou	471	6.0 (± 0.2)	3.5 (± 0.1)	1.90	473	25.7 (± 0.3)
Robinson Bayou	333	6.0 (± 0.2)	2.7 (± 0.1)	1.48	439	24.9 (± 0.3)
Stone Quarry Bayou	344	14.1 (± 0.1)	0.9 (± 0.0)	0.20	482	25.5 (± 0.3)
Texar Bayou	402	11.4 (± 0.2)	2.6 (± 0.1)	0.75	501	24.8 (± 0.3)
Trout Bayou	406	10.6 (± 0.2)	1.4 (± 0.1)	0.40	506	26.0 (± 0.3)
Weakley Bayou	383	11.3 (± 0.2)	2.3 (± 0.1)	0.72	498	26.7 (± 0.3)

Table 3-4. Mean (± standard error) and number of days measured for seasonal gross primary production (GPP), ecosystem respiration (ER), and net ecosystem metabolism (NEM). ND indicates "no data."

		GPP (mmol O_2 $m^{-2}d^{-1}$)				ER (mmol O_2 $m^{-2}d^{-1}$)				NEM (mmol O_2 $m^{-2}d^{-1}$)			
Site		Spring	Summer	Autumn	Winter	Spring	Summer	Autumn	Winter	Spring	Summer	Autumn	Winter
Indian	n	78	125	60	57	78	126	60	57	78	125	60	57
	mean	719	212	191	114	-598	-579	-509	-368	-418	-366	-318	-254
	SE	14	16	30	11	34	21	41	25	28	13	32	22
Long	n	72	140	ND	36	72	140	ND	36	72	140	ND	36
	mean	306	284	ND	154	-542	-690	ND	-270	-236	-406	ND	-116
	SE	22	13	ND	12	49	28	ND	23	36	25	ND	16
Manuel	n	77	167	23	25	77	167	23	25	77	167	23	25
	mean	318	247	198	299	-844	-712	-831	-652	-527	-465	-632	-352
	SE	30	12	36	61	73	26	103	71	56	24	84	41
Mulat	n	81	144	16	24	81	144	16	24	81	144	16	24
	mean	194	226	143	133	-570	-687	-661	-412	-376	-460	-517	-279
	SE	15	13	32	20	37	26	108	40	33	20	88	33
Texar	n	89	164	89	65	89	164	89	65	89	164	89	65
	mean	226	254	186	92	-471	-492	-371	-188	-245	-238	-185	-96
	SE	11	9	12	8	20	14	20	11	16	12	15	7
Weakley	n	88	136	65	85	88	136	65	85	88	136	65	85
	mean	213	263	226	183	-763	-682	-580	-571	-550	-419	-354	-388
	SE	15	23	24	10	41	33	39	28	37	18	22	24

Table 3-5. Summary of stepwise regression models for seasonal averages of gross primary production (GPP), ecosystem respiration (ER), and net ecosystem metabolism (NEM). Models are ranked according to AICc scores. Data from SWAT outputs have been log transformed (see Table 3-2).

Variable	Rank	Model Covariates	AIC	ΔAIC	Final r2	Final p
GPP	1	Temp	222.01	34.57	0.29	0.01
	2	Temp, SalAmp	224.73	31.85	-	-
	3	Temp, SalAmp, RB	227.24	29.34	-	-
	4	Temp, SalAmp, RB, NO3	230.93	25.65	-	-
	5	Temp, SalAmp, RB, NO3, SalMean	235.58	21.00	-	-
	6	Temp, SalAmp, RB, NO3, SalMean, MinP	241.27	15.31	-	-
	7	Temp, SalAmp, RB, NO3, SalMean, MinP, Flow	248.15	8.43	-	-
	8	Temp, SalAmp, RB, NO3, SalMean, MinP, Flow, NH4	256.58	0.00	-	-
ER	1	Temp, RB, SalMean, NH4	261.71	23.33	0.50	0.02
	2	Temp, RB, SalMean, NH4, NO3	265.66	19.38	-	-
	3	Temp, RB, SalMean, NH4, NO3, Flow	270.46	14.58	-	-
	4	Temp, RB, SalMean, NH4, NO3, Flow, MinP	277.12	7.92	-	-
	5	Temp, RB, SalMean, NH4, NO3, Flow, MinP, SalAmp	285.04	0.00	-	-
NEM	1	RB, SalMean, NH4	253.62	26.15	0.45	0.02
	2	RB, SalMean, NH4, Flow	256.8	22.97	-	-
	3	RB, SalMean, NH4, Flow, Temp	260.32	19.45	-	-
	4	RB, SalMean, NH4, Flow, Temp, NO3	265.72	14.05	-	-
	5	RB, SalMean, NH4, Flow, Temp, NO3, MinP	271.67	8.10	-	-
	6	RB, SalMean, NH4, Flow, Temp, NO3, MinP, SalAmp	279.77	0.00	-	-

Table 3-6. Mean (± standard error) of Soil and Water Assessment Tool (SWAT) outputs across the entire study period (June 2019-October 2020).

Site	Flow (cms)	NH4 (µg/L)	NO3 (µg/L)	Mineral P (µg/L)
Bayou Grande	0.038 (± 0.004)	1.7 (± 0.1)	24.3 (± 1.2)	3.2 (± 0.3)
Graham Creek	0.032 (± 0.005)	2.2 (± 2.0)	194.1 (± 78.9)	6.9 (± 0.7)
Heron Bayou	0.037 (± 0.005)	1.7 (± 1.0)	25.7 (± 1.4)	3.8(± 0.3)
Indian Bayou	0.043 (± 0.008)	4.1 (± 0.3)	19.1 (± 1.6)	0.1 (± 0.0)
Long Bayou	0.032 (± 0.005)	1.3 (± 1.0)	38.6 (± 15.6)	2.1 (± 0.2)
Manuel Bayou	0.034 (± 0.005)	4.2 (± 0.4)	187.7 (± 93.6)	6.8 (± 0.8)
Mulat Bayou	0.044 (± 0.008)	4.6 (± 0.3)	33.9 (± 1.8)	1.0 (± 0.1)
Robinson Bayou	0.042 (± 0.007)	1.5 (± 0.1)	132.5 (± 36.1)	0.2 (± 0.0)
Stone Quarry Bayou	0.036 (± 0.004)	0.1 (± 0.0)	11.4 (± 0.8)	0.2 (± 0.1)
Texar Bayou	0.034 (± 0.006)	9.3 (± 0.7)	71.1 (± 6.6)	10.1 (± 0.6)
Trout Bayou	0.043 (± 0.008)	2.1 (± 0.2)	45.8 (± 2.4)	0.8 (± 0.1)
Weakly Bayou	0.042 (± 0.005)	0.8 (± 0.0)	8.6 (± 0.4)	1.1 (± 0.1)

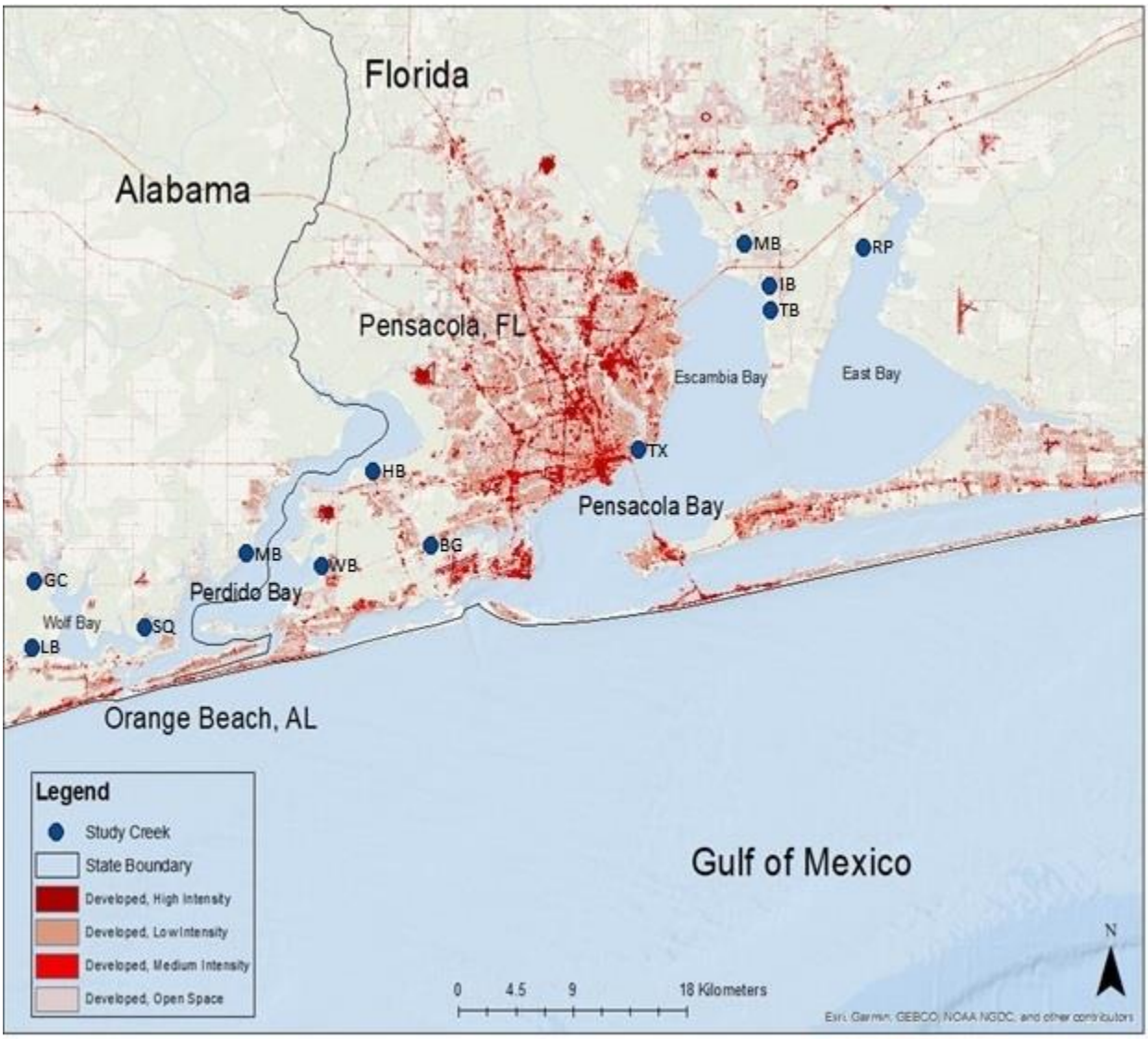

Figure 3-1. Map of the study region. Blue dots represent sampling sites within study creeks and red shading represents intensity of urban land use (data from 2016 NLCD). See Table 3-1 for site abbreviations.

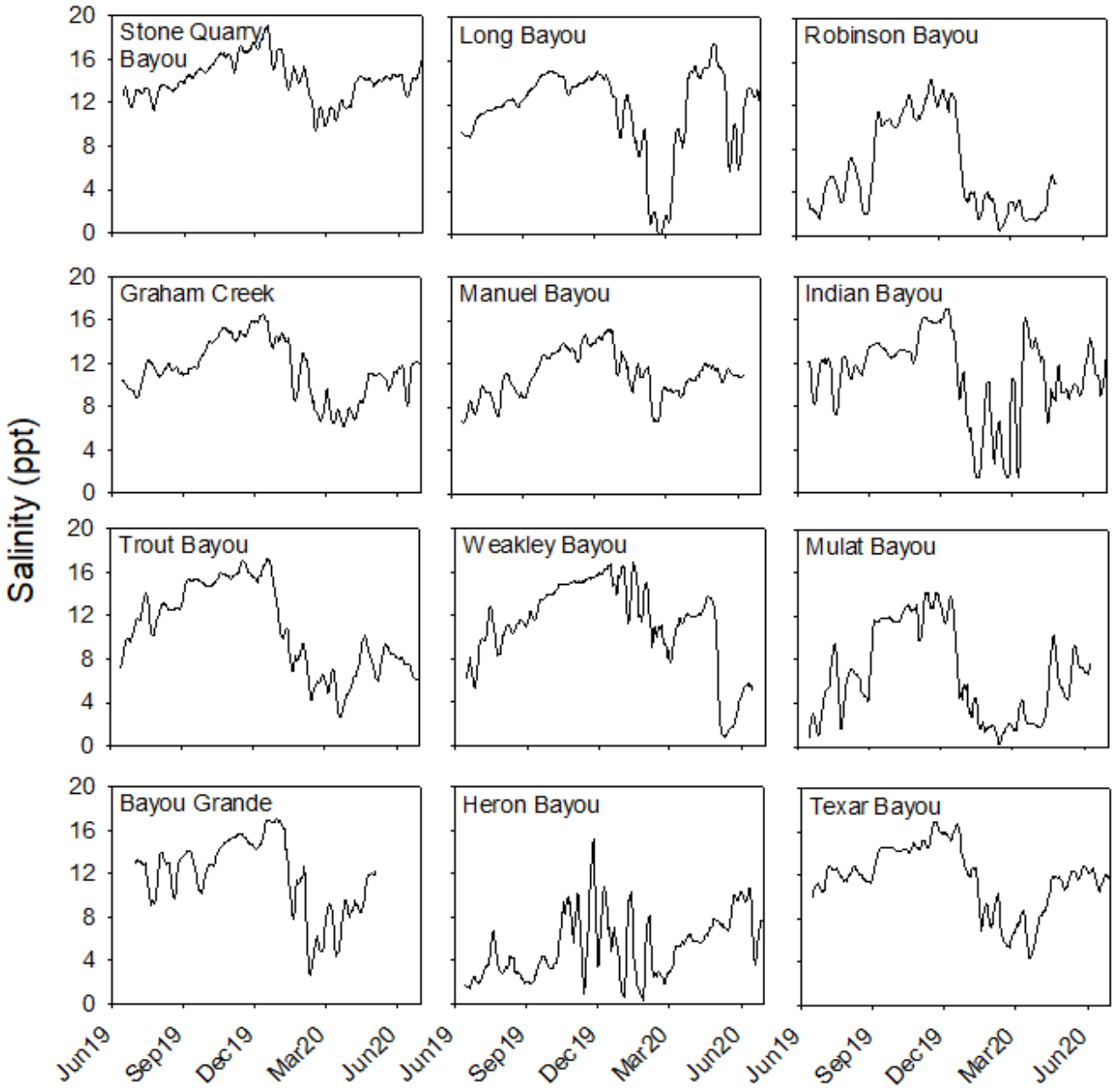

Figure 3-2. Time series of 7-day moving average salinity across all twelve sites from June 2019 to June 2020.

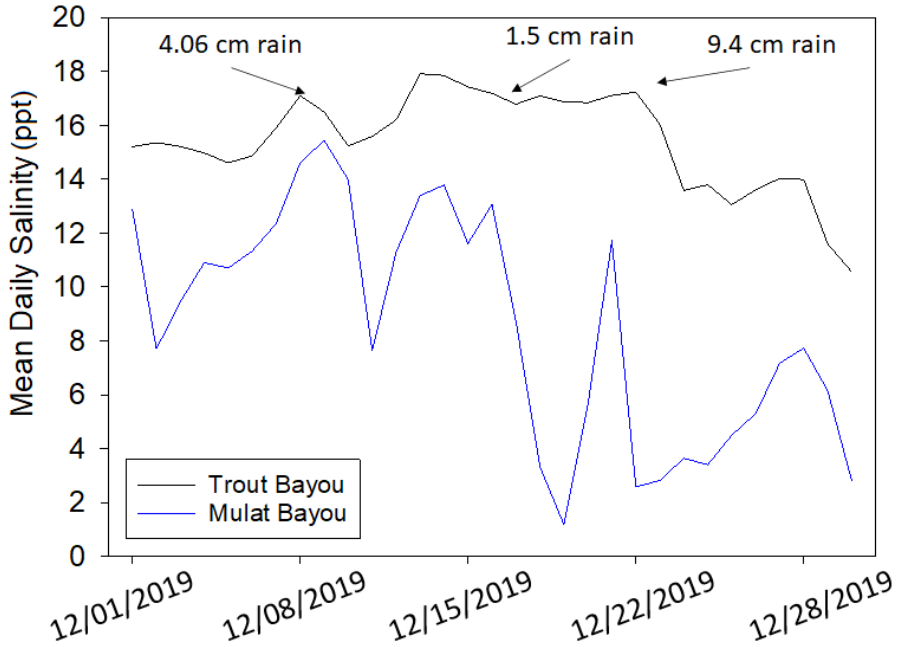

Figure 3-3. Mean daily salinity (ppt) response at Trout and Mulat Bayous following rain events.

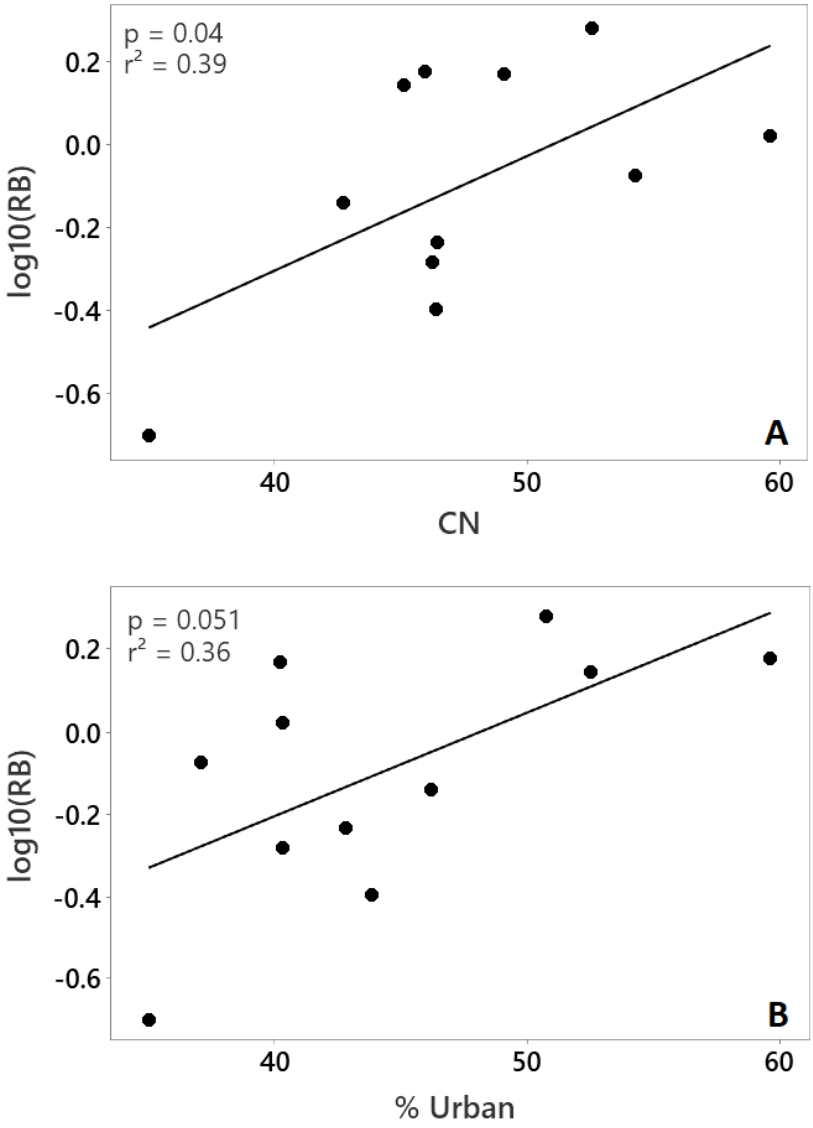

Figure 3-4. Linear regressions between mean seasonal RB-index and watershed curve number (A) and the proportion of tidal creek watersheds as urban land cover (B). Texar Bayou data not included in regression (see text).

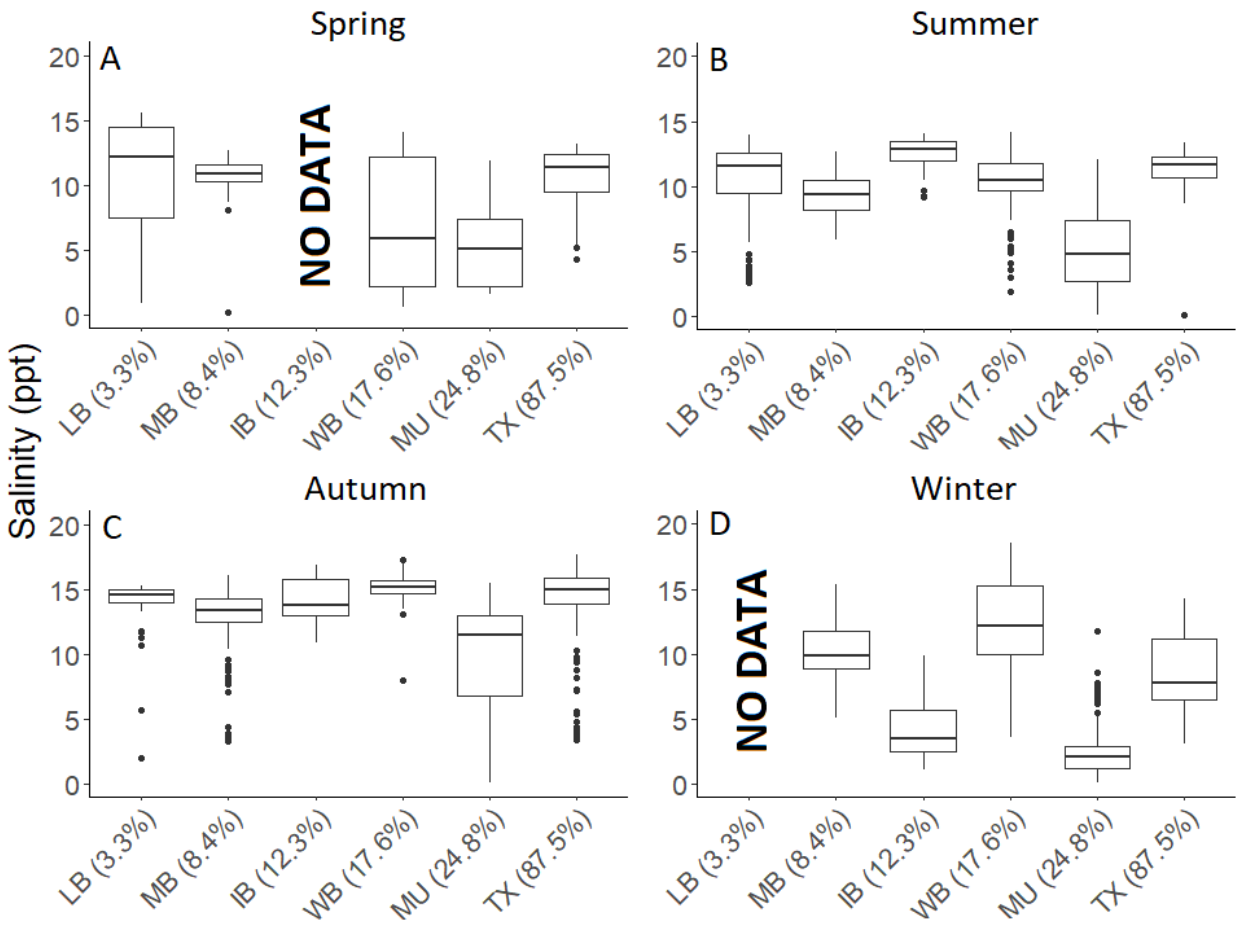

Figure 3-5. Box plots summarizing mean daily salinity (ppt) data at Long Bayou (LB), Manuel Bayou (MB), Indian Bayou (IB), Weakley Bayou (WB), Mulat Bayou (MU), and Texar Bayou (TX) during spring (A), summer (B), autumn (C), and winter (D). Values in parentheses are % urban land cover. The horizontal line within each box indicates the median, the edges of the boxes indicate the 25th and 75th percentiles, and whiskers represent the 10th and 90th percentiles. Black circles represent outlier datapoints. No data indicates periods when salinity sensors malfunctioned.

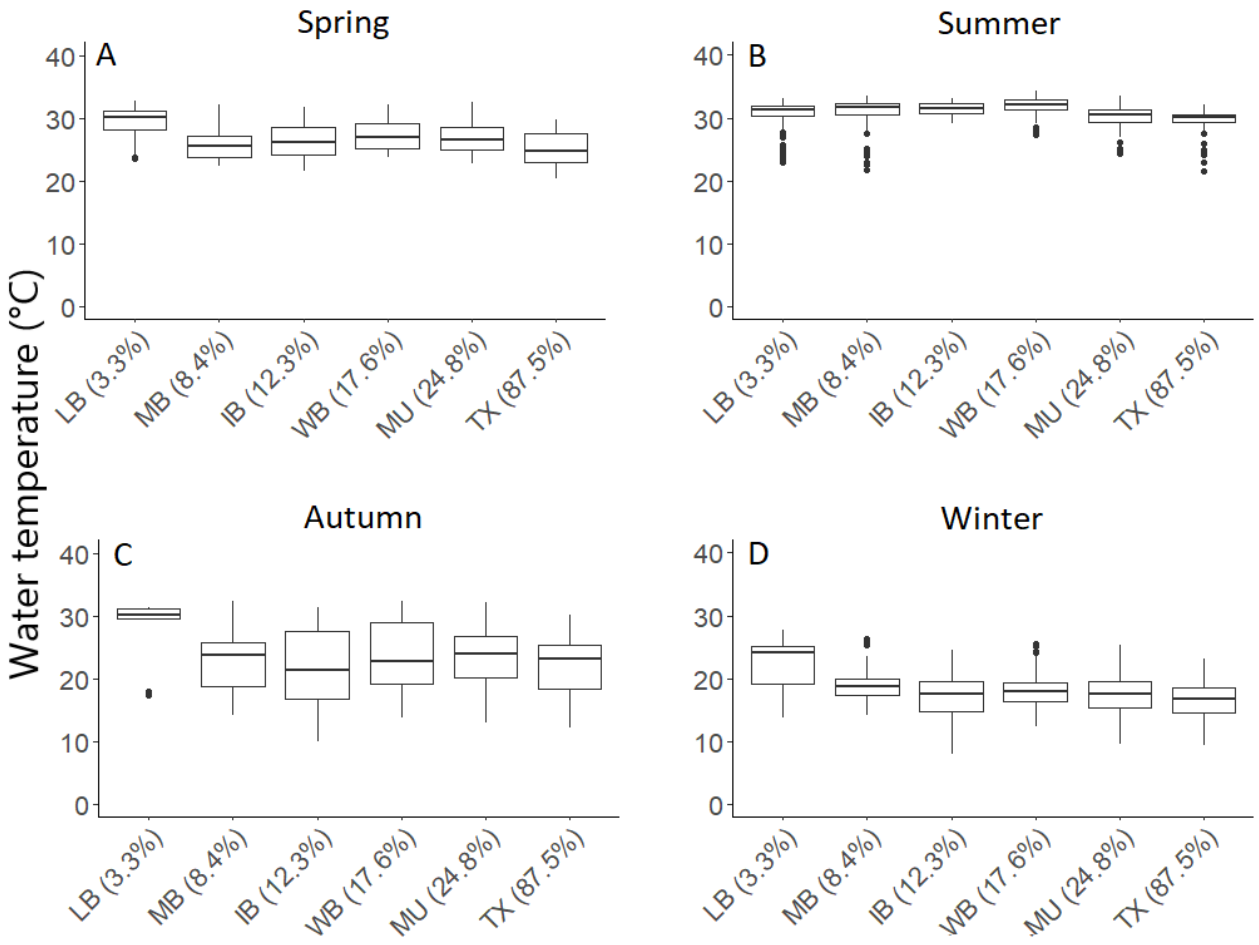

Figure 3-6. Box plots of mean daily water temperature (°C) at Long Bayou (LB), Manuel Bayou (MB), Indian Bayou (IB), Weakley Bayou (WB), Mulat Bayou (MU), and Texar Bayou (TX) during spring (A), summer (B), autumn (C), and winter (D). Values in parentheses are % urban land cover. The horizontal line within each box indicates the median, the edges of the boxes indicate the 25th and 75th percentiles, and whiskers represent the 10th and 90th percentiles. Black circles represent outlier datapoints.

A

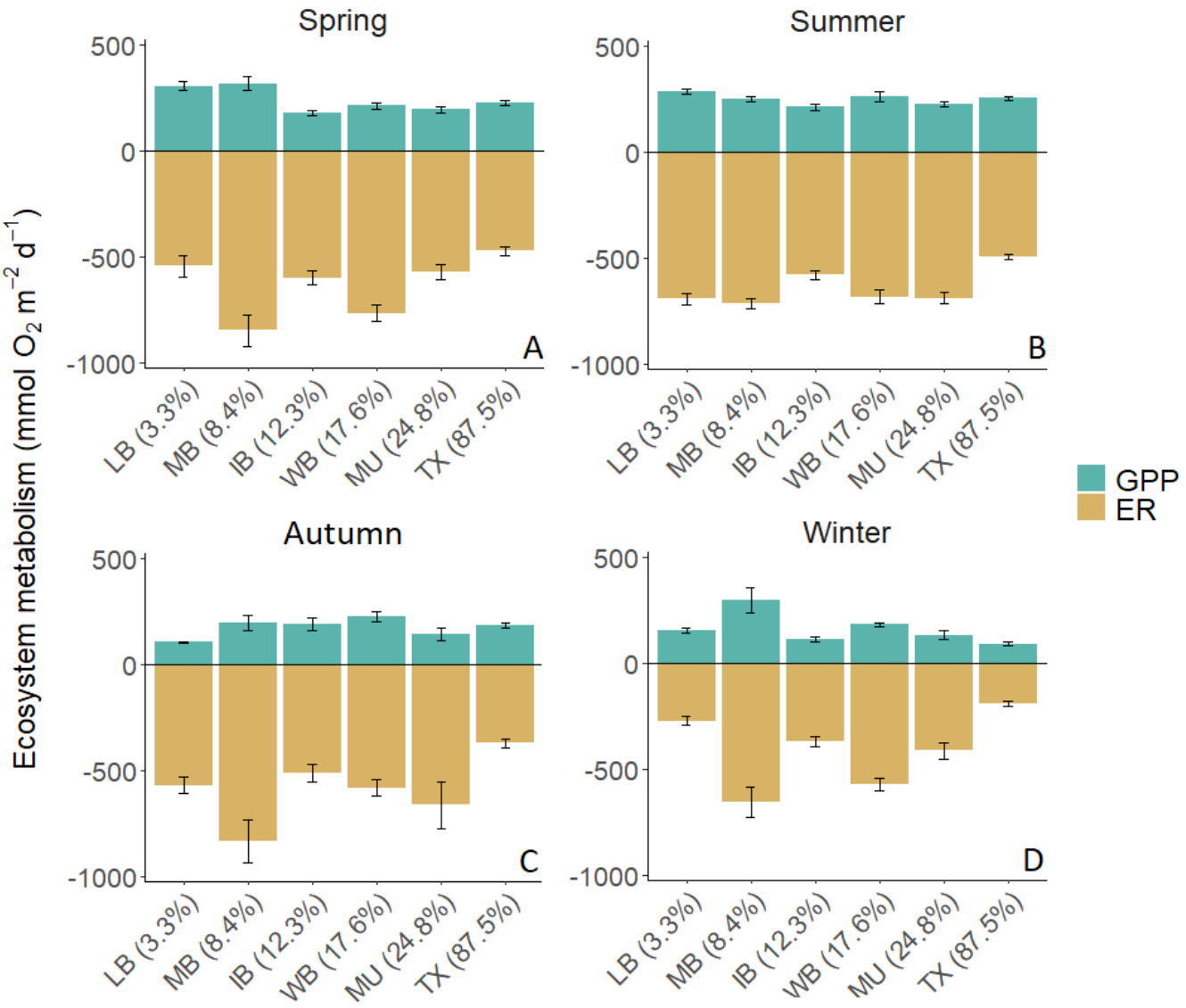

Figure 3-7. Mean (± standard error) seasonal ecosystem metabolism (mmol O_2 m^{-2} d^{-1}) as measured by gross primary production (GPP) and ecosystem metabolism (ER) at Long Bayou (LB), Manuel Bayou (MB), Indian Bayou (IB), Weakley Bayou (WB), Mulat Bayou (MU), and Texar Bayou (TX) during spring (A), summer (B), autumn (C), and winter (D). Values in parentheses are % urban land cover.

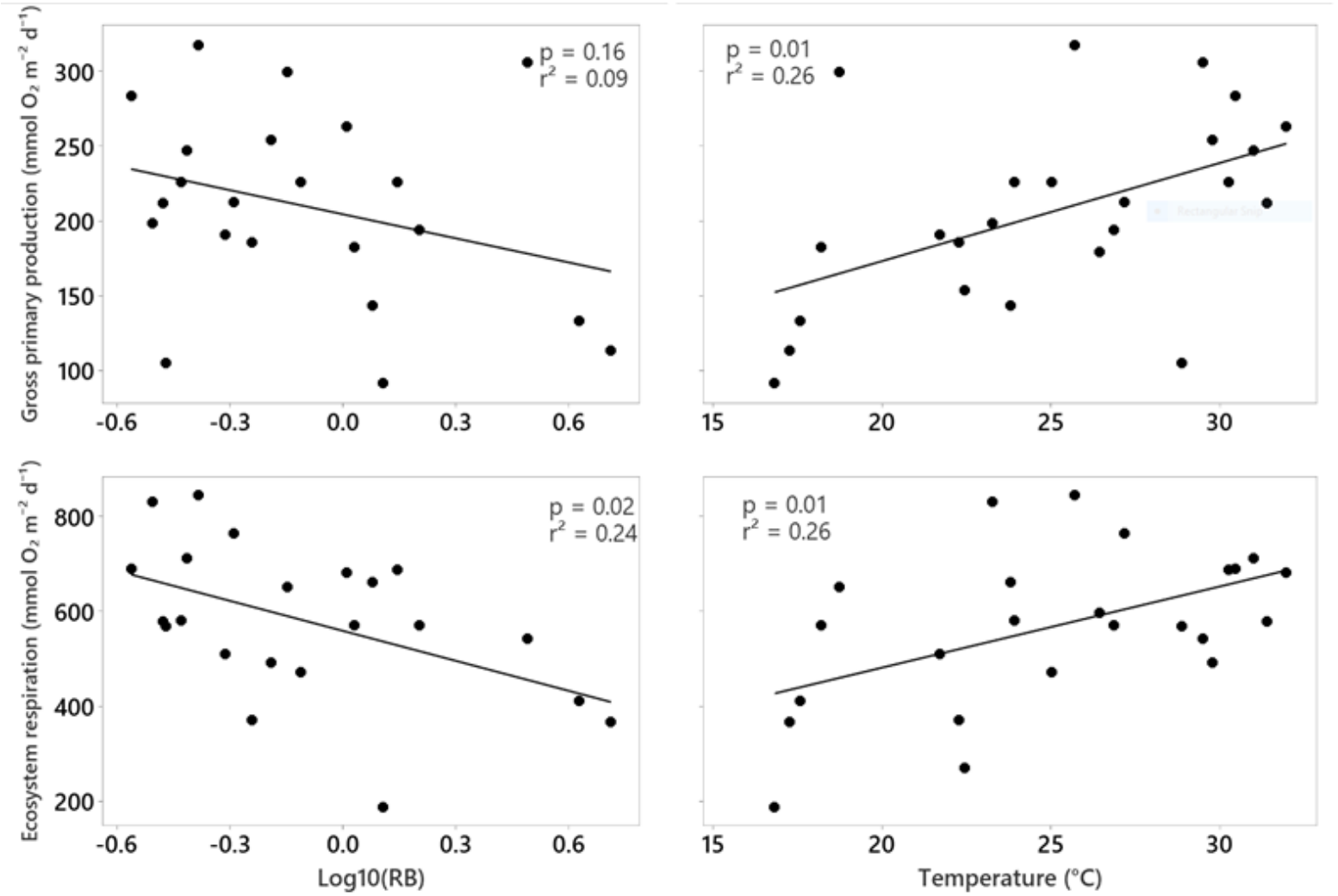

Figure 3-8. Linear regressions of gross primary productivity (mmol O_2 $m^{-2}d^{-1}$) summarized by season in relation to RB-index (A) and temperature (B), and ecosystem respiration (mmol O_2 $m^{-2}d^{-1}$) summarized by season in relation to RB-index (C) and temperature (D). Black line indicates trend in data only.

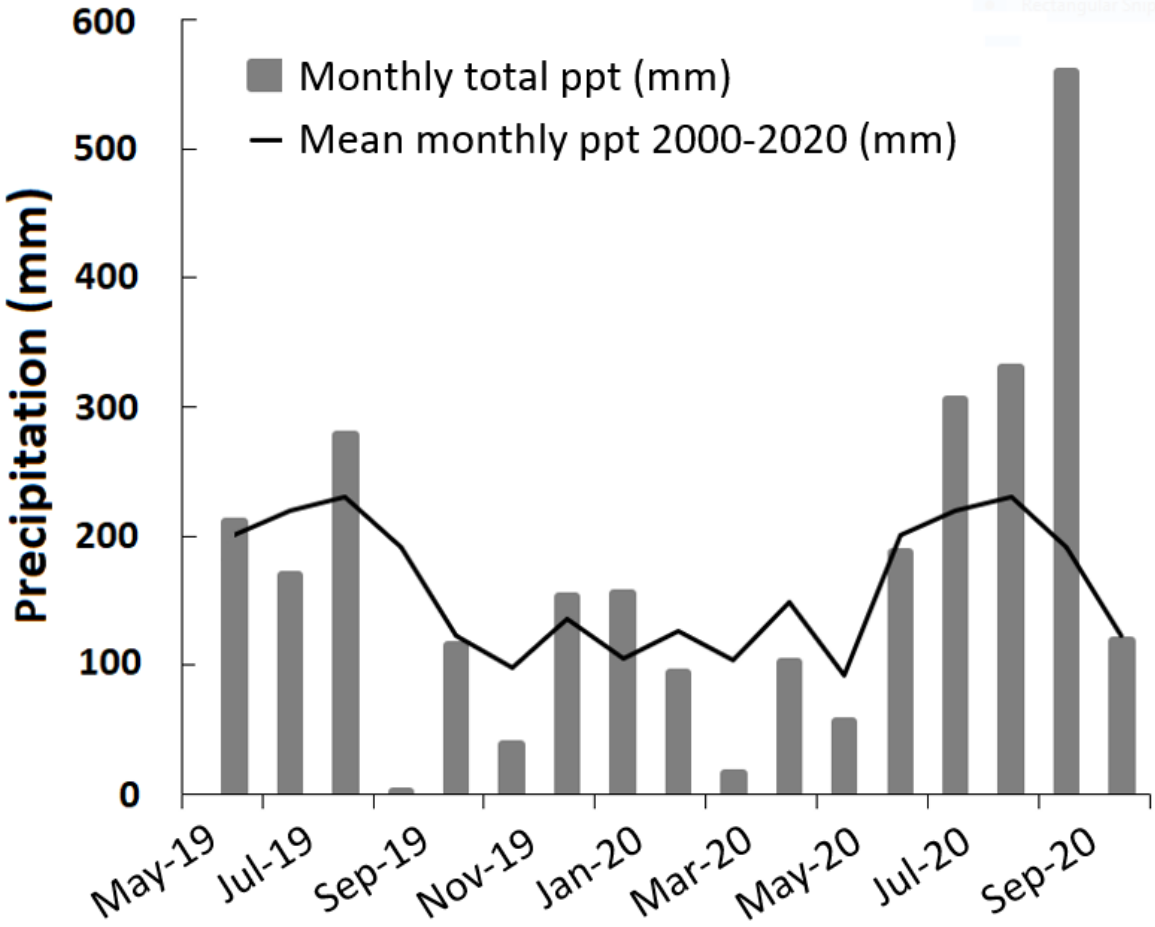

Figure 3-9. Monthly precipitation totals (mm; grey bars) during the study period (June 2019-October 2020) and average monthly precipitation totals (mm; black line) based on 2000-2020 precipitation data from PRISM dataset for Pensacola, Florida, USA.

Chapter 4: Changes in the abundance of *Fundulus grandis* in response to salinity regime

Abstract

Salinity is understood to be a primary determinant of community structure in estuaries. Although salinity varies naturally, there is evidence watershed urbanization increases freshwater input and salinity variation, which can influence biota. *Fundulus grandis*, a regionally dominant resident salt marsh fish along the northern Gulf of Mexico (GOM) coastline, were collected in 12 tidal creeks (2nd to 3rd order) along a salinity and urbanization gradient. At each creek, we measured salinity continuously for over one year and quantified mean salinity and salinity variability (using a modified Richard Baker (RB)-index of flashiness). To examine potential changes in *F. grandis* abundance over time, we compared these results to a dataset from 2012 (coinciding with a regional drought) that sampled salinity and resident fish similarly at a subset (n = 6) of the same sites. We found that *F. grandis* abundance (based on catch per unit effort, CPUE) in 2019-2020 increased with mean site salinity and decreased with RB-index. Further, CPUE declined between 2012 and 2019-2020 coinciding with decreased salinity related to more normal precipitation. These results indicate that *F. grandis* abundance tends to decline with increasing freshwater input and that salinity variability caused by watershed development, even at low-to-moderate levels typical for this region, may reduce *F. grandis* abundance. Our results indicate an

important linkage between tidal creek salinity and biota that should be considered in relation to a changing coastal landscape and climate.

Introduction

Salinity has long been recognized as structuring fish assemblages along estuarine salinity gradients, and many studies have found the greatest abundance of estuarine fish in mesohaline to polyhaline conditions (Martino and Able 2003, 2003, Harrison and Whitfield 2006, Whitfield et al. 2006, Franco et al. 2019). Changes in baseline salinity may alter not only estuarine fish assemblages, but also lead to changes in fish abundance. Along the northern Gulf of Mexico (GOM), *Fundulus grandis* (Gulf killifish) is a ubiquitous fish species in the Cyprinidae family and is a dominant resident fish species in tidal creeks and salt marshes (Peterson and Turner 1994, Lowe and Peterson 2015). *Fundulus* species have been shown to have a preference for more polyhaline conditions (Wagner and Austin 1999, Bucking et al. 2012, Marshall et al. 2016), and this preference may be detected as lower catch per unit effort (CPUE) in mesohaline conditions. While *F. grandis* is able to osmotically regulate across a wide range of conditions (Nordlie and Haney 1998), compared to saltier waters, growth rate and survival of *F. grandis* is lower, and the embryonic mortality rate is higher in lower salinity conditions (Patterson et al. 2012, Ramee et al. 2016, Ramee and Allen 2016). Based on this evidence, it is likely that important thresholds in *F. grandis* habitat suitability occur as estuaries transition to oligohaline conditions, either due to natural changes in the environment or due to human activities.

In addition to naturally occurring salinity gradients that exist in estuaries, it is increasingly recognized that fluctuations in salinity can be caused by human activities. This is

particularly evident in tidal creeks that directly receive watershed runoff from developed watersheds. When considering coastal land use, variations and alterations to hydrology have long been demonstrated to be a driver of environmental changes (Bain et al. 1988, Poff et al. 1997, Walsh et al. 2005a, Poff and Zimmerman 2010,Schneid et al. 2017). Peak runoff and runoff volume increased following discrete storm events with urbanization and impervious surface coverage in Eight Mile Creek in coastal Alabama (Noori et al. 2016). Increased runoff from urbanized areas may also lead to changes to the frequency and magnitude of salinity fluctuations in tidal creeks (Lerberg et al. 2000, Holland et al. 2004, Sanger et al. 2008). These alterations in runoff and resulting salinity fluctuations may represent important habitat changes and potential stressors to resident fish communities in these tidal creeks.

Previous work along the northern GOM has provided some evidence of differences in *F. grandis* abundance between urban and non-urban tidal creeks. This is notable because *F. grandis* is a resident tidal marsh species and tend not to migrate in response to environmental or life-history changes, and therefore is a suitable indicator species (Whitfield and Elliott 2002). Lowe and Peterson (2014) found *F. grandis* CPUE along the Mississippi coast was highest in undisturbed salt marshes with intact marsh edge but declined with salt-marsh fragmentation associated with urbanization. Similarly, Wedge and Anderson (2017) found that *F. grandis* CPUE was highest in non-urban tidal creeks compared to more urban tidal creeks along the Alabama coast. Salinity was a significant factor in structuring the entire tidal creek fish assemblage, suggesting that resident fish species assemblages are structured by both baseline environmental conditions and watershed disturbances (Wedge and Anderson 2017). However, not all related studies have detected an urban effect. Abundance of *F. heteroclitus* in Atlantic

slope tidal creeks did not differ with impervious surface coverage (Holland et al. 2004), suggesting adaptation to more disturbed habitat. Although there may be variation across taxa and regions, it is expected that as coastal development increases, so does the potential for disturbances to coastal aquatic ecosystems.

It has been estimated that a third of the global population lives within 100 km of the coast (Gittman et al. 2016), and 29% of the population of the United States reside within a county along either the Pacific, Atlantic, or Gulf of Mexico coastlines (U.S. Census 2017). Along the Gulf of Mexico (GOM), population grew by 3 million people between 2000 and 2016, to a total of 15.8 million people living in coastal GOM counties (US Census 2017), which has led to increased low- and moderate-density urbanization (Wilson and Fischetti 2010, Xian et al. 2012). As the human population continues to grow in coastal areas along the GOM, there is an increasing risk to coastal aquatic resources that receive drainage from these urban lands. In addition to urbanization, increased extreme precipitation associated with climate change has the potential to increase freshwater flows and lower baseline salinity in coastal waters (Du and Park 2019, Des et al. 2021). The identification of indicator species and important salinity thresholds is needed to aid in monitoring the overall health of coastal ecosystems as land use change and climate change continue.

Using a combination of new (2019-2020) and previously measured (2012-2013) *F. grandis* abundance and salinity data, this study examined the how abundance and salinity regimes have changed across 12 tidal creeks located along a natural mesohaline salinity gradient

in the northern GOM. These creeks also represented an urban gradient which has been shown to increase the variability of creek salinity related to urban runoff when calculated for a multi-month period of record. It was expected that increased precipitation in the Southeastern United States associated with climate change has potentially led to increased freshwater flows and subsequent lower salinity conditions along the northern GOM. Further, it was expected that that the abundance of *F. grandis* would decrease with both decreasing salinities and the magnitude and frequency of salinity fluctuations associated with watershed development. To examine changes between in *F. grandis* abundance in response to changes in salinity regime, 2019-2020 and 2012-2013 abundance and salinity regime data were compared. The 2019-2020 dataset was also used to examine how *F. grandis* abundance responded to changes in watershed development and across a mesohaline salinity gradient. The goal of this study was to better understand the contributions of these factors on fish abundance and relate these factors to changes in both watershed and estuarine conditions.

Methods

Study species and study sites

Fundulus grandis is a member of the Cyprinodontidae family and an abundant resident salt marsh fish along the Gulf of Mexico (Rozas and Reed 1993, Rozas and Zimmerman 2000, Lowe and Peterson 2015). As a resident salt marsh fish, tidal inundation structures much of *F. grandis* life history. For example, high tide represents a period where *F. grandis* has greater access to the marsh surface, enabling it to forage before retreating towards the marsh and tidal creeks at ebb tide (Rozas and LaSalle 1990). During spring and early summer, the peak

spawning period for *F. grandis*, females lay their eggs on marsh vegetation during spring tide, where they incubate for 14 ± 1 days before hatching during the next spring tide (Greeley and MacGregor 1983). *F. grandis* has a limited home range, moving only about 100 m in either direction (Nelson et al. 2014). Because of their abundance and high site fidelity to salt marshes, they likely represent an important prey species for transient fish entering tidal creeks.

Twelve second- or third-order tidal creeks draining to either the Wolf-Perdido Bay or the Pensacola-East Bay in the northern GOM (Alabama to west-Florida, USA) were selected for this study (Fig. 4-1). Field visits confirmed the occurrence of fringing Black Needlerush (*Juncus roemerianus*) near the mouth of each creek, which served as an initial indicator of comparable habitat and salinity range between sites. Site selection was also based on identifying creeks along a gradient of urbanization typical to the region (Table 4-1), with some preference being given to sites accessible by small boat. Watershed urban land cover within the Wolf-Perdido Bay sites (n=6) ranged from 0.0-38.8% (30-m resolution; NLCD 2016) and watershed area ranged from 0.4-13.6 km^2 (Table 4-1). Watershed urban land cover within the Pensacola-East Bay sites (n=6) ranged from 8.2-87.5% (NLCD 2016) and watershed area ranged from 2.5-46.4 km^2 (Table 4-1). One site (Texar Bayou) was characterized as high-density urban given its location near downtown Pensacola, FL. The remaining sites were generally characterized as low- to moderate-urban dominated by residential and commercial land use. Each creek was tidally influenced and

dominated by *J. roemerianus* with other common marsh vegetation being a mix of Smooth Cordgrass (*Spartina alterniflora*) and Sawgrass (*Cladium jamaicense)*.

Salinity

Salinity was continuously measured at each creek starting in June 2019, generally following Wedge and Anderson (2017). A HOBO U-24-002-C saltwater conductivity sensor (Onset Computer Corporation, Bourne, Massachusetts) was deployed in June 2019 – October 2020 to continually measure hourly conductivity (µS/cm) and temperature (°C) at all 12 sites. Conductivity/temperature data were routinely downloaded and converted to salinity (ppt) and used to generate daily averages throughout the study period. Daily averages of salinity were used to evaluate base level salinity at each creek. In some cases, sensors malfunctioned, and data gaps were filled with modeled estimates of daily average salinity (Isik et al. *in preparation*). Because of sensor malfunctions, exceedance probability curves of the seven-day moving average of mean daily salinity were prepared for graphical comparison between sites for the most complete period of record, June 2019-May 2020. To assess the frequency and magnitude of salinity change, we used a modified index of flashiness based on the Richard-Baker (RB) index (Baker et al. 2004a). The RB-index measures the change in salinity between timesteps (15-minutes) compared to overall salinity at a site, and has been used to quantify salinity and streamflow variability

elsewhere in the region (Barksdale et al. 2014, Wedge and Anderson 2017, Rezaeianzadeh et al. 2017).

Fish sampling

Fish were sampled seasonally during autumn 2019 (October), summer 2020 (July), and autumn 2020 (October). For each sampling event, all 12 sites were sampled over the course of two weeks following methodology in Wedge and Anderson (2017). In each creek, four fringing marshes were selected, and three baited (commercially available frozen bait fish: *Brevortia* sp. and *Selar crumenophthalmus*) minnow traps (22.9 cm x 44.5 cm, with a 2.5 cm opening on each end) were randomly deployed along the periphery of each marsh at falling tide. While minnow traps do not adequately sample the entire salt marsh fish community (Rozas and Minello 1997), it does bias towards Fundulid species (Layman and Smith 2001) and provides a highly replicable sampling effort. Minnow traps were placed just below the water surface (as close to the marsh edge as possible) and secured to the marsh edge with a small metal stake. Surface water salinity was measured at each marsh using a YSI model 85 handheld meter. Fish were collected from the traps four hours after deployment and immediately placed on ice until returned to the laboratory

where fish were enumerated. Creek-level abundance was estimated as catch per unit effort (*n* fish/*n* traps; CPUE).

Historical fish and salinity data

To compare potential longer-term shifts in salinity and fish, historical data were utilized as collected and reported by Wedge and Anderson (2017). Daily average salinity was available at a subset of six sites (Stone Quarry, Long Bayou, Graham Creek, Manuel Bayou, Weakley Bayou, and Bayou Grande) for April 2012 – March 2013. These data (2012-13) were also used to build seven-day moving average frequency graphs and visually compared to graphs prepared for 2019-20 salinity data. Because fish capture methods were the same between studies, we compared CPUE of *F. grandis* between 2012-13 and 2019-20. To align similar seasonal sampling events, fish sampling data and CPUE from July and September 2012 were compared with July and October 2020 data collected as part of this study (see below).

The 2012-13 data were collected during a period when 24% of the Choctawhatchee-Escambia watershed (draining into Escambia Bay, see Fig. 4-1) experienced severe to exceptional drought (Akyuz 2017) and mean monthly rainfall between March 2011 and March 2012 was only 105 mm (±22), which contributed to reduced freshwater flows to estuaries. There was more precipitation between April 2012- March 2013 (coinciding with Wedge and Anderson 2017; average monthly precipitation = 149 mm [± 38]), but this period was still dryer than the June 2019-October 2020 period (this study; 170 mm [± 42]) and was closer to the 30-year (1990-2020) monthly average for the Pensacola, FL region (145 mm [±104]; Fig. 4-4). Much of the

rainfall between June 2019-October 2020 was the result of the 2020 Atlantic Hurricane season being the most active on record, and Hurricane Sally made landfall near Gulf Shores, Alabama on September 19, 2020 (one month before October 2020 sampling) and 630-760 mm of rainfall was reported in the region (Beven 2021). Therefore, the 2012-2013 dataset represents more extreme dry conditions, while the 2019-2020 dataset represents more extreme wet conditions. These circumstances provided a valuable dataset of extreme conditions to compare longer term changes in salinity and *F. grandis* abundance in response to changing environmental conditions.

Statistical Analysis

Concurrent creek salinity and fish data from 2019-20 were combined with 2012-13 data to evaluate the potential influence of salinity and salinity variability on *F. grandis* abundance. Using continuous daily average salinity, salinity for the three months preceding fish collection was averaged. Because fundulids have high site fidelity (Teo and Able 2003, Skinner et al. 2006, Nelson and DeVries 2014), it is reasonable to assume that sampled fish experienced salinity conditions that were observed within tidal creeks at least 1-4 months prior to sampling. Linear regression was used to examine the seasonal *F. grandis* abundance (CPUE) per creek and its relationship with the three-month preceding measure of salinity. To further evaluate the influence of salinity on *F. grandis* abundance, linear regression between average *F. grandis* CPUE for each sampling event and average creek salinity for the entire study period, and between average *F. grandis* CPUE for each sampling event and RB-index for the entire study

period were used. Regression was used to examine relationships between average creek salinity measured in the field and *F. grandis* CPUE from each fish sampling event.

To interpret interannual shifts in salinity (2012-13 to 2019-20) and salinity variability on *F. grandis*, we compared climatic data from the two time periods leading up to the respective data collection periods. Average monthly precipitation (mm) for a 30-year period (1990-2020) was calculated and averaged across April 2012-March 2013 and October 2019-September 2020 using data at Pensacola, Florida (mm; PRISM Climate Group). Additionally, the number of rain days (precipitation > 15 mm) for each study period were summed. A linear mixed-effects model (LMM) was used to test whether there were differences in abundance between 2012 (summer and autumn) and 2020 (summer and autumn). The response variable was CPUE, year (2012 and 2020) and season (summer and autumn) were fixed effects, and site was a random effect.

Model parameter normality was assessed using probability plots and Anderson-Darling normality tests using Minitab Statistical Software v. 20.3 (Minitab 17 Statistical Software 2022). For linear regressions of *F. grandis* abundance, CPUE and salinity metrics across both the 2020 and 2012 study periods were averaged. Additionally, linear regressions were used to analyze CPUE for each sample using mean site salinity metrics. Sample CPUE was log10 transformed to meet assumptions of normality Because LMMs are robust to violations of linear model assumptions, mean CPUE averaged for the entire period (2012 and 2020) was not transformed to meet assumptions of normality for the long-term abundance analysis. R statistical software was

used for regression and LMM analysis (R Core Team 2021). LMM analysis was done using the *nlme* package (Pinheiro et al. 2017), and ANOVA tables were generated to produce *p*-values.

Results

Salinity

Across all sites, salinity followed a seasonally predictable trend and increased steadily from June 2019 until January 2020 when the highest salinities were observed across all sites. Between January 2020 and March 2020 salinities rapidly decreased, before rising again in June 2020. Based on comparisons between 2012-13 data and 2019-20 data, salinity at all creeks examined (Stone Quarry, Long Bayou, Manuel Bayou, Graham Creek, Weakly Bayou, and Bayou Grande) was consistently lower during 2020 than during 2012 (Fig. 4-2). Mean salinity across all six sites during 2020 (11.8 ppt ±0.3) was 25% lower than during 2012 (15.2 ppt ±0.3) (ANOVA, $p < 0.001$, $F = 177.7$).

Fish assemblage and abundance

A total of 3,550 fish representing 12 species were captured over three sampling events (October 2019, July 2020, and October 2020). *Fundulus grandis* was the most commonly captured species (49.9% of total) however *Lagodon rhomboides* was also frequently encountered (34.2% of total). The remaining ten species represented <15.9% of the total caught and included: *Poecillia latipinna* (4.2% of total), *Gambusia holbrooki* (3.3% of total), *Adinia xenica* (2.7% of total), *Fundulus jekenksi* (2.5% of total), *Fundulus confluentus* (1.4% of total), *Cyprinodon*

variegatus (1.2% of total), *Fundulus pulvereus* (0.4% of total), *Anchoa mitchilli* (0.1% of total), *Centroprisis striata* (<0.1% of total), *and Fundulus similis* (<0.1% of total). *Fundulus jekenkski* is considered threatened (Chao et al. 2014) and all specimens of this species were released when it was identified within minnow traps.

A total of 829 *F. grandis* were captured in October 2019, 675 in July 2020, and 266 in October 2020, and creek-level measures of species CPUE were calculated (Table 4-2). *F. grandis* CPUE was highest during October 2019 and decreased through October 2020 with each sample, however this pattern was not consistent at each site, and there was apparent variability in CPUE among sites and across seasons (Table 4-2). CPUE averaged across all samples was highest at Indian Bayou and lowest at Heron Bayou (Table 4-2). Four sites had consistently low *F. grandis* and overall CPUE (Robinson, Manuel, Mulat, Heron) across all samples (Table 4-2).

Relationship between salinity and F. grandis abundance over time

Combining both the 2019-2020 and 2012 datasets, there was a positive relationship between CPUE and 3-month salinity ($p = 0.06$, $r^2 = 0.29$) and mean study period salinity ($p = 0.03$, $r^2 = 0.36$), and a negative relationship between CPUE and RB-index ($p = 0.06$, $r^2 = 0.29$) (Fig. 4-3). Abundance trends among sites were consistent between 2012 and 2020, with CPUE

being highest at Long Bayou during both 2012 and 2020, and lowest at Graham Creek and Manuel Bayou (Table 4-2).

Mean CPUE differed between years ($p = 0.053$, $F = 4.4$), and was higher in 2012 (7.98 ± 2.03) than during 2020 (4.92 ± 1.43). There were also differences between season ($p < 0.01$, $F = 9.2$), with mean CPUE being higher during summer (8.67 ± 1.85) than during autumn (4.23 ± 1.51).

Discussion

This study examined the effects of salinity on *F. grandis* abundance and found that it was positively associated with salinity and negatively associated with RB-index. While *F. grandis* can be found across a wide range of salinities (Griffith 1974, Crego and Peterson 1997), fish at our study sites were found to favor higher salinities in both this study and Wedge and Anderson (2017). Previous studies have found that estuarine fish species abundance is often greatest in mesohaline and polyhaline waters (Martino and Able 2003, 2003, Harrison and Whitfield 2006, Whitfield et al. 2006, Franco et al. 2019), and this response is likely driven by fish physiology. For example, low-salinity conditions can lead to increased metabolic costs associated with osmoregulation for *F. grandis* (Patterson et al. 2012), and can also lead to changes in the ionic balance of intracellular fluids, which can degrade proteins and damage cells (Evans and Kültz 2020). Further, low-salinity conditions have been shown to reduce *F. grandis* growth rates and increase mortality (Patterson et al. 2012, Ramee et al. 2016, Ramee and Allen 2016). While this was not observed in this study, it is possible that the timing of freshwater flows into tidal creeks during some years may coincide with peak *F. grandis* spawning within the marsh during the

spring, with the greatest amount of activity occurring during spring high tides (Greeley and MacGregor 1983), further reducing *F. grandis* abundance as embryonic and juvenile *F. grandis* are exposed to low salinity conditions.

Previous work has shown that watershed urban cover can contribute to increased flashiness in tidal creek salinity (Sanger et al. 2015, Wedge and Anderson 2017, Bickley et al. Chapter 2). The negative relationship between salinity RB-Index and *F. grandis* abundance, coupled with an increase in RB-index associated with development (Bickley et al. Chapter 2), suggest that coastal watershed urbanization leads to decreased *F. grandis* abundance in *Juncus*-dominated tidal creeks. This appears to occur even at low- to moderate-levels of watershed development observed at the majority of the study sites.

F. grandis (and all fish) were noticeably absent or present in lower-than-expected numbers at Mulat Bayou, Heron Bayou, Robinson Bayou, and Manuel Bayou across multiple sampling events. Of these sites Heron Bayou, Robinson Bayou, and Mulat Bayou had the lowest mean salinity (5.48 – 6.03 ppt) among sites but were also the study sites furthest north in their respective bay systems (Fig. 4-1), possibly limiting the effects of tidally advected marine waters which would increase salinity. Abundance was also low at Graham Creek during summer 2019 and autumn 2020, which was not surprising given that previous sampling efforts at this tidal creek also had lower than expected abundance for *F. grandis*, possibly related to a steep marsh edge slope which may enhance predator access (Wedge and Anderson 2017). Interestingly, Mulat, Trout, and Indian Bayou which were within 5 km of each other along the western

Escambia Bay coastline (Fig. 4-1), had very different abundances of *F. grandis*. Mulat Bayou (one of the more urbanized watersheds) ranked among the lowest creeks in terms of CPUE of *F. grandis* and total fish (Table 4-2), while both Trout and Indian Bayou (with more moderate levels of urban cover) (Table 4-2) were both among the highest creeks in CPUE. The proximity of these sites would likely preclude any geographical influence on base level salinity and *F. grandis* distributions and indicates that differences in watershed land cover are important here. Previous studies have indicated that *F. grandis* is a suitable indicator species (Nelson et al. 2014, Vastano et al. 2017, Jensen et al. 2019, Serafin et al. 2019), however these results suggest it is important to consider both base level salinity and watershed effects when interpreting their abundance.

The decrease in *F. grandis* abundance between 2012 and 2020 at the subset of comparable sites (Stone Quarry, Long Bayou, Manuel Bayou, Graham Creek, Weakly Bayou, and Bayou Grande) can be partially explained by the trend of decreasing salinity and increased precipitation within the region. During the present study, average monthly precipitation values (range = 15-566 mm, mean =170 mm [± 42]) were greater than the 30-year (1990-2020) average (145 mm [±104]) for the Pensacola, Florida region. This was consistent with a regional trend of decreasing salinity observed between 2012 and 2020 and at three nearby National Estuarine Research Reserve sites along the northern Gulf Coast (NOAA 2022). Our results, when contextualized with long-term datasets from the region suggest that salinities have decreased between the 2012 and 2020 study, and that decrease in salinity is driving a decline in *F. grandis* abundance. The freshening of coastal waters along the northern GOM will likely continue as precipitaiton is expected to intensify in the Southeastern United States under climate change

(Sinha et al. 2017, Armal et al. 2018), potentially further reducing *F. grandis* abundance in these tidal creeks.

While the focus of this study was on *F. grandis*, there were some notable observations in regard to other creek species. The fish species captured during 2019-2020 were similar to other species observations within tidal marshes along the northern GOM (Lowe and Peterson 2014b, Wedge and Anderson 2017) and the broader GOM region (Subrahmanyam and Coultas 1980, Krucynski and Ruth 1990, Rozas and Minello 1998, Gelwick et al. 2001, Minello et al. 2003). However, there were differences in the composition of the fish assemblage captured in 2019-2020 comapred to that captured in 2012-2013. For example, *P. latipinna* was the second most dominant species captured in 2012-13 and represented 15% of all fish sampled, but only represented 4.2% of fish sampled in 2019-2020. Similarly, *L. rhomboides* was not captured in 2012-13 but represented 34.2% of the sample collected in 2019-2020 and was captured at the same six sites sampled in 2012-2013. Though *P. latipinna* tolerates a wide range of salinity (Nordlie et al. 1992), field experiments have demonstrated decreased juvenile growth rate under freshwater conditions (Trexler and Travis 1990), suggesting that decreased salinity may have reduced *P. latipinna* abundance. *L. rhomboides* (20-100mm) like those captured in 2019-2020 are also a common species found in tidal creeks and salt marshes (Rozas and Minello 1998, Potthoff and Allen 2003), so it's absence in the 2012-2013 sample is peculiar, and it's presence during the 2019-2020 sample may be another indicator of a return to historical precipitation and salinity conditions. Like *P. latipinna*¸ *L. rhomboides* is also tolerant of a wide range of salinity (Shervette et al. 2007), suggesting that other environmental factors outside of the tidal creek salinity may be responsible for these changes in abundance over time. For example, the 2020 Atlantic Hurricane season was the most active on record and resulted in record amounts of

rainfall in the region. Tidal pumping following large storm events that occurred within the region may have forced some species out the tidal creeks in ebb tide, while also allowing for species from the wider bay to more easily enter as more marine seawater enters during spring tide (Brown et al. 2000, Du and Park 2019).

While there were observed changes in the composition of fish captured by minnow traps between 2020 and 2012, our ability to infer changes to the broader salt marsh fish assemblage during this period is limited due to the limitations of sampling equipment. Sampling of salt marsh fish assemblage is recognized as a difficult undertaking and gear choice can significantly influence what fish are caught and in what numbers (Rozas and Minello 1997). In a comparison of exhaustive seining vs. minnow traps in shallow tidal pools, seining captured both more individual fish and a greater number of fish species compared to minnow traps, with 99.5% of all captured fish in minnow traps being *F. heteroclitus*, a cogener of *F. grandis* (Layman and Smith 2001). Additionally, the size of minnow trap openings can exclude large fish species, while the wire mesh can allow juvenile fish to escape (Layman and Smith 2001). During minnow trap retrieval, small, juvenile fish were observed escaping through the minnow trap mesh, thereby biasing our catch towards large individuals (personal observation). However, the sampling gear used was suitable because this study's question was specifically focused on differences in abundance of *F. grandis* captured by minnow traps between sites and did not set out to capture

the larger salt marsh fish assemblage, and this sampling technique allowed for a direct comparison to 2012-2013 abundance data.

Conclusion

This study examined how watershed development alters the abundance of the resident marsh fish, *F. grandis*, in tidal creeks along the northern GOM, and found that *F. grandis* abundance decreased with RB-index, which was associated with urbanization. *F. grandis* abundance increased with mean salinity, and decreased between 2012 and 2020, likely in part because of decreased salinity as because precipitation was higher in 2020 than 2012. Other factors associated with large storm events and hurricanes in 2020, such as tidal pumping forcing fish out of tidal creeks, may have also led to decreased *F. grandis* abundance in tidal creeks. These results represent an important record of understudied tidal creek ecosystems along the northern GOM that are experiencing increased pressure from both land use and climate change. Without interventions at the watershed scale, the potential for both decreased base level salinity and increased salinity variability along the northern GOM coast, driven in part by increased precipitation and runoff associated with climate change in the Southeastern United States, will

likely lead to further decreases of *F. grandis* abundance, and continue to threaten tidal creek and salt marsh ecosystems.

Literature cited

Armal, S., N. Devineni, and R. Khanbilvardi. 2018. Trends in Extreme Rainfall Frequency in the Contiguous United States: Attribution to Climate Change and Climate Variability Modes. Journal of Climate 31:369–385.

Baker, D. B., R. P. Richards, T. T. Loftus, and J. W. Kramer. 2004. A new flashiness index: Characteristics and applications to Midwestern rivers and streams. Journal of the American Water Resources Association 40:503–522.

Barksdale, W. F., C. J. Anderson, and L. Kalin. 2014. The influence of watershed run-off on the hydrology, forest floor litter and soil carbon of headwater wetlands. Ecohydrology 7:803–814.

Beven, J. L. 2021. The 2020 Atlantic Hurricane Season: The Most Active Season on Record. Weatherwise 74:33–43.

Brown, C. A., G. A. Jackson, and D. A. Brooks. 2000. Particle transport through a narrow tidal inlet due to tidal forcing and implications for larval transport. Journal of Geophysical Research: Oceans 105:24141–24156.

Bucking, C., C. M. Wood, and M. Grosell. 2012. Diet influences salinity preference of an estuarine fish, the killifish *Fundulus heteroclitus*. Journal of Experimental Biology 215:1965–1974.

Chao, L., U. Bruce Collette (Smithsonian, R. Robertson (STRI), H. E.-P. (National U. of Mexico), J. M. (Texas A. University), C. C. Frank Pezold (Texas A&M University, J. Brenner (TNC), J. Carlson (NOAA), J. C. (Tulane University), P. C. (Louisiana S. University), J. S. (Texas A. University), L. T. (Texas A. University), D. G. (Florida S. University), C. F. D. James Tolan (Texas Parks and Wildlife Department, U. M. Maria Eugenia Vega-Cendejas (CINVESTAV-IPN, and H. J. (USGS S. E. S. Center). 2014. IUCN Red List of Threatened Species: Fundulus jenkinsi. IUCN Red List of Threatened Species.

Crego, G. J., and M. S. Peterson. 1997. Salinity Tolerance of Four Ecologically Distinct Species of Fundulus (Pisces: Fundulidae) from the Northern Gulf of Mexico. Gulf of Mexico Science 15.

Des, M., D. Fernández-Nóvoa, M. deCastro, J. L. Gómez-Gesteira, M. C. Sousa, and M. Gómez-Gesteira. 2021. Modeling salinity drop in estuarine areas under extreme precipitation events within a context of climate change: Effect on bivalve mortality in Galician Rías Baixas. Science of The Total Environment 790:148147.

Du, J., and K. Park. 2019. Estuarine salinity recovery from an extreme precipitation event: Hurricane Harvey in Galveston Bay. Science of The Total Environment 670:1049–1059.

Evans, T. G., and D. Kültz. 2020. The cellular stress response in fish exposed to salinity fluctuations. Journal of Experimental Zoology Part A: Ecological and Integrative Physiology 333:421–435.

Franco, T. P., L. M. Neves, and F. G. Araújo. 2019. Better with more or less salt? The association of fish assemblages in coastal lagoons with different salinity ranges. Hydrobiologia 828:83–100.

Gelwick, F. P., S. Akin, D. A. Arrington, and K. O. Winemiller. 2001. Fish Assemblage Structure in Relation to Environmental Variation in a Texas Gulf Coastal Wetland. Estuaries 24:285.

Gittman, R. K., S. B. Scyphers, C. S. Smith, I. P. Neylan, and J. H. Grabowski. 2016. Ecological Consequences of Shoreline Hardening: A Meta-Analysis. BioScience 66:763–773.

Greeley, M. S., and R. MacGregor. 1983. Annual and Semilunar Reproductive Cycles of the Gulf Killifish, Fundulus grandis, on the Alabama Gulf Coast. Copeia 1983:711.
Griffith, R. W. 1974. Environment and Salinity Tolerance in the Genus Fundulus. Copeia 1974:319.
Harrison, T. D., and A. K. Whitfield. 2006. Temperature and salinity as primary determinants influencing the biogeography of fishes in South African estuaries. Estuarine, Coastal and Shelf Science 66:335–345.
Jensen, O., C. Martin, K. Oken, F. Fodrie, P. López-Duarte, K. Able, and B. Roberts. 2019. Simultaneous estimation of dispersal and survival of the gulf killifish Fundulus grandis from a batch-tagging experiment. Marine Ecology Progress Series 624:183–194.
Krucynski, W. L., and B. F. Ruth. 1990. Fishes and Invertebrates. Pages 131–172 Ecology and Management of Tidal Marshes: A Model from the Gulf of Mexico.
Layman, C. A., and D. E. Smith. 2001. Sampling bias of minnow traps in shallow aquatic habitats on the Eastern Shore of Virginia. Wetlands 21:145–154.
Lowe, M. R., and M. S. Peterson. 2014. Effects of Coastal Urbanization on Salt-Marsh Faunal Assemblages in the Northern Gulf of Mexico. Marine and Coastal Fisheries 6:89–107.
Lowe, M. R., and M. S. Peterson. 2015. Body Condition and Foraging Patterns of Nekton from Salt Marsh Habitats Arrayed Along a Gradient of Urbanization. Estuaries and Coasts 38:800–812.
Marshall, W. S., J. C. Tait, and E. W. Mercer. 2016. Salinity Preference in the Estuarine Teleost Fish Mummichog (*Fundulus heteroclitus*): Halocline Behavior. Physiological and Biochemical Zoology 89:225–232.
Martino, E. J., and K. W. Able. 2003. Fish assemblages across the marine to low salinity transition zone of a temperate estuary. Estuarine, Coastal and Shelf Science 56:969–987.
Minello, T., K. Able, M. Weinstein, and C. Hays. 2003. Salt marshes as nurseries for nekton: Testing hypotheses on density, growth and survival through meta-analysis. Marine Ecology Progress Series 246:39–59.
Minitab 17 Statistical Software. 2022. Minitab, Inc.
Nelson, T. R., D. Sutton, and D. R. DeVries. 2014. Summer Movements of the Gulf Killifish (Fundulus grandis) in a Northern Gulf of Mexico Salt Marsh. Estuaries and Coasts 37:1295–1300.
NOAA, N. E. R. R. S. (NERRS). 2022. System-wide Monitoring Program. Data accessed from the NOAA NERRS Centralized Data Management Office website: Http://www.nerrsdata.org. (Available from: http://www.nerrsdata.org)
Noori, N., L. Kalin, S. Sen, P. Srivastava, and C. Lebleu. 2016. Identifying areas sensitive to land use/land cover change for downstream flooding in a coastal Alabama watershed. Regional Environmental Change 16:1833–1845.
Nordlie, F. G., and D. C. Haney. 1998. Adaptations in salt marsh teleosts to life in waters of varying salinity. Italian Journal of Zoology 65:405–409.
Nordlie, F. G., D. C. Haney, and S. J. Walsh. 1992. Comparisons of Salinity Tolerances and Osmotic Regulatory Capabilities in Populations of Sailfin Molly (Poecilia latipinna) from Brackish and Fresh Waters. Copeia 1992:741.
Patterson, J., C. Bodinier, and C. Green. 2012. Effects of low salinity media on growth, condition, and gill ion transporter expression in juvenile Gulf killifish, Fundulus grandis. Comparative Biochemistry and Physiology Part A: Molecular & Integrative Physiology 161:415–421.

Peterson, G. W., and R. E. Turner. 1994. The value of salt marsh edge vs interior as a habitat for fish and decapod crustaceans in a Louisiana tidal marsh. Estuaries 17:235–262.
Potthoff, M. T., and D. M. Allen. 2003. Site fidelity, home range, and tidal migrations of juvenile pinfish, Lagodon rhomboides, in salt marsh creeks. Environmental Biology of Fishes 67:231–240.
R Core Team. 2021. R: A language and environment for statistical computing. R Foundation for Statistical Computing, Vienna, Austria.
Ramee, S., C. Green, and P. J. Allen. 2016. Effects of Low Salinities on Osmoregulation, Growth, and Survival of Juvenile Gulf Killifish. North American Journal of Aquaculture 78:8–19.
Ramee, S. W., and P. J. Allen. 2016. Freshwater influences on embryos, hatching and larval survival of euryhaline Gulf killifish *Fundulus grandis* and potential constraints on habitat distribution: Early survival of *f. grandis* in fresh water. Journal of Fish Biology 89:1466–1472.
Rezaeianzadeh, M., L. Kalin, and C. J. Anderson. 2017. Wetland Water-Level Prediction Using ANN in Conjunction with Base-Flow Recession Analysis. Journal of Hydrologic Engineering 22:D4015003.
Rozas, L. P., and M. W. LaSalle. 1990. A Comparison of the Diets of Gulf Killifish, Fundulus grandis Baird and Girard, Entering and Leaving a Mississippi Brackish Marsh. Estuaries 13:332.
Rozas, L. P., and T. J. Minello. 1997. Estimating Densities of Small Fishes and Decapod Crustaceans in Shallow Estuarine Habitats: A Review of Sampling Design with Focus on Gear Selection. Estuaries 20:199.
Rozas, L. P., and T. J. Minello. 1998. Nekton Use of Salt Marsh, Seagrass, and Nonvegetated Habitats in a South Texas (USA) Estuary. Bulletin of Marine Science 63:21.
Rozas, L., and D. Reed. 1993. Nekton use of marsh-surface habitats in Louisiana (USA) deltaic salt marshes undergoing submergence. Marine Ecology Progress Series 96:147–157.
Rozas, L., and R. Zimmerman. 2000. Small-scale patterns of nekton use among marsh and adjacent shallow nonvegetated areas of the Galveston Bay Estuary, Texas (USA). Marine Ecology Progress Series 193:217–239.
Sanger, D., A. Blair, G. DiDonato, T. Washburn, S. Jones, G. Riekerk, E. Wirth, J. Stewart, D. White, L. Vandiver, and A. F. Holland. 2015. Impacts of Coastal Development on the Ecology of Tidal Creek Ecosystems of the US Southeast Including Consequences to Humans. Estuaries and Coasts 38:49–66.
Schneid, B. P., C. J. Anderson, and J. W. Feminella. 2017. The influence of low-intensity watershed development on the hydrology, geomorphology, physicochemistry and macroinvertebrate diversity of small coastal plains streams. Ecological Engineering 108:380–390.
Serafin, J., S. C. Guffey, T. Bosker, R. J. Griffitt, S. De Guise, C. Perkins, M. Szuter, and M. S. Sepúlveda. 2019. Combined effects of salinity, temperature, hypoxia, and Deepwater Horizon oil on Fundulus grandis larvae. Ecotoxicology and Environmental Safety 181:106–113.
Shervette, V. R., N. Ibarra, and F. Gelwick. 2007. Influences of Salinity on Growth and Survival of Juvenile Pinfish Lagodon rhomboides (Linnaeus). Environmental Biology of Fishes 78:125–134.

Sinha, E., A. M. Michalak, and V. Balaji. 2017. Eutrophication will increase during the 21st century as a result of precipitation changes. Science 357:405–408.
Subrahmanyam, B., and L. Coultas. 1980. Studies on the Animal Communities in Two North Florida Salt Marshes Part III. Seasonal Fluctuations of Fish and Macroinvertebrates. 30:790–818.
Trexler, J. C., and J. Travis. 1990. Phenotypic Plasticity in the Sailfin Molly, *Poecilia Latipinna* (Pisces: Poeciliidae). I. Field Experiments. Evolution 44:143–156.
Vastano, A. R., K. W. Able, O. P. Jensen, P. C. López-Duarte, C. W. Martin, and B. J. Roberts. 2017. Age validation and seasonal growth patterns of a subtropical marsh fish: The Gulf Killifish, Fundulus grandis. Environmental Biology of Fishes 100:1315–1327.
Wagner, M. C., and H. M. Austin. 1999. Correspondence between environmental gradients and summer littoral fish assemblages in low salinity reaches of the Chesapeake Bay, USA. Marine Ecology Progress Series 177:197–212.
Wedge, M., and C. J. Anderson. 2017. Urban Land use Affects Resident Fish Communities and Associated Salt Marsh Habitat in Alabama and West Florida, USA. Wetlands 37:715–727.
Wedge, M., C. J. Anderson, and D. DeVries. 2015. Evaluating the Effects of Urban Land Use on the Condition of Resident Salt Marsh Fish. Estuaries and Coasts 38:2355–2365.
Whitfield, A. K., and M. Elliott. 2002. Fishes as indicators of environmental and ecological changes within estuaries: A review of progress and some suggestions for the future. Journal of Fish Biology 61:229–250.
Whitfield, A. K., R. H. Taylor, C. Fox, and D. P. Cyrus. 2006. Fishes and salinities in the St Lucia estuarine system—A review. Reviews in Fish Biology and Fisheries 16:1–20.

Table 4-1. Study creek watershed area (km^2), land cover (% of watershed coverage from 2016 NLCD), RB-Index and mean annual salinity (± standard error).

Site	Area (km2)	Urban* (%)	Forest/Herb. (%)	Wetland* (%)	Shrub (%)	Ag* (%)	Barren/Water (%)	RB-index	Salinity (ppt)
Wolf-Perdido Bay									
Stone Quarry (SQ)	0.4	0	93.6	6.4	0	0	0	0.2	14.68 (± 0.12)
Manuel Bayou (MB)	6.2	8.4	37.3	6.2	1.4	46	0.2	0.52	10.60 (± 0.10)
Weakley Bayou (WB)	6.7	17.6	24.2	55.2	1.7	0.6	0.4	0.72	11.25 (± 0.22)
Long Bayou (LB)	6.8	3.3	23.1	61	0.2	11	0.4	0.84	9.94 (± 0.23)
Graham Creek (GC)	8.8	8.4	45.6	21.3	1.4	21	2.2	1.05	11.42 (± 0.14)
Escambia-Pensacola-East Bay									
Trout Bayou (TB)	2.5	13.9	10.5	73.5	0.1	0.5	1.4	0.4	10.6 (± 0.20)
Robinson Pointe (RP)	3.1	8.2	33.9	37.3	2	13	4.5	1.48	5.99 (± 0.24)
Indian Bayou (IB)	5.1	12.3	1.9	84.7	0	0	1	0.58	10.67 (± 0.19)
Mulat Bayou (MB)	10.3	24.8	13.3	57.2	0.6	2.7	1.2	1.9	6.03 (± 0.20)
Heron Bayou (HB)	13.6	38.8	10.3	48.1	0.4	1.2	0.5	1.5	5.43 (± 0.16)
Bayou Grande (BG)	18.3	27.6	19.8	47.5	0.5	2.2	1.4	1.39	11.60 (± 0.22)
Texar Bayou (TX)	46.4	87.5	6.6	2	0.2	0.2	3.1	0.75	11.41 (± 0.16)

*Urban includes all levels of development (open, low, medium, high), wetland includes woody and emergent wetlands, and Ag includes pasture and row crops.

Table 4-2. Catch per unit effort of *Fundulus grandis* during July 2012, September 2012, October 2019, July 2020, and October 2020 across all study sites and mean (±SE) catch per unit effort for each sample season. % in parentheses represents proportion of urban land cover. Dashed lines indicate sites not part of the Wedge and Anderson (2017) dataset. No sample indicates that a sample was not collected. Zero indicates no *F. grandis* were captured.

Site	July 2012	September 2012	October 2019	July 2020	October 2020
Stone Quarry (0%)	10.3	7.55	3.58	4.08	1.50
Long Bayou (3.3%)	23.95	18.8	6.25	14.33	5.58
Robinson Bayou (8.2%)	-	-	0.33	0.00	0.00
Graham Creek (8.4%)	2.85	0.85	0.08	6.83	0.17
Manuel Bayou (8.4%)	3.75	4.8	1.83	0.00	0.00
Indian Bayou (12.3%)	-	-	19.25	no sample	6.33
Trout Bayou (13.9%)	-	-	17.75	6.17	2.50
Weakley Bayou (17.0%)	10.15	6.15	4.67	12.42	2.00
Mulat Bayou (24.8%)	-	-	0.00	0.00	1.00
Bayou Grande (27.6%)	5.65	1.00	12.75	9.75	2.42
Heron Bayou (38.8%)	-	-	0.00	0.00	0.17
Texar Bayou (87.5%)	-	-	2.58	2.67	1.75
Mean	9.44 (±2.90)	6.32 (±2.94)	5.76 (±1.93)	5.11 (±0.50)	1.95 (±0.58)

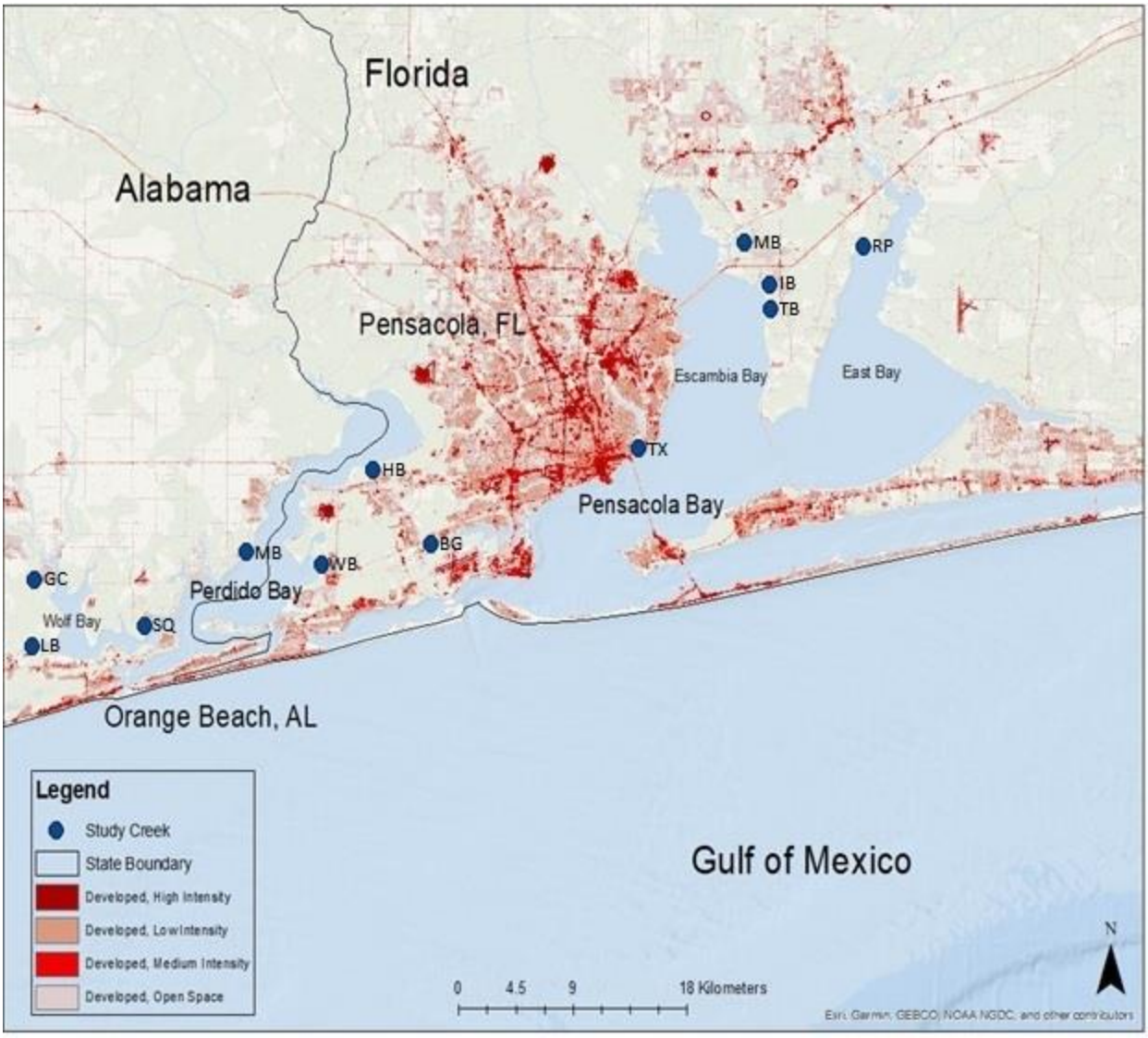

Figure 4-1. Map of study region. Blue dots represent a study site and red shading represents intensity of development, from 2016 NLCD (see Table 4-1 for creek abbreviation names).

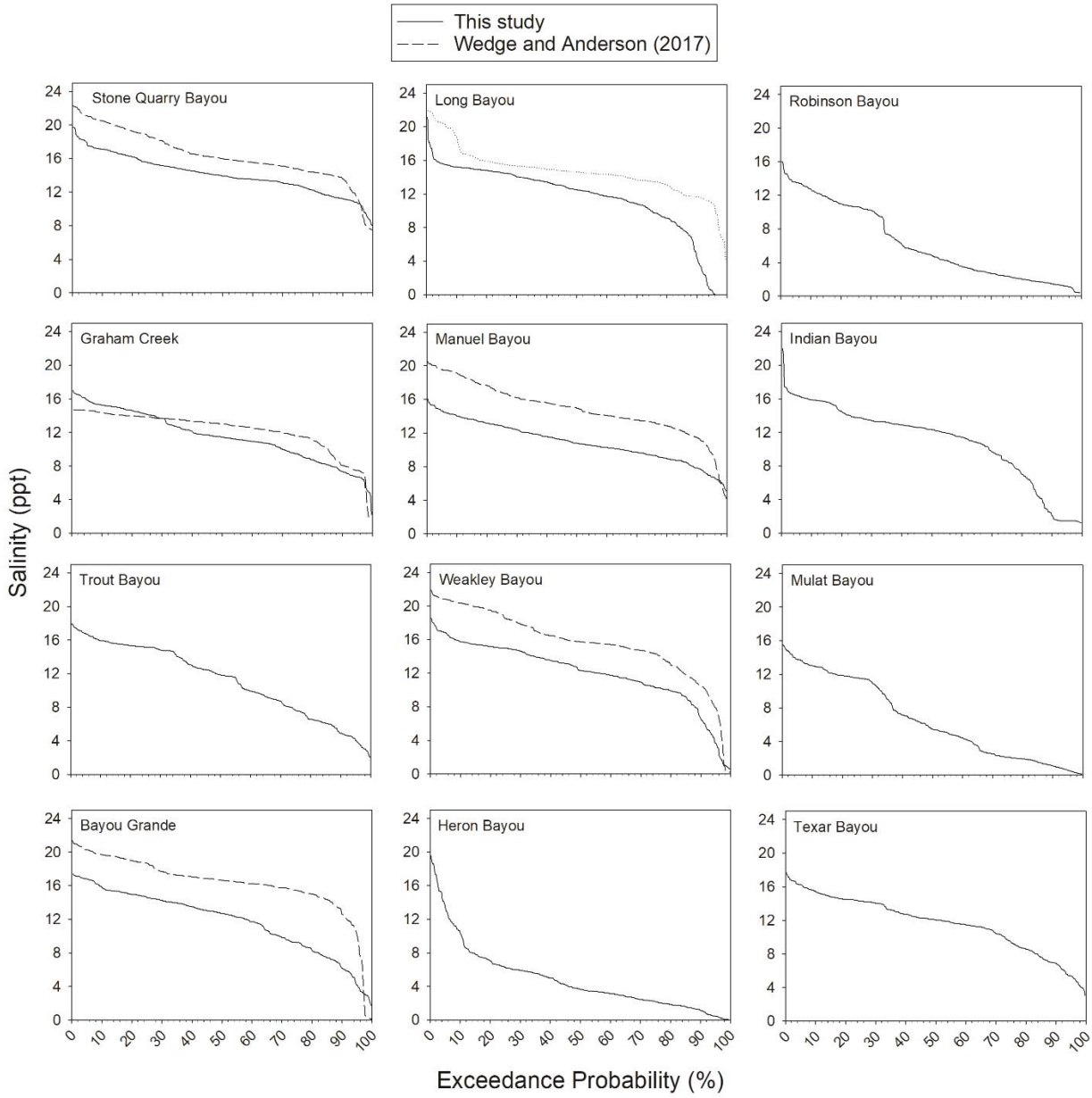

Figure 4-2. Exceedance probability curves for salinity measured all 12 study sites across the entire current study period (solid line, June 2019-May 2020) and from Wedge and Anderson 2017 (dashed line; April 2012-March 2013). Gaps in data were filled using predicted values from Isik et al. (in preparation).

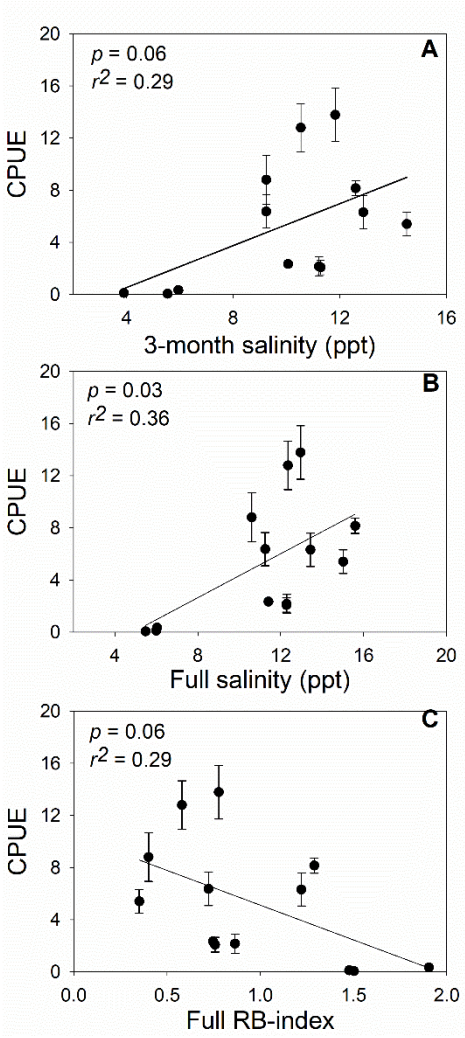

Figure 4-3. Regression analysis of (A) mean *F. grandis* catch per unit effort (CPUE) and mean 3-month salinity (ppt) preceding sampling averaged across all samples collected during July and September 2012 and June 2020-October 2020, (B) mean *F. grandis* CPUE and mean site salinity (ppt) averaged across all samples collected during April 2012-March 2013 and June 2020-October 2020, and (C) mean *F. grandis* CPUE and mean RB-index averaged across all samples collected during April 2012-March 2013 and June 2020-October 2020. Error bars represent standard error.

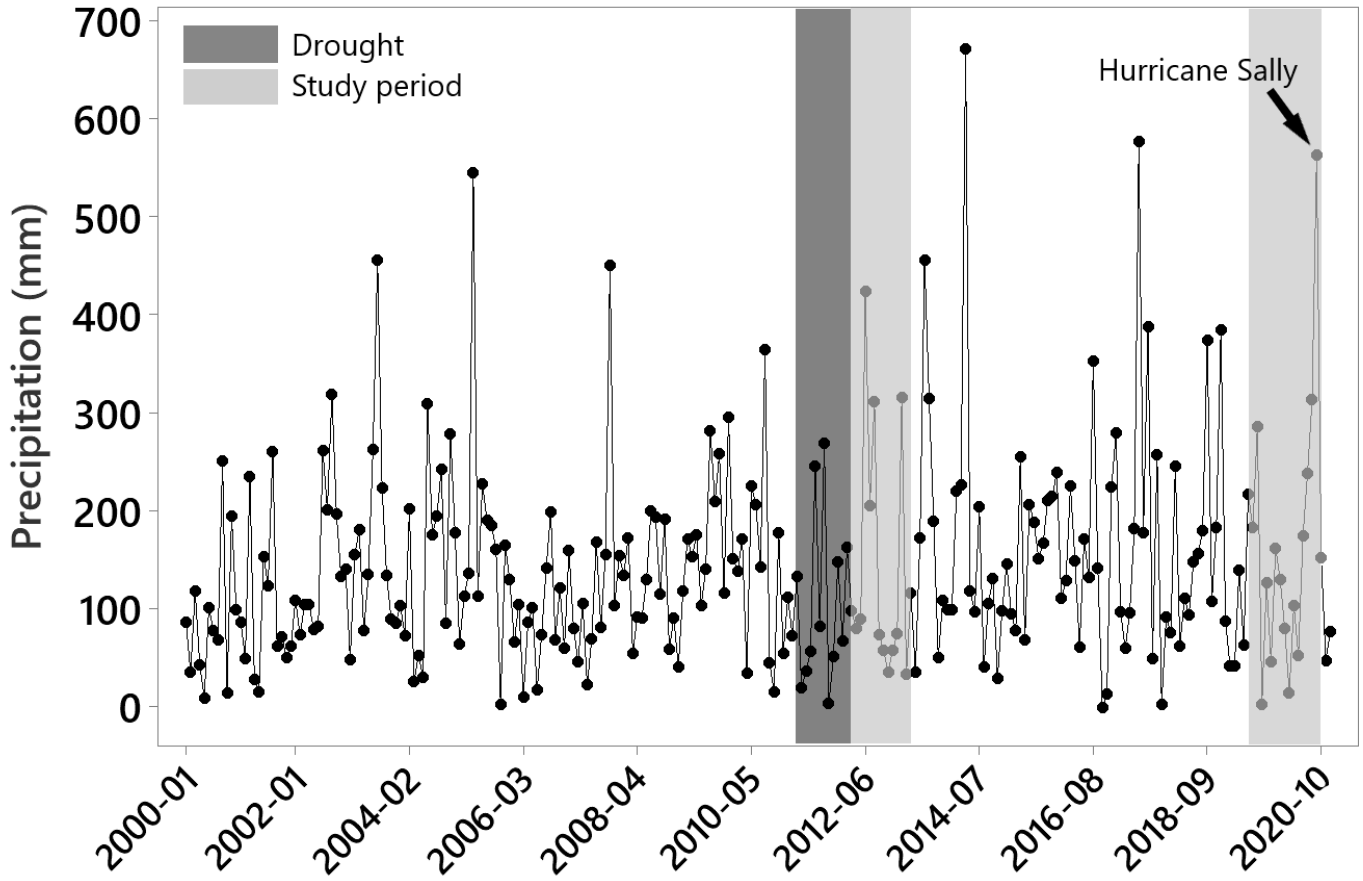

Figure 4-2. Mean monthly precipitation for Pensacola, Florida between January 2000 and December 2020. Study periods (April 2012-March 2013 and June 2019-October 2020) are highlighted in light gray and drought preceding April 2011-March 2012 sample is highlighted in dark gray. Hurricane Sally is indicated by the black arrow. Data from PRISM.

Chapter 5: Effects of watershed development and diet on the condition of *Fundulus grandis.*

Abstract

Measures of fish condition have been used to indicate the general health of an individual fish and can also be used to indicate changes in the environmental condition of an ecosystem. Here, we captured *Fundulus grandis*, a resident salt marsh fish, from 12 tidal creeks (2^{nd} to 3^{rd} order) located along a gradient of urbanization and salinity along the northern Gulf of Mexico (GOM). We quantified the frequency of occurrence (%FO) and weight (%W) of dietary items found in *F. grandis* stomachs (n=205) over three seasons and estimated the caloric density and other measures of condition of captured fish (n=125) over two seasons. We found that *F. grandis* diet was similar across sites and seasons and had a higher %FO of fish compared to other dietary studies of *F. grandis* in salt marshes along the northern GOM. Further, caloric density of fish increased with the %FO of fish and decreased with the %FO of macroinvertebrates. We found no effect of watershed development on measures of fish condition, but %FO of fish was greatest at lower salinities and %FO of macroinvertebrates was greatest at higher salinities. These two dietary items were also inversely related, suggesting a shift in diet along the salinity gradient. Our findings suggest that the prevalence of fish in *F. grandis* diet is due to heavy utilization of

the salt marsh surface by calorically rich juvenile fish and highlights the importance of fringing salt marshes along higher-order tidal creeks as nursery and forage habitat.

Introduction

Various measures of fish condition have been used since the early 20th century in fisheries science to indicate overall health of a fish (Fulton 1904, Froese 2006). Condition indices can be as simple as fish length to weight ratios (Fulton 1904) or the slope of length-weight regressions (Le Cren 1951), to more intensive, physiological measurements such as liver somatic index (Delahunty and de Vlaming 1980, Adams and Mcleans 1985), caloric density (Hartman and Brandt 1995), or RNA to DNA ratios (Clemmesen et al. 2003). Because each conditional measure describes something physiologically different (Bolger and Connolly 1989, Jakob et al. 1996, Stevenson and Woods 2006), multiple measurements are ideally used (Adams and Mcleans 1985, Ferraro et al. 2001, Brown and Murphy 2004, Wedge et al. 2015) so as to take into account the different factors that affect fish condition.

Fish condition is often assessed based on morphological or physiological measurements that can reflect changes in season, sexual reproductive status, and nutritional status of individual fish or fish populations (Booth and Keast 1986, Bolger and Connolly 1989, Mézin and Hale 2000). The Gulf killifish (*Fundulus grandis*) is a ubiquitous fish species in the Cyprinidae family that is commonly detected as a resident in salt marshes in the GOM. In a study along coastal Alabama, it was noted that *F. grandis* had lower measures of both caloric density and liver somatic index (LSI) during the summer compared to other seasons, possibly as a result of

increased energy expenditure related to reproduction (Wedge et al. 2015). Similarly, LSI (reported as hepatosomatic index) of largemouth bass (*Micropterus salmoides)* varied with season and size class, with large fish having higher LSI in April and lower levels in May, before increasing during summer, while small and medium fish had low LSI levels during late summer, likely in response to high temperature (28.8 to 29.7°C) above the optimum temperatures for feeding (27 °C; Brown and Murphy 2004). In addition to reduced feeding rates associated with seasonality, the availability and abundance of prey items likely play an important role in determining fish condition. Mummichog (*Fundulus heteroclitus)*, a cogener of *F. grandis*, saw increased metabolic costs as benthic prey abundances decreased in a Staten Island, New York estuary (Goto and Wallace 2010), while the slope of the length-weight relationship of *F. grandis* from landscapes where fish had higher frequencies of empty stomachs was lower than compared to fish from other landscapes with more abundant prey items (Lowe and Peterson 2015).

In addition to prey availability, the composition and quality of diet may also influence fish condition (Weisberg and Lotrich 1982, Goto and Wallace 2010). As the availability of animal prey decreases, omnivorous fish such as *F. grandis* are capable of shifting their diet to feed on more readily available, lesser-quality resources, such as algae, detritus, mollusks, and crustaceans (Persson 1983, Brabrand 1985, Rozas and Lasalle 1990, Pothoven et al. 2004). For example, Rozas and Lasalle (1990) found that *F. grandis* in St. Louis Bay, Mississippi fed mainly on less calorically-dense (Weisberg and Lotrich 1982) fiddler crabs (*Uca pugnax*), which were abundant on the marsh surface. The availability and abundance of prey items may be a key factor when considering the growth and vigor of fish. Reduced growth rates were observed when *F. grandis* were fed a diet of fiddler crabs compared to a diet of opossum shrimp (*Palaemonetes*

pugoi), which is likely a result of the lower caloric content in fiddler crabs (Weisberg and Lotrich 1982). The ability of *F. grandis* to shift foraging behavior depending on prey availability has also been observed in the closely related *F. heteroclitus* (Goto and Wallace 2011).

As the omnivorous fish shift to less calorically rich, yet more abundant food items, they may show decreased body condition. For example, following the invasion of zebra mussels (*Dreissena polymorpha*) in southeastern Lake Michigan in 1992, densities of high-quality amphipods declined and lake whitefish (*Coregonus clupeaformis*) diet shifted to include more zebra mussels, which led to a decrease in mean body length and weight post-invasion (Pothoven et al. 2004). Some fish, however, can shift diet with no detrimental effects on body condition. For example, when the diet of rainbow trout shifted due to urban development, there was no change in condition (Brumm 2019). The trophic position of *Awaous stamineous*, a native Hawaiian goby, was found to be elevated in urban streams, as their diet shifted away from algae to exotic macroinvertebrates, though this shift in diet caused no change in measured condition (Lisi et al. 2018). Similarly, redbreast sunfish (*Lepomis auratus*) diet not only shifted to include terrestrial prey when aquatic prey abundance decreased in association with changes in land use, but their trophic position decreased as they fed in more productive urban streams (Helms et al. 2018). Changes in habitat suitability associated with watershed development may represent an important alteration to fish diet composition, with differing effects on fish condition.

Because measures of fish condition are a product of the physiological status of a fish as determined by seasonality, reproductive status, the availability and composition of prey, and

habitat suitability, conditional indices may be a useful indicator of watershed disturbance or urbanization (Ferraro et al. 2001, Krebs et al. 2014, Lowe and Peterson 2015, Wedge et al. 2015). For example, *F. grandis* in more urbanized watersheds have been shown to have lower measures of condition (measured as length-weight slope; Lowe and Peterson 2015). The difference in diet as a function of watershed urbanization in Lowe and Peterson (2015) was supported by high frequencies of empty stomachs in fish from more urban watersheds, which is likely a product of decreased macroinvertebrate abundances in more developed watersheds (Stepenuck et al. 2002, Wang and Kanehl 2003, Partyka and Peterson 2008, Washburn and Sanger 2011, Lisi et al. 2018, Brumm et al. 2019). Urban conditions have been shown to result in increased nutrient loading (Walsh et al. 2005) which may increase the abundance of algae for fish consumption. Food quality that is poorer in more urbanized watersheds may lead to changes in fish size and body condition (Pothoven et al. 2004, Lowe and Peterson 2014).

Recent development along the northern GOM within 10-50 km of the coast has been extensive and characterized by low-density residential and commercial development (Xian et al. 2012). Coastal watersheds are often linked to coastal waters through tidal creeks and their associated fringing salt marshes, and the water-quality of these tidal creeks and salt marshes is reflective of changes within the watershed (Holland et al. 2004). Because tidal creeks represent an important transition between watersheds and estuaries, these areas may be particularly sensitive to water quality and habitat shifts related to urbanization. Even low to moderate-intensity urban land use may still be enough to see changes in habitat suitability or prey availability for the salt marsh resident *F. grandis* (Partyka and Peterson 2008, Washburn and Sanger 2011, Lowe and Peterson 2015). Although most work has been focused on freshwater

systems (see Washburn and Sanger 2011), multiple studies using other aquatic environments have shown deleterious effects of land use change on macroinvertebrate communities (Stepenuck et al. 2002, Wang and Kanehl 2003, Partyka and Peterson 2008, Washburn and Sanger 2011, Lisi et al. 2018, Brumm et al. 2019). Factors explaining the negative effects include reduced riparian shoreline and sub-aquatic vegetation, altered flow regimes, reduced habitat substrate, increased suspended solids input, increased temperature, and increased toxicant inputs (Rozas and Reed 1994, Walsh et al. 2005, Francis and Schindler 2006, 2009). Examining low-order freshwater streams on the Alabama coast, Schneid et al. (2017) found that some changes to macroinvertebrate communities were related to drainage from impervious surfaces, even when focusing only on low-density residential areas. Contrary to freshwater streams, low-order tidal creeks are influenced by a combination of watershed and estuarine processes, however negative effects have been detected here too. Highly urbanized tidal creeks along Tampa Bay, Florida had very low abundances of grass shrimp (*Palaemonetes* spp.) when compared to undeveloped, and even industrial, tidal creeks (Krebs et al. 2013). A similar negative relationship was observed along the Biloxi Bay estuary, where both macroinvertebrate (dominated by grass shrimp) and macroinfaunal (dominated by oligochaetes) abundances decreased as urban land use and marsh fragmentation increased (Lowe and Peterson 2014). Amphipod and bivalve species were absent along the Pascagoula River estuary shorelines with both medium and high levels of alteration (Partyka and Peterson 2008). Not only do potential fish prey items, represented above as macroinvertebrate and macroinfaunal assemblages, decrease with increasing development, but the composition of these assemblages can shift to include more pollution tolerant species and less pollution sensitive species (Lerberg et al. 2000, Washburn and Sanger 2011). As the suite of prey

items available to *F. grandis* and other resident salt marsh fish changes, their diets will reflect this change in land use and subsequent prey availability.

In urbanizing tidal creeks, salinity variation has been identified as potentially important disturbance in estuarine systems (Lerberg et al. 2000, Holland et al. 2004, Sanger et al. 2015, Wedge and Anderson 2017). Changes in *F. grandis* diet associated with land use change have been documented (Lowe and Peterson 2015), but is yet unknown what effect increased salinity variation associated with watershed development has on the diet of the common resident fish *F. grandis* in tidal creeks. Similarly, few studies have assessed *F. grandis* diet from tidal creeks with smaller, fringing salt marsh habitat.

Here, I investigated the relationship between low-intensity coastal watershed development and fish diet, and whether changes in fish diet associated with development and environmental changes lead to changes in fish condition. Specifically, I hypothesized that low-intensity urbanization affects *F.grandis* diet and body condition because urban-related changes in salinity and nutrient concentrations alter the composition and abundance of the available prey base. I predicted that *F. grandis* from watersheds with higher salinity variation and nutrient concentrations will have diets composed of smaller proportions of fish and macroinvertebrates and larger proportions of algae and detritus when compared to watersheds with lower levels of salinity variation and nutrient concentrations. I predicted that *F. grandis* with diets composed of larger proportions of fish and macroinvertebrates and small proportions of algae and detritus will have greater measures of condition. This study is one of the few to analyze *F. grandis* diet, and

the only other study to examine the effects of land use on *F. grandis* diet. As coastal development continues, more studies are needed to understand the effects of low-intensity urbanization on fish diet and the potential bioenergetic changes that may result.

Methods

Study sites

I sampled 12 second- to third-order, mesohaline tidal creeks located in coastal Alabama and northwest Florida (Fig. 5-1). Watersheds for each creek were delineated using ArcMap (v10.7.1) using 3-m digital elevation models (DEM). Using the 2016 National Land Cover Dataset (NLCD 2016), I quantified land cover in each watershed and each land cover class was presented as a percentage of the watershed. Five creeks were in the Wolf-Perdido Bay system, where developed land-cover within each watershed ranged from 0.0 to 17.6% (NLCD 2016) and watershed area ranged from 0.4 to 8.8 km^2 (Table 5-1). Seven creeks were in the Escambia-Pensacola-East Bay system, where developed land-cover in each watershed ranged from 8.2% to 87.5% (the only highly urbanized study site; NLCD 2016) and watershed area ranged from 2.5 to 46.4 km^2 (Table 5-1). All sites were tidally influenced coastal creeks with fringing salt marshes, dominated by *Juncus roemerianus* (black needlerush), with other marsh vegetation including *Spartina alterniflora* (smooth cordgrass) and *Cladium jamaicense* (sawgrass). *Juncus roemerianus* was used as an indicator of comparable salinity regimes across creeks. Watershed development is primarily low-to medium-intensity residential development, with bulkheads and docks being common along the creeks. The largest and most heavily developed watershed, Texar

Bayou, was in downtown Pensacola and was a mix of residential, commercial, and industrial development.

Salinity, and SWAT modeling of nutrient concentrations

HOBO U-24-002-C saltwater conductivity sensors (Onset Computer Corporation, Bourne, Massachusetts) were deployed in the summer of 2019 at each site and collected data from June 2019 – October 2020. Sensors measured surface water hourly conductivity (µS/cm) and temperature (°C), with conductivity being converted to salinity (ppt). Sensor malfunctions results in some site data gaps that were filled with modeled estimates (see Chapter 2). Using the salinity data, a modified index of flashiness based on the Richard-Baker (RB) index (Baker et al. 2004) was used to evaluate the "flashiness" of salinity changes in tidal creeks. Salinity RB-index has previously been used to evaluate changes in salinity and streamflow along the northern GOM coast (Barksdale et al. 2014, Wedge and Anderson 2017, Rezaeianzadeh et al. 2017). RB-index and mean salinity were calculated for the entire study period (June 2019-October 2020), and mean salinity three months prior to fish sampling was calculated (see Chapter 3). Although the primary intent of the study design was to capture an urban gradient related to creek watersheds, the sites selected also represented a natural salinity gradient related to proximity to major bay freshwater sources and the Gulf of Mexico. Because of this, sites varied in mean salinity (5.5 ± 0.2 - 14.1 ± 0.1 ppt) and represented a range of mesohaline conditions. For each creek, modelled mean daily estimated nitrate (NO_3), ammonium (NH_4), and mineralized phosphorous (MinP) loads from the Soil and Water Assessment Tool (SWAT) were used to evaluate the effects of

land use practices on fish diet and condition (see Chapter 3 for details). SWAT estimates were averaged for the 3-month period prior to fish sampling.

Fish collection

Fundulus grandis were sampled in October (autumn) 2019, July (summer) 2020, and October (autumn) 2020 in all 12 creeks over the course of two weeks. In each creek, three minnow traps (22.9 x 44.5cm, with a 2.5 cm opening on each end) baited with commercially available baitfish (generally *Brevortia* sp. and *Selar crumenophthalmus*) were deployed at four different marshes. Minnow traps were randomly deployed just below the water surface along the edge of the marsh at falling tide. Minnow traps were deployed for four hours before being collected, inspected, and fish placed on ice until return to the laboratory. Fish collected during October 2019 were fixed in formalin, preserved in 95% ethanol, and deposited in the Auburn University Museum of Natural History. Fish collected during July and October 2020 were not preserved.

Diet analysis

During each sampling event per season, *F. grandis* >50 mm in length were collected from each creek for dietary analysis and attempted to analyze at least 30 guts per creek, but analysis of this many guts was not always possible based on limited catch numbers. Stomachs were opened according to protocols described in Gelwick and Matthews (2007) and prey items identified to the lowest taxonomic level possible (Heard 1982, Abele and Kim 1986). Because some diet items were only parts, both the frequency of occurrence and percent weight methods (Hyslop 1980) were used for dietary analysis. Dietary items were classified as “algal or vegetation,”

"detritus," "crab," "macroinvertebrates (non-crab macroinvertebrates; gastropods, terrestrial arthropods and arachnids, crustaceans)" and "fish." Unidentifiable material was classified as "unknown," and fish without any stomach contents were classified as "empty stomach."

The frequency of occurrence method does not quantify the amount of a specific food item in a stomach, but only whether a specific dietary item occurred in a stomach and presents this as a percentage of all stomachs in the analysis. Frequency of occurrence is calculated as follows:

$$\%FO_i = \frac{N_i}{N} \times 100$$

Where FO_i is the frequency of occurrence of dietary item $\boldsymbol{i}$, $\boldsymbol{N_i}$ is the number of consumer fish with dietary item $\boldsymbol{i}$ present, and $\boldsymbol{N}$ is the number of total fish analyzed for that sample (Manko 2016). The %FO was calculated for each dietary item per creek and per sampling event.

The percent weight (%W) of each dietary item quantifies the amount of each dietary item found in all sample stomachs and presents this as a percentage of all stomachs analyzed from that sample and is calculated as follows:

$$\%\boldsymbol{W} = \frac{W_i}{W_t} \times 100$$

Where %W is the proportion of a dietary item $\boldsymbol{i}$ from each sample, $\boldsymbol{W_i}$ is the weight of item $\boldsymbol{i}$, and $\boldsymbol{W_t}$ is the total weight of all dietary items from all stomachs from that sample. The %W was calculated for each dietary item per creek and per sampling event.

Fish condition

Fundulus grandis collected during summer and autumn 2020 were analyzed for caloric density (summer $n = 50$, autumn $n = 75$). *F.grandis* collected during autumn 2020 were not analyzed for caloric condition because they were preserved in alcohol. For caloric density analysis, fish were selected to represent the observed size range at each site. Each fish was weighed (wet weight), then the whole fish was ground to homogenization and oven dried. One pellet per fish (0.07-0.20 g pellets) was ignited in a semi-micro bomb calorimeter (Parr instrument Co., Molline, Illinois). Measured caloric density of each pellet was used to calculate caloric density per dry weight. Caloric density per wet weight was used for statistical analysis and was calculated as follows (Glover et al. 2010):

$$\text{caloric density} = \text{calorie per gram dry weight} \times \frac{\text{wet weight}}{\text{dry weight}}$$

Fulton's condition factor

Fulton's condition factor (*K*) (Fulton 1904, Froese 2006) can be used to describe the weight of a fish given its length, and how that varies from the weight *expected* based on length, and has been used as a standardized measure of fish condition in fisheries science (Froese 2006).

Fulton's *K* was calculated as follows:

$$K = \frac{W}{L^3} \times 100$$

Where *K* = Fulton's condition factor, W = whole body wet weight (g), and L = length (cm), and the factor of 100 allows *K* to be close to 1. $K > 1$ indicates a fish that is heavier than would be

expected at a given length and $K < 1$ indicates a fish that is lighter than would be expected at a given weight. Fulton's *K* was calculated for all *F. grandis* sampled in all three sampling seasons.

Statistical analysis

Two principal component analyses (PCA) were used to understand the patterns of diet, environmental conditions, and body condition across sites and seasons. Using individual fish data, the first PCA was used to visualize diet composition across sites in Euclidean space based on presence/absence of each dietary item and subsequent correlations to creek salinity, nutrient concentrations, and fish size. Normality of explanatory variables was assessed using probability plots and Anderson-Darling normality tests using Minitab Statistical Software v. 20.3 ("Minitab 17 Statistical Software" 2022), and all explanatory variables (length, RB-index, full salinity, 3-month salinity, temperature, NO_3^-, NH_4^+, and MinP) were log10 transformed to meet normality assumptions of PCA.

The second PCA was used to visualize fish condition in Euclidean space based on individual fish caloric density, Fulton's K, and length, across sites and seasons and subsequent correlations to dietary items. Caloric density, Fulton's *K* and caloric density were log10 transformed to meet PCA assumptions of normality, while length was untransformed. For each

fish, the presence/absence of each dietary item was indicated and utilized (without being transformed) in the PCA to detect correlations with condition measures.

To examine creek-level patterns, a linear mixed-effects model (LMM; Harrison et al. 2018) was used to detect the statistical relationship between mean fish condition and mean %FO and %W of fish dietary items at each site. Six separate models were run using length, Fulton's *K*, and caloric density as response variables, with three models using %FO of dietary items and three models using %W of dietary items. For each model, fixed effects were dietary items (empty stomachs, algae and vegetation, crab, detritus, fish, and macroinvertebrates). Because we were interested in the effects of specific dietary items on fish condition, unknown dietary items were not included in these models. Site was included as a random effect to take into account variation among tidal creeks. Because LMM's are robust to violations of model assumptions pertaining to normality, fixed effects were not transformed to meet those assumptions. R statistical software (version 3.3.3; R Project for Statistical Computing, Vienna, Austria) and the *lme4* package (Bates et al. 2015) were used for all LMM analyses. The *car* package (Fox and Weisberg 2019) was used to analyze fixed effects on response variables, which generated a type-II analysis of variance (ANOVA) table for each LMM, and we then used the partial likelihood

ratio test (Fox and Weisberg 2019) to generate *p*-values. In addition to PCA and LMM analysis, Analysis of variance (ANOVA) was used to analyze differences in caloric density by season.

Results

Creek salinity, salinity variation, and nutrient concentrations

Mean salinity across all sites was between 10.6 ppt (Manuel Bayou) to 14.1 ppt (Stone Quarry Bayou) (see Table 3-3), and 3-month salinity varied by season, with mean salinity being 12.7 ppt during autumn 2019, 10.4 ppt during summer 2020, and 9.2 ppt during autumn 2020. Full RB-index for all sites where diet analysis was complete was between 0.20 (Stone Quarry Bayou) and 1.39 (Bayou Grande) (see Table 3-3). Across the entire study period and at sites where diet analysis was completed, SWAT modeled MinP, NH_4^+, and NO_3^- concentrations were greatest at Texar Bayou (10.1 µg/L, 9.3 µg/L, and 71.1 µg/L respectively). MinP was lowest at Indian Bayou (0.1 µg/L), NH_4^+ was lowest at Stone Quarry Bayou (0.1 µg/L), and NO_3^- was lowest at Weakley Bayou (8.6 µg/L) (see Table 3-6).

Fish diet and condition

Of the 829 *F. grandis* captured during the study, 512 fish guts were analyzed and were used in the PCA analysis of diet and environmental conditions. Caloric density was measured for 125 *F. grandis*, 105 of which also had gut contents analyzed, and were included in the PCA

analysis of diet and condition. The remaining 317 *F. grandis* were used for abundance estimates in Chapter 4.

Mean fish length across all seasons ranged from 74.1 mm (Weakley Bayou, autumn 2019) to 114.2 mm (Bayou Grande, autumn 2020), and increased with each season (84.5 mm during autumn 2019, 88.5 mm during summer 2020, and 93.4 mm during autumn 2020). Mean fish weight across all seasons ranged from 5.7 g (Weakley Bayou, autumn 2019) to 21.4 g (Bayou Grande, autumn 2020), and increased with each season (8.1 g during autumn 2019, 10.8 g during summer 2020, and 13.7 g during autumn 2020). Fulton's *K* across all seasons ranged from 1.05 (Weakley Bayou, autumn 2019) to 1.48 (Weakley Bayou, summer 2020). Mean Fulton's *K* was 1.10 during autumn 2019, 1.39 during summer 2020, and 1.33 during autumn 2020.

A total of 205 *F. grandis* stomachs were analyzed in autumn 2019, 160 in summer 2020, and 147 in autumn 2020. *F. grandis* diet across all the samples (autumn 2019, summer 2020, autumn 2020) was broad and represented both aquatic and terrestrial origins (Fig. 5-2). Dietary aquatic organisms were most represented by the following: fish (likely *F. grandis* juveniles based upon otolith identification Tammy DeVries, personal communication); *Melampus bidentus*, the common marsh snail; *Minuca spp.*, fiddler crab; detritus, identified as a mix of sediment and organic matter; and vegetation. Additionally, low numbers of the following aquatic organisms were represented: Polychaetea; Oligochaeta; Amphipoda; Isopoda; Tanaidacea, and

Penaeidae. Terrestrial organisms were represented by spiders (likely *Pardosa sp.)* and Hymenoptera sp.

There was consistency in the %FO of dietary items in *F. grandis* diets across all seasons (Fig. 5-3). Across all sites, diet was dominated by %FO of fish (24-31%), unknown (18-28%) and macroinvertebrates (16-23%) (Fig. 5-2). Fish were the highest %W across all seasons (49-52%), followed by unknown (13-30%), and crab (6-10%) (Fig. 5-3). The first two axes of the PCA analysis of diet explained 54.92% of the total variation in *F. grandis* diet. Differences among samples were driven primarily by fish (Pearson's R = -0.97) and macroinvertebrates (R = 0.96) (Fig. 5-4). Environmental (e.g., mean salinity, RB-index, nutrient concentrations) and size (e.g., length, weight, Fulton's K) variables were not associated with *F. grandis* diet and there was no obvious grouping by site.

A total of 125 *F. grandis* individuals were further analyzed for caloric density between summer 2020 (n = 50) and autumn 2020 (n = 75). The mean caloric density was higher in summer (1925.7±77 cal g^{-1} wet $weight^{-1}$) compared to autumn (938.4±16 cal g^{-1} wet $weight^{-1}$) (ANOVA, $p < 0.001$, df = 1, f = 92.47). During the summer, *F. grandis* from Long Bayou had the highest caloric content (2718 cal g^{-1} wet $weight^{-1}$), compared to Indian Bayou, which had the lowest caloric content during the summer (934 cal g^{-1} wet $weight^{-1}$) (Table 5-2). During autumn,

F. grandis at Weakley Bayou had the highest caloric content (1004 cal g^{-1} wet weight $^{-1}$), compared to Texar Bayou (993 cal g^{-1} wet weight $^{-1}$) (Table 5-2).

The first two axes of the PCA analysis of condition explained 79% of the total variance in *F. grandis* condition. The effect of the different conditional measures on structuring samples was driven by length ($R = 0.72$), Fulton's K ($R = -0.87$), and caloric density ($R = -0.82$). Diet and environmental conditions did not influence condition, but samples were strongly differentiated by seasonal differences (Fig. 5-5).

The results of the LMM analysis of %FO of dietary items with caloric density as a response variable found that the only dietary items that affected caloric density in this model were %FO of empty stomachs (ANOVA, $p = 0.01$, $X^2 = 5.92$) and %FO of fish ($p = 0.08$, $X^2 = 3.08$), with caloric density decreasing with %FO of empty stomachs (beta = -147.32, $t = -2.43$) and weakly increasing with %FO of fish (beta = 54.75, $t = 1.76$). The LMM analysis found that increased %FO of detritus led to a decrease in Fulton's K (beta = -0.02, $t = -2.29$), and that this was the only dietary item affecting Fulton's K in the model ($p = 0.02$, $X^2 = 5.25$). LMM analysis found no effect of %FO of dietary items on *F. grandis* length.

The results of the LMM analysis of %W of dietary items with caloric density as a response variable found that the only dietary items that affected caloric density in this model were algae and vegetation ($p = 0.02$, $X^2 = 5.77$) and detritus ($p = 0.05$, $X^2 = 3.77$), with caloric density increasing with algae and vegetation (beta = 42.87, t = 2.40) and detritus (beta = 197.99, t = 1.94). The relationship between caloric density and algae and vegetation was driven largely by the summer 2020 sample at Long Bayou, which had an algae and vegetation %W of 48.75%,

much higher than the mean of 3.77% across all sites and samples. Conversely, LMM analysis also found that Fulton's *K* decreased with %W of detritus (beta = -0.03, t = 1.89), and this was the only dietary item affecting Fulton's *K* in this model ($p = 0.06$, $X^2 = 3.55$). LMM analysis found no effect of %W of dietary items on *F. grandis* length.

Discussion

This study examined *F. grandis* diets in mesohaline tidal creeks along the northern GOM in relation to environmental variables associated with urban land use. *F. grandis* diets were broad and appear to be robust to changes in urban-induced salinity variation. Diet was similar across all sites and was dominated by fish, macroinvertebrates, unknown items, and crabs. However, across all samples the proportion (%FO and %W) of fish making up *F. grandis* diet (range = 8%-59%, mean = 29.76 ± 2.32%) was greater than other diet studies in the region which have found diets dominated more by shrimp, crabs, and other small crustaceans (Rozas and Lasalle 1990, Lowe and Peterson 2015).

One possibility for the disparity in reported *F. grandis* diets among studies is the variation in sampling locations geographically and within tidal marshes/creeks. In St. Louis Bay, Mississippi, *F. grandis* exiting the marsh surface during an ebb tide were found to prefer fiddler crabs, compared to a preference for amphipods in low and sub-tidal habitats, which was likely a reflection of the abundance of fiddler crabs within the marsh (Rozas and Lasalle 1990). Notably, fish were sampled exiting the marsh surface during an ebb tide in this study as well, yet *F. grandis* appeared to prefer fish as a dietary item, while also consuming crabs. However, Rozas and Lasalle (1990) sampled three small rivulets within a larger salt-marsh complex, while we

sampled fringing marsh along larger tidal creeks. In first-order tidal creeks arrayed along a gradient of urbanization in the Pascagoula River and Biloxi Bay estuaries, *F. grandis* fed on large brown shrimp in urbanized creeks, while fish in less urbanized creeks preferred grass shrimp and fish (Lowe and Peterson 2015). Tidal creeks sampled by Lowe and Peterson (2015) were smaller than those in this study, and the %FO of fish was never >20% at any site, compared to 19 of the 23 site-season combinations from this study (autumn 2019 n = 8 sites, summer 2020 n = 8 sites, autumn 2020 n = 7 sites) where %FO was >20%, and ranged from 8% (Texar Bayou, autumn 2020) to 59% (Trout Bayou, summer 2020). The tidal creeks in this study are larger mesohaline, tidally influenced coastal streams and are not fully represented in the estuarine literature, making this one of the first studies of fish diet from this size of tidal creek ecosystem.

Another possibility for the greater proportion of fish in *F. grandis* diets is that we captured larger fish that were more prone to piscivory. Odum (1970) detected fish as a primary dietary item in *F. grandis* captured between 46-98 mm, a similar size range as this study (32-143 mm, mean = 75.15 ± 0.52 mm, n = 1750; Chapter 3). On the contrary, *F. grandis* captured by Rozas and Lasalle (1990) were generally smaller than those from this study, ranging in size from 30-82 mm, while those captured by Lowe and Peterson (2015) represented the smaller end of the *Fundulus* size range, being between 18-110 mm. As mentioned, these studies detected other dietary items in the guts of *F. grandis*. However, guts from fish in this study were found to contain fish or fish parts, indicating that there was no dietary shift to or away from fish within our sampled range. Any identifiable part of a fish (scales, bones, whole fish) found in a gut counted as an occurrence of fish, and guts from larger fish did contain more intact fish, while

smaller fish were more likely to contain scales or bones, and fish and fish parts represented the largest proportion of prey items by %W.

Fundulus grandis preference for fish as a primary dietary item may also be driven by the higher caloric content of fish compared to macroinvertebrates, detritus, and vegetation (Cumminns and Wuycheck 1971, Griffiths 1977, Weisberg and Lotrich 1982). In our study, the caloric density of *F. grandis* weakly increased with %FO (but not %W) of fish. Similar to observations made by Rozas and Lasalle (1990), *F. grandis* may shift foraging behavior to focus on a combination of the most abundant and calorically rich prey items. Prey selection has been well studied in animals (Stephens and Krebs 1986, Lima and Dill 1990). Optimal foraging theory (Werner and Hall 1974) predicts that fish select prey based on energy gained (calories consumed) vs. energy expended (handling time, forage time). For example, Atlantic cod fed in a lab preferred fish over shrimp and crabs, likely because handling time increased with prey size compared to fish length (Arnott and Pihl 2000). Prey pursuit, however, can increase energy expenditure of fish and optimal foraging theory would suggest that fish would favor less evasive but abundant prey items (Manatunge and Asaeda 1999), such as macroinvertebrates. One possible explanation for the greater proportion of fish in *F. grandis* diet is that because of a high abundance of small fish using the salt marsh surface, *F. grandis* can select more evasive fish as prey because of high encounter rates. Because of the high %FO of fish compared to other studies, coupled with fish being the dominant prey by weight, these findings suggest that the *F. grandis* diet composition observed in this study compared to others is not due to the effects of coastal watershed development, but is instead driven by the increased abundance of small prey fish utilizing the marsh surface in these tidal creeks. This highlights the importance of fringing

salt marshes and tidal creeks as both important nursery and forage habitat for resident fish species.

The finding that %FO of empty stomachs decreased caloric density of *F. grandis* was not surprising. In smaller tidal creeks sampled in Mississippi, empty stomachs were more common in urban watersheds, and fish from those locations also had lower length-weight ratios (Lowe and Peterson 2015). Empty stomachs are commonly found when conducting gut analyses (Cortés 1997, Lowe and Peterson 2015, Manko 2016, Helms et al. 2018), but, only accounted for 6.12% of analyzed guts in this study, which was comparable to the 5.56% of *F. grandis* found with empty stomachs captured exiting a large salt marsh in Mississippi (Rozas and Lasalle 1990). These findings suggest that these tidal creeks and fringing salt marshes currently provision enough resources to maintain sufficient *F. grandis* body condition, as evidenced by Fulton's *K* measures >1.2 at all sites. However, if development in these watersheds continue, available prey resources may be reduced, leading to increased empty stomachs and reduced body condition.

The findings of this study should be interpreted with care as there are limitations associated with the use of *F. grandis* as a bioindicator, the use of gut analyses to explain fish condition, and caloric condition as a measure of body condition. For example, the lack of effect of salinity variation and nutrient concentrations associated with development on *F. grandis* diet and body condition suggest that *F. grandis*, at least in these tidal creeks, may be robust to these environmental changes. Because of *F. grandis*' well-documented environmental tolerances (Griffith 1974, Nordlie et al. 1992, Crego and Peterson 1997, Love and Rees 2002), they may not be the most suitable indicator species when examining low-intensity watershed development.

Similarly, gut analysis, a low-cost, but time-intensive method of assessing fish diet, is also limited in its ability infer effects on fish condition. For example, not all consumed items are equal and assimilation of different items is variable, and therefore dietary analysis using %FO or %W likely does not represent assimilation of these items by fish (Edwards and Horn 1982, Pandian and Marian 1985). Detritus was included in dietary analysis because it was found in the gut of *F. grandis* and is not an uncommon dietary item found in *Fundulus* guts (Harrington and Harrington 1982, Rozas and LaSalle 1990, Allen et al. 1994), but its consumption is likely incidental and has little effect on fish condition, regardless of any association between %FO and %W and condition. Additionally, prey digestive state can confound dietary item identification, with some dietary items like hard crab carapaces or snail shells persisting in guts longer and in a more identifiable state than smaller, more digestible dietary items (Buckland et al. 2017). More costly methods such as stable isotope analysis, coupled with gut content analysis, could provide a greater understanding of trophic dynamics and *F. grandis* body condition in these tidal creeks along the northern GOM (Gu et al. 1996, McMahon et al. 2005, 2015, Muñoz et al. 2011, Davis et al. 2012, Newton 2016). Lastly, caloric density analysis indicated significant differences between autumn and summer, likely due to changes in energy allocation associated with spawning during summer, which may have confounded any effects of salinity variation or diet

composition on *F. grandis* condition. These limitations taken together suggest that care must be taken when choosing suitable bioindicators of environmental change.

Conclusion

I found that *F. grandis* in tidal creeks along the northern GOM consumed more fish as a prey item compared to other studies in the region, likely due to increased small and juvenile fish using these tidal creeks and fringing salt marsh as nursery habitat, highlighting the important role that tidal creeks play in the transfer of energy within the coastal landscape. The lack of any effect of salinity variation or other watershed development metrics on measures of diet and body condition suggests that *F. grandis* are robust to the low-level residential development common along the northern GOM. However, there may be important limitations to the use of the environmentally tolerant *F. grandis* as a bioindicator species. Understanding how *F. grandis* diet and condition responds to future changes in salinity and land use is vital to understanding how estuaries may respond to increased pressures from both climate and land use change.

Literature cited

Abele, L. G., and W. Kim. 1986. An illustrated guide to the marine decapods of Florida. Technical Series 8.

Adams, S. M., and R. B. Mcleans. 1985. Estimation of largemouth bass, Micropterus salmoides Lacbpkde, growth using the liver somatic index and physiological variables. Journal of Fish Biology 26:111–126.

Allen, E. A., P. E. Fell, M. A. Peck, J. A. Gieg, C. R. Guthke, and M. D. Newkirk. 1994. Gut Contents of Common Mummichogs, Fundulus heteroclitus L., in a Restored Impounded Marsh and in Natural Reference Marshes. Estuaries 17:462.

Arnott, S., and L. Pihl. 2000. Selection of prey size and prey species by 1-group cod Gadus morhua:effects of satiation level and prey handling times. Marine Ecology Progress Series 198:225–238.

Baker, D. B., R. P. Richards, T. T. Loftus, and J. W. Kramer. 2004. A new flashiness index: Characteristics and applications to Midwestern rivers and streams. Journal of the American Water Resources Association 40:503–522.

Barksdale, W. F., C. J. Anderson, and L. Kalin. 2014. The influence of watershed run-off on the hydrology, forest floor litter and soil carbon of headwater wetlands. Ecohydrology 7:803–814.

Bates, D., M. Mächler, B. Bolker, and S. Walker. 2015. Fitting Linear Mixed-Effects Models Using lme4. Journal of Statistical Software 67.

Bolger, T., and P. L. Connolly. 1989. The selection of suitable indices for the measurement and analysis of fish condition. Journal of Fish Biology 34:171–182.

Booth, D. J., and J. A. Keast. 1986. Growth energy partitioning by juvenile bluegill sunfish, Lepomis macrochirus Rafinesque. Journal of Fish Biology 28:37–45.

Brabrand, Å. 1985. Food of roach (Rutilus rutilus) and ide (Leusiscus idus): Significance of diet shift for interspecific competition in omnivorous fishes. Oecologia 66:461–467.

Brown, M. L., and B. R. Murphy. 2004. Seasonal dynamics of direct and indirect condition indices in relation to energy allocation in largemouth bass Micropterus salmoides (Lacèpede). Ecology of Freshwater Fish 13:23–36.

Brumm, K. J., J. L. Jonas, C. G. Prichard, N. M. Watson, and K. L. Pangle. 2019. Land cover influences on juvenile Rainbow Trout diet composition and condition in Lake Michigan tributaries. Ecology of Freshwater Fish 28:11–19.

Buckland, A., R. Baker, N. Loneragan, and M. Sheaves. 2017. Standardising fish stomach content analysis: The importance of prey condition. Fisheries Research 196:126–140.

Clemmesen, C., V. Buhler, G. Carvalho, and R. Case. 2003. Variability in condition and growth of Atlantic cod larvae and juveniles reared …. Journal of Fish … 706–723.

Cortés, E. 1997. A critical review of methods of studying fish feeding based on analysis of stomach contents: Application to elasmobranch fishes. 54:13.

Crego, G. J., and M. S. Peterson. 1997. Salinity Tolerance of Four Ecologically Distinct Species of Fundulus (Pisces: Fundulidae) from the Northern Gulf of Mexico. Gulf of Mexico Science 15.

Le Cren, E. D. 1951. The Length-Weight Relationship and Seasonal Cycle in Gonad Weight and Condition in the Perch (Perca fluviatilis) Author (s): E. D. Le Cren Source: Journal of Animal Ecology , Vol. 20 , No. 2 (Nov ., 1951), pp. 201-219 Published by: British Ec. Journal of Animal Ecology 20:201–219.

Cumminns, K. W., and J. C. Wuycheck. 1971. Caloric Equivalents for Investigations in Ecological Energetics: With 2 figures and 3 tables in the text. SIL Communications, 1953-1996 18:1–158.
Davis, A. M., M. L. Blanchette, B. J. Pusey, T. D. Jardine, and R. G. Pearson. 2012. Gut content and stable isotope analyses provide complementary understanding of ontogenetic dietary shifts and trophic relationships among fishes in a tropical river: Isotopic ecology of some tropical fishes. Freshwater Biology 57:2156–2172.
Delahunty, G., and V. L. de Vlaming. 1980. Seasonal relationships of ovary weight, liver weight and fat stores with body weight in the goldfish, Carassius auratus (L.). Journal of Fish Biology 16:5–13.
Edwards, T. W., and M. H. Horn. 1982. Assimilation efficiency of a temperate-zone intertidal fish (Cebidichthys violaceus) fed diets of macroalgae. Marine Biology 67:247–253.
Ferraro, M. L., L. A. E. Kaplan, J. Leamon, and J. F. Crivello. 2001. Variations in physiological biomarkers among mummichogs collected from Connecticut salt marshes. Journal of Aquatic Animal Health 13:246–256.
Francis, T. B., and D. E. Schindler. 2006. Degradation of Littoral Habitats by Residential Development: Woody Debris in Lakes of the Pacific Northwest and Midwest, United States. AMBIO: A Journal of the Human Environment 35:274–280.
Francis, T. B., and D. E. Schindler. 2009. Shoreline urbanization reduces terrestrial insect subsidies to fishes in North American lakes. Oikos 118:1872–1882.
Froese, R. 2006. Cube law, condition factor and weight-length relationships: History, meta-analysis and recommendations. Journal of Applied Ichthyology 22:241–253.
Fulton, T. W. 1904. The rate of growth of fishes. Fisheries Board of Scotland.
Glover, D. C., D. R. DeVries, R. A. Wright, and D. A. Davis. 2010. Sample Preparation Techniques for Determination of Fish Energy Density via Bomb Calorimetry: An Evaluation Using Largemouth Bass. Transactions of the American Fisheries Society 139:671–675.
Goto, D., and W. G. Wallace. 2010. Bioenergetic responses of a benthic forage fish (Fundulus heteroclitus) to habitat degradation and altered prey community in polluted salt marshes. Canadian Journal of Fisheries and Aquatic Sciences 67:1566–1584.
Goto, D., and W. G. Wallace. 2011. Altered feeding habits and strategies of a benthic forage fish (Fundulus heteroclitus) in chronically polluted tidal salt marshes. Marine Environmental Research 72:75–88.
Griffith, R. W. 1974. Environment and Salinity Tolerance in the Genus Fundulus. Copeia 1974:319.
Griffiths, D. 1977. Caloric Variation in Crustacea and Other Animals. The Journal of Animal Ecology 46:593.
Gu, B., C. L. Schelske, and M. V. Hoyer. 1996. Stable isotopes of carbon and nitrogen as indicators of diet and trophic structure of the fish community in a shallow hypereutrophic lake. Journal of Fish Biology 49:1233–1243.
Harrington, R. W., and E. S. Harrington. 1982. Effects on fishes and their forage organisms of impounding a Florida salt marsh to prevent breeding by salt marsh mosquitoes. Deep Sea Research Part B. Oceanographic Literature Review 29:792.
Harrison, X. A., L. Donaldson, M. E. Correa-Cano, J. Evans, D. N. Fisher, C. E. D. Goodwin, B. S. Robinson, D. J. Hodgson, and R. Inger. 2018. A brief introduction to mixed effects modelling and multi-model inference in ecology. PeerJ 6:e4794.

Hartman, K. J., and S. B. Brandt. 1995. Estimating Energy Density of Fish. Transactions of the American Fisheries Society 124:347–355.
Heard, R. W. 1982. Guide to common tidal marsh invertebrates of the northeastern Gulf of Mexico.
Helms, B. S., N. A. Bickford, N. W. Tubbs, and J. W. Feminella. 2018. Feeding, growth, and trophic position of redbreast sunfish (Lepomis auritus) in watersheds of differing land cover in the lower Piedmont, USA. Urban Ecosystems 21:107–117.
Holland, A. F., D. M. Sanger, C. P. Gawle, S. B. Lerberg, M. S. Santiago, G. H. M. Riekerk, L. E. Zimmerman, and G. I. Scott. 2004. Linkages between tidal creek ecosystems and the landscape and demographic attributes of their watersheds. Journal of Experimental Marine Biology and Ecology 298:151–178.
Hyslop, E. J. 1980. Stomach contents analysis-a review of methods and their application. Journal of Fish Biology 17:411–429.
Jakob, E. M., S. D. Marshall, G. W. Uetz, E. M. Jakob, S. D. Marshall, G. W. Uetz, and G. W. Estimating. 1996. Estimating Fitness: A Comparison of Body Condition Indices indices. Oikos 77:61–67.
Krebs, J. M., S. S. Bell, and C. C. McIvor. 2014. Assessing the Link Between Coastal Urbanization and the Quality of Nekton Habitat in Mangrove Tidal Tributaries. Estuaries and Coasts 37:832–846.
Krebs, J. M., C. C. McIvor, and S. S. Bell. 2013. Nekton Community Structure Varies in Response to Coastal Urbanization Near Mangrove Tidal Tributaries. Estuaries and Coasts 37:815–831.
Lerberg, S. B., A. F. Holland, and D. M. Sanger. 2000. Responses of tidal creek macrobenthic communities to the effects of watershed development. Estuaries 23:838–853.
Lima, S. L., and L. M. Dill. 1990. Behavioral decisions made under the risk of predation: A review and prospectus. Canadian Journal of Zoology 68:619–640.
Lisi, P. J., E. S. Childress, R. B. Gagne, E. F. Hain, B. A. Lamphere, R. P. Walter, J. D. Hogan, J. F. Gilliam, M. J. Blum, and P. B. McIntyre. 2018. Overcoming urban stream syndrome: Trophic flexibility confers resilience in a Hawaiian stream fish. Freshwater Biology 63:492–502.
Love, J. W., and B. B. Rees. 2002. Seasonal Differences in Hypoxia Tolerance in Gulf Killifish, Fundulus Grandis (Fundulidae). Environmental Biology of Fishes 63:103–115.
Lowe, M. R., and M. S. Peterson. 2014. Effects of Coastal Urbanization on Salt-Marsh Faunal Assemblages in the Northern Gulf of Mexico. Marine and Coastal Fisheries 6:89–107.
Lowe, M. R., and M. S. Peterson. 2015. Body Condition and Foraging Patterns of Nekton from Salt Marsh Habitats Arrayed Along a Gradient of Urbanization. Estuaries and Coasts 38:800–812.
Manatunge, J., and T. Asaeda. 1999. Optimal foraging as the criteria of prey selection by two centrarchid fishes. 18.
Manko, P. 2016. Stomach content analysis in freshwater fish feeding ecology.
McMahon, K. W., B. J. Johnson, and W. G. Ambrose. 2005. Diet and movement of the killifish,Fundulus heteroclitus, in a Maine salt marsh assessed using gut contents and stable isotope analyses. Estuaries 28:966–973.
McMahon, K. W., S. R. Thorrold, T. S. Elsdon, and M. D. McCarthy. 2015. Trophic discrimination of nitrogen stable isotopes in amino acids varies with diet quality in a

marine fish: Trophic discrimination of amino acids. Limnology and Oceanography 60:1076–1087.
Mézin, L. C., and R. C. Hale. 2000. Effects of Contaminated Sediment on the Epidermis of Mummichog, Fundulus Heteroclitus. Environmental Toxicology and Chemistry 19:2779.
Minitab 17 Statistical Software. 2022. Minitab, Inc.
Muñoz, R., C. Currin, and P. Whitfield. 2011. Diet of invasive lionfish on hard bottom reefs of the Southeast USA: Insights from stomach contents and stable isotopes. Marine Ecology Progress Series 432:181–193.
Newton, J. 2016. Stable Isotopes as Tools in Ecological Research. Pages 1–8 *in* John Wiley & Sons Ltd (editor). ELS. John Wiley & Sons, Ltd, Chichester, UK.
Nordlie, F. G., D. C. Haney, and S. J. Walsh. 1992. Comparisons of Salinity Tolerances and Osmotic Regulatory Capabilities in Populations of Sailfin Molly (Poecilia latipinna) from Brackish and Fresh Waters. Copeia 1992:741.
Pandian, T. J., and M. P. Marian. 1985. Nitrogen content of food as an index of absorption efficiency in fishes. Marine Biology 85:301–311.
Partyka, M. L., and M. S. Peterson. 2008. Habitat Quality and Salt-Marsh Species Assemblages along an Anthropogenic Estuarine Landscape. Journal of Coastal Research 246:1570–1581.
Persson, L. 1983. Food Consumption and the Significance of Detritus and Algae to Intraspecific Competition in Roach Rutilus rutilus in a Shallow Eutrophic Lake. Oikos 41:118.
Pothoven, S. A., T. F. Nalepa, P. J. Schneeberger, and S. B. Brandt. 2004. Changes in Diet and Body Condition of Lake Whitefish in Southern Lake Michigan Associated with Changes in Benthos. North American Journal of Fisheries Management 21:876–883.
Rezaeianzadeh, M., L. Kalin, and C. J. Anderson. 2017. Wetland Water-Level Prediction Using ANN in Conjunction with Base-Flow Recession Analysis. Journal of Hydrologic Engineering 22:D4015003.
Rozas, L. P., and M. W. Lasalle. 1990. A Comparison of the Diets of Gulf Killifish , Fundulus grandis Baird and Girard , Entering and Leaving a Mississippi Brackish Marsh. Estuaries 13:332–336.
Rozas, L. P., and M. W. LaSalle. 1990. A Comparison of the Diets of Gulf Killifish, Fundulus grandis Baird and Girard, Entering and Leaving a Mississippi Brackish Marsh. Estuaries 13:332.
Rozas, L. P., and D. J. Reed. 1994. Comparing nekton assemblages of subtidal habitats in pipeline canals traversing brackish and saline marshes in coastal Louisiana. Wetlands 14:262–275.
Sanger, D., A. Blair, G. DiDonato, T. Washburn, S. Jones, G. Riekerk, E. Wirth, J. Stewart, D. White, L. Vandiver, and A. F. Holland. 2015. Impacts of Coastal Development on the Ecology of Tidal Creek Ecosystems of the US Southeast Including Consequences to Humans. Estuaries and Coasts 38:49–66.
Stepenuck, K. F., R. L. Crunkilton, and L. Wang. 2002. Impacts of urban landuse on macroinvertebrate communities in southeastern Wisconsin streams. Journal of the American Water Resources Association 38:1041–1051.
Stephens, D. W., and J. R. Krebs. 1986. Foraging theory. Princeton University Press, Princeton, N.J.
Stevenson, R. D., and W. A. Woods. 2006. Condition indices for conservation: New uses for evolving tools. Integrative and Comparative Biology 46:1169–1190.

Walsh, C. J., A. H. Roy, J. W. Feminella, P. D. Cottingham, P. M. Groffman, R. P. M. Ii, and R. A. P. M. O. Ii. 2005. The urban stream syndrome: Current knowledge and the search for a cure. North American Benthological Society 24:706–723.

Wang, L., and P. Kanehl. 2003. Influences of watershed urbanization and instream habitat on macroinvertebrates in cold water streams. Journal of the American Water Resources Association 39:1181–1196.

Washburn, T., and D. Sanger. 2011. Land use effects on macrobenthic communities in southeastern United States tidal creeks. Environmental Monitoring and Assessment 180:177–188.

Wedge, M., and C. J. Anderson. 2017. Urban Land use Affects Resident Fish Communities and Associated Salt Marsh Habitat in Alabama and West Florida, USA. Wetlands 37:715–727.

Wedge, M., C. J. Anderson, and D. DeVries. 2015. Evaluating the Effects of Urban Land Use on the Condition of Resident Salt Marsh Fish. Estuaries and Coasts 38:2355–2365.

Weisberg, S. B., and V. A. Lotrich. 1982. Ingestion, egestion, excretion, growth, and conversion efficiency for the mummichog, Fundulus heteroclitus (L.). Journal of Experimental Marine Biology and Ecology 62:237–249.

Werner, E. E., and D. J. Hall. 1974. Optimal Foraging and the Size Selection of Prey by the Bluegill Sunfish (Lepomis Macrochirus). Ecology 55:1042–1052.

Xian, G., C. Homer, B. Bunde, P. Danielson, J. Dewitz, J. Fry, and R. Pu. 2012. Quantifying urban land cover change between 2001 and 2006 in the Gulf of Mexico region. Geocarto International 27:479–497.

Table 5-1. Area (km^2), mean (±SE) salinity (ppt), salinity RB-index, and land-cover (% of watershed coverage), from 2016 NLCD. Development includes all levels of development (open, low, medium, high), wetland includes woody and emergent wetlands, and Agric. includes pasture and row crops. Abbreviations of creek names in parentheses.

Site	Area (km^2)	Mean salinity (ppt)	RB-index	Urban	Forest/ Herb-aceous	Wet-land	Shrub-land	Agric.	Barren Land & Open Water
Wolf-Perdido Bay									
Stone Quarry (SQ)	0.4	14.1 (± 0.1)	0.20	0.0	93.6	6.4	0.0	0.0	0.0
Manuel Bayou (MB)	6.2	10.6 (± 0.1)	0.52	8.4	37.3	6.2	1.4	46.1	0.2
Weakley Bayou (WB)	6.7	11.3 (± 0.2)	0.72	17.6	24.2	55.2	1.7	0.6	0.4
Long Bayou (LB)	6.8	11.8 (± 0.2)	0.84	3.3	23.1	61.0	0.2	11.1	0.4
Graham Creek (GC)	8.8	11.4 (± 0.1)	1.05	8.4	45.6	21.3	1.4	21.0	2.2
Escambia-Pensacola-East Bay									
Trout Bayou (TB)	2.5	10.6 (± 0.2)	0.40	13.9	10.5	73.5	0.1	0.5	1.4
Robinson Pointe (RP)	3.1	6.0 (± 0.2)	1.48	8.2	33.9	37.3	2.0	13.4	4.5
Indian Bayou (IB)	5.1	12.4 (± 0.3)	0.58	12.3	1.9	84.7	0.0	0.0	1.0
Mulat Bayou (MB)	10.3	6.0 (± 0.2)	1.90	24.8	13.3	57.2	0.6	2.7	1.2
Heron Bayou (HB)	13.6	5.5 (± 0.2)	1.5	38.8	10.3	48.1	0.4	1.2	0.5
Bayou Grande (BG)	18.3	11.6 (± 0.2)	1.39	27.6	19.8	47.5	0.5	2.2	1.4
Texar Bayou (TX)	46.4	11.4 (± 0.2)	0.75	87.5	6.6	2.0	0.2	0.2	3.1

Table 5-2. Number of diets analyzed, mean (±SE) length (mm), mean (±SE) weight (g), mean length: weight ratio, mean Fulton's *K*, and mean (±SE) caloric density (kcal/g wet weight) of *Fundulus grandis* across sites during autumn 2019, summer 2020, and autumn 2020. Asterisk indicates that caloric density was not measured during autumn 2020. Double asterisk indicates samples that were lost.

Sample	Site	*n* diets	Length (mm)	Weight (g)	Length: weight ratio	Fulton's *K*	Caloric Density (kcal/g wt weight)
Autumn 2019	Bayou Grande	29	90.13 (±2.10)	8.86 (±0.59)	10.17	1.08 (±0.01)	NA*
	Indian Bayou	30	82.14 (±2.42)	7.28 (±0.50)	11.28	1.08 (±0.01)	NA*
	Long Bayou	20	97.14 (±3.27)	11.86 (±1.06)	8.19	1.14 (±0.01)	NA*
	Manuel Bayou	9	78.85 (±4.28)	6.56 (±1.15)	12.02	1.09 (±0.02)	NA*
	Stone Quarry	25	79.62 (±3.12)	6.78 (±0.78)	11.74	1.09 (±0.04)	NA*
	Texar Bayou	28	85.31 (±3.95)	9.04 (±0.83)	9.44	1.15 (±0.01)	NA*
	Trout Bayou	30	88.57 (±2.26)	9.08 (±0.74)	9.75	1.09 (±0.02)	NA*
	Weakley Bayou	29	74.06 (±3.22)	5.71 (±0.69)	12.97	1.05 (±0.02)	NA*
Summer 2020	Bayou Grande	26	80.35 (±2.36)	7.71 (±0.70)	10.42	1.32 (±0.01)	1808.68 (± 99.43)
	Graham Creek	20	85.61 (±3.32)	10.56 (±1.12)	8.11	1.41 (±0.02)	1417.08 (± 53.06)
	Long Bayou	14	82.56 (±5.58)	9.17 (±0.99)	9.00	1.31 (±0.04)	2717.65 (± 272.02)
	Indian Bayou	27	99.40 (±5.21)	12.28 (±2.43)	8.09	1.42 (±0.03)	1050.40 (± 41.79)
	Stone Quarry	15	81.18 (±2.06)	8.52 (±0.81)	9.53	1.44 (±0.02)	1891.87 (± 233.47)
	Texar Bayou	24	88.00 (±2.43)	10.46 (±0.75)	8.41	1.42 (±0.03)	1949.16 (± 141.08)
	Trout Bayou	25	90.24 (±2.50)	10.84 (±0.90)	8.32	1.35 (±0.04)	2009.03 (± 228.60)
	Weakley Bayou	8	100.63 (±3.91)	13.90 (±1.15)	7.24	1.48 (±0.23)	2283.94 (± 144.03)
Autumn 2020	Bayou Grande	28	114.15 (±3.22)	21.45 (±1.63)	5.32	1.29 (±0.01)	970.41 (± 39.46)
	Indian Bayou	21	87.65 (±3.53)	11.08 (±1.46)	7.91	1.37 (±0.06)	NA**
	Long Bayou	27	98.90 (±4.15)	13.74 (±1.60)	7.20	1.25 (±0.02)	NA**
	Stone Quarry	20	85.12 (±4.13)	10.87 (±1.78)	7.83	1.46 (±0.03)	904.25 (± 28.72)
	Texar Bayou	19	99.51 (±2.48)	13.29 (±1.34)	7.49	1.22 (±0.08)	848.21 (± 39.88)
	Trout Bayou	15	93.21 (±5.94)	15.34 (±2.37)	6.08	1.41 (±0.03)	996.18 (± 30.77)
	Weakley Bayou	16	75.64 (±7.43)	10.22 (±2.59)	7.40	1.28 (±0.04)	1004.66 (± 41.10)

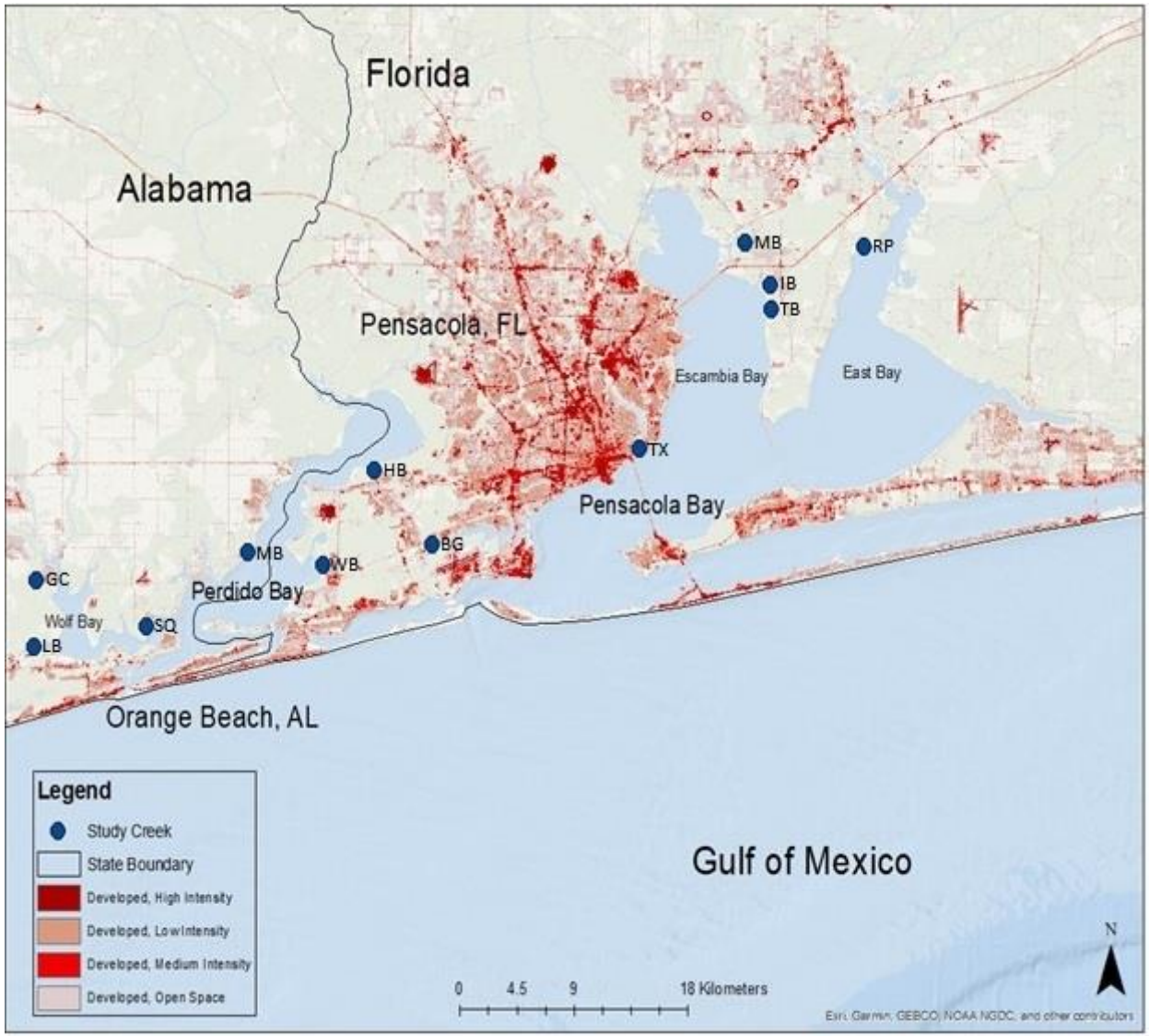

Figure 5-1. Map of study region. Blue dots represent a study site and red shading represents intensity of development, from 2011 NLCD (see Table 5-1 for creek abbreviation names).

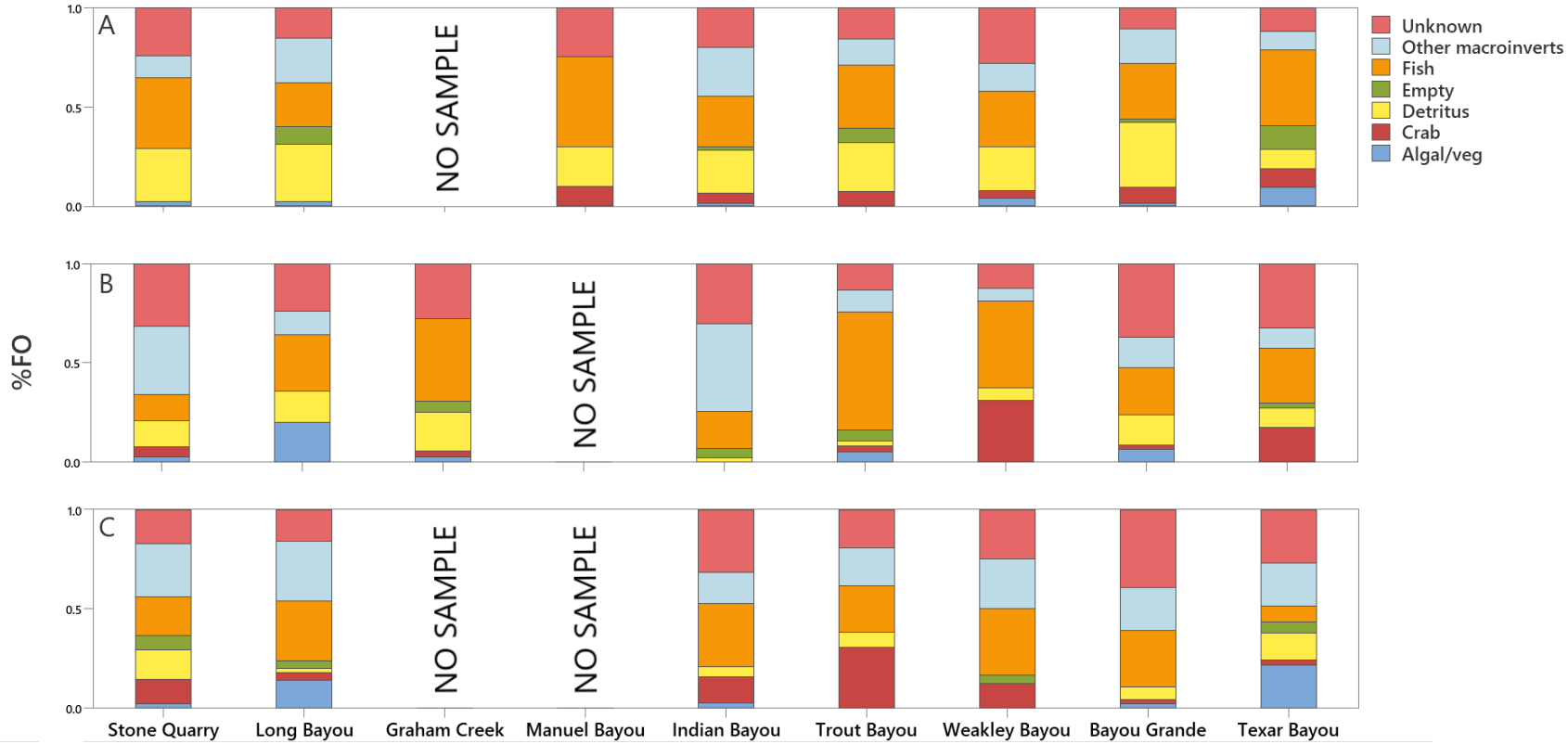

Figure 5-2. Percent frequency (%FO) of *Fundulus grandis* dietary items across each sampled site during autumn 2019 (A), summer 2020 (B), and autumn 2020 (C).

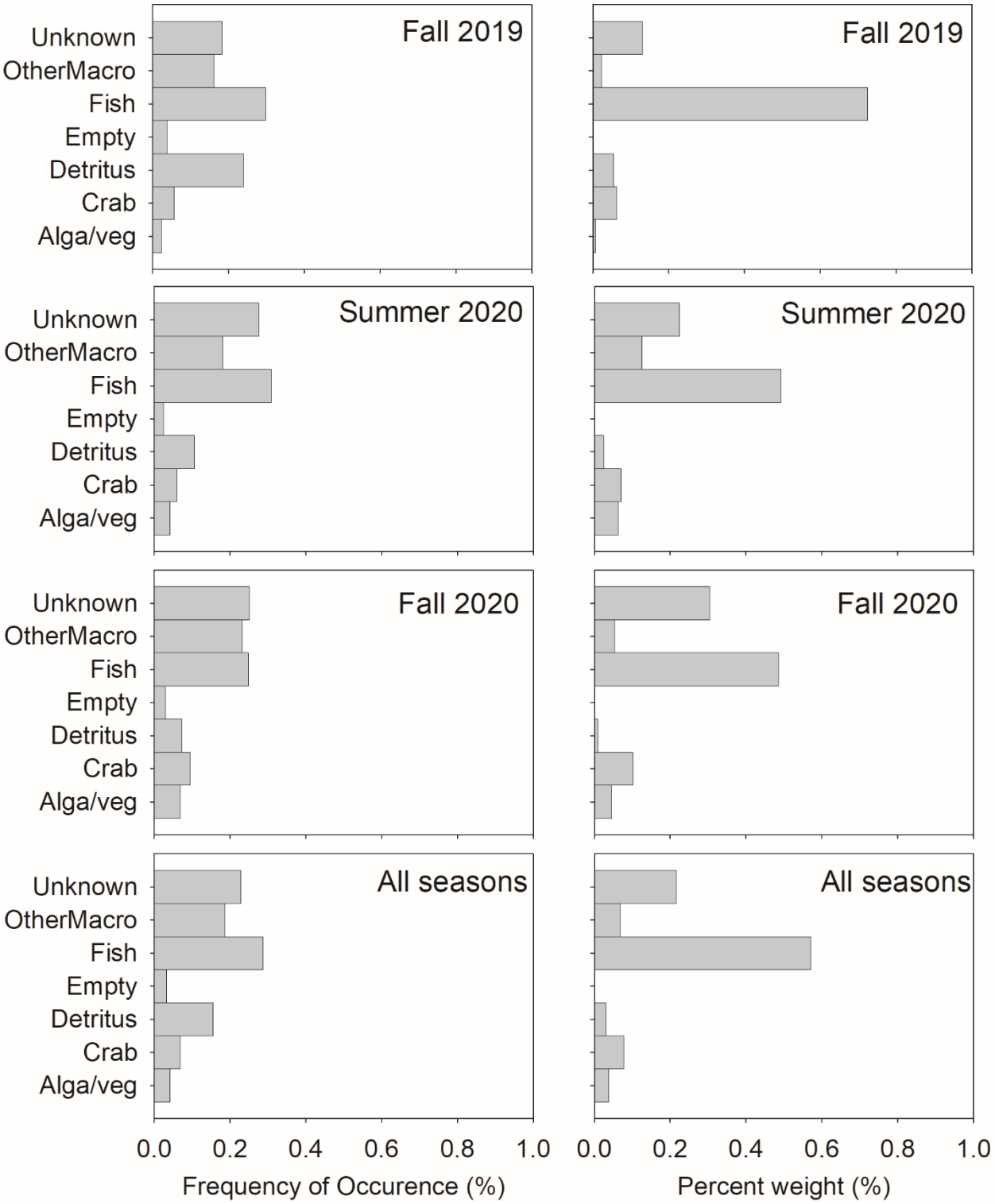

Figure 5-3. Frequency of occurrence (%) and percent weight (%) of each dietary item at all sites for autumn 2019, summer 2020, autumn 2020, and across all three sampling events.

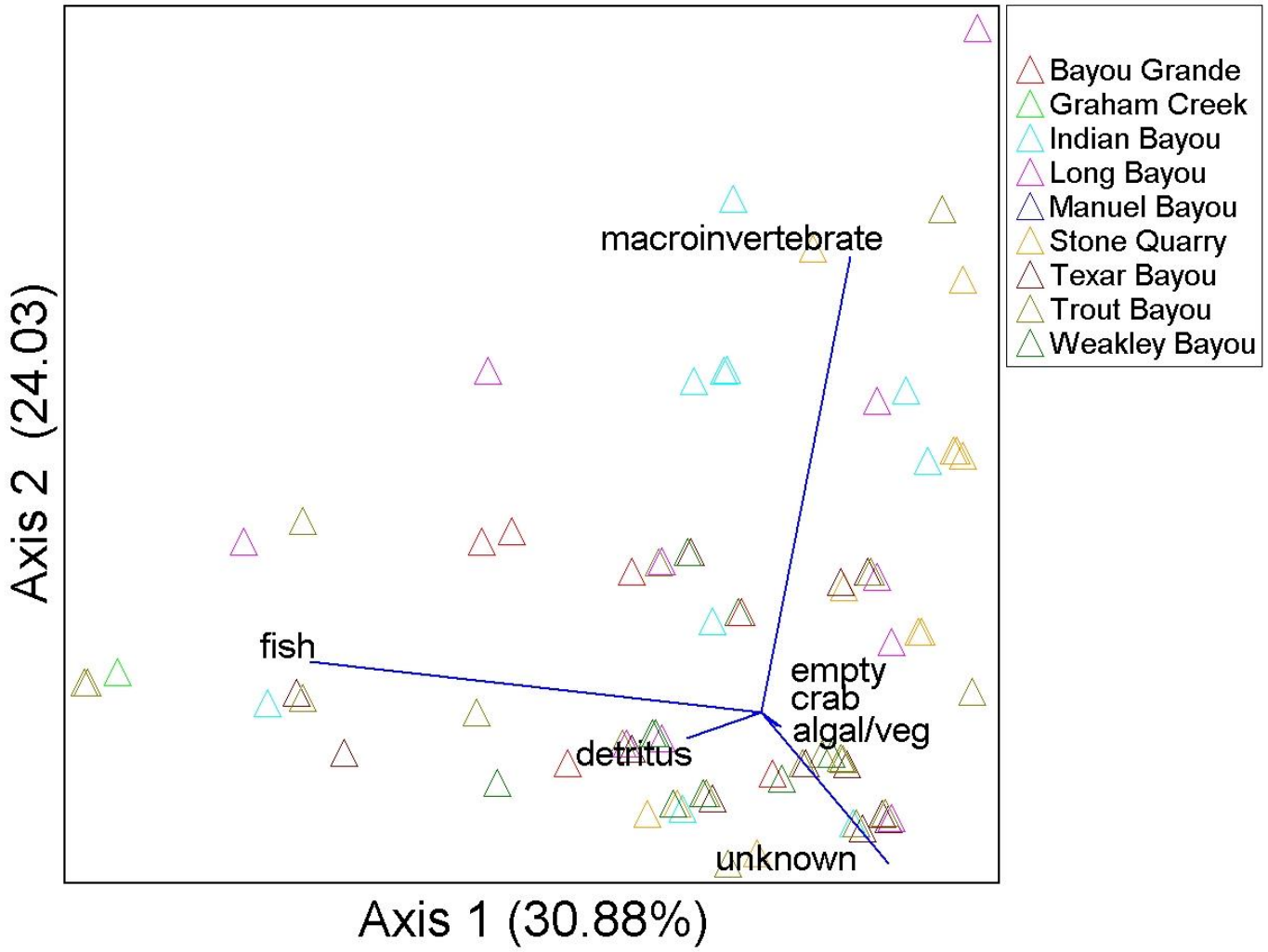

Figure 5-4. Principal component analysis of *Fundulus grandis* diet composition at Bayou Grande, Graham Creek, Indian Bayou, Long Bayou, Manuel Bayou, Stone Quarry, Texar Bayou, Trout Bayou, and Weakley Bayou. Blue vectors indicate the strength and direction of relationships to dietary items.

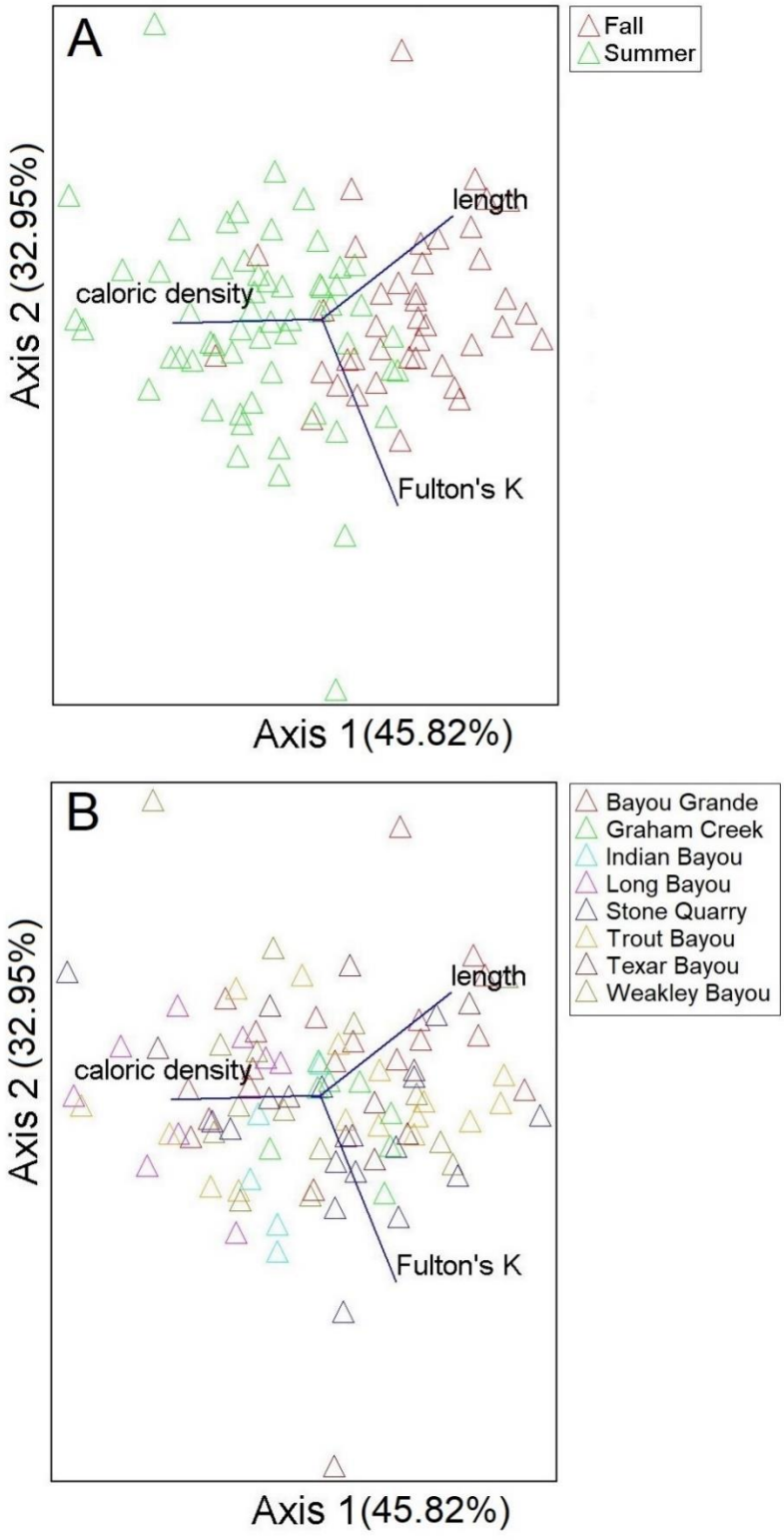

Figure 5-5. Principal component analysis of *Fundulus grandis* length, caloric density, and Fulton's *K* by A) season and B) site.

Chapter 6: Conclusions

Aquatic ecosystems are experiencing increased pressures associated with urbanization and climate change. This pressure has resulted in the degradation of streams, rivers, lakes, and coastal waters. As these resources continue to be threatened, particularly due to widespread development and exurban sprawl, there is a need to understand whether the negative effects of development can either be ameliorated or reversed. Additionally, climate change will continue to lead to increased precipitation, particularly in the Southeastern United States, which may further hinder society's ability to maintain ecosystem services provided by aquatic resources.

Chapter 2 of this dissertation was the first study to address the lack of long-term assessments of coarse woody debris dams (CWD) as a stream restoration technique to improve water quality and ecosystem functioning. Fourteen years following CWD installation, there was no observed increase in ecosystem functioning or change in water quality. This study was one of only a handful to assess a restoration project over a longer period of time (> 10 years) and highlights the difficult nature of restoring aquatic ecosystems. Additionally, it appears that there were changes in the watershed (revegetation of bare ground, BMPs) that likely contributed to changes in water quality *regardless of restoration status*. This supports the conclusion that improving instream habitat or water quality is unlikely to occur without changes in the watershed, and therefore may limit the usefulness of certain instream restoration techniques.

Chapter 3 of this dissertation was the first study to 1) estimate water column ecosystem metabolism in tidal creeks along the northern GOM, and 2) assess the effects of watershed

disturbance on salinity regime and ecosystem function in these same tidal creeks. This research found that low-level urbanization is increasing salinity variability in these streams, and that this is leading to decreased rates of ecosystem metabolism. Because tidal creeks and their fringing salt marshes are important sources of energy transferred across the coastal landscape, it is important to understand how these systems respond to watershed development and any effect this may have on the fate and transport of organic matter.

Chapter 4 of this dissertation examined the effect of watershed urbanization and subsequent salinity variation on the abundance of the common resident marsh fish *Fundulus grandis* and examined how this species responded to changes in salinity, likely a result of differences in precipitation, over 8 years. This research found that *F. grandis* abundance was lower in 2020 than in 2012, when salinities across a subset of 6 study sites were higher following a drought. Salinity during 2020 was lower than in 2012, likely due to increased precipitation during this period. *F. grandis* abundance decreased with the increase of salinity variability associated with watershed urbanization. Resident marsh species are important linkages in the transfer of energy from tidal creeks and fringing salt marshes, and these findings suggest that their ability to transfer energy to the estuary and open ocean may decrease as coastal watersheds face increased development pressure and climate change.

Chapter 5 of this dissertation examined the effect of changes in land use and *F. grandis* diet on *F. grandis* body condition. Considering the findings that increased salinity variability and decreased base-level salinity led to reductions in *F. grandis* abundance, it is important to

understand how this important trophic linkage is altered as *F. grandis* diet may also potentially change with land use. *F. grandis* body condition and diet appeared to be robust to changes in the watershed associated with urbanization. While these findings suggest low-level urbanization may not be leading to changes in body condition in these tidal creeks, effects may still be observed in species of fish less suited to freshwater conditions resulting from changes to salinity regime. Likewise, there may be an as-of-yet unidentified threshold of effect for coastal watershed urbanization that was not captured in the levels of urbanization in the watersheds used in this study.

There were, however, limitations in this dissertation that must be acknowledged. For example, the findings of Chapter 2 suggest that restoration results are likely highly site specific and variability among restored streams may confound our ability to detect differences. Further, one site in the Chapter 2 study, Bonham Creek, was considered an outlier and was dropped from some analyses, possibly further reducing an ability to detect an effect of restoration. But consideration of outliers when examining changes to an ecosystem is important because these systems are part of the landscape and may be the most vulnerable to degradation. Similarly to Bonham Creek, Chapters 3-5 included Texar Bayou, the only highly urbanized site in those studies. However, Texar Bayou is representative of tidal creeks found in the few large urban areas along the northern GOM and may be particularly vulnerable to the effects of development on tidal creeks. Interestingly, our findings suggest that Texar Bayou does not experience the

same increased variability in salinity as the low-level urbanized tidal creeks in the region, and thus it was important to include this site in these studies.

Additional limitations include the use of *F. grandis* as a study species when examining the impact of development on tidal creeks. Because *F. grandis* is tolerant of a wide range of conditions, it may not be the first tidal creek resident to exhibit changes in abundance, diet, or condition. Similarly, the use of gut analysis to infer body condition is limited at best and care should be taken when drawing conclusions. So, while there was no observed effect of dietary changes or body condition for *F. grandis*, natural abundance stable isotope or fatty acid analysis may be more useful tools to examine these changes because they can more accurately describe assimilation of dietary items vs. simple observation within fish stomachs.

This dissertation lays the foundation for future studies that may more thoroughly define a potential "urban tidal creek syndrome." The identification of RB-index as a responsive metric of watershed development is helpful but should be further evaluated in tidal creeks in different regions and at more moderate (20-60%) levels of urbanization. Similarly, the physiological effects of salinity variation on tidal creek biota should be assessed directly in lab experiments. The interaction between increased salinization of coastal waters due to sea level rise and increased salinity variability associated with watershed development and increased precipitation should also be examined, as these two stressors may potentially lead to novel structural and functional changes within these systems and climate and land use continue to change. Future work should also further examine the long-term effects of different restoration techniques, with

the emphasis being on whether explicitly defined restoration goals have been met over this period. Long-term studies are costly and are necessarily time consuming, but these studies are important to our understanding of society's ability to maintain or restore ecosystem structure and function in a changing world.

Overall, the results of this dissertation suggests that 1) to restore instream water quality and habitat, the most important changes occur in the watershed, 2) low-level urbanization of coastal watersheds is currently leading to detectable changes in salinity regime, ecosystem function, and *F. grandis* abundance, and 3) changes in climate, coupled with watershed development are further threatening tidal creek ecosystems. As the climate continues to change in both predictable and unpredictable ways, it is vital to understand how low-order headwater and tidal creek ecosystems respond to these changes. By understanding how these systems operate under the current (yet changing) climate regime, researchers, land managers, and communities can better predict how these systems will respond in the future, allowing society to protect these important aquatic resources.

Figure 2-S1. Gantt chart indicating when water quality, NH_4^+ uptake, and ecosystem metabolism were measured in the pre-restoration (PRE), 1-3 y post-restoration (POST-ST), and 14-15 y post-restoration (POST-LT) periods. CWD was added to restored streams in October

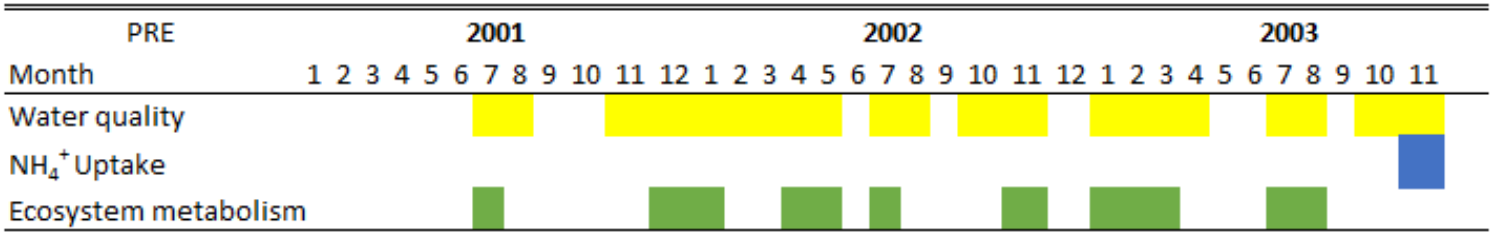

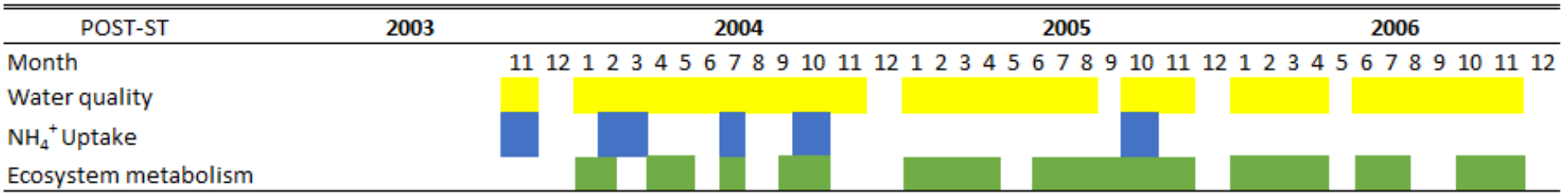

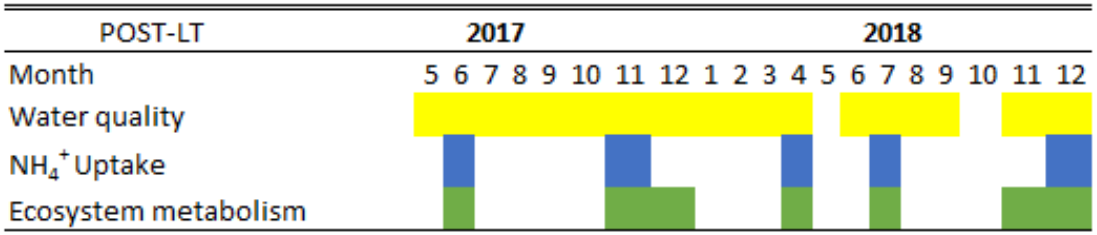

Supplemental Material (not copyedited or formatted) for: Samuel Bickley, Brian S. Helms, Daniel Isenberg, Jack W. Feminella, Brian J. Roberts, Natalie A. Griffiths. 2021. "Lack of Long-Term Effect of Coarse Woody Debris Dam Restoration on Ecosystem Functioning and Water Quality in Coastal Plain Streams." Freshwater Science 40(4). DOI: https://doi.org/10.1086/717325.

Figure 2-S2. Relationships between mean (± SE) streamwater TSS, NO_3^-, NH_4^+, SRP, DOC concentrations and specific conductance and % watershed disturbance across all streams (both restored and unrestored) in the PRE (top row), POST-ST (middle row), and POST-LT (bottom row) periods. Solid line indicates positive or negative relationship based on $r^2 > 0.5$.

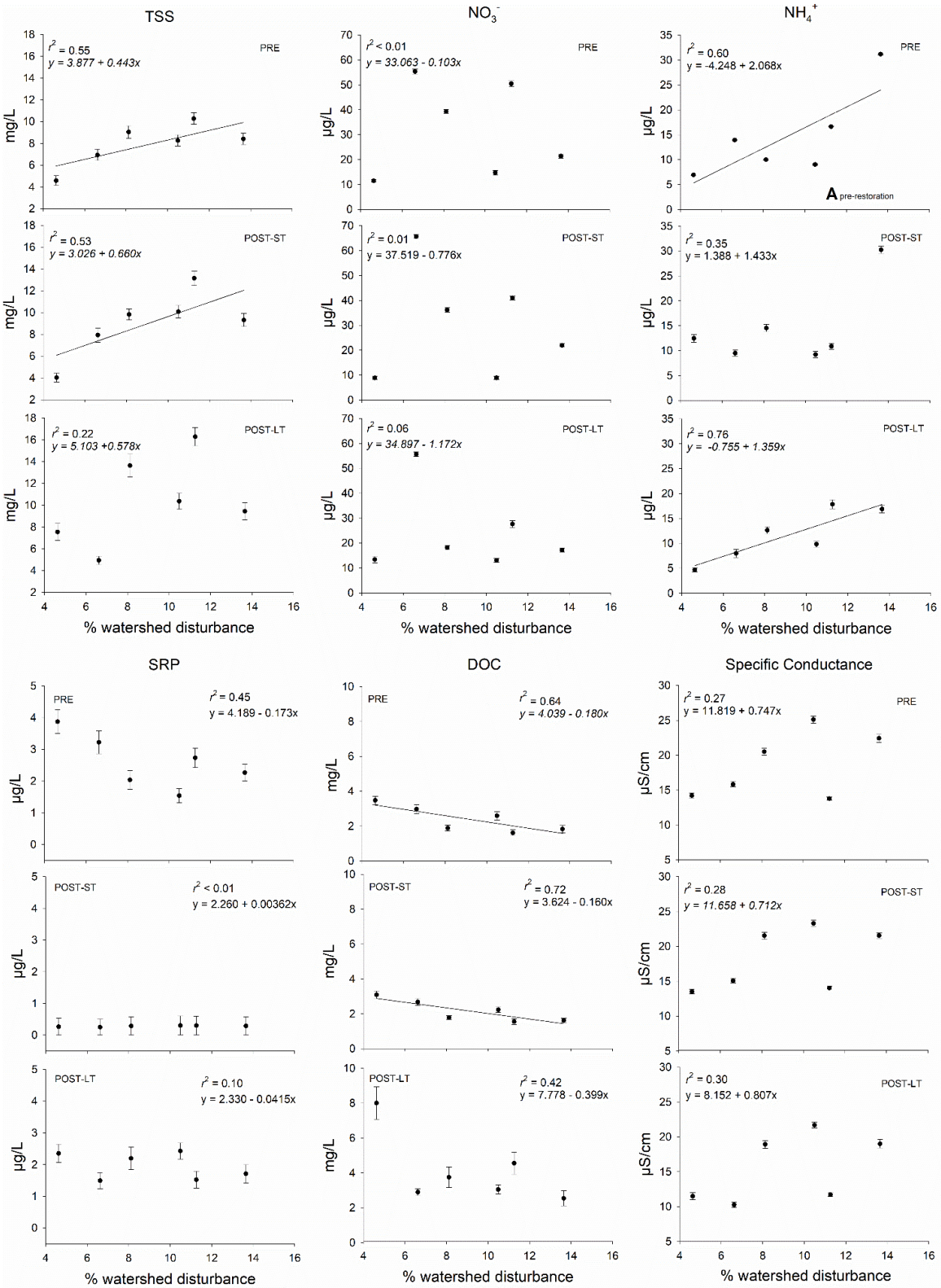

Supplemental Material (not copyedited or formatted) for: Samuel Bickley, Brian S. Helms, Daniel Isenberg, Jack W. Feminella, Brian J. Roberts, Natalie A. Griffiths. 2021. "Lack of Long-Term Effect of Coarse Woody Debris Dam Restoration on Ecosystem Functioning and Water Quality in Coastal Plain Streams." Freshwater Science 40(4). DOI: https://doi.org/10.1086/717325.

Table 2-S1. Type-II ANOVA table of areal coarse woody debris (CWD) response to CWD additions.

Response	**Fixed effects**	**Wald $\chi 2$**	**df**	***p*-value**
Areal CWD n = 7	treatment	0.23	1	0.63

Table 2-S2. Mean (± SE) values of water quality metrics (total suspended solid [TSS], pH, specific conductance [Sp. cond.], nitrate [NO_3^-], ammonium [NH_4^+], soluble reactive phosphorus [SRP], and dissolved organic carbon [DOC] concentrations) in 3 unrestored and 4 restored streams in the pre-restoration (PRE), 1 to 3 y post-restoration (POST-ST), and 14 y post-restoration (POST-LT) periods at Fort Benning Military Installation, Georgia, USA. See text for further details.

Stream	Period	TSS (mg/L)	pH	Sp. cond. (µS/cm)	NO_3^- (µg N/L)	NH_4^+ (µg N/L)	SRP (µg P/L)	DOC (mg/L)
Unrestored								
Hollis Branch	PRE	6.9 ± 1.2	5.2 ± 0.1	15.8 ± 0.5	55.4 ± 4.2	14.0 ± 2.9	3.2 ± 0.6	3.0 ± 0.2
	POST-ST	4.3 ± 2.0	5.6 ± 0.1	15.1 ± 0.4	65.7 ± 3.3	9.5 ± 1.7	2.3 ± 0.3	2.7 ± 0.2
	POST-LT	5.0 ± 0.5	5.1 ± 0.2	10.3 ± 0.5	55.7 ± 3.3	8.0 ± 2.7	1.5 ± 0.3	2.9 ± 0.1
Bonham Creek	PRE	3.9 ± 0.8	4.7 ± 0.1	24.6 ± 0.5	4.1 ± 1.6	7.2 ± 1.3	3.6 ± 0.6	1.5 ± 0.1
	POST-ST	4.3 ± 0.5	5.0 ± 0.1	21.5 ± 0.5	2.9 ± 0.5	14.8 ± 2.7	3.1 ± 0.4	2.4 ± 0.2
	POST-LT	5.0 ±2.0	4.9 ± 0.2	20.9 ± 0.8	1.8 ± 1.1	5.5 ± 0.8	2.2 ± 0.6	3.1 ± 0.6
Sally Branch 4	PRE	8.4 ± 1.1	5.7 ± 0.1	22.4 ± 1.4	21.4 ± 2.8	31.2 ± 3.1	2.3 ± 0.3	1.8 ± 0.2
	POST-ST	9.3 ± 1.5	5.8 ± 0.1	21.5 ± 0.7	22.0 ± 2.1	30.3 ± 2.5	2.3 ± 0.4	1.6 ± 0.1
	POST-LT	9.5 ± 1.8	5.7 ± 0.2	19.0 ± 1.3	17.2 ± 2.3	16.9 ± 2.1	1.7 ± 0.3	2.5 ± 0.6
Restored								
King's Mill	PRE	4.6 ± 0.8	5.0 ± 0.0	14.2 ± 0.5	11.5 ± 1.0	6.9 ± 1.4	3.9 ± 0.6	3.5 ± 0.2
	POST-ST	4.0 ± 0.7	5.6 ± 0.1	13.5 ± 0.4	8.9 ± 1.5	12.5 ± 2.4	2.4 ± 0.3	3.1 ± 0.2

	POST-LT	7.6 ± 2.2	5.1 ± 0.2	11.5 ± 0.9	13.4 ± 6.8	4.7 ± 0.7	2.4 ± 0.3	8.0 ± 3.5
Sally Branch 2	PRE	9.0 ± 1.4	6.1 ± 0.0	20.5 ± 1.1	39.3 ± 2.6	10.0 ± 1.4	2.0 ± 0.4	1.9 ± 0.1
	POST-ST	9.8 ± 1.2	6.2 ± 0.1	21.5 ± 1.0	36.2 ± 3.5	14.5 ± 2.3	1.2 ± 0.4	1.8 ± 0.1
	POST-LT	13.6 ± 3.6	5.6 ± 0.2	18.9 ± 1.1	18.2 ± 2.4	12.7 ± 1.9	2.2 ± 0.5	3.8 ± 1.2
Sally Branch 3	PRE	8.3 ± 1.1	6.2 ± 0.1	25.1 ± 1.1	14.7 ± 4.0	9.0 ± 1.6	1.5 ± 0.2	2.6 ± 0.2
	POST-ST	10.2 ± 1.4	6.3 ± 0.1	23.3 ± 0.9	8.9 ± 1.9	9.2 ± 1.8	2.5 ± 0.4	2.2 ± 0.1
	POST-LT	10.4 ± 1.7	5.8 ± 0.2	21.7 ± 0.6	13.1 ± 2.0	9.8 ± 1.4	2.4 ± 0.2	3.0 ± 0.2
Little Pine Knot	PRE	10.3 ± 1.1	5.5 ± 0.0	13.8 ± 0.2	50.5 ± 5.7	16.6 ± 3.1	2.7 ± 0.4	1.6 ± 0.1
	POST-ST	13.2 ± 1.9	5.7 ± 0.1	14.0 ± 0.2	41.0 ± 2.6	10.7 ± 1.4	2.3 ± 0.4	1.6 ± 0.1
	POST-LT	16.3 ± 2.6	5.1 ± 0.2	11.7 ± 0.4	27.7 ± 7.3	17.9 ± 3.4	1.5 ± 0.3	4.6 ± 1.7

Supplemental Material (not copyedited or formatted) for: Samuel Bickley, Brian S. Helms, Daniel Isenberg, Jack W. Feminella, Brian J. Roberts, Natalie A. Griffiths. 2021. "Lack of Long-Term Effect of Coarse Woody Debris Dam Restoration on Ecosystem Functioning and Water Quality in Coastal Plain Streams." Freshwater Science 40(4). DOI: https://doi.org/10.1086/717325.

Table 2-S3. Type-II ANOVA tables, with Benjamini-Hochberg (BH) corrected p-values, of water quality metric (total suspended solid [TSS], pH, specific conductance [Sp. cond.], nitrate [NO_3^-], ammonium [NH_4^+], soluble reactive phosphorus [SRP], and dissolved organic carbon [DOC] concentrations) response to CWD additions. *n* = number of observations associated with each model.

Response	**Fixed effects**	**Wald $\chi 2$**	**df**	**BH corrected *p*-value**
TSS n = 375				
	treatment	1.50	1	0.46
	period	2.80	2	0.43
	season	48.93	3	< 0.01
	treatment x period	4.84	2	0.32
	treatment x season	0.67	3	0.88
	period x season	9.31	6	0.37
	treatment x period x season	3.16	6	0.88
pH n = 383				
	treatment	0.92	1	0.39
	period	61.57	2	< 0.01
	season	33.97	3	< 0.01
	treatment x period	11.70	2	< 0.01
	treatment x season	2.27	3	0.52
	period x season	50.48	6	< 0.01
	treatment x period x season	7.14	6	0.40
Specific conductance n = 368				
	treatment	0.16	1	0.81
	period	34.68	2	< 0.01
	season	26.90	3	< 0.01
	treatment x period	4.29	2	0.21
	treatment x season	2.19	3	0.74
	period x season	26.02	6	< 0.01
	treatment x period x season	1.53	6	0.96

NO_3^- n = 376				
	treatment	0.04	1	0.85
	period	5.73	2	0.14
	season	15.43	3	< 0.01
	treatment x period	2.06	2	0.63
	treatment x season	0.80	3	0.85
	period x season	13.29	6	0.14
	treatment x period x season	3.35	6	0.85
NH_4^+ n = 379				
	treatment	0.64	1	0.58
	period	6.10	2	0.18
	season	22.14	3	< 0.01
	treatment x period	4.60	2	0.23
	treatment x season	0.88	3	0.83
	period x season	4.53	6	0.71
	treatment x period x season	6.81	6	0.58
SRP n = 397				
	treatment	0.36	1	0.65
	period	7.86	2	0.05
	season	20.11	3	< 0.01
	treatment x period	2.37	2	0.54
	treatment x season	1.94	3	0.65
	period x season	18.20	6	0.02
	treatment x period x season	4.17	6	0.65
DOC n = 364				
	treatment	0.99	1	0.37
	period	16.76	2	< 0.01
	season	1.86	3	0.60
	treatment x period	6.76	2	0.05
	treatment x season	5.51	3	0.20
	period x season	26.49	6	< 0.01
	treatment x period x season	16.94	6	0.02

Table 2-S*4*. Type-II ANOVA tables of water quality metric (total suspended solid [TSS], pH, specific conductance [Sp. cond.], nitrate [NO_3^-], ammonium [NH_4^+], soluble reactive phosphorus [SRP], and dissolved organic carbon [DOC] concentrations) differences among restoration period (PRE, POST-ST, and POST-LT). n = number of observations associated with each model.

Response	**Fixed effects**	**Wald χ^2**	**df**	***p*-value**
TSS n = 375				
	period	3.52	2	0.18
pH n = 383				
	period	29.98	2	< 0.01
Specific conductance n = 368				
	period	27.64	2	< 0.01
NO_3^- n = 376				
	period	4.79	2	0.09
NH_4^+ n = 379				
	period	3.42	2	0.14
SRP n = 397				
	period	8.18	2	0.02
DOC n = 364				
	period	10.81	2	< 0.01

Table 2-S5. Type-II ANOVA tables of water quality metric (total suspended solid [TSS], pH, specific conductance [Sp. cond.], nitrate [NO_3^-], ammonium [NH_4^+], soluble reactive phosphorus [SRP], and dissolved organic carbon [DOC] concentrations) response to CWD additions during the POST-LT period. *n* = number of observations associated with each model.

Response	**Fixed effects**	**Wald χ^2**	**df**	***p*-value**
TSS n = 98				
	treatment	5.6	1	0.01
	season	5.02	3	0.17
	treatment x season	0.078	3	0.86
pH n = 98				
	treatment	0.07	1	0.80
	season	26.64	3	< 0.01
	treatment x season	3.20	3	0.36
Specific conductance n = 98				
	treatment	0.03	1	0.86
	season	17.13	3	< 0.01
	treatment x season	3.06	3	0.38
NO_3^- n = 106				
	treatment	0.21	1	0.65
	season	0.28	3	0.96
	treatment x season	1.87	3	0.60
NH_4^+ n = 107				
	treatment	0.02	1	0.88
	season	4.73	3	0.19
	treatment x season	4.46	3	0.33
SRP n = 106				
	treatment	1.15	1	0.28
	season	17.43	2	< 0.01
	treatment x season	2.17	3	0.54
DOC n = 107				

treatment	2.36	1	0.12
season	9.28	2	0.03
treatment x season	8.01	3	0.05

Table 2-S6. Type-II ANOVA table of nutrient uptake metrics (U, v_f) response to CWD additions during summer. n = number of observations associated with each model.

Response	**Fixed effects**	**Wald χ2**	**df**	***p*-value**
U				
n = 21	treatment	0.612	1	0.43
	period	0.35	1	0.55
	treatment x period	1.18	1	0.28
v_f				
n = 21	treatment	0.59	1	0.44
	period	1.45	1	0.23
	treatment x period	0.52	1	0.47

Table 2-S7. Type-II ANOVA table of nutrient uptake metrics (U, v_f) response to CWD additions during autumn. n = number of observations associated with each model.

Response	**Fixed effects**	**Wald χ2**	**df**	***p*-value**
U				
n = 42	treatment	< 0.01	1	0.97
	period	3.81	2	0.15
	treatment x period	0.76	2	0.68
v_f				
n = 42	treatment	1.16	1	0.28
	period	6.614	2	0.04
	treatment x period	3.65	2	0.16

Supplemental Material (not copyedited or formatted) for: Samuel Bickley, Brian S. Helms, Daniel Isenberg, Jack W. Feminella, Brian J. Roberts, Natalie A. Griffiths. 2021. "Lack of Long-Term Effect of Coarse Woody Debris Dam Restoration on Ecosystem Functioning and Water Quality in Coastal Plain Streams." Freshwater Science 40(4). DOI: https://doi.org/10.1086/717325.

Table 2-S8. Type-II ANOVA table of nutrient uptake metrics (U, v_f) response to CWD additions during spring. n = number of observations associated with each model.

Response	**Fixed effects**	**Wald χ2**	**df**	***p*-value**
U				
n = 14	treatment	3.83	1	0.05
	period	1.69	1	0.19
	treatment x period	0.13	1	0.72
v_f				
n = 14	treatment	7.05	1	< 0.01
	period	5.33	1	0.02
	treatment x period	4.69	1	0.03

Table 2-S9. Mean ammonium uptake velocity (v_f ; mm/s) and areal ammonium uptake rate (U; mg N m^{-2} d^{-1}) and physical characteristics (stream discharge [Q], wetted width, water velocity [v], and water depth [z]) of each stream during the fall, in the pre-restoration (PRE), 1-3 y post-restoration (POST-ST), and 14-15 y post-restoration (POST-LT) periods. NU* indicates no measurable uptake. *n* indicates the number of NH_4^+ uptake measurements conducted per period in each stream during fall.

Stream	Period	*n*	Mean v_f (mm/s)	Mean U (mg N m^{-2} d^{-1})	Mean Q (L/s)	Mean width (m)	Mean v (m/s)	Mean z (m)
Unrestored								
HB	PRE	1	0.01	51.4	18.4	1.80	0.08	0.12
	POST-ST	3	0.01	26.5	16.6	1.88	0.07	0.13
	POST-LT	2	0.02	9.1	22.9	2.43	0.05	0.21
BC	PRE	1	0.03	88.9	7.5	1.34	0.04	0.14
	POST-ST	3	0.02	69.5	10.8	1.22	0.05	0.17
	POST-LT	2	0.06	16.3	11.2	1.83	0.03	0.18
SB4	PRE	1	NU*	NU*	7.9	1.24	0.11	0.06

	POST-ST	3	< 0.01	2.9	11.2	1.66	0.12	0.06
	POST-LT	2	0.04	50.0	24.3	1.78	0.11	0.11
Restored								
	PRE	1	0.02	72.1	29.3	2.03	0.10	0.14
KM	POST-ST	3	0.02	72.6	24.1	2.18	0.08	0.15
	POST-LT	2	NU*	NU*	41.3	2.49	0.09	0.19
	PRE	1	0.01	24.0	14.3	1.50	0.13	0.07
SB2	POST-ST	3	0.01	17.7	16.4	1.77	0.11	0.08
	POST-LT	2	0.04	31.4	30.2	2.18	0.06	0.14
	PRE	1	0.02	67.8	5.8	1.19	0.09	0.05
SB3	POST-ST	3	0.01	35.0	7.2	1.31	0.08	0.07
	POST-LT	2	0.01	3.7	14.3	1.76	0.13	0.06
	PRE	1	0.01	23.7	3.4	0.89	0.10	0.04
LPK	POST-ST	3	0.01	49.8	4.5	1.05	0.09	0.05
	POST-LT	2	0.02	13.6	3.2	1.40	0.08	0.04

Table 2-S10. Type-II ANOVA table of nutrient uptake metrics (U, v_f) response to CWD additions during POST-LT restoration period. n = number of observations associated with each model.

Response	**Fixed effects**	**Wald χ2**	**df**	***p*-value**
U				
n = 36				
	treatment	0.09	1	0.76
v_f				
n = 36				
	treatment	1.51	1	0.22

Table 2-S11. Type-II ANOVA table of whole-stream metabolism indicators (daily amplitude of dissolved oxygen (DO) deficit, maximum daily DO deficit) response to CWD additions during spring. n = number of observations associated with each model.

Response	**Fixed effects**	**Wald χ2**	**df**	***p*-value**
daily amplitude of dissolved oxygen deficit				
n = 221	treatment	0.04	1	0.85
	period	4.71	2	0.09
	treatment x period	0.10	2	0.95
maximum daily DO deficit				
n = 221	treatment	0.02	1	0.89
	period	14.60	2	< 0.01
	treatment x period	1.93	2	0.38

Table 2-S12. Type-II ANOVA table of whole-stream metabolism indicators (daily amplitude of dissolved oxygen (DO) deficit, maximum daily DO deficit) response to CWD additions during summer. *n* = number of observations associated with each model.

Response	**Fixed effects**	**Wald χ2**	**df**	***p*-value**
daily amplitude of dissolved oxygen deficit				
n = 218	treatment	< 0.01	1	0.97
	period	4.76	2	0.09
	treatment x period	0.73	2	0.69
maximum daily DO deficit				
n = 218	treatment	1.4	1	0.23
	period	54.86	2	< 0.01
	treatment x period	3.27	2	0.19

Table 2-S13. Type-II ANOVA table of whole-stream metabolism indicators (daily amplitude of dissolved oxygen (DO) deficit, maximum daily DO deficit) response to CWD additions during autumn. *n* = number of observations associated with each model.

Response	**Fixed effects**	**Wald χ2**	**df**	***p*-value**
daily amplitude of dissolved oxygen deficit				
n = 132	treatment	0.02	1	0.88
	period	3.46	2	0.18
	treatment x period	1.13	2	0.57
maximum daily DO deficit				
n = 132	treatment	0.55	1	0.46
	period	11.84	2	< 0.01
	treatment x period	1.963	2	0.38

Supplemental Material (not copyedited or formatted) for: Samuel Bickley, Brian S. Helms, Daniel Isenberg, Jack W. Feminella, Brian J. Roberts, Natalie A. Griffiths. 2021. "Lack of Long-Term Effect of Coarse Woody Debris Dam Restoration on Ecosystem Functioning and Water Quality in Coastal Plain Streams." Freshwater Science 40(4). DOI: https://doi.org/10.1086/717325.

Table 2-S14. Mean whole-stream metabolism indicators, daily amplitude of dissolved oxygen (DO) deficit (mg/L) (an indicator of gross primary production) and maximum daily DO deficit (mg/L) (an indicator of ecosystem respiration), in each stream across all seasons in the pre-restoration (PRE), 1-3 y post-restoration (POST-ST), and 14-15 y post-restoration (POST-LT) periods. *n* indicates the number of metabolism measurements conducted per period in each stream.

Stream	Period	*n*	Daily amplitude of DO deficit (mg/L)	Maximum daily DO deficit (mg/L)
Unrestored				
HB	PRE	9	0.44	0.86
	POST-ST	12	0.36	0.77
	POST-LT	5	0.25	1.34
BC	PRE	9	0.62	1.76
	POST-ST	11	0.42	1.16
	POST-LT	5	0.48	1.90
SB4	PRE	8	0.48	0.90
	POST-ST	12	0.34	0.73
	POST-LT	5	0.41	1.49
Restored				
KM	PRE	8	0.68	1.34

	POST-ST	11	0.53	1.24
	POST-LT	5	0.30	1.51
	PRE	8	0.62	1.04
SB2	POST-ST	12	0.31	0.96
	POST-LT	5	0.36	1.42
	PRE	8	0.29	0.74
SB3	POST-ST	11	0.41	0.87
	POST-LT	5	0.46	1.42
	PRE	7	0.26	0.80
LPK	POST-ST	11	0.45	0.85
	POST-LT	3	0.60	1.52

Table 2-S15. Type-II ANOVA table of whole-stream metabolism indicators (daily amplitude of dissolved oxygen (DO) deficit, maximum daily DO deficit) response to CWD additions during the POST-LT restoration period. *n* = number of observations associated with each model.

Response	**Fixed effects**	**Wald χ2**	**df**	***p*-value**
daily amplitude of dissolved oxygen deficit *n* = 168				
	treatment	0.30	1	0.58
maximum daily DO deficit *n* = 168				
	treatment	0.53	1	0.46

Table 2-S16. r^2 and Benjamini-Hochberg (BH) corrected *P*-values from the regression analyses examining the effects of % watershed disturbance on areal ammonium uptake rate (*U*; mg N m^{-2} d^{-1}) and ammonium uptake velocity (v_f; mm/s) by year and season across pre-restoration (PRE), 1-3 y post-restoration (POST-ST), and 14-15 y post-restoration (POST-LT) periods.

			n	U			v_f;		
Period	Year	Season		U r^2	Direction	BH corrected *P*-value	v_f r^2	Direction	BH corrected *P*-value
PRE	2003	Fall	6	0.51	-	0.44	0.6	-	0.28
POST-ST	2003	Fall	6	0.63	-	0.44	0.85	-	0.11
POST-ST	2004	Winter	6	< 0.01	+	0.99	< 0.01	+	0.98
POST-ST	2004	Spring	6	0.15	-	0.81	0.3	-	0.78
POST-ST	2004	Summer	6	0.14	-	0.81	0.06	-	0.92
POST-ST	2004	Fall	6	< 0.01	-	0.99	0.1	-	0.92
POST-ST	2005	Fall	6	0.15	-	0.81	0.15	-	0.92
POST-LT	2017	Summer	6	0.03	+	0.94	< 0.01	-	0.98
POST-LT	2017	Fall	6	0.02	-	0.94	0.04	-	0.92

POST-LT	2018	Spring	6	0.25	+	0.81	0.02	-	0.94
POST-LT	2018	Summer	6	0.06	-	0.94	0.12	-	0.92
POST-LT	2018	Fall	6	0.57	+	0.44	0.67	+	0.28

Table 2-S17. r^2 and Benjamini-Hochberg (BH) corrected *P*-values for regression analyses of the effects of % watershed disturbance on total suspended solids (TSS; mg/L), specific conductance (Sp. Cond.; µS/cm), and pH by year and season across pre-restoration (PRE), 1-3 y post-restoration (POST-ST), and 14-15 y post-restoration (POST-LT) periods in restored and unrestored streams. "No data" indicates no data was collected.

Period	Year	Season	TSS (mg/L)				Sp. Cond. (µS/cm)				pH			
			r^2	Direction of relationship	BH corrected *P*-value	n	r^2	Direction of relationship	BH corrected *P*-value	n	r^2	Direction of relationship	BH corrected *P*-value	n
PRE	2001	Summer	0.84	+	0.17	5	0.47	+	0.49	5	0.37	+	0.51	5
PRE	2001	Fall	0.86	+	0.13	6	0.3	+	0.49	6	0.29	+	0.51	6
PRE	2002	Winter	0.31	+	0.47	6	0.24	+	0.49	6	0.04	+	0.81	6
PRE	2002	Spring	0.34	+	0.46	6	0.22	+	0.49	6	0.26	+	0.53	6
PRE	2002	Summer	0.06	+	0.75	6	0.14	+	0.52	6	0.36	+	0.51	6
PRE	2002	Fall	0.2	+	0.53	6	0.25	+	0.49	6	0.18	+	0.55	6
PRE	2003	Winter	0.18	+	0.53	6	0.3	+	0.49	6	0.35	+	0.51	6
PRE	2003	Spring	0.51	+	0.37	6	0.27	+	0.49	6	0.21	+	0.55	6
PRE	2003	Summer	0.38	+	0.46	6	0.26	+	0.49	6	0.37	+	0.51	6
PRE	2003	Fall	0.13	+	0.91	6	0.23	+	0.49	6	0.3	+	0.51	6
1-3y PR	2003	Fall	No data				0.5	+	0.49	6	0.01	+	0.90	6
1-3y PR	2004	Winter	0.71	+	0.53	3	0.58	+	0.45	3	0.16	+	0.83	3
1-3y PR	2004	Spring	0.77	+	0.14	6	0.24	+	0.32	6	0.16	+	0.55	6

1-3y PR	2004	Summer	0.79	+	0.14	6	0.23	+	0.33	6	< 0.01	-	0.94	6
1-3y PR	2004	Fall	0.36	-	0.46	6	0.12	+	0.51	6	0.19	+	0.55	6
1-3y PR	2005	Winter	0.11	+	0.65	6	0.14	+	0.47	6	0.29	+	0.51	6
1-3y PR	2005	Spring	0.77	+	0.37	4	0.45	+	0.49	4	0.94	-	0.51	4
1-3y PR	2005	Summer		No data					No data			No data		
1-3y PR	2005	Fall	0.44	+	0.42	6	0.41	+	0.49	6	0.34	+	0.51	6
1-3y PR	2006	Winter	0.57	+	0.37	6	0.25	+	0.49	6	0.34	+	0.51	6
1-3y PR	2006	Spring	0.2	+	0.53	6	0.26	+	0.49	6	0.3	+	0.51	6
1-3y PR	2006	Summer	0.34	+	0.46	6	0.31	+	0.52	4	0.59	+	0.51	6
1-3y PR	2006	Fall	0.97	+	0.37	3		No data			0.36	+	0.71	3
14-15y PR	2017	Spring	< 0.01	+	0.95	6	0.25	+	0.49	6	0.51	+	0.51	6
14-15y PR	2017	Summer	0.16	+	0.55	6	0.38	+	0.49	6	0.43	+	0.51	6
14-15y PR	2017	Fall	< 0.01	-	0.95	6	0.13	+	0.52	6	0.17	+	0.55	6
14-15y PR	2018	Winter	0.21	+	0.53	6	0.19	+	0.93	6	0.15	+	0.55	6
14-15y PR	2018	Spring	0.93	+	0.13	5	0.53	-	0.49	5	< 0.01	-	0.91	5
14-15y PR	2018	Summer	0.2	+	0.53	6	0.47	+	0.49	6	0.67	+	0.51	6
14-15y PR	2018	Fall	< 0.01	+	0.95	6	0.18	+	0.52	6	0.37	+	0.51	6

Table 2-S17 (continued). r^2 and Benjamini-Hochberg (BH) corrected *P*-values for regression analyses of the effects of % watershed disturbance on mean physiochemical parameters by year and season across pre-restoration (PRE), 1-3 y post-restoration (POST-ST), and 14-15 y post-restoration (POST-LT) periods in restored and unrestored streams. “No data” indicates no data was collected.

Supplemental Material (not copyedited or formatted) for: Samuel Bickley, Brian S. Helms, Daniel Isenberg, Jack W. Feminella, Brian J. Roberts, Natalie A. Griffiths. 2021.
"Lack of Long-Term Effect of Coarse Woody Debris Dam Restoration on Ecosystem Functioning and Water Quality in Coastal Plain Streams."
Freshwater Science 40(4). DOI: https://doi.org/10.1086/717325.

			NO_3^- (µg N/L)				NH_4^+ (µg N/L)				SRP (µg P/L)				DOC (mg/L)			
Period	Year	Season	r^2	Direction	BH corrected *p*-value	n	r^2	Direction	BH corrected *p*-value	n	r^2	Direction	BH corrected *p*-value	n	r^2	Direction	BH corrected *p*-value	n
PRE	2001	Summer	0.04	-	0.98	5	0.50	+	0.35	5	0.61	-	0.47	5		No data		
PRE	2001	Fall	< 0.01	-	0.98	6	0.71	+	0.35	6	0.56	-	0.44	6		No data		
PRE	2002	Winter	0.05	-	0.98	6	0.59	+	0.35	6	0.10	-	0.78	6	0.77	-	0.13	6
PRE	2002	Spring	< 0.01	+	0.98	6	0.55	+	0.35	6	0.64	+	0.41	6	0.38	-	0.31	6
PRE	2002	Summer	0.24	+	0.98	6	0.15	+	0.52	6	0.61	-	0.41	6	0.26	-	0.37	6
PRE	2002	Fall	0.01	+	0.98	6	0.59	+	0.35	6	0.79	-	0.29	6		No data		
PRE	2003	Winter	< 0.01	+	0.98	6	0.37	+	0.35	6	0.15	-	0.78	6	0.83	-	0.13	6
PRE	2003	Spring	< 0.01	-	0.98	6	0.49	+	0.35	6	0.06	-	0.82		0.69	-	0.13	6
PRE	2003	Summer	< 0.01	-	0.98	6	0.44	+	0.35	6	0.02	+	0.90		0.61	-	0.16	6
PRE	2003	Fall	0.14	-	0.98	6	0.10	+	0.57	6	0.45	+	0.48		0.68	-	0.13	6
1-3y PR	2003	Fall	< 0.01	+	0.98	6	0.03	-	0.73	6	0.39	+	0.52	6	< 0.01	+	0.98	6
1-3y PR	2004	Winter	0.11	+	0.98	3	0.73	+	0.48	3	0.59	+	0.78	3	0.84	-	0.36	3
1-3y PR	2004	Spring	0.05	-	0.98	6	0.39	+	0.35	6	0.10	+	0.78	6	0.71	-	0.13	6
1-3y PR	2004	Summer	0.03	-	0.98	6	0.40	+	0.35	6	0.27	-	0.75	6	0.58	-	0.16	6
1-3y PR	2004	Fall	0.04	-	0.98	6	0.23	+	0.48	6	< 0.01	+	0.98	6	0.52	-	0.18	6
1-3y PR	2005	Winter	0.03	-	0.98	6	0.22	+	0.52	6	0.12	-	0.78	6	0.35	-	0.32	6
1-3y PR	2005	Spring	0.65	-	0.98	4	0.90	+	0.35	4	0.94	+	0.29	4	0.25	-	0.57	4
1-3y PR	2005	Summer	No data				No data				No data				No data			
1-3y PR	2005	Fall	< 0.01	+	0.98	6	0.38	+	0.35	6	0.20	-	0.78	6	0.51	-	0.18	6
1-3y PR	2006	Winter	0.02	-	0.98	6	0.47	+	0.35	6	0.14	+	0.78	6	0.69	-	0.13	6

1-3y PR	2006	Spring	0.02	+	0.98	6	0.27	+	0.45	6	0.08	+	0.78	6	0.57	-	0.16	6
1-3y PR	2006	Summer	0.33	-	0.98	4	0.41	+	0.48	4	0.84	+	0.29	6	0.15	+	0.53	6
1-3y PR	2006	Fall	No data				No data				0.23	+	0.82	3	1.00	-	0.13	3
14-15y PR	2017	Spring	0.30	-	0.98	6	0.15	+	0.52	6	0.48	-	0.47	6	0.58	-	0.16	6
14-15y PR	2017	Summer	< 0.01	-	0.98	6	0.59	+	0.35	6	0.26	+	0.75	6	0.57	-	0.16	6
14-15y PR	2017	Fall	0.26	-	0.98	6	0.14	+	0.52	6	0.08	-	0.78	6	0.52	-	0.18	6
14-15y PR	2018	Winter	< 0.01	-	0.98	6	0.56	+	0.35	6	< 0.01	+	0.99	6	0.27	-	0.36	6
14-15y PR	2018	Spring	0.15	+	0.98	5	0.20	-	0.52	5	0.03	-	0.89	5	< 0.01	+	0.98	5
14-15y PR	2018	Summer	< 0.01	-	0.98	6	0.36	+	0.35	6	0.01	-	0.90	6	< 0.01	-	0.98	6
14-15y PR	2018	Fall	0.05	-	0.98	6	0.47	+	0.35	6	0.21	-	0.78	6	0.68	-	0.13	6

Table 2-S18. r^2 and Benjamini-Hochberg (BH) corrected *P*-values for regression analyses of the effects of % watershed disturbance on stream metabolism indicators, mean maximum daily dissolved oxygen (DO) deficit and mean daily DO deficit amplitude (both mg/L), by year and season across pre-restoration (PRE), 1-3 y post-restoration (POST-ST), and 14-15 y post-restoration (POST-LT) periods.

Period	Year	Season	n	Max daily DO deficit r^2	Direction	Max daily DO deficit BH corrected *P*-value	Daily amplitude of the DO deficit r^2	Direction	Daily amplitude of the DO deficit BH corrected P-value
PRE	2001	Summer	4	0.67	-	0.47	0.58	+	0.69
PRE	2001	Fall	6	0.24	-	0.62	0.1	-	0.82
PRE	2002	Spring	6	0.27	-	0.62	0.3	-	0.75
PRE	2002	Summer	5	< 0.01	-	0.88	0.19	+	0.82
PRE	2002	Fall	6	0.04	-	0.88	0.5	-	0.68
PRE	2002	Winter	6	< 0.01	-	0.88	0.19	-	0.82
PRE	2003	Spring	5	0.28	-	0.62	0.46	-	0.68
PRE	2003	Summer	4	0.1	-	0.88	< 0.01	+	0.99
PRE	2003	Winter	6	0.42	-	0.47	0.14	-	0.82
POST-ST	2004	Spring	6	0.73	-	0.39	0.61	-	0.61
POST-ST	2004	Summer	6	0.29	-	0.62	0.18	+	0.82

POST-ST	2004	Fall	6	0.65	-	0.43	0.09	-	0.82
POST-ST	2004	Winter	6	<0.01	-	0.88	0.05	+	0.83
POST-ST	2005	Spring	5	0.03	-	0.88	0.56	-	0.68
POST-ST	2005	Summer	5	0.29	-	0.62	0.11	+	0.82
POST-ST	2005	Fall	5	0.51	-	0.47	0.14	+	0.82
POST-ST	2005	Winter	6	< 0.01	-	0.88	< 0.01	-	0.99
POST-ST	2006	Spring	6	0.55	-	0.47	0.05	-	0.83
POST-ST	2006	Summer	6	0.04	-	0.88	0.05	+	0.83
POST-ST	2006	Fall	6	0.02	-	0.88	0.36	+	0.68
POST-ST	2006	Winter	6	0.51	+	0.47	< 0.01	+	0.99
POST-LT	2017	Summer	6	0.5	+	0.47	0.97	+	< 0.01
POST-LT	2017	Fall	4	0.73	-	0.47	0.97	-	0.26
POST-LT	2018	Spring	6	0.79	-	0.39	0.37	-	0.68

POST-LT	2018	Summer	5	0.07	-	0.88	0.1	+	0.82
POST-LT	2018	Fall	6	0.02	-	0.88	< 0.01	-	0.99

Table 1. Catch per unit effort (CPUE) for all species at each site during Autumn 2019, Summer 2020, and Autumn 2020 and mean CPUE (± standard error) for each species across all sites. NS = No sample.

Date	Species	Stone Quarry	Long Bayou	Robinson Bayou	Manuel Bayou	Graham Creek	Indian Bayou	Heron Bayou	Trout Bayou	Weakley Bayou	Mulat Bayou	Bayou Grande	Texar Bayou	Mean CPUE (± SE)
Oct 2019														
	Fundulus grandis	**3.58**	**6.25**	**0.33**	**1.83**	**0.08**	**19.25**	**0.00**	**17.75**	**4.67**	**0.00**	**12.75**	**2.58**	**5.76 (1.93)**
	Poecillia latipinna	0.08	0.08	0.00	0.58	1.25	0.00	0.00	0.50	1.33	0.00	0.17	0.00	0.33 (0.14)
	Lagodon rhomboides	1.00	0.00	0.00	0.08	0.00	0.00	0.00	0.00	1.42	0.00	0.33	0.08	0.24 (0.13)
	Adinia xenica	0.17	0.08	0.00	0.00	0.00	0.25	0.00	0.75	0.00	0.00	0.00	0.00	0.10 (0.06)
	Fundulus jekenkski	0.25	0.00	0.08	0.25	0.00	0.33	0.00	0.08	0.08	0.00	0.00	0.08	0.10 (0.03)
	Fundulus confluentus	0.00	0.00	0.00	0.00	0.00	0.17	0.00	0.33	0.00	0.00	0.00	0.00	0.04 (0.03)
	Gambusia holbrooki	0.00	0.00	0.00	0.00	0.25	0.08	0.00	0.00	0.00	0.00	0.00	0.00	0.03 (0.02)
	Fundulus pulvereus	0.00	0.00	0.00	0.00	0.25	0.00	0.00	0.00	0.00	0.00	0.00	0.00	0.02 (0.02)
	Cyprinodon variegatus	0.00	0.17	0.00	0.00	0.00	0.00	0.00	0.00	0.00	0.00	0.00	0.00	0.01 (0.01)
	Total	5.08	6.58	0.42	2.75	1.83	20.08	0.00	19.42	7.50	0.00	13.25	2.75	6.64 (2.00)
Jul 2020														
	Lagodon rhomboides	9.67	0.00	0.00	0.92	0.00	NS	0.00	18.92	13.17	0.00	2.92	21.67	6.11 (2.39)
	Fundulus grandis	**4.08**	**14.33**	**0.00**	**0.00**	**6.83**	NS	**0.00**	**6.17**	**12.42**	**0.00**	**9.75**	**2.67**	5.11 (1.51)
	Poecillia latipinna	0.25	0.75	0.00	1.75	0.58	NS	0.00	0.75	2.92	0.00	0.00	0.33	0.67 (0.26)
	Adinia xenica	0.33	0.83	0.00	0.00	0.00	NS	0.00	2.83	1.17	0.00	0.83	0.75	0.61 (0.25)
	Fundulus jekenkski	0.08	0.33	0.67	0.00	0.00	NS	0.00	0.25	2.25	0.00	0.58	0.08	0.39 (0.19)
	Cyprinodon variegatus	0.50	1.50	0.00	0.00	0.50	NS	0.00	0.67	0.00	0.00	0.00	0.00	0.29 (0.14)
	Fundulus confluentus	0.08	0.25	0.00	0.00	0.00	NS	0.00	0.00	2.08	0.00	0.00	0.42	0.26 (0.18)
	Gambusia holbrooki	0.25	0.08	0.00	1.00	0.17	NS	0.25	0.00	0.00	0.00	0.00	0.33	0.19 (0.09)
	Fundulus pulvereus	0.00	0.08	0.17	0.00	0.08	NS	0.00	0.00	0.17	0.00	0.00	0.00	0.05 (0.02)
	Anchoa mitchilli	0.00	0.00	0.00	0.00	0.00	NS	0.00	0.17	0.00	0.00	0.00	0.00	0.02 (0.01)
	Fundulus similis	0.00	0.00	0.00	0.00	0.00	NS	0.00	0.00	0.00	0.00	0.00	0.08	0.01 (0.01)
	Total	15.25	18.17	0.83	3.67	8.17	NS	0.25	29.75	34.17	0.00	14.08	26.33	13.70 (3.55)
Oct 2020														
	Lagodon rhomboides	15.25	0.00	0.00	1.75	0.00	2.08	0.00	2.00	0.50	0.00	0.58	10.58	2.73 (1.36)
	Fundulus grandis	**1.50**	**5.58**	**0.00**	**0.00**	**0.17**	**6.33**	**0.17**	**2.50**	**2.00**	**1.00**	**2.42**	**1.75**	**1.95 (0.58)**
	Gambusia holbrooki	0.17	0.00	0.00	5.33	0.33	0.00	1.00	0.33	0.00	0.33	0.00	0.00	0.63 (0.42)

Fundulus jekenkski	0.00	0.08	0.00	0.92	0.00	0.00	0.42	0.50	0.08	0.08	0.00	0.00	0.17 (0.08)
Poecillia latipinna	0.17	0.00	0.00	0.33	0.25	0.00	0.00	0.00	0.25	0.00	0.00	0.00	0.08 (0.04)
Fundulus confluentus	0.00	0.00	0.00	0.08	0.00	0.00	0.00	1.17	0.00	0.08	0.00	0.00	0.11 (0.09)
Fundulus pulvereus	0.00	0.08	0.00	0.00	0.00	0.00	0.00	0.33	0.00	0.17	0.00	0.00	0.05 (0.03)
Cyprinodon variegatus	0.00	0.08	0.00	0.00	0.00	0.00	0.00	0.17	0.00	0.00	0.00	0.00	0.02 (0.01)
Centroprisis Striata	0.08	0.00	0.00	0.00	0.00	0.00	0.00	0.00	0.00	0.00	0.00	0.00	0.01 (0.01)
Total	17.17	5.83	0.00	8.42	0.75	8.42	1.58	7.00	2.83	1.67	3.00	12.33	5.75 (1.44)

Table 2. Fish species length and weight averaged for each sampling event by site and season.

Site	Species	Year	Season	*n* fish	Length (mm)	Length SE	Weight (g)	Weight SE
Bayou Grande	Fundulus grandis	2019	autumn	153	78.64	1.56	6.32	0.38
Bayou Grande	Lagodon rhomboides	2019	autumn	4	66.50	3.28	4.80	0.78
Bayou Grande	Poecillia latipinna	2019	autumn	2	51.50	1.50	1.69	0.18
Graham Creek	Fundulus grandis	2019	autumn	3	76.33	4.18	5.10	1.01
Graham Creek	Fundulus pulvereus	2019	autumn	3	46.33	3.84	1.15	0.36
Graham Creek	Gambusia holbrooki	2019	autumn	7	37.14	1.75	0.52	0.07
Graham Creek	Poecillia latipinna	2019	autumn	18	38.94	0.86	0.79	0.07
Indian Bayou	Adinia xenica	2019	autumn	3	37.33	1.76	0.80	0.16
Indian Bayou	Fundulus confluentus	2019	autumn	2	53.00	1.00	1.44	0.06
Indian Bayou	Fundulus grandis	2019	autumn	231	72.48	1.20	4.97	0.29
Indian Bayou	Fundulus jekenkski	2019	autumn	4	51.75	2.72	1.06	0.16
Indian Bayou	Gambusia holbrooki	2019	autumn	1	42.00	NA	0.61	NA
Long Bayou	Adinia xenica	2019	autumn	1	38.00	NA	0.92	NA
Long Bayou	Cyprinodon variegatus	2019	autumn	2	45.00	4.00	1.74	0.57
Long Bayou	Fundulus grandis	2019	autumn	51	88.27	2.17	8.81	0.71
Long Bayou	Poecillia latipinna	2019	autumn	1	52.00	NA	1.86	NA
Manuel Bayou	Fundulus grandis	2019	autumn	22	64.55	3.37	3.47	0.77
Manuel Bayou	Fundulus jekenkski	2019	autumn	3	54.33	4.63	1.29	0.36
Manuel Bayou	Lagodon rhomboides	2019	autumn	1	55.00	NA	2.70	NA
Manuel Bayou	Poecillia latipinna	2019	autumn	7	38.86	3.51	0.72	0.13
Robinson Bayou	Fundulus grandis	2019	autumn	4	99.75	4.89	12.43	1.63
Robinson Bayou	Fundulus jekenkski	2019	autumn	1	40.00	NA	0.43	NA
Stone Quarry	Adinia xenica	2019	autumn	2	37.50	5.50	0.79	0.32
Stone Quarry	Fundulus grandis	2019	autumn	43	70.33	3.81	5.50	0.85
Stone Quarry	Fundulus jekenkski	2019	autumn	3	50.33	3.28	0.97	0.19
Stone Quarry	Lagodon rhomboides	2019	autumn	12	67.08	1.50	4.27	0.27
Stone Quarry	Poecillia latipinna	2019	autumn	1	48.00	NA	1.29	NA
Texar Bayou	Fundulus grandis	2019	autumn	31	83.27	3.65	7.92	1.00
Texar Bayou	Fundulus jekenkski	2019	autumn	1	85.00	NA	6.55	NA
Texar Bayou	Lagodon rhomboides	2019	autumn	1	67.00	NA	5.43	NA
Trout Bayou	Adinia xenica	2019	autumn	9	42.22	1.89	0.96	0.09
Trout Bayou	Fundulus confluentus	2019	autumn	4	56.75	3.20	1.96	0.40
Trout Bayou	Fundulus grandis	2019	autumn	213	75.33	1.42	5.66	0.34
Trout Bayou	Fundulus jekenkski	2019	autumn	1	53.00	NA	1.11	NA
Trout Bayou	Poecillia latipinna	2019	autumn	6	55.33	2.60	1.99	0.22
Weakley Bayou	Fundulus grandis	2019	autumn	56	73.75	2.73	5.56	0.65
Weakley Bayou	Fundulus jekenkski	2019	autumn	1	46.00	NA	0.80	NA
Weakley Bayou	Lagodon rhomboides	2019	autumn	17	63.65	0.57	4.17	0.14
Weakley Bayou	Poecillia latipinna	2019	autumn	16	48.69	1.40	1.36	0.12

Bayou Grande	Fundulus grandis	2020	autumn	19	104.42	5.58	16.68	2.26
Bayou Grande	Lagodon rhomboides	2020	autumn	7	93.86	8.95	14.44	4.33
Heron Bayou	Fundulus grandis	2020	autumn	2	62.00	2.00	2.83	0.48
Heron Bayou	Fundulus jekenkski	2020	autumn	5	51.00	1.05	1.19	0.08
Heron Bayou	Gambusia holbrooki	2020	autumn	12	34.00	2.32	0.44	0.14
Indian Bayou	Fundulus grandis	2020	autumn	66	80.38	3.57	10.24	1.12
Indian Bayou	Lagodon rhomboides	2020	autumn	25	77.96	3.15	8.15	1.09
Long Bayou	Cyprinodon variegatus	2020	autumn	1	54.00	NA	2.78	NA
Long Bayou	Fundulus grandis	2020	autumn	91	85.80	1.96	9.07	0.72
Long Bayou	Fundulus jekenkski	2020	autumn	1		NA		NA
Long Bayou	Fundulus pulvereus	2020	autumn	1	58.00	NA	2.41	NA
Manuel Bayou	Fundulus confluentus	2020	autumn	1	47.00	NA	1.48	NA
Manuel Bayou	Fundulus jekenkski	2020	autumn	11	47.64	2.56	1.32	0.26
Manuel Bayou	Gambusia holbrooki	2020	autumn	64	29.75	0.57	0.24	0.02
Manuel Bayou	Lagodon rhomboides	2020	autumn	21	48.43	1.37	1.93	0.20
Manuel Bayou	Poecillia latipinna	2020	autumn	4	40.50	3.86	0.95	0.20
Mulat Bayou	Fundulus confluentus	2020	autumn	1	56.00	NA	2.05	NA
Mulat Bayou	Fundulus grandis	2020	autumn	12	70.58	4.99	5.25	1.24
Mulat Bayou	Fundulus jekenkski	2020	autumn	1	55.00	NA	1.68	NA
Mulat Bayou	Fundulus pulvereus	2020	autumn	2	43.00	3.00	1.05	0.06
Mulat Bayou	Gambusia holbrooki	2020	autumn	4	41.50	2.87	0.79	0.20
Stone Quarry	Centropristis Striata	2020	autumn	1	60.00	NA	3.63	NA
Stone Quarry	Fundulus grandis	2020	autumn	8	68.63	5.12	5.44	1.53
Stone Quarry	Gambusia holbrooki	2020	autumn	2	45.50	1.50	1.31	0.03
Stone Quarry	Lagodon rhomboides	2020	autumn	183	70.08	0.76	6.04	0.21
Stone Quarry	Poecillia latipinna	2020	autumn	2	55.00	5.00	3.04	0.83
Texar Bayou	Fundulus grandis	2020	autumn	11	100.18	4.00	14.60	1.56
Texar Bayou	Lagodon rhomboides	2020	autumn	127	72.55	1.36	7.12	0.52
Trout Bayou	Cyprinodon variegatus	2020	autumn	1	49.00	NA	2.66	NA
Trout Bayou	Fundulus confluentus	2020	autumn	7	50.43	1.73	2.04	0.25
Trout Bayou	Fundulus grandis	2020	autumn	5	59.80	6.26	3.38	1.21
Trout Bayou	Fundulus jekenkski	2020	autumn	3	53.67	5.21	1.64	0.34
Trout Bayou	Fundulus pulvereus	2020	autumn	2	47.50	1.50	1.51	0.13
Trout Bayou	Gambusia holbrooki	2020	autumn	2	38.00	1.00	0.60	0.07
Trout Bayou	Lagodon rhomboides	2020	autumn	12	72.33	3.62	6.39	0.95
Weakley Bayou	Fundulus grandis	2020	autumn	14	47.93	3.99	1.79	0.46
Weakley Bayou	Fundulus jekenkski	2020	autumn	1	30.00	NA	0.28	NA
Weakley Bayou	Lagodon rhomboides	2020	autumn	6	63.67	3.31	4.24	0.74
Weakley Bayou	Poecillia latipinna	2020	autumn	3	42.00	3.00	1.28	0.24
Bayou Grande	Adinia xenica	2020	summer	10	35.13	0.69	0.64	0.04
Bayou Grande	Fundulus grandis	2020	summer	117	71.52	1.96	5.30	0.45
Bayou Grande	Fundulus jekenkski	2020	summer	7	50.00	1.63	1.13	0.12
Bayou Grande	Lagodon rhomboides	2020	summer	35	61.29	1.32	3.14	0.24

Graham Creek	Cyprinodon variegatus	2020	summer	6	41.17	1.78	1.34	0.05
Graham Creek	Fundulus grandis	2020	summer	82	61.78	1.90	3.67	0.50
Graham Creek	Fundulus pulvereus	2020	summer	1	49.00	NA	1.36	NA
Graham Creek	Gambusia holbrooki	2020	summer	2	40.00	0.00	0.38	0.13
Graham Creek	Poecillia latipinna	2020	summer	7	44.57	3.08	0.88	0.12
Heron Bayou	Gambusia holbrooki	2020	summer	3	28.33	8.35	0.33	0.26
Long Bayou	Adinia xenica	2020	summer	10	37.00	1.22	0.82	0.11
Long Bayou	Cyprinodon variegatus	2020	summer	18	46.78	2.33	2.17	0.33
Long Bayou	Fundulus confluentus	2020	summer	3	54.33	0.67	1.85	0.10
Long Bayou	Fundulus grandis	2020	summer	172	76.05	1.51	6.13	0.36
Long Bayou	Fundulus jekenkski	2020	summer	4	52.50	1.50	1.18	0.16
Long Bayou	Fundulus pulvereus	2020	summer	1	54.00	NA	1.00	NA
Long Bayou	Gambusia holbrooki	2020	summer	1	40.00	NA	0.51	NA
Long Bayou	Poecillia latipinna	2020	summer	9	40.33	1.95	0.76	0.11
Manuel Bayou	Gambusia holbrooki	2020	summer	12	28.25	1.00	0.25	0.03
Manuel Bayou	Lagodon rhomboides	2020	summer	11	47.73	1.62	1.84	0.28
Manuel Bayou	Poecillia latipinna	2020	summer	21	37.86	0.88	0.85	0.05
Robinson Bayou	Fundulus jekenkski	2020	summer	8	53.00	2.51	1.48	0.29
Robinson Bayou	Fundulus pulvereus	2020	summer	2	44.50	1.50	0.91	0.12
Stone Quarry	Adinia xenica	2020	summer	4	36.00	1.78	0.73	0.13
Stone Quarry	Cyprinodon variegatus	2020	summer	6	39.33	2.09	0.88	0.16
Stone Quarry	Fundulus confluentus	2020	summer	1	55.00	NA		NA
Stone Quarry	Fundulus grandis	2020	summer	49	62.83	2.50	4.72	0.71
Stone Quarry	Fundulus jekenkski	2020	summer	1	50.00	NA		NA
Stone Quarry	Gambusia holbrooki	2020	summer	3	44.00	0.58	0.86	0.05
Stone Quarry	Lagodon rhomboides	2020	summer	116	60.41	0.87	3.40	0.19
Stone Quarry	Poecillia latipinna	2020	summer	3	51.67	10.48	3.04	1.62
Texar Bayou	Adinia xenica	2020	summer	9	33.44	0.65	0.59	0.05
Texar Bayou	Fundulus confluentus	2020	summer	5	57.00	2.83	2.21	0.39
Texar Bayou	Fundulus grandis	2020	summer	32	81.50	3.13	8.31	0.84
Texar Bayou	Fundulus jekenkski	2020	summer	1	46.00	NA	0.76	NA
Texar Bayou	Fundulus similis	2020	summer	1	90.00	NA	7.06	NA
Texar Bayou	Gambusia holbrooki	2020	summer	4	44.50	0.29	0.79	0.06
Texar Bayou	Lagodon rhomboides	2020	summer	260	52.27	0.61	2.27	0.08
Texar Bayou	Poecillia latipinna	2020	summer	4	51.75	8.20	1.80	0.79
Trout Bayou	Adinia xenica	2020	summer	34	34.44	0.40		NA
Trout Bayou	Anchoa mitchilli	2020	summer	2	45.50	2.50		NA
Trout Bayou	Cyprinodon variegatus	2020	summer	8	54.75	1.01		NA
Trout Bayou	Fundulus grandis	2020	summer	74	80.73	2.34	10.51	0.72
Trout Bayou	Fundulus jekenkski	2020	summer	3	52.00	2.52		NA
Trout Bayou	Lagodon rhomboides	2020	summer	227	59.89	0.59		NA
Trout Bayou	Poecillia latipinna	2020	summer	9	53.67	2.85		NA
Weakley Bayou	Adinia xenica	2020	summer	14	34.36	0.55	0.48	0.02

Weakley Bayou	Fundulus confluentus	2020	summer	25	49.52	0.78	0.98	0.07
Weakley Bayou	Fundulus grandis	2020	summer	149	73.50	1.90	6.05	0.46
Weakley Bayou	Fundulus jekenkski	2020	summer	27	51.11	0.82	1.06	0.06
Weakley Bayou	Fundulus pulvereus	2020	summer	2	42.00	0.00	0.53	0.04
Weakley Bayou	Lagodon rhomboides	2020	summer	158	55.73	0.71	2.18	0.09
Weakley Bayou	Poecillia latipinna	2020	summer	35	46.94	1.34	1.20	0.24

Table 3. Caloric density (kcal/g wet weight), length (mm), and weight (g) of *Fundulus grandis.*

Site	FishID	Season	Year	Length (mm)	Weight (g)	Caloric Density (kcal/g wet weight)
Bayou Grande	BG1	Autumn	2020	103	16.22	748.91
Bayou Grande	BG2	Autumn	2020	142	44.87	954.50
Bayou Grande	BG3	Autumn	2020	136	35.72	979.34
Bayou Grande	BG4	Autumn	2020	104	15.08	896.71
Bayou Grande	BG5	Autumn	2020	142	37.79	909.35
Bayou Grande	BG6	Autumn	2020	115	19.82	885.10
Bayou Grande	BG7	Autumn	2020	143	37.53	953.00
Bayou Grande	BG8	Autumn	2020	129	30	1247.75
Bayou Grande	BG9	Autumn	2020	72	4.32	1047.75
Bayou Grande	BG10	Autumn	2020	132	22.99	860.20
Bayou Grande	BG1	Summer	2020	113	19.26	1381.85
Bayou Grande	BG2	Summer	2020	90	9.45	1752.65
Bayou Grande	BG3	Summer	2020	109	17.61	1508.02
Bayou Grande	BG4	Summer	2020	75	5.8	2291.56
Bayou Grande	BG5	Summer	2020	110	16.94	1554.83
Bayou Grande	BG6	Summer	2020	88	10.55	1559.06
Bayou Grande	BG7	Summer	2020	94	9.74	1898.21
Bayou Grande	BG8	Summer	2020	89	9.36	1843.17
Bayou Grande	BG9	Summer	2020	79	6.37	2231.48
Bayou Grande	BG10	Summer	2020	78	6.41	2066.01
Graham Creek	GC1	Summer	2020	102	14.56	1416.12
Graham Creek	GC2	Summer	2020	102	15.02	1551.76
Graham Creek	GC3	Summer	2020	106	18.24	1230.97
Graham Creek	GC4	Summer	2020	100	13.78	1496.05
Graham Creek	GC5	Summer	2020	101	13.68	1417.24
Graham Creek	GC6	Summer	2020	84	8.53	1705.23
Graham Creek	GC7	Summer	2020	113	21.47	1306.56
Graham Creek	GC8	Summer	2020	100	16.11	1276.72
Graham Creek	GC10	Summer	2020	109	18.17	1353.02
Indian Bayou	IB2	Summer	2020	90	9.4	1107.82
Indian Bayou	IB3	Summer	2020	68	4.1	1184.97
Indian Bayou	IB4	Summer	2020	64	3.68	1031.15
Indian Bayou	IB5	Summer	2020	55	2.17	905.54
Indian Bayou	IB6	Summer	2020	52	2.07	994.72
Indian Bayou	IB7	Summer	2020	52	1.89	1015.39
Indian Bayou	IB8	Summer	2020	51	1.67	1137.56
Indian Bayou	IB9	Summer	2020	50	1.71	1006.10
Indian Bayou	IB10	Summer	2020	47	1.57	958.39
Long Bayou	LB1	Summer	2020	106	15.92	2215.10

Long Bayou	LB2	Summer	2020	81	7.74	3760.22
Long Bayou	LB3	Summer	2020	85	7.53	3539.15
Long Bayou	LB4	Summer	2020	101	13.13	2177.33
Long Bayou	LB5	Summer	2020	108	17.08	2120.19
Long Bayou	LB6	Summer	2020	73	5.29	2355.14
Long Bayou	LB7	Summer	2020	72	5.87	2059.92
Long Bayou	LB8	Summer	2020	71	4.54	4060.12
Long Bayou	LB9	Summer	2020	85	7.07	2171.72
Stone Quarry	SQ1	Autumn	2020	137	41.24	828.93
Stone Quarry	SQ2	Autumn	2020	73	5.64	811.44
Stone Quarry	SQ3	Autumn	2020	77	6.34	818.46
Stone Quarry	SQ4	Autumn	2020	108	20.31	893.69
Stone Quarry	SQ5	Autumn	2020	68	3.83	849.84
Stone Quarry	SQ6	Autumn	2020	122	23.99	904.16
Stone Quarry	SQ7	Autumn	2020	76	6.32	961.24
Stone Quarry	SQ8	Autumn	2020	83	9.11	859.28
Stone Quarry	SQ9	Autumn	2020	85	8.09	1045.93
Stone Quarry	SQ10	Autumn	2020	113	20.37	1015.17
Stone Quarry	SQ1	Summer	2020	81	7.35	1959.31
Stone Quarry	SQ2	Summer	2020	91	12.09	1513.60
Stone Quarry	SQ3	Summer	2020	69	3.38	2904.62
Stone Quarry	SQ4	Summer	2020	82	9.98	1566.81
Stone Quarry	SQ5	Summer	2020		5.3	2397.32
Stone Quarry	SQ6	Summer	2020	61	3.03	3460.24
Stone Quarry	SQ7	Summer	2020	80	7.52	1903.50
Stone Quarry	SQ8	Summer	2020	91	12.09	1524.18
Stone Quarry	SQ9	Summer	2020	79	6.7	2081.11
Stone Quarry	SQ10	Summer	2020	111	21.26	1325.77
Trout Bayou	TB1	Autumn	2020	129	33.05	873.24
Trout Bayou	TB2	Autumn	2020	124	29.69	1008.85
Trout Bayou	TB3	Autumn	2020	135	37.01	905.90
Trout Bayou	TB4	Autumn	2020	68	4.75	1014.16
Trout Bayou	TB5	Autumn	2020	111	19.94	976.73
Trout Bayou	TB6	Autumn	2020	107	18.53	1043.16
Trout Bayou	TB7	Autumn	2020	68	4.42	944.77
Trout Bayou	TB8	Autumn	2020	115	22.89	1159.47
Trout Bayou	TB9	Autumn	2020	102	14.36	988.73
Trout Bayou	TB10	Autumn	2020	96	12.79	1013.40
Trout Bayou	TB1	Summer	2020	106	17.53	1539.99
Trout Bayou	TB2	Summer	2020	72	5.06	2458.10
Trout Bayou	TB3	Summer	2020	105	13.57	1360.92
Trout Bayou	TB4	Summer	2020	108	19.84	1315.94
Trout Bayou	TB5	Summer	2020	79	7.44	2109.36

Trout Bayou	TB6	Summer	2020	73	5.73	2199.37
Trout Bayou	TB7	Summer	2020	62	2.99	3266.07
Trout Bayou	TB8	Summer	2020	108	16.62	1380.16
Trout Bayou	TB9	Summer	2020	95	9.93	1758.27
Trout Bayou	TB10	Summer	2020	66	4.16	2610.37
Texar Bayou	TX1	Autumn	2020	88	8.14	903.31
Texar Bayou	TX2	Autumn	2020	128	27.73	804.57
Texar Bayou	TX3	Autumn	2020	90	10	861.02
Texar Bayou	TX4	Autumn	2020	87	9.75	939.03
Texar Bayou	TX5	Autumn	2020	113	20.17	1002.23
Texar Bayou	TX6	Autumn	2020	99	12.46	851.12
Texar Bayou	TX7	Autumn	2020	135	31.74	791.36
Texar Bayou	TX8	Autumn	2020	96	9.94	796.80
Texar Bayou	TX9	Autumn	2020	96	12.96	858.83
Texar Bayou	TX10	Autumn	2020	66	3.87	675.03
Texar Bayou	TX1	Summer	2020	104	15.9	2311.00
Texar Bayou	TX3	Summer	2020	99	11.71	1606.21
Texar Bayou	TX4	Summer	2020	74	5.53	2309.90
Texar Bayou	TX5	Summer	2020	75	5.3294	2408.57
Texar Bayou	TX6	Summer	2020	85	8.71	1668.18
Texar Bayou	TX7	Summer	2020	69	7.05	1898.64
Texar Bayou	TX8	Summer	2020	75	5.54	2047.67
Texar Bayou	TX9	Summer	2020	75	5.04	2235.57
Texar Bayou	TX10	Summer	2020	96	12.2	1694.36
Weakley Bayou	WB1	Autumn	2020	143	38.84	808.76
Weakley Bayou	WB2	Autumn	2020	113	20.92	1047.79
Weakley Bayou	WB3	Autumn	2020	102	13.33	1033.02
Weakley Bayou	WB4	Autumn	2020	118	25.91	1135.24
Weakley Bayou	WB5	Autumn	2020	89	9.33	1050.55
Weakley Bayou	WB6	Autumn	2020	78	6.73	1070.78
Weakley Bayou	WB7	Autumn	2020	59	2.96	860.46
Weakley Bayou	WB8	Autumn	2020	54	1.92	947.48
Weakley Bayou	WB9	Autumn	2020	49	1.49	1106.75
Weakley Bayou	WB10	Autumn	2020	112	22.51	974.50
Weakley Bayou	WB1	Summer	2020	99	12.43	2465.87
Weakley Bayou	WB2	Summer	2020	106	17.23	2254.00
Weakley Bayou	WB3	Summer	2020	106	15.76	2310.35
Weakley Bayou	WB4	Summer	2020	118	19.15	2028.06
Weakley Bayou	WB5	Summer	2020	95	13.7	3023.99
Weakley Bayou	WB6	Summer	2020	99	8.14	1997.00
Weakley Bayou	WB8	Summer	2020	85	8.3	1908.32
Weakley Bayou	WB9	Summer	2020	77	5.5	2423.28
Weakley Bayou	WB10	Summer	2020	76	4.85	2562.63

Table 4. Mean daily salinity (ppt) at 12 tidal creeks during the study period (6/11/2019-10/26/2020).

Date	Trout Bayou	Stone Quarry Bayou	Texar Bayou	Mulat Bayou	Manuel Bayou	Robinson Point	Long Bayou	Indian Bayou	Bayou Grande	Heron Bayou	Graham Creek	Weakley Bayou
6/11/2019		10.25	8.16		6.38						9.84	
6/12/2019	6.09	11.50	8.65	0.20	7.56	0.34					10.68	2.94
6/13/2019	6.54	11.93	9.67	0.19	7.34	0.96	9.27				10.56	5.13
6/14/2019	7.30	11.63	11.16	0.91	6.44	1.42	9.59				9.98	7.35
6/15/2019	8.79	11.03	11.66	2.93	5.86	2.21	9.72				9.65	8.63
6/16/2019	9.49	11.27	11.58	3.55	5.94	2.34	9.70				9.55	8.24
6/17/2019	10.13	11.87	11.89	3.79	6.78	2.41	9.75				9.46	8.20
6/18/2019	10.26	12.65	10.08	4.74	6.98	2.49	9.72				9.39	9.26
6/19/2019	10.06	13.54	10.41	3.44	8.41	2.48	9.54				9.23	8.66
6/20/2019	9.88	13.92	11.12	1.94	9.03	2.34	9.29				9.73	6.19
6/21/2019	9.71	13.84	10.99	1.12	8.05	2.11	8.64			0.68	9.89	3.57
6/22/2019	9.68	13.54	11.47	0.74	8.17	1.78	8.82			0.49	9.97	4.10
6/23/2019	9.68	13.30	12.41	0.68	8.73	1.64	9.07			0.43	9.48	4.90
6/24/2019	9.92	13.41	10.37	1.19	9.25	1.60	9.43			0.68	9.09	5.39
6/25/2019	9.71	13.67	8.72	0.98	8.57	1.24	9.27			1.62	8.94	6.01
6/26/2019	9.50	11.78	9.19	1.29	6.49	1.11	9.25			2.36	8.69	6.44
6/27/2019	9.26	10.94	10.21	1.31	6.42	1.07	9.15			3.02	8.52	7.85
6/28/2019	9.95	10.98	11.14	2.00	7.34	2.24	9.12			2.90	8.73	8.72
6/29/2019	11.72	11.09	11.45	2.74	7.67	4.05	9.01			2.75	8.68	9.78
6/30/2019	11.84	11.14	11.72	4.70	6.94	4.06	8.69			2.31	9.16	10.50
7/1/2019	11.81	12.05	11.84	5.28	7.76	4.27	8.76		13.51	2.13	9.46	10.32
7/2/2019	11.73	12.99	12.35	4.50	8.74	4.82	9.08		13.13	2.03	9.61	9.97
7/3/2019	11.60	12.87	13.25	4.72	9.12	4.72	10.20		12.24	1.95	9.65	9.60
7/4/2019	11.52	12.65	13.36	4.60	8.58	4.95	10.35		11.93	1.88	10.14	9.26
7/5/2019	11.60	12.98	13.11	4.74	9.19	4.91	10.55		13.12	1.94	10.43	9.35
7/6/2019	11.66	13.04	12.79	5.35	9.40	5.28	10.62		12.63	1.89	10.68	9.61

7/7/2019	11.67	13.47	12.21	5.67	10.50	5.45	10.73		12.22	1.93	10.92	10.02
7/8/2019	11.67	13.69	12.09	5.68	10.78	5.30	10.82		12.25	1.98	11.51	10.06
7/9/2019	11.66	13.56	11.30	5.45	10.60	5.20	10.99		12.99	2.35	12.26	10.25
7/10/2019	11.94	13.12	11.91	4.83	10.26	5.47	10.99		13.84	2.99	12.22	10.19
7/11/2019	14.68	12.41	13.16	7.13	9.07	5.79	11.01		13.83	3.02	12.28	12.89
7/12/2019	14.67	12.29	13.15	10.22	8.50	5.60	11.25		13.85	3.17	12.41	14.15
7/13/2019	14.54	12.61	13.00	9.98	8.60	5.78	11.29		6.84	3.26	12.47	13.84
7/14/2019	14.32	12.86	12.94	9.60	8.79	5.33	11.07		9.30	3.29	12.15	13.43
7/15/2019	14.02	13.28	12.28	9.89	10.18	5.34	10.99		9.34	3.43	12.17	13.41
7/16/2019	13.44	13.63	11.65	9.25	10.26	4.65	10.91		9.22	3.46	12.00	11.71
7/17/2019	12.84	13.59	11.60	8.96	9.58	4.42	11.12		9.21	3.78	11.77	10.08
7/18/2019	12.33	13.62	11.61	8.54	9.10	4.31	11.35		9.73	3.78	11.77	9.75
7/19/2019	12.02	13.45	11.85	8.16	9.33	3.86	11.52		10.62	3.71	11.76	9.65
7/20/2019	9.49	12.83	11.94	4.46	8.70	3.79	11.52		10.93	3.39	11.76	9.88
7/21/2019	8.16	12.88	12.26	0.55	7.87	3.33	11.57		7.73	4.29	11.65	9.95
7/22/2019	9.27	13.36	11.65	0.70	8.98	3.13	11.49		8.55	7.42	11.50	9.85
7/23/2019	8.62	13.90	10.16	0.99	9.04	2.50	11.38		8.75	8.03	11.42	8.13
7/24/2019	9.32	12.73	10.09	0.46	8.23	1.09	11.27		10.65	8.64	10.59	1.85
7/25/2019	11.81	11.95	11.49	0.59	7.08	2.71	11.45		12.21	8.51	9.88	8.49
7/26/2019	11.81	11.28	12.13	3.52	6.74	3.71	11.49		13.58	6.08	10.66	9.89
7/27/2019	12.03	10.81	12.13	4.63	6.15	3.68	11.51		14.03	3.80	10.78	10.41
7/28/2019	11.44	10.64	12.60	5.09	6.56	4.21	11.54		14.34	3.39	10.86	9.82
7/29/2019	11.66	10.96		5.92	7.22	4.72	11.57		14.26	3.37	10.95	9.86
7/30/2019	11.88	11.60		6.35	7.85	5.68	11.65		14.43	3.46	11.00	10.05
7/31/2019	12.16	12.22		6.27	8.75	6.71	11.68	13.06	14.04	3.62	11.08	10.09
8/1/2019	12.24	12.94		6.31	9.64	7.06	11.74	12.77	13.64	3.52	11.14	10.07
8/2/2019	12.60	12.99		6.42	10.25	7.07	11.82	12.60	13.22	3.32	11.24	10.53
8/3/2019	13.04	12.96		7.16	10.40	7.54	12.01	12.55	12.48	2.32	11.53	11.44
8/4/2019	13.50	13.06		7.65	10.81	7.40	12.03	12.63	12.04	1.49	11.75	11.95
8/5/2019	13.53	13.71		7.29	11.24	7.55	11.95	12.64	12.62	2.49	11.82	11.77
8/6/2019	13.32	13.92		7.37	11.35	7.30	11.72	12.61	13.21	3.41	11.71	11.41

8/7/2019	13.10	13.99	7.00	11.43	7.31	11.68	12.52	13.23	3.45	12.01	10.80
8/8/2019	12.85	13.91	6.88	11.48	6.52	11.70	12.34	13.28	3.83	12.22	10.14
8/9/2019	12.58	13.59	6.77	11.26	6.06	11.82	10.51	13.38	4.56	12.36	10.08
8/10/2019	11.71	12.73	6.62	10.06	5.21	11.86	9.64	12.74		11.94	10.60
8/11/2019	12.64		6.59	10.39	5.30	12.03	9.13	12.82		11.40	10.25
8/12/2019	12.51		6.17	10.82	6.44	12.06	9.28	12.65		10.93	9.63
8/13/2019	12.43		6.35	10.58	5.85	12.19	10.43	7.82		10.05	10.51
8/14/2019	12.34		6.98	9.42	5.11	12.44	11.91	8.18		11.26	10.95
8/15/2019	12.61		7.31	9.36	5.27	12.44	12.01	9.10		11.80	11.26
8/16/2019	12.52		5.24	10.05	3.79	12.52	11.52	9.25		12.42	11.34
8/17/2019	12.54		5.11	10.28	3.42	12.46	11.35	10.19		12.21	11.18
8/18/2019	12.10		6.54	9.65	3.32	12.60	11.51	11.21		12.00	11.41
8/19/2019	12.46		5.55	10.26	3.53	12.37	11.46	11.96		11.39	11.62
8/20/2019	12.45		4.70	10.14	2.45	12.29	11.43	12.66		11.11	11.15
8/21/2019	12.71		2.86	8.86	1.75	12.32		12.93		10.56	10.93
8/22/2019	13.08		5.08	7.87	1.97	12.36		13.33		10.71	12.04
8/23/2019	13.00		4.63	9.12	0.84	12.59		13.49		10.92	12.36
8/24/2019	12.81		4.92	8.85	1.27	12.61		13.51		11.10	11.30
8/25/2019	12.50		4.69	9.45	2.67	12.69		13.68		11.31	11.06
8/26/2019	12.46		6.11	8.73	3.40	12.46		13.30		11.57	11.20
8/27/2019	12.11		4.21	9.74	1.86	11.75		13.45		11.63	10.37
8/28/2019	11.65		2.10	9.77	1.91	10.90		13.97		9.83	8.80
8/29/2019	13.03		2.93	9.32	3.42	10.89		14.13		9.97	10.18
8/30/2019	13.86		5.41	8.40	4.23	11.91		13.75		11.38	11.44
8/31/2019	13.91		9.31	8.02	5.23	12.15		11.43		11.68	11.98
9/1/2019	14.29		11.56	7.84	5.62	12.25	13.27	12.73		11.68	13.25
9/2/2019	14.76		11.93	9.31	6.21	12.32	13.02	14.01		11.35	12.74
9/3/2019	15.59		11.82	9.60	6.91	12.36	13.27	14.08		11.21	12.68
9/4/2019	15.59		11.62	10.21	7.09	12.44	13.75	14.42		11.17	12.07
9/5/2019	15.36		11.73	10.10	7.74	12.49	12.86	14.05		11.40	11.78
9/6/2019	15.31		10.80	10.53	9.97	12.54	13.37	14.05		11.50	11.50

9/7/2019	15.49		11.10	10.31	11.97	12.61	12.90	14.05	11.53	11.27
9/8/2019	15.40		11.58	10.46	12.46	12.77	13.78	13.68	11.81	11.03
9/9/2019	14.98		11.40	10.64	11.64	12.84	13.24	13.02	11.73	11.15
9/10/2019	15.12		11.99	10.65	10.83	12.98	13.47	12.19	11.70	11.63
9/11/2019	14.77		11.62	10.71	10.21	13.03	13.82	11.43	11.57	12.78
9/12/2019	15.16		11.76	10.97	9.71	13.19	13.80	11.64	11.45	13.17
9/13/2019	15.16		11.77	11.19	9.72	13.29	13.90	11.94	11.38	13.19
9/14/2019	15.32		11.88	11.30	10.09	13.38	14.02	12.67	11.45	13.46
9/15/2019	15.66		11.87	11.23	10.39	13.44	14.07	12.46	11.50	13.83
9/16/2019	15.82		11.99	11.55	10.60	13.51	14.07	11.38	11.81	13.64
9/17/2019	15.55		11.81	12.05	10.70	13.46	13.78	6.94	12.33	13.38
9/18/2019	15.23		11.63	12.02	10.29	13.49	13.43	7.68	12.76	13.16
9/19/2019	15.17		11.54	11.93	10.80	13.69	13.30	9.97	12.95	13.10
9/20/2019	15.18		11.80	12.02	10.72	13.77	13.45	11.69	12.81	13.23
9/21/2019	15.14		11.91	12.36	10.61	13.80	13.27	11.71	12.66	13.60
9/22/2019	15.12		12.07	12.69	10.61	13.96	13.53	11.62	12.66	14.02
9/23/2019	15.13	14.86	12.10	12.87	10.71	14.19	13.56	11.56	12.61	14.28
9/24/2019	15.16	15.14	12.05	13.21	10.85	14.39	13.39	10.95	12.85	14.21
9/25/2019	15.10	15.17	11.86	13.03	11.31	14.42	13.08	11.44	13.43	14.03
9/26/2019	14.92	15.05	11.66	13.06	10.61	14.51	13.12	12.44	13.99	13.81
9/27/2019	14.73	15.15	11.55	12.82	10.53	14.64	12.95	12.83	14.26	13.62
9/28/2019	14.74	15.12	11.46	12.46	9.59	14.70	12.89	12.86	14.19	13.46
9/29/2019	14.70	14.88	11.43	11.85	9.45	14.80	12.84	12.93	14.07	13.85
9/30/2019	14.72	14.69	11.47	12.10	9.48	14.86	12.73	12.98	13.91	14.20
10/1/2019	14.74	14.66	11.46	12.47	9.83	14.92	11.57	12.97	13.75	14.14
10/2/2019	14.75	14.68	11.42	12.79	10.20	15.03	12.57	12.67	13.68	14.06
10/3/2019	14.77	14.74	11.49	12.95	10.68	14.74	12.59	12.54	13.84	14.05
10/4/2019	14.75	14.79	11.50	13.13	10.65	13.83	12.57	12.82	14.05	13.92
10/5/2019	14.71	14.94	11.38	12.90	10.40	15.11	12.59	12.94	14.01	13.89
10/6/2019	14.72	15.15	11.49	12.73	10.31	15.24	12.65	12.56	14.12	14.39
10/7/2019	14.80	15.31	11.60	12.69	10.20	15.20	12.79	12.72	14.08	15.07

10/8/2019	14.84	15.33		11.62	13.07	10.97	15.16	12.34	13.30	14.29	14.84
10/9/2019	14.91	15.39		11.83	13.37	12.36	15.13	12.85	14.38	14.48	14.71
10/10/2019	15.11	15.49		12.27	13.22	11.93	15.08	13.07	14.48	14.44	14.74
10/11/2019	15.21	15.61	14.21	12.83	13.07	11.47	15.09	12.98	14.41	14.47	14.92
10/12/2019	15.12	15.60	13.98	12.91	13.02	11.09	14.85	13.25	14.28	14.56	15.00
10/13/2019	15.03	15.73	14.17	12.87	13.15	11.73	14.97	13.31	14.04	14.66	14.96
10/14/2019	15.48	15.61	14.04	12.91	13.12	12.24	15.08	13.28	14.18	15.01	14.98
10/15/2019	15.68	15.48	13.65	13.10	13.07	12.07	14.94	13.21	14.38	15.38	14.92
10/16/2019	15.60	15.83	13.86	12.85	13.82	12.67	14.78	12.97	14.74	15.51	14.63
10/17/2019	15.46	16.19	14.58	12.47	13.77	13.18	14.74	12.97	14.99	15.40	14.57
10/18/2019	15.91	16.49	15.21	12.74	13.82	13.43	14.90	13.31	15.02	15.09	14.43
10/19/2019	16.92	16.72	14.99	13.75	14.18	13.77	14.90	13.58	15.05	15.15	15.21
10/20/2019	16.57	16.55	15.22	13.30	14.25	13.80	14.80	13.36	14.96	15.33	15.19
10/21/2019	15.53	16.14	14.57	13.08	13.63	12.58	14.60	13.19	14.95	15.21	15.00
10/22/2019	15.02	16.31	14.82	11.82	13.47	11.23	14.30	12.74	14.96	14.87	14.63
10/23/2019	15.22	16.80	15.08	10.54	13.68	11.35	14.46	12.78	14.80	14.77	14.48
10/24/2019	15.51	16.83	14.33	12.12	13.41	11.01	14.62	12.92	14.92	14.85	14.74
10/25/2019	16.47	16.36	14.24	13.05	12.93	10.35	14.70	13.00	15.11	14.72	15.22
10/26/2019	16.46	16.31	13.87	14.38	13.20	10.23	14.65	13.28	15.41	14.65	15.33
10/27/2019	15.86	16.73	14.48	13.37	13.94	10.52	14.47	13.27	15.30	14.96	15.20
10/28/2019	15.45	16.55	14.38	12.37	13.61	10.73	14.62	13.27	15.24	15.12	15.01
10/29/2019	15.21	15.86	14.34	12.49	12.90	11.02	14.43	13.20	15.32	15.04	15.11
10/30/2019	15.35	15.24	14.85	13.21	11.84	10.66	13.31	12.91	15.46	14.33	15.59
10/31/2019	15.17	16.17	15.46	10.10	13.56	10.58	10.71	12.57	15.44	14.68	14.96
11/1/2019	15.23	17.24	15.42	6.03	14.25	9.95	11.65	11.09	15.38	11.35	14.39
11/2/2019	15.30	17.07	15.67	6.36	14.20	10.18	13.25	12.65	15.43	14.01	14.96
11/3/2019	15.91	17.09	15.46	7.78	13.57	9.92	13.57	13.31	15.41	14.18	14.77
11/4/2019	16.69	16.44	14.74	12.51	12.61	9.37	13.61	14.29	15.35	14.83	15.31
11/5/2019	15.62	15.31	14.59	13.61	12.08	11.89	13.64	14.64	15.43	15.18	15.30
11/6/2019	15.87	14.81	14.12	14.38	11.08	13.35	13.61	14.94	15.70	15.00	15.32
11/7/2019	15.63	14.10	14.16	14.72	10.40	10.55	13.51	15.12	16.18	14.84	14.96

11/8/2019	15.47	13.61	14.52	12.12	11.98	11.85	13.48	15.27	16.04	14.44	14.47
11/9/2019	15.88	14.54	14.52	13.63	13.67	14.21	13.64	15.68	15.37	15.09	15.02
11/10/2019	16.15	15.03	14.75	14.82	13.41	13.50	13.62	15.80	15.27	14.99	15.12
11/11/2019	16.43	15.26	15.13	14.93	12.98	12.59	13.60	15.84	15.33	14.93	15.14
11/12/2019	16.45	16.55	16.68	13.63	13.65	8.96	13.61	15.25	15.55	14.16	15.43
11/13/2019	14.18	17.43	16.32	12.74	14.64	12.20	13.89	15.37	15.54	13.95	15.29
11/14/2019	17.33	17.50	16.23	14.14	14.66	13.04	13.96	16.65	15.64	14.69	15.66
11/15/2019	17.75	17.47	17.36	12.97	14.96	14.90	13.92	16.56	15.29	14.73	15.74
11/16/2019	17.53	17.43	17.64	8.75	14.96	14.06	13.84	16.19	15.14	14.26	14.98
11/17/2019	17.51	17.05	17.10	10.99	14.34	12.56	13.93	14.99	15.20	14.49	15.32
11/18/2019	15.83	17.04	17.14	12.55	14.33	12.99	14.01	15.86	15.04	14.85	15.63
11/19/2019	16.15	17.11	16.72	13.32	14.46	14.06	14.04	15.72	14.69	15.69	15.39
11/20/2019	16.10	16.96	16.32	13.21	14.25	11.43	13.97	15.79	14.70	15.72	15.17
11/21/2019	16.10	16.35	15.68	14.42	12.94	11.20	14.00	15.90	13.02	15.61	15.48
11/22/2019	16.71	15.49	15.95	15.37	12.42	11.03	14.01	15.81	13.30	15.64	16.26
11/23/2019	15.60	16.61	15.63	15.19	13.60	12.83	14.06	15.71	13.23	15.82	15.10
11/24/2019	15.52	17.48	15.79	13.55	14.45	13.12	14.14	15.86	14.81	15.92	15.09
11/25/2019	15.45	17.21	15.72	12.96	14.37	12.69	14.45	15.91	14.70	16.18	15.39
11/26/2019	15.95	16.51	16.29	12.53	13.77	11.50	14.67	15.74	14.70	16.25	15.21
11/27/2019	15.92	16.69	15.83	13.76	13.36	11.66	14.49	15.44	13.94	15.93	14.88
11/28/2019	15.48	16.96	15.79	10.11	14.23	10.86	14.49	15.34	13.97	15.15	15.73
11/29/2019	15.67	16.86	15.59	9.72	13.69	10.30	14.65	13.88	13.76	15.11	15.86
11/30/2019	15.35	16.33	15.87	11.80	13.34	10.43	14.86	15.41	14.08	15.92	15.82
12/1/2019	15.22	17.27	15.50	12.90	14.26	13.91	14.78	15.52	14.40	16.68	15.71
12/2/2019	15.36	18.27	16.20	7.70	14.87	11.09	11.26	15.65	15.02	15.40	16.00
12/3/2019	15.22	18.28	15.89	9.44	14.97	10.95	11.75	15.96	15.10	16.19	15.46
12/4/2019	14.98	18.20	15.26	10.91	15.32	12.01	15.23	15.89	14.92	16.47	15.70
12/5/2019	14.61	17.94	14.73	10.70	14.41	8.43	15.25	15.30	13.58	16.40	15.70
12/6/2019	14.87	16.48	15.07	11.34	13.65	10.51	15.19	15.82	11.12	16.84	16.20
12/7/2019	15.91	15.97	15.26	12.36	13.80	12.13	15.06	15.67	12.91	16.33	16.53
12/8/2019	17.11	16.31	15.16	14.61	14.02	12.71	15.13	16.17	15.47	16.51	17.04

12/9/2019	16.50	17.12	14.95	15.45	14.02	12.41	15.05	16.49	16.42	16.61	16.86
12/10/2019	15.24	16.96	16.26	13.99	14.49	11.47	14.94	16.46	16.74	16.64	15.66
12/11/2019	15.59	17.49	16.11	7.63	15.63	5.68	13.29	10.82	16.85	15.11	15.51
12/12/2019	16.21	18.23	16.79	11.29	15.36	8.71	15.19	14.14	16.51	15.09	16.38
12/13/2019	17.92	18.29	16.32	13.40	15.26	11.73	15.12	16.85	16.82	15.23	17.23
12/14/2019	17.85	18.62	16.66	13.79	15.29	12.52	14.97	14.46	17.19	16.18	17.08
12/15/2019	17.43	18.31	16.84	11.61	14.81	10.10	14.98	16.37	17.28	16.03	16.80
12/16/2019	17.19	17.17	16.68	13.07	13.42	9.57	14.89	16.45	17.12	15.53	16.75
12/17/2019	16.79	18.57	16.64	8.73	15.36	8.09	14.40	16.65	16.13	14.29	17.02
12/18/2019	17.10	19.69		4.63	16.05	6.53	5.66		12.75	9.21	13.11
12/19/2019	16.88	19.73	15.06	1.87	15.64		1.95		13.01	9.55	7.97
12/20/2019	16.85	19.61	15.32	5.62	14.59	10.00			13.21	14.01	15.69
12/21/2019	17.11	18.86	12.75	11.72	13.91	9.28			15.61	14.70	17.59
12/22/2019	17.24	18.10	11.66	2.58	14.86	9.71			10.18	13.62	16.81
12/23/2019	16.04	18.67	13.95	2.81	15.38	8.91			12.63	16.79	15.52
12/24/2019	13.59	18.05	13.10	4.31	14.00	7.11			15.77	14.68	10.67
12/25/2019	13.80	16.06	14.24	4.03	11.61	5.24			17.11	14.21	13.48
12/26/2019	13.06	14.82	12.71	5.47	10.26	5.00			16.81	12.81	15.67
12/27/2019	13.61	13.57	11.24	5.30	9.78	4.03			16.99	13.96	15.83
12/28/2019	14.04	13.38	11.02	7.17	8.15	3.11			17.07	13.58	16.63
12/29/2019	13.99	13.38	11.63	7.73	8.80	3.18			16.19	14.22	18.08
12/30/2019	11.60	16.61	11.44	6.14	13.85	3.06			13.32	15.09	17.06
12/31/2019	10.57	17.09	12.11	2.81	14.09	2.44			12.24	15.33	15.41
1/1/2020	10.73	17.22	13.27	2.17	13.26	3.45			17.21	14.56	14.86
1/2/2020	10.77	16.12	13.33	6.87	11.13	4.13			15.79	15.35	15.50
1/3/2020	10.32	16.71	10.07	7.39	12.60	4.11			14.45	15.14	15.24
1/4/2020	10.10	17.21	11.93	2.00	13.77	3.41			12.78	15.14	12.91
1/5/2020	8.80	17.18	13.95	0.89	12.45	1.65			14.88	9.45	3.54
1/6/2020	9.84	16.82	13.23	1.38	12.67	4.05			13.79	13.50	7.70
1/7/2020	9.62	17.39	13.13	1.34	12.90	4.22			4.99	13.49	11.83
1/8/2020	9.93	17.10	12.60	2.48	12.10	5.50			6.73	13.96	9.98

1/9/2020	11.73	15.90	12.02	4.27	10.44	4.18		14.37	15.68	15.56
1/10/2020	12.33	15.63	11.89	7.56	9.95	3.30		12.43	15.29	18.02
1/11/2020	11.80	15.63	9.30	8.57	10.47	3.54		9.94	15.32	18.51
1/12/2020	10.77	16.30	6.64	5.33	13.34	2.93		10.17	13.24	17.69
1/13/2020	10.07	13.50	7.23	2.43	7.43	3.06		6.33	7.17	16.73
1/14/2020	8.15	12.47	7.06	1.04	7.63	1.94		7.18	8.10	16.06
1/15/2020	5.29	13.05	5.59	0.30	10.33	0.63		7.45	8.58	15.35
1/16/2020	4.56	13.54	5.60	0.17	10.18	0.31		9.10	8.83	13.23
1/17/2020	7.77	12.39	7.25	1.36	9.01	1.39		9.29	6.35	15.07
1/18/2020	9.14	12.75	8.50	6.32	8.77	1.81		8.81	10.06	16.95
1/19/2020	6.38	14.37	10.83	1.81	11.80	1.98		10.45	12.12	14.47
1/20/2020	6.37	14.96	12.49	0.70	12.65	2.81		9.51	8.28	7.58
1/21/2020	6.75	15.12	9.76	0.80	12.32	3.62		13.80	6.62	5.47
1/22/2020	9.06	15.29	7.05	1.51	12.07	2.94		14.13	8.29	9.57
1/23/2020	9.56	15.24	8.64	2.28	11.33	2.37		13.10	10.63	14.49
1/24/2020	8.89	15.65	8.33	2.57	11.68	3.76		8.17	13.27	15.36
1/25/2020	6.02	16.15	6.93	0.97	11.92	5.11		4.66	13.55	12.35
1/26/2020	6.56	15.42	6.30	0.93	10.72	3.87		10.09	12.73	12.30
1/27/2020	8.36	13.42	6.97	1.48	9.35	3.16		12.33	11.88	14.75
1/28/2020	9.44	13.35	7.42	1.50	10.90	4.85		14.09	12.98	14.88
1/29/2020	9.00	13.34	7.96	2.52	9.82	2.98		14.42	12.94	15.38
1/30/2020	9.82	13.36	7.65	2.01	11.19	3.43		14.07	12.73	16.57
1/31/2020	10.06	13.39	7.36	2.37	11.61	2.58		11.39	12.72	15.89
2/1/2020	10.20	14.33	9.29	2.13	11.46	2.99		8.82	13.08	14.17
2/2/2020	9.06	14.97	11.18	1.06	11.85	5.43		4.78	10.77	5.46
2/3/2020	7.65	15.30	11.23	1.38	12.09	3.30		3.21	10.62	6.05
2/4/2020	7.37	15.07	10.11	2.52	11.62	2.69		1.85	12.62	12.12
2/5/2020	7.55	14.80	11.13	2.96	10.68	3.15		1.79	9.69	13.02
2/6/2020	7.44	15.56	9.30	2.29	11.87	3.02		3.75	8.40	13.15
2/7/2020	3.83	17.26	10.42	0.27	12.47	1.58		3.09	9.16	7.81
2/8/2020	4.20	14.96	7.04	0.12	8.86	0.90	1.11	3.12	7.10	6.36

2/9/2020	5.12	14.26	6.20	0.15	6.62	0.68	1.40	2.95		8.20	9.61
2/10/2020	5.44	11.69	4.59	0.31	5.25	0.45	2.51	4.00		8.56	13.13
2/11/2020	4.30	11.68	3.92	0.41	6.73	0.32	2.91	4.13		9.77	13.20
2/12/2020	3.42	10.81	6.49	0.24	5.44	0.27	2.53	5.87		8.07	10.30
2/13/2020	3.06	13.30	6.97	0.56	7.16	0.28	2.94	6.09		7.96	9.99
2/14/2020	3.74	13.65	6.96	0.37	7.82	0.20	2.48	6.57		4.46	8.81
2/15/2020	7.54	13.20	6.09	0.44	7.77	0.39	5.52	6.68		6.01	7.65
2/16/2020	7.91	12.50	4.79	1.79	6.92	1.10	9.91	5.74		7.73	11.43
2/17/2020	7.48	11.37	4.63	2.67	6.34	1.41	9.55	7.35		8.29	12.24
2/18/2020	5.12	9.02	3.04	2.04	5.10	1.10	8.66	6.85	1.97	8.93	12.16
2/19/2020	4.01	8.18	4.03	1.34	6.08	0.87	5.92	3.67	3.04	8.07	11.66
2/20/2020	4.31	8.03	6.48	1.21	6.80	1.04	5.20	3.17	2.93	6.68	11.16
2/21/2020	4.91	8.72	7.05	1.33	9.62	2.28	2.07	2.91	2.53	2.40	4.36
2/22/2020	7.07	10.32	5.43	1.87	9.69	2.54	3.99	3.79	3.63	4.11	5.12
2/23/2020	7.62	10.79	6.99	2.41	9.76	2.94	4.27	4.87	3.45	7.34	9.40
2/24/2020	7.32	11.34	5.22	3.63	9.54	2.42		7.13	1.78	9.80	12.30
2/25/2020	6.33	12.24	6.13	2.59	10.45	1.92		7.37	1.67	10.31	12.20
2/26/2020	5.52	12.09	6.88	1.51	9.93	2.60		7.02	1.67	10.30	9.09
2/27/2020	6.17	12.32	8.04	1.64	9.71	4.79		6.50	2.68	9.63	5.25
2/28/2020	6.06	11.21	8.21	1.18	9.40	4.29		9.35	2.54	9.50	6.38
2/29/2020	6.15	11.46	5.91	0.88	9.62	2.75		7.58	1.79	8.61	4.74
3/1/2020	6.00	9.53	7.71	0.91	9.41	2.91		9.80	1.84	8.74	6.84
3/2/2020	5.97	8.67	7.80	2.31	9.09	2.47		10.06	0.95	8.11	10.09
3/3/2020	4.31	9.18	7.62	2.10	9.85	1.99		10.12	1.24	7.87	11.09
3/4/2020	3.19	8.87	7.59	1.90	9.91	1.75		9.52	5.32	7.15	10.86
3/5/2020	3.96	10.05	6.82	1.89	9.75	1.85		7.78	5.84	6.71	11.43
3/6/2020	4.90	11.23	9.59	1.08	9.89	2.76		7.89	3.10	5.06	10.25
3/7/2020	6.28	11.10	9.60	0.72	9.55	4.73		7.35	2.26	4.14	6.40
3/8/2020	8.63	11.03	8.98	3.76	8.81	4.81		5.99	1.28	6.21	10.57
3/9/2020	9.53	11.33	8.37	6.68	8.92	3.59		5.67	2.46	7.32	12.96
3/10/2020	8.82	11.62	9.09	6.96	8.79	2.93		4.63	2.74	7.65	13.19

3/11/2020	5.93	12.09	9.01	4.38	9.25	2.12	3.19	5.13	7.96	11.83
3/12/2020	4.50	12.25	5.96	3.23	10.41	1.74	2.72	6.19	8.37	11.00
3/13/2020	3.66	11.36	4.11	2.85	10.59	1.46	3.38	6.33	8.40	10.54
3/14/2020	3.16	10.61	4.01	2.25	9.90	1.23	5.01	6.11	7.69	10.70
3/15/2020	2.81	10.65	4.24	2.21	8.91	1.26	7.47	5.59	7.09	11.41
3/16/2020	2.80	10.81	3.94	2.12	8.68	1.31	6.80	3.74	6.73	11.43
3/17/2020	3.04	10.37	3.68	2.10	9.04	1.55	5.43	3.24	6.67	11.65
3/18/2020	3.00	9.64	4.98	2.01	8.55	1.57	6.83	4.98	6.54	11.98
3/19/2020	2.48	9.55	5.34	2.09	8.03	1.57	7.92	6.16	6.33	12.25
3/20/2020	2.06	10.60	5.39	2.07	8.65	1.63	9.66	6.56	6.82	12.27
3/21/2020	2.15	12.01	4.31	1.96	10.26	1.35	10.62	5.84	5.73	12.32
3/22/2020	3.59	12.51	5.15	2.01	9.87	1.43	10.65	6.04	4.98	12.03
3/23/2020	4.62	12.87	5.44	2.19	9.48	1.51	10.40	5.97	6.02	12.19
3/24/2020	4.59	13.14	5.39	2.21	9.78	1.81	10.02	5.17	7.89	12.00
3/25/2020	4.55	13.02	6.71	2.18	11.31	1.68	7.30	5.18	8.47	11.93
3/26/2020	4.62	11.26	8.72	1.91	10.83	1.44	8.04	4.76	8.02	11.73
3/27/2020	4.66	11.12	8.69	1.96	10.13	1.42	8.50	5.41	7.93	11.80
3/28/2020	4.85	11.03	8.01	1.96	10.34	1.60	8.75	7.05	7.91	11.90
3/29/2020	4.92	11.12	7.18	1.92	10.77	1.75	6.64	7.45	7.75	11.96
3/30/2020	4.76	11.33	8.78	1.81	10.58	1.35	7.84	7.54	7.20	11.82
3/31/2020	4.79	12.55	8.04	1.96	10.64	1.35	9.42	6.03	7.27	11.99
4/1/2020	4.64	11.89	8.55	1.75	10.79	1.04	9.99	5.26	6.97	11.97
4/2/2020	6.15	11.28	8.55	1.60	10.01	1.78	9.74	5.80	6.82	11.57
4/3/2020	6.50	11.49	8.66	1.64	10.23	1.97	9.02	5.96	6.71	11.95
4/4/2020	5.90	11.65	8.46	1.88	10.65	1.98	9.41	5.80	6.69	12.17
4/5/2020	6.12	11.51	8.93	2.00	10.60	2.32	9.53	5.77	6.64	12.18
4/6/2020	6.90	11.50	9.12	2.02	10.72	2.30	9.81	5.86	6.79	12.09
4/7/2020	6.63	11.74	8.48	2.14	10.26	2.32	9.41	5.73	7.74	12.11
4/8/2020	6.57	13.56	8.80	2.55	11.04	2.02	8.76	5.90	8.71	12.23
4/9/2020	6.56	13.89	9.34	2.71	11.56	2.21	7.73	5.87	9.02	12.19
4/10/2020	6.41	13.42	10.98	2.58	11.22	2.05	8.51	6.01	8.61	11.93

4/11/2020	8.20	13.66	11.95	2.58	10.80	2.65		8.20	5.73	7.92	11.83
4/12/2020	8.09	13.62	10.83	6.18	10.16	2.60		7.87	5.55	8.58	13.65
4/13/2020	7.55	14.53	10.54	5.06	11.54	2.76		8.45	5.35	9.05	13.80
4/14/2020	7.31	14.05	11.89	4.30	12.13	2.23		9.31	5.39	7.77	13.04
4/15/2020	8.76	14.39	12.28	4.30	11.77	4.46		9.49	5.05	7.63	13.51
4/16/2020	11.00	14.65	12.59	7.27	12.05	6.33		10.15	5.99	8.72	13.64
4/17/2020	12.04	14.52	12.02	10.18	11.62	6.03		10.30	6.44	9.59	13.93
4/18/2020	11.19	14.34	12.36	11.89	11.57	6.36		11.15	5.75	10.52	14.07
4/19/2020	9.73	14.51	10.62	11.17	12.42	5.04		11.34	6.27	11.01	13.79
4/20/2020	8.31	14.77	11.37	10.69	12.54	4.97		11.69	5.54	10.91	13.60
4/21/2020	8.91	14.08	12.02	9.67	12.04	4.73		11.99	6.18	10.75	13.16
4/22/2020	8.96	13.81	12.35	8.76	11.29			12.16	7.29	10.81	12.89
4/23/2020	9.08	13.99	10.87	9.06	10.58			12.29	6.95	11.24	13.44
4/24/2020	8.77	14.20	12.72	7.67	12.64			12.23	6.42	11.10	13.26
4/25/2020	7.98	14.04	12.49	7.15	11.89			11.19	5.96	11.39	12.81
4/26/2020	8.02	14.27	11.35	5.35	12.18			11.84	5.94	10.90	12.27
4/27/2020	8.44	14.27	9.48	4.83	11.91			11.84	8.06	10.81	11.54
4/28/2020	8.10	14.03	12.05	5.18	10.98			12.23	7.82	10.71	8.99
4/29/2020	7.80	14.07	11.49	6.68	11.15				8.14	10.98	5.66
4/30/2020	6.99	14.56	10.40	6.51	12.31				7.18	10.87	3.15
5/1/2020	6.54	14.13	9.60	5.19	11.44				6.54	10.92	2.14
5/2/2020	6.29	13.76	10.35	4.85	11.16				7.93	10.77	1.66
5/3/2020	5.98	13.55	10.96	4.71	11.07				8.62	10.90	1.25
5/4/2020	5.76	13.47	11.11	4.60	11.47				7.99	11.08	0.94
5/5/2020	5.68	13.41	11.25	4.62	11.74				8.43	11.03	0.66
5/6/2020	5.78	13.42	12.10	4.48	11.50				7.23	10.93	0.58
5/7/2020	6.42	13.36	12.78	4.23	10.69				6.42	11.14	0.69
5/8/2020	6.23	13.78	12.07	4.24					7.38	11.00	0.88
5/9/2020	6.37	14.60	12.44	4.02	0.13				7.84	10.75	0.99
5/10/2020	7.98	14.57	12.02	3.97	0.14		15.16		7.38	10.61	1.06
5/11/2020	8.11	14.13	12.32	4.11	0.13		15.57		7.16	10.47	1.16

5/12/2020	9.84	14.03	12.52	5.09	0.13	15.56	7.28	10.55	1.30
5/13/2020	9.63	13.92	12.66	7.44	0.13	15.55	7.11	10.46	1.45
5/14/2020	9.38	13.81	12.30	8.97		15.57	7.11	10.42	1.53
5/15/2020	9.40	13.88	12.10	9.94		15.46	7.20	10.46	1.62
5/16/2020	9.38	13.89	12.25	9.68		15.32	7.01	10.43	1.69
5/17/2020	9.33	13.71	11.01	9.69		14.88	6.81	10.42	1.77
5/18/2020	9.08	14.68	10.94	9.75		14.79	7.04	5.59	1.79
5/19/2020	8.85	14.85	10.68	9.20		14.74	6.45	8.71	1.74
5/20/2020	8.69	14.71	11.87	8.19		14.50	6.41	10.86	1.77
5/21/2020	8.47	14.45	12.59	7.40		14.14	6.59	11.54	1.97
5/22/2020	8.28	14.17	12.58	7.09		13.88	6.73	11.74	2.20
5/23/2020	8.27	13.79	12.65	7.17		5.69	8.02	11.28	3.22
5/24/2020	8.26	13.90	12.79	7.17		3.98	10.04	10.70	3.61
5/25/2020	8.40	14.13	12.91	7.41		5.38	10.67	10.84	3.77
5/26/2020	8.56	14.41	12.71	7.72		2.21	10.90	10.94	3.97
5/27/2020	8.86	14.35	13.15	7.41		3.56	10.84	11.14	4.10
5/28/2020	8.58	14.58	12.76	7.39		8.21	9.37	11.34	4.33
5/29/2020	8.06	14.62	12.05	7.18		10.17	9.56	11.52	4.58
5/30/2020	7.48	14.62	11.68	6.62		11.54	8.65	11.39	4.79
5/31/2020	7.40	14.56	11.44	6.35		12.06	9.39	11.28	4.89
6/1/2020	8.13	14.57	11.79	6.02		12.46	9.92	11.64	5.24
6/2/2020	8.53	14.55	12.45	6.76		10.32	9.96	12.01	5.62
6/3/2020	8.48	14.52	12.64	7.80		5.86	10.05	12.31	5.83
6/4/2020	8.47	14.06	12.52			9.55	10.75	10.33	5.94
6/5/2020	7.87	13.98	12.55			6.96	10.85	11.47	5.66
6/6/2020	7.63	14.27	12.74			6.84	10.82	12.68	5.30
6/7/2020	8.42	14.48	12.91			3.64	10.02	11.70	5.56
6/8/2020	7.90	15.37	12.83			0.83	8.91	8.08	5.84
6/9/2020	7.49	14.94	11.51			7.46	9.16	2.48	5.76
6/10/2020	7.06	14.57	9.12			9.91	9.08	5.15	5.14
6/11/2020	6.64	14.30	10.35			10.87	9.25	7.12	

6/12/2020	7.46	13.60	10.91		11.47	9.91	10.10
6/13/2020	8.24	12.62	11.34		12.17	9.90	11.76
6/14/2020	8.01	12.45	10.43		12.50	9.92	11.80
6/15/2020	7.62	12.41	10.32		12.74	10.33	12.18
6/16/2020	7.52	12.40	10.73		13.10	11.17	12.09
6/17/2020	7.02	12.26	10.92		13.31	12.33	11.91
6/18/2020	6.36	12.30	11.48		13.49	11.73	12.03
6/19/2020	6.40	12.75	11.82		13.79	8.26	11.91
6/20/2020	6.01	13.47	12.35		13.89	3.89	11.96
6/21/2020	6.04	14.03	12.39		13.82	1.65	12.10
6/22/2020	6.02	14.43	11.94		13.43	1.80	12.31
6/23/2020	6.24	14.65	12.07		13.20	3.53	12.24
6/24/2020	6.22	14.65	12.23		13.30	4.20	12.06
6/25/2020	5.97	14.55	11.35		12.57	3.47	12.30
6/26/2020	5.87	14.14	10.92		11.76	6.08	11.87
6/27/2020	5.96	13.69			12.35	7.58	11.43
6/28/2020		13.90			12.75	8.05	11.68
6/29/2020		14.26	0.04		13.08	7.78	11.96
6/30/2020		14.22	0.04		13.44	7.96	12.31
7/1/2020		13.93	0.04		13.55	7.92	
7/2/2020			0.05		13.57	7.57	
7/3/2020			0.04	3.94	13.65	7.27	
7/4/2020				4.30	13.42	7.54	
7/5/2020				4.48	8.09	7.90	
7/6/2020				5.35	10.34	7.82	
7/7/2020				5.51	7.36	8.10	
7/8/2020				4.96	10.08	8.17	
7/9/2020				4.53	7.94	7.54	
7/10/2020				4.19	4.35	7.21	
7/11/2020				4.26	7.27	7.02	
7/12/2020				4.15	9.31		

7/13/2020	4.88	10.52
7/14/2020	3.89	11.49
7/15/2020	4.05	11.83
7/16/2020	2.69	11.82
7/17/2020	2.73	12.82
7/18/2020	5.21	13.12
7/19/2020	4.48	13.13
7/20/2020	2.74	13.01
7/21/2020	3.22	12.73
7/22/2020	4.55	12.70
7/23/2020	4.98	13.05
7/24/2020	4.68	13.08
7/25/2020	2.30	13.14
7/26/2020	1.56	5.93
7/27/2020	3.56	3.85
7/28/2020	3.01	5.81
7/29/2020	0.51	3.48
7/30/2020	0.05	2.90
7/31/2020	0.08	2.53
8/1/2020	0.13	2.64
8/2/2020	0.17	2.77
8/3/2020	0.35	3.03
8/4/2020	0.55	3.22
8/5/2020	1.09	3.16
8/6/2020	1.67	3.24
8/7/2020	2.00	3.18
8/8/2020	1.96	3.44
8/9/2020	2.14	3.58
8/10/2020	2.49	4.23
8/11/2020	2.78	4.73
8/12/2020	3.03	5.66

8/13/2020	2.47	6.20
8/14/2020	3.47	6.43
8/15/2020	3.28	
8/16/2020	3.05	
8/17/2020	3.41	
8/18/2020	4.44	
8/19/2020	5.11	
8/20/2020	6.57	
8/21/2020	8.63	
8/22/2020	9.94	
8/23/2020	10.00	
8/24/2020	6.89	
8/25/2020	2.91	
8/26/2020	6.39	
8/27/2020	6.23	
8/28/2020	5.26	
8/29/2020	2.30	
8/30/2020	0.22	
8/31/2020	0.16	
9/1/2020	0.13	
9/2/2020	0.13	
9/3/2020	0.15	
9/4/2020	0.25	
9/5/2020	0.34	
9/6/2020	2.81	
9/7/2020	7.93	
9/8/2020	10.27	
9/9/2020	10.14	
9/10/2020	11.19	
9/11/2020	11.14	
9/12/2020	10.85	

9/13/2020			11.60					
9/14/2020			11.93					
9/15/2020			8.66					
9/16/2020			0.08					
9/17/2020			0.05					
9/18/2020			0.09					
9/19/2020			2.38					
9/20/2020			6.35					
9/21/2020			8.23					
9/22/2020			6.96					
9/23/2020			5.60					
9/24/2020			4.08					
9/25/2020			2.08					
9/26/2020			0.97					
9/27/2020			0.95					
9/28/2020			0.86					
9/29/2020			0.58					
9/30/2020			0.60					
10/1/2020			0.58					
10/2/2020			0.54					
10/3/2020	6.56	3.90	1.43		1.02	7.76		
10/4/2020	6.76	4.06	4.05	3.23	1.01	8.67		5.65
10/5/2020	7.70	4.11	6.33	3.52	1.78	8.85		6.86
10/6/2020	8.31	4.21	8.36	3.85	2.97	9.24		7.22
10/7/2020	8.12	4.42	8.51	3.80	4.12	9.66		7.25
10/8/2020	7.45	4.74	7.84	3.87	3.86	9.66		7.71
10/9/2020	7.78	5.62	6.75	3.37	3.76	9.61		11.94
10/10/2020	5.42	4.40	4.10	4.37	2.10	5.02		14.30
10/11/2020	0.18	3.39	0.09	9.56	0.12	0.09		9.65
10/12/2020	1.48	3.68	0.13	8.75	0.42	0.21	0.12	7.21
10/13/2020	2.74	5.34	0.15	8.68	0.60	0.31	0.12	4.84

10/14/2020	4.50	7.15	0.27	8.24	2.14	2.43		0.15	7.32
10/15/2020	5.64	7.30	0.68	7.99	1.52	7.52		0.21	9.05
10/16/2020	6.13	8.20	0.43	7.93	1.05	6.61		0.85	8.31
10/17/2020	9.92	8.76	2.31	8.94	2.56	7.94		2.65	9.09
10/18/2020	11.66	9.33	4.23	8.21	2.80	11.37		4.39	10.44
10/19/2020	9.90	9.61	4.48	7.65	3.39	11.76		8.21	12.31
10/20/2020	9.54	9.79	4.29	7.07	3.18	10.91		8.26	13.27
10/21/2020	10.31	9.52	5.01	9.19	3.99	10.94		5.49	13.68
10/22/2020	12.76	10.26	7.18	9.16	5.00	11.71	2.50	3.85	
10/23/2020	10.52	11.33	7.69	9.95	5.68	12.70	2.35	2.40	
10/24/2020	9.82		6.93		5.06	12.17	2.33	3.90	
10/25/2020	9.18		6.83		5.02	11.18	2.31	4.18	
10/26/2020	9.40				8.92		2.47	3.75	

Table 5. Gross primary production (GPP, mmol O_2 $m^{-2}d^{-1}$) and absolute ecosystem respiration (ER, mmol O_2 $m^{-2}d^{-1}$) at 6 tidal creeks.

Date	Indian Bayou GPP	Indian Bayou ER	Long Bayou GPP	Long Bayou ER	Manuel Bayou GPP	Manuel Bayou ER	Mulat Bayou GPP	Mulat Bayou ER	Texar Bayou GPP	Texar Bayou ER	Weakley Bayou GPP	Weakley Bayou ER
6/11/2019					129.86	564.98						
6/12/2019					325.21	616.21	259.45	408.97	221.37	108.72	332.58	607.59
6/13/2019			447.45	391.27	363.85	529.66	7.22	416.76	167.08	139.40	166.71	497.12
6/14/2019			333.02	455.18	430.49	619.66	171.95	510.53	186.56	182.24	187.85	407.96
6/15/2019			294.18	498.20	403.81	661.19	99.61	532.60	216.65	194.04	196.63	596.14
6/16/2019			319.36	544.75	429.86	663.58	156.74	553.39	253.71	224.36	629.49	1177.04
6/17/2019			373.06	617.18	527.76	759.68	181.16	628.57	294.96	278.38	1115.99	1691.22
6/18/2019			508.73	838.73	499.74	850.97	301.91	939.23	312.89	321.37	1274.87	1823.60
6/19/2019			562.57	1083.61	419.88	1045.36	490.09	1643.84	300.34	332.29	1432.41	2176.99
6/20/2019			343.47	922.21	284.96	1051.51	170.28	1483.11	266.83	326.15	1323.42	2250.98
6/21/2019			286.54	685.84	344.70	816.91			309.43	393.48	1254.72	2031.94
6/22/2019			383.16	685.48	544.66	897.69	16.56	542.93	363.93	439.12	1239.56	1886.51
6/23/2019			356.83	783.35	419.04	1056.91	110.95	999.46	321.61	352.15	1150.37	2008.91
6/24/2019			123.45	659.43	119.07	813.20			229.95	271.81	611.56	1204.29
6/25/2019			114.01	429.36	554.40	740.85	126.35	648.05	142.59	193.82	273.98	697.99
6/26/2019			259.82	564.35	715.38	868.75	351.65	776.09	93.20	163.82		
6/27/2019			255.31	837.20	594.34	829.68	222.62	1050.07	31.99	139.79	159.90	966.75
6/28/2019			267.14	764.50	442.09	617.10	15.01	715.40	17.42	130.50	450.14	1063.19
6/29/2019			373.23	701.30	445.90	588.93	13.87	400.19	70.56	170.60	628.02	1009.52
6/30/2019			377.88	822.22	497.32	737.27	349.09	784.20	341.54	458.89	431.09	888.27
7/1/2019			384.19	870.49	369.33	711.82	296.20	751.52	265.20	363.63	229.37	603.47
7/2/2019			446.47	878.42	251.58	650.97	247.98	720.76	280.48	410.10	99.49	239.06
7/3/2019			452.12	840.85	262.90	684.56	251.25	768.06	283.66	388.40		
7/4/2019			441.18	807.95	377.63	828.73	388.13	855.09	298.65	404.00	103.89	372.90
7/5/2019			259.83	704.64	314.81	929.68	279.86	686.25	166.35	234.77	353.06	618.66

7/6/2019			211.08	747.69	230.50	915.86	284.58	750.25	114.34	298.85	841.98	1100.88
7/7/2019			199.97	772.73	260.71	1004.58	233.16	774.11	173.89	389.17	511.52	216.00
7/8/2019			185.20	797.01	209.64	1025.91	209.69	771.37	211.09	423.66		
7/9/2019			137.60	690.68	114.68	819.14	168.22	628.97	160.20	350.04		
7/10/2019			391.75	888.47	447.99	1129.90	451.84	880.97	250.24	451.43		
7/11/2019			537.95	1754.33	716.64	2310.87	696.59	1644.69	317.52	803.33		
7/12/2019			348.80	2473.58	575.86	3097.93	588.23	2192.93	209.64	1127.96		
7/13/2019			43.92	2054.69	5.28	2368.51	232.14	1712.64				
7/14/2019			453.19	1604.08	218.62	1535.07	364.38	1174.78	126.34	768.98	234.01	1675.73
7/15/2019			392.66	1187.06			250.44	766.09	75.91	563.31	189.24	1331.06
7/16/2019			573.48	908.36	178.45	543.27	356.82	605.73	189.88	414.41	295.42	750.99
7/17/2019			572.39	937.87	66.49	606.94	391.29	700.89	196.86	425.85	371.01	1071.88
7/18/2019			408.77	801.69	59.94	817.06	294.69	610.65	147.25	358.20	275.45	896.93
7/19/2019			282.14	605.82	392.92	994.26	221.06	446.97	199.29	391.37		
7/20/2019			253.83	547.52	686.22	1074.38	188.19	381.62	231.36	419.86		
7/21/2019			346.61	663.08	559.95	909.51	230.00	502.17	265.13	464.35		
7/22/2019			334.35	779.03	259.36	814.43	178.12	542.98	261.18	496.60		
7/23/2019			314.24	817.51	234.54	863.76	27.54	507.41	281.65	541.69	26.97	432.21
7/24/2019			272.65	705.69	245.02	777.62			290.05	514.39	64.20	381.78
7/25/2019			392.46	711.51	395.94	803.72			379.70	555.10	194.31	427.35
7/26/2019			295.89	694.90	151.40	689.10			339.75	543.13	178.81	445.75
7/27/2019			429.29	693.00	176.04	548.23			434.15	587.25	166.66	396.29
7/28/2019			393.65	721.59	161.68	573.73	18.47	453.85	347.24	560.60	183.20	477.20
7/29/2019			393.10	741.74	104.30	485.37	104.11	478.85	344.16	572.89	219.94	496.05
7/30/2019			327.61	709.72			174.22	591.87	342.65	548.73	206.51	488.04
7/31/2019	448.28	424.08	304.23	659.66			287.30	712.44	389.10	570.04	247.22	513.01
8/1/2019	265.38	408.19	192.70	567.48			255.91	684.73	320.53	493.95	188.62	467.05
8/2/2019	284.74	413.21	283.17	537.65	54.05	379.10	342.55	649.70	340.14	481.17	234.41	434.38
8/3/2019	277.13	453.31	286.54	610.03	178.06	580.83	274.73	655.89	319.96	496.05	233.78	481.79
8/4/2019	245.08	415.12	270.76	593.03	230.77	621.20	209.58	603.39	310.04	483.57	279.59	562.07
8/5/2019	282.84	482.66	361.99	700.74	367.09	777.38	250.62	667.94	389.56	597.88	333.48	647.79

8/6/2019	252.08	552.71	268.27	738.68	277.55	803.27	113.54	687.05	308.62	599.30	229.33	660.17
8/7/2019	306.37	642.40	276.43	760.94	343.15	817.31	189.00	747.61	373.60	678.09	264.36	675.66
8/8/2019	448.43	919.70	196.93	852.89	282.49	874.88	83.00	839.47	329.39	728.82	201.84	747.95
8/9/2019	491.67	907.26	128.71	707.47	158.12	723.50			217.65	596.60	113.90	639.85
8/10/2019	577.16	872.05	359.84	741.21	297.74	728.95	204.02	688.59	339.49	610.52	242.53	621.16
8/11/2019	390.43	720.21	222.03	729.43	80.72	655.88	873.75	1353.27	112.84	489.52	17.81	516.92
8/12/2019	415.44	589.75	177.42	453.96			720.85	923.91	367.43	533.85		
8/13/2019	545.81	693.79	251.93	444.77	70.63	268.72	527.20	687.15	687.76	751.68	36.42	183.02
8/14/2019	649.10	903.83	271.96	654.75	160.06	544.14	223.11	644.35	627.59	783.97		
8/15/2019	548.85	798.10	236.64	596.50	114.94	512.48	81.30	537.16	454.00	636.61		
8/16/2019	588.36	764.54	353.96	596.35			296.57	675.04	446.41	566.32		
8/17/2019	524.01	835.26	203.07	639.82			257.43	917.08	330.90	630.68		
8/18/2019	452.55	788.39	62.86	540.94			236.60	963.76	259.30	578.52	147.32	648.19
8/19/2019	346.16	637.38					48.53	653.61	110.80	380.73	132.88	556.83
8/20/2019			23.57	241.43			28.42	323.40	75.16	239.96	206.26	436.15
8/21/2019			53.49	325.74					194.50	389.61	176.30	447.79
8/22/2019									165.89	404.10	109.26	398.16
8/23/2019					262.14	473.76					222.32	406.78
8/24/2019					103.88	366.08					206.51	500.01
8/25/2019					113.49	467.76	54.58	454.21			201.60	546.53
8/26/2019			31.65	436.36	281.32	666.22	116.65	567.98	579.55	916.40	245.81	605.73
8/27/2019			34.46	586.86	330.08	833.95	127.97	843.56	779.50	1136.77	258.71	736.71
8/28/2019			44.38	670.29	216.36	787.51	198.72	1137.99	380.64	881.39	191.34	743.02
8/29/2019			145.67	545.47	181.07	580.61	274.55	962.77	109.65	477.21	201.47	566.96
8/30/2019			299.65	618.80	257.32	608.54	895.75	1738.44	263.61	539.79	361.32	650.44
8/31/2019		622.22	229.64	667.76	214.48	738.95			207.28	542.65	280.12	668.56
9/1/2019	233.17	578.52	262.87	651.74	271.93	731.48			163.33	420.13	289.73	617.25
9/2/2019	78.27	391.41	199.27	632.47	229.54	684.24			127.04	421.46	211.25	573.32
9/3/2019	2.37	283.56	224.54	614.72	235.67	582.63			175.74	417.60	217.20	547.23
9/4/2019	75.06	456.06	248.37	754.38	189.17	615.29			282.21	566.78	267.24	681.63
9/5/2019			101.58	810.82	54.45	692.83			207.18	586.67	149.04	701.91

9/6/2019			38.99	601.55	36.70	560.33	2.15	363.25	120.29	542.53
9/7/2019			103.70	496.59	123.31	501.34			188.12	492.32
9/8/2019			66.92	488.05	127.52	507.85			154.36	487.85
9/9/2019			79.13	450.81	245.79	563.86	194.68	390.25	168.80	453.51
9/10/2019	138.42	386.91	98.23	496.59	350.47	708.79	245.21	443.43	256.87	518.81
9/11/2019	221.82	506.48	20.45	449.49	428.14	964.61	248.04	466.17	218.45	493.56
9/12/2019	177.24	455.98					235.34	458.20	158.16	438.52
9/13/2019	148.35	415.73					212.07	426.09	116.45	407.59
9/14/2019	130.78	370.60					192.21	383.80	183.51	430.79
9/15/2019	128.17	341.84					220.61	410.51	218.96	435.90
9/16/2019	141.34	424.61					260.64	514.15	172.61	444.98
9/17/2019	108.19	462.03					228.12	564.26	97.95	411.62
9/18/2019	159.38	576.94					345.34	787.78	195.08	554.43
9/19/2019							192.64	801.37	102.78	691.74
9/20/2019	37.36	537.43					222.06	615.46	83.14	458.40
9/21/2019	62.24	456.45					228.55	550.27		
9/22/2019	13.57	361.59					293.22	570.93		
9/23/2019	53.02	475.02					329.04	669.09	179.97	602.12
9/24/2019							270.21	636.81	246.01	702.43
9/25/2019	143.31	646.76					376.82	672.72	134.72	411.49
9/26/2019	116.65	683.21					300.77	647.69		
9/27/2019	140.64	510.52					269.61	499.07		
9/28/2019	157.51	450.81					296.08	468.98	311.90	642.14
9/29/2019	53.34	401.96					258.83	428.06	337.24	653.72
9/30/2019	40.33	308.01					244.21	356.33	341.93	517.87
10/1/2019							187.34	316.62	170.28	456.42
10/2/2019							195.61	345.54	408.86	871.56
10/3/2019							176.77	342.91	703.17	1183.41
10/4/2019							83.78	202.90	583.97	932.52
10/5/2019	156.65	580.31					79.95	224.37	502.96	814.82
10/6/2019	64.50	703.03					13.07	223.29	440.28	935.18

10/7/2019	208.59	643.06	58.54	229.46	605.87	958.50
10/8/2019	284.08	875.22	175.17	490.21	612.51	1036.74
10/9/2019	176.21	860.95	170.62	587.06	480.05	1097.97
10/10/2019	102.55	592.05	226.08	541.69	773.02	1271.34
10/11/2019	75.10	480.69	308.41	565.62	792.16	1222.03
10/12/2019	89.92	389.42	358.87	571.64	393.02	812.69
10/13/2019	50.46	300.47	376.31	543.91	150.10	523.10
10/14/2019	47.02	336.93	393.11	556.04	80.49	465.14
10/15/2019	123.63	539.02	418.68	660.76	79.52	556.95
10/16/2019	29.19	621.47	333.40	681.90		
10/17/2019	83.04	579.84	374.08	665.99		
10/18/2019	134.04	795.57	295.05	656.80		
10/19/2019						
10/20/2019	174.06	402.74	134.59	280.75	40.64	292.67
10/21/2019	169.92	686.22	144.06	462.78	70.58	629.36
10/22/2019			29.06	417.50		
10/23/2019			66.58	247.84	89.64	306.20
10/24/2019	194.36	621.94	156.68	483.67	202.71	532.94
10/25/2019	254.83	1211.74	213.74	980.57	76.87	889.82
10/26/2019						
10/27/2019			111.73	245.40	39.45	262.30
10/28/2019	37.41	153.60	156.93	223.68	91.46	180.21
10/29/2019	80.77	390.64	170.31	349.45		
10/30/2019	103.90	891.00	177.44	577.40		
10/31/2019			29.49	519.53		
11/1/2019						
11/2/2019						
11/3/2019						
11/4/2019						
11/5/2019					8.20	312.84
11/6/2019					103.66	286.19

11/7/2019	109.14	429.61	121.67	443.25	359.09	836.54
11/8/2019			70.24	507.57	310.76	1162.25
11/9/2019			104.01	186.83	286.34	490.87
11/10/2019			76.17	118.90	193.35	325.60
11/11/2019	60.98	376.45	150.96	401.22	255.19	755.37
11/12/2019			22.75	389.15		
11/13/2019			36.08	136.13	39.41	264.35
11/14/2019			56.86	238.62	128.06	439.01
11/15/2019						
11/16/2019						
11/17/2019			23.60	83.14	38.41	154.18
11/18/2019			107.00	165.49	28.52	179.01
11/19/2019			157.78	199.46	0.93	88.90
11/20/2019	32.53	121.49	158.30	212.64		
11/21/2019	86.17	227.89	84.06	173.29		
11/22/2019	73.41	195.08	138.76	227.45	80.67	237.44
11/23/2019			123.63	239.34	3.03	261.12
11/24/2019			124.27	187.83		
11/25/2019	43.95	162.84	178.84	244.20	50.98	140.53
11/26/2019	95.41	395.71	199.98	353.37	56.33	422.94
11/27/2019	32.54	347.89	161.79	273.74		
11/28/2019	49.89	158.01	100.71	182.90		
11/29/2019	159.70	248.03	204.37	264.32	142.10	324.75
11/30/2019	244.73	462.27	182.56	347.20	338.09	869.20
12/1/2019	292.36	487.81	248.26	321.38	346.77	1010.91
12/2/2019	105.74	237.98	172.42	355.19	200.13	669.47
12/3/2019			332.35	398.07	201.61	367.49
12/4/2019			122.50	155.12	152.37	311.22
12/5/2019					149.94	259.37
12/6/2019					143.96	312.41
12/7/2019					13.83	363.72

12/8/2019					47.18	372.38
12/9/2019	134.11	405.68			180.63	573.44
12/10/2019	374.89	519.73			118.65	802.88
12/11/2019	275.57	333.07				
12/12/2019	14.79	105.23			51.27	366.21
12/13/2019			18.57	69.15	47.16	288.31
12/14/2019	94.16	153.35	59.65	106.14	118.55	344.47
12/15/2019	401.69	467.63	168.90	214.94	210.24	541.33
12/16/2019	651.68	597.89	381.98	339.45	505.61	1084.53
12/17/2019	1177.89	764.67	669.30	560.25	300.45	1100.67
12/18/2019	449.77	418.03			190.19	785.64
12/19/2019	13.12	77.79			150.77	407.04
12/20/2019	37.38	61.87	98.31	88.76	187.08	440.48
12/21/2019			61.61	104.81	155.78	566.21
12/22/2019			52.27	70.13	55.59	501.98
12/23/2019			41.42	48.95	46.83	315.20
12/24/2019			49.77	56.20	54.15	188.40
12/25/2019			57.02	91.44	99.26	214.15
12/26/2019			59.17	66.47	70.58	265.91
12/27/2019			47.44	81.67	174.55	506.06
12/28/2019			61.07	119.33	203.09	804.79
12/29/2019			72.68	120.10	212.51	705.43
12/30/2019	28.24	307.86	47.73	127.40	114.24	457.76
12/31/2019	0.69	201.30	6.02	85.40	87.26	297.43
1/1/2020	133.73	490.84	36.12	148.20	254.04	641.15
1/2/2020	140.37	963.32			217.68	1091.54
1/3/2020	107.26	806.42			135.75	984.17
1/4/2020					114.08	664.99
1/5/2020					169.73	454.47
1/6/2020	9.36	171.12			230.52	605.17
1/7/2020					118.93	553.73

1/8/2020					212.29	511.58
1/9/2020			26.43	178.94	96.41	565.17
1/10/2020	103.17	724.21	108.71	298.14	326.36	1154.47
1/11/2020			59.42	184.27	80.59	584.37
1/12/2020	62.90	143.30	94.75	160.36	174.44	223.54
1/13/2020	55.52	251.99	109.62	249.79	51.94	233.07
1/14/2020			88.21	229.08		
1/15/2020			113.08	192.56	91.59	385.66
1/16/2020			124.45	232.62	246.83	524.42
1/17/2020			3.87	125.95	118.27	633.39
1/18/2020					359.59	1000.01
1/19/2020					272.13	1318.02
1/20/2020					113.53	1131.15
1/21/2020						
1/22/2020					104.14	304.83
1/23/2020					68.94	257.52
1/24/2020					70.43	211.56
1/25/2020					99.81	214.21
1/26/2020	16.81	183.01	34.70	123.39	149.89	270.17
1/27/2020	97.69	232.07	66.79	111.75	134.44	341.89
1/28/2020	158.50	332.77	40.98	101.90	227.95	458.87
1/29/2020	114.19	411.62			134.92	393.49
1/30/2020	188.53	392.14			147.66	283.08
1/31/2020	253.02	498.76	15.73	79.98	108.75	277.18
2/1/2020	416.27	798.62	37.21	51.85	99.45	293.24
2/2/2020	416.84	704.26			37.64	309.58
2/3/2020	304.48	606.88			91.70	439.44
2/4/2020	27.53	428.38			123.35	634.77
2/5/2020					192.53	845.80
2/6/2020			68.50	41.12		
2/7/2020	36.21	479.27	18.51	116.09	37.63	466.63

2/8/2020	91.83	330.94	233.55	400.16	667.05	816.54			99.53	184.48	158.06	510.76
2/9/2020			152.22	366.38	880.75	1052.67			41.11	218.00	106.04	551.81
2/10/2020			30.06	187.30	880.93	1009.07			29.56	170.56	86.42	436.73
2/11/2020	85.53	288.43	73.82	233.62	926.32	1191.76	54.29	394.28	157.01	289.18	302.19	712.01
2/12/2020	68.88	512.13	96.86	373.34	892.72	1422.73	8.58	664.81	130.28	324.75	396.85	1155.92
2/13/2020	35.18	607.18	162.80	550.88	578.03	1413.64			95.72	293.79	301.00	1164.99
2/14/2020	35.38	473.43	67.03	262.16	307.48	795.01			66.13	244.63	166.58	757.95
2/15/2020	152.70	368.55	138.21	295.12	296.11	390.04	16.75	265.85	114.96	234.91	253.56	555.72
2/16/2020	138.55	361.28	150.58	286.33	128.14	280.07			119.45	229.16	181.71	525.63
2/17/2020	195.09	330.84	154.55	205.46	64.59	171.78			82.26	78.59	201.74	438.00
2/18/2020	165.32	221.01	165.37	259.74	15.97	87.75					243.16	476.40
2/19/2020	148.34	295.06	320.58	549.81					46.88	126.37	415.28	863.27
2/20/2020	193.78	658.77	258.65	571.06			153.41	654.28	205.54	326.83	297.60	1278.79
2/21/2020	43.19	525.88	12.74	184.64					95.61	265.01		
2/22/2020	196.65	247.14	91.05	101.61					66.53	91.26	173.19	377.17
2/23/2020	113.12	186.90	90.20	135.90							205.81	483.02
2/24/2020	80.94	181.87	122.59	134.22							136.24	409.59
2/25/2020	186.84	324.70	191.46	282.67			43.00	237.20	60.07	133.77	426.59	764.70
2/26/2020	90.93	439.77	150.51	161.60					13.55	171.67	195.60	839.69
2/27/2020	125.68	394.86	52.58	21.97					24.75	119.06	227.75	694.38
2/28/2020	119.17	354.67					89.89	443.57	12.31	115.25	230.70	588.92
2/29/2020	128.89	340.68					224.51	560.60	30.24	142.03	221.88	540.56
3/1/2020	124.95	353.24			214.16	761.72	394.58	785.78	72.32	221.15	271.71	667.04
3/2/2020					69.57	568.82	247.46	724.99	62.11	209.20	93.29	578.41
3/3/2020	107.65	301.10	53.61	17.53	180.88	416.06	310.48	532.66	146.34	293.55	242.13	525.54
3/4/2020	50.15	248.07	85.69	70.80	68.24	390.14	65.42	372.21	152.18	269.35	191.54	600.48
3/5/2020	88.58	363.06	154.07	250.40	82.67	482.45	182.21	672.37	168.03	297.14	273.95	740.62
3/6/2020	13.46	345.31	180.21	239.84			126.17	608.49	159.86	332.91	123.05	668.92
3/7/2020	112.00	346.98	169.16	265.67	109.35	538.59	193.26	442.07	172.47	271.09	256.67	649.15
3/8/2020	112.00	319.06	162.80	298.68	114.22	786.93	64.23	334.02	132.43	262.44	251.56	682.67
3/9/2020	62.69	229.72	124.54	195.29	64.23	650.05	47.75	264.04	127.19	224.44	181.08	579.81

3/10/2020	107.38	224.17	114.32	177.29	120.95	514.31	84.86	197.60	149.34	216.81	249.02	521.65
3/11/2020	111.98	246.36	166.89	282.91	198.87	625.21	54.13	137.93	162.42	240.38	293.09	567.24
3/12/2020	76.51	193.29	216.43	315.28	255.70	711.89			181.38	277.82	289.68	525.11
3/13/2020	77.11	138.59	226.50	263.65	228.87	286.81	17.56	101.85	238.18	330.05	303.41	432.81
3/14/2020	102.85	163.53	238.62	295.20			114.82	181.09	273.90	297.08	278.25	417.77
3/15/2020	64.92	171.33	236.27	322.95			154.52	274.78	198.17	230.22	123.69	385.80
3/16/2020	6.64	120.93	197.62	263.86			166.77	272.16	125.80	158.39	112.72	359.25
3/17/2020	85.14	211.08	251.84	390.01	43.65	347.89	205.42	326.39	130.97	244.71	247.55	522.06
3/18/2020	118.67	405.75	245.53	511.07	93.89	577.96	175.98	437.41	208.73	482.72	341.51	905.82
3/19/2020	86.23	401.31	200.83	506.76	16.25	557.20	82.71	370.38	233.93	486.35	233.77	826.45
3/20/2020	81.28	294.86	168.49	347.83	111.66	616.29	59.84	248.35	235.90	413.41	179.12	567.16
3/21/2020	114.14	263.58	195.80	323.91	320.13	782.48	88.68	211.25	280.32	406.73	263.16	482.10
3/22/2020	160.18	377.40	239.17	413.47	664.02	1274.84	94.42	270.13	337.51	528.54	332.98	644.94
3/23/2020	184.43	591.20	269.28	526.40	823.47	2135.88	51.56	396.86	357.47	717.37	340.66	962.90
3/24/2020	80.04	588.65	159.67	379.42	267.85	2263.90			192.82	606.13	108.03	897.76
3/25/2020	64.87	332.42	126.98	217.55	259.18	1447.99	20.04	258.09	177.07	352.28	78.03	472.21
3/26/2020	238.04	407.20	231.68	309.52	905.38	1562.93	220.49	355.02	335.98	497.44	307.41	525.15
3/27/2020	217.72	689.33	285.26	461.36	721.99	2349.31	168.81	567.93	338.26	769.30	244.60	897.42
3/28/2020	159.40	691.35	214.65	497.83	726.91	2411.44	61.47	547.90	244.15	720.76	134.50	867.72
3/29/2020	146.90	440.24	223.83	369.30	591.41	1459.00	45.06	347.05	176.74	448.64	128.22	590.21
3/30/2020	339.70	608.26	555.15	916.13	1534.95	2711.22	211.20	470.15	352.46	641.26	614.29	1221.85
3/31/2020			207.39	500.23	181.45	1826.36			27.27	575.11		
4/1/2020	155.75	405.87	136.52	278.34	329.22	711.67			85.96	247.49	205.99	591.16
4/2/2020	190.55	353.92	147.64	237.13					72.52	194.29	238.21	488.46
4/3/2020	232.78	336.57	194.28	264.19			5.34	122.29	173.63	330.18	259.63	439.11
4/4/2020	176.13	268.04	224.54	340.96			16.07	157.68	233.57	351.48	232.92	492.61
4/5/2020	43.39	180.35	149.72	255.73	157.94	369.92			141.49	265.54	43.26	338.46
4/6/2020	101.22	232.84	233.98	362.99	310.64	429.54	75.75	240.06	224.54	334.35	109.85	289.94
4/7/2020	141.83	414.39	280.21	520.17	224.93	565.29	141.56	526.30	250.26	464.65	100.81	551.31
4/8/2020	113.54	462.76	239.63	481.46	92.73	559.69	104.06	632.32	164.09	438.75	49.01	635.79
4/9/2020	238.15	573.43	383.44	645.29	206.43	606.30	248.88	752.11	253.41	505.51	243.39	755.82

4/10/2020	191.61	636.44	277.00	502.03	105.61	559.17	72.36	781.83	186.20	482.71	97.07	779.10
4/11/2020	464.57	970.06	482.23	878.93	402.40	829.54	465.05	1171.71	389.53	745.40	438.48	1081.53
4/12/2020	287.33	1006.28	424.28	752.19	114.00	830.31	107.20	1211.75	234.66	810.53	162.79	1194.56
4/13/2020	274.41	659.79	338.85	533.16	170.10	632.11	165.47	892.45	264.80	643.79	254.26	873.18
4/14/2020	339.17	692.03	445.80	675.69	349.17	773.49	409.60	1063.02	378.51	717.29	418.33	931.85
4/15/2020	5.95	475.41	301.48	474.58	174.23	569.25	104.31	880.00	204.33	568.72	73.50	708.18
4/16/2020	37.31	240.33	250.02	410.92	510.17	712.26	427.95	780.41	263.43	427.20	377.75	638.67
4/17/2020			173.19	307.70	597.69	828.56	343.09	778.34	124.71	279.87	301.17	649.77
4/18/2020	117.00	389.22	298.07	546.79	738.01	908.50	444.48	765.55	85.25	219.95	361.85	746.88
4/19/2020	11.03	467.87	304.93	442.92	341.09	456.98	76.21	587.76	8.16	331.21	57.77	714.84
4/20/2020	78.37	321.11	182.01	210.14	63.22	88.66	64.24	308.72	19.65	202.11	100.00	350.43
4/21/2020	170.13	369.17	182.88	287.63			122.41	291.26	155.73	328.36	160.95	312.43
4/22/2020	317.38	818.66	442.01	756.77			325.60	805.64	363.12	716.41	305.27	716.09
4/23/2020			253.22	371.54			106.56	924.40	179.35	634.70	57.25	769.92
4/24/2020	216.35	561.28	111.87	194.03			288.07	666.23	239.98	410.90	235.92	563.98
4/25/2020	182.56	713.12	156.45	272.34			308.56	875.12	188.30	407.44	252.66	802.00
4/26/2020			136.23	149.62	0.19	502.53	76.38	589.38	97.17	294.94	83.67	626.36
4/27/2020	179.55	448.27	391.82	715.84	279.75	533.94	277.16	589.10	166.86	292.93	285.10	610.92
4/28/2020	134.94	667.95	1137.55	1693.46	328.88	714.93	256.51	757.08	102.49	328.59	349.67	1056.65
4/29/2020			776.47	661.74	84.76	368.48					88.50	1118.07
4/30/2020					37.71	158.87						
5/1/2020	26.37	305.16			41.20	105.07	38.30	185.38			42.55	405.92
5/2/2020	188.34	435.88			140.41	195.01	238.85	373.45	105.61	251.52	113.35	396.42
5/3/2020	263.25	522.85			222.77	303.95	252.99	258.45	367.15	588.82	125.66	504.95
5/4/2020	220.58	496.35					80.49	136.11	468.97	618.98	88.33	549.66
5/5/2020	435.93	876.72			30.11	358.52	146.90	269.02	566.86	837.35	425.14	1093.14
5/6/2020	64.85	902.00					77.87	341.15	210.55	557.02		
5/7/2020	340.64	864.93			140.89	399.19	195.29	381.59	315.29	572.49	327.95	1062.40
5/8/2020	127.33	940.27			48.49	308.96	63.56	362.92	294.47	682.54	66.86	1184.92
5/9/2020	66.37	666.20			133.28	315.81	119.84	437.31	191.79	396.17		
5/10/2020	330.57	701.52			270.95	569.13	360.60	625.45	92.00	183.24	233.41	630.39

5/11/2020	208.69	762.27			238.59	622.12	237.13	581.64			158.30	781.35
5/12/2020	290.27	689.31			211.14	380.01	289.66	554.17	25.65	180.59	417.72	815.39
5/13/2020	493.79	1168.23			182.27	456.27	505.01	979.41	291.34	613.30	471.37	1125.48
5/14/2020	110.44	1267.65					240.24	920.97	268.32	729.10	71.11	1236.25
5/15/2020	80.58	814.13					182.00	588.02	193.62	503.89	131.38	859.25
5/16/2020	266.65	764.83			99.40	512.82	261.06	519.74	269.28	521.95	415.20	918.37
5/17/2020	118.75	936.29			115.80	638.10	146.87	549.84	241.20	626.15	386.66	1219.32
5/18/2020			262.31	709.73	157.74	653.42	41.41	365.90	146.88	487.44	123.57	1053.16
5/19/2020	25.47	495.04	240.57	379.22	307.01	626.42	121.02	261.84	148.59	324.46	38.97	604.52
5/20/2020	83.96	361.37	258.03	331.23	360.93	560.13	168.12	268.84	154.00	272.05	104.15	443.89
5/21/2020	198.66	538.87	388.96	545.05	376.78	712.52	196.55	347.28	187.09	328.87	284.16	711.15
5/22/2020			369.83	570.62	324.07	887.75	148.05	515.59	80.75	336.54	99.82	856.13
5/23/2020			244.67	412.70	465.65	857.80	175.03	491.40	95.90	301.52	189.06	703.12
5/24/2020	203.53	704.48	389.45	633.67	635.33	1062.35	338.15	663.29	269.92	444.50	549.01	1002.54
5/25/2020			307.56	556.22	244.02	982.14	160.60	689.18	331.37	559.81	305.73	960.12
5/26/2020	57.58	520.58	330.41	509.34	336.42	751.73	242.32	545.98	357.81	493.65	309.89	679.74
5/27/2020	241.10	650.55	569.51	838.40	421.75	775.40	277.45	494.85	439.18	594.69	407.94	756.30
5/28/2020	70.39	568.88	493.46	696.30	60.04	417.39	97.98	364.14	367.92	522.98	199.50	641.50
5/29/2020	172.60	441.37	369.02	456.39	15.82	143.17	210.12	427.60	262.85	341.50	211.48	476.85
5/30/2020	187.33	562.56	298.00	457.34			401.12	683.46	237.36	385.67	166.45	547.17
5/31/2020	148.34	588.14	197.48	334.28			405.34	655.96	213.73	429.80	69.77	544.05
6/1/2020	256.18	677.14	199.28	307.17			431.41	673.97	325.13	582.64	163.62	631.80
6/2/2020	104.67	566.70	36.38	70.91			316.81	572.42	273.62	475.79	12.18	543.73
6/3/2020	247.58	455.02			94.79	307.62	318.73	448.83	271.77	346.29	191.72	438.81
6/4/2020	261.13	573.13			159.00	459.08	322.41	529.11	196.89	312.46	191.41	563.84
6/5/2020	323.82	865.14	105.33	394.39	281.57	689.38	345.35	721.95	213.94	423.58	270.81	812.49
6/6/2020	755.55	2194.60	1034.59	2299.37	814.07	1848.71	613.35	1645.12	407.81	927.67	836.29	2142.10
6/7/2020			431.31	2743.66	745.54	3123.36	73.15	2399.29	168.31	1240.58	271.23	3138.93
6/8/2020					373.72	2441.44			172.56	903.77		
6/9/2020	2.51	1457.33	355.09	881.89	156.30	1408.68			232.75	551.18	15.28	1376.97
6/10/2020			612.60	999.91	231.75	920.94			217.22	399.55	130.03	953.90

6/11/2020			412.39	821.01	417.58	1021.77			230.13	376.84	160.46	829.01
6/12/2020			58.86	332.17	541.96	1157.50			211.09	314.41	104.09	675.08
6/13/2020	27.14	377.07	139.85	248.55	613.85	970.65	76.80	505.11	172.99	228.31	100.92	459.88
6/14/2020	133.74	411.29	373.36	446.23	691.21	869.99	152.60	449.78	192.76	260.17	185.96	482.95
6/15/2020	122.31	525.23	401.33	492.07	536.21	796.04	110.56	539.56	211.40	339.88	162.69	640.62
6/16/2020	52.69	425.37	295.30	390.50	232.34	442.38	47.72	480.55	209.00	359.26	54.12	559.84
6/17/2020	161.82	416.17	283.02	388.79	103.12	228.30	100.60	373.88	233.19	356.51	117.98	439.21
6/18/2020	135.76	406.04	224.83	345.39	48.21	268.62	94.38	375.23	217.73	338.48	107.26	411.62
6/19/2020	94.95	358.41	225.51	417.74	90.06	358.33	157.44	440.24	245.04	349.88	190.61	491.60
6/20/2020	69.20	489.59	291.22	614.80	226.13	653.67	214.68	629.98	244.12	371.29	222.26	694.59
6/21/2020	19.04	566.82	268.95	602.97	281.29	781.28	216.76	623.63	243.17	407.57	95.24	655.09
6/22/2020	191.06	693.33	380.32	780.26	390.70	826.36	274.33	527.07	374.03	630.24	137.78	614.12
6/23/2020	38.61	689.45	86.73	515.37	66.84	639.93	90.46	411.76	339.85	665.05		
6/24/2020	83.82	497.86			21.82	391.28	126.97	433.87	281.47	475.75	33.46	554.77
6/25/2020	118.26	364.51			134.57	384.20	239.35	472.33	243.68	338.99	176.75	483.25
6/26/2020	87.82	292.84			208.78	399.08	296.56	489.98	194.89	260.21	192.08	392.55
6/27/2020	189.91	440.19	306.98	552.70	294.42	476.12	361.87	558.12	256.84	383.11	212.08	472.83
6/28/2020	98.16	485.37	417.16	651.19	251.90	514.80	154.00	450.29	252.42	411.66	57.45	504.14
6/29/2020	128.58	409.91	512.39	794.51	381.29	573.57	120.17	342.92	258.07	382.44	161.37	465.44
6/30/2020	98.72	531.38	404.01	856.98	337.66	624.36	216.84	539.08	267.97	445.13	205.11	611.42
7/1/2020	36.57	545.43	213.56	714.52	193.74	554.17	129.94	485.70	280.33	454.76	56.57	566.29
7/2/2020	78.29	485.36	319.76	744.59	222.80	511.29	130.49	430.65	280.65	415.60	33.06	479.34
7/3/2020	38.77	425.12	294.06	530.54	162.61	439.37	131.09	431.95	236.82	358.80	64.03	455.97
7/4/2020	136.94	383.13	303.51	457.68	253.03	414.74	206.98	405.74	224.56	303.41	327.67	522.28
7/5/2020	161.74	411.22	316.66	537.55	262.33	457.54	204.44	415.86	193.81	285.42	418.98	593.54
7/6/2020	235.26	608.53	494.03	834.66	293.76	620.63	232.46	496.67	302.60	481.14	446.80	807.85
7/7/2020	70.19	637.59	302.25	695.10	90.24	638.33	74.54	429.74	326.96	597.65	317.91	936.19
7/8/2020	139.26	570.90	490.60	807.59	104.95	532.83	161.77	467.11	426.12	635.29	478.85	948.83
7/9/2020	85.20	548.79	458.93	641.79	78.82	629.75	436.27	903.88	356.40	551.39	373.27	841.53
7/10/2020	93.71	588.49	334.21	514.73	178.91	935.42	646.94	1176.48	236.01	507.49	185.96	711.05
7/11/2020	104.14	672.73	249.98	510.67	90.52	1050.05	521.04	1081.27	199.42	645.44	43.35	759.06

7/12/2020	83.96	632.36	263.05	538.77			251.51	707.50	258.94	759.57	85.99	814.31
7/13/2020	209.16	567.52	375.69	668.62	640.28	1041.88	315.26	585.21	472.73	791.20	410.36	917.59
7/14/2020	164.57	384.91	332.02	495.83	877.77	1042.34	364.85	551.56	410.71	581.50		
7/15/2020	239.15	343.24	388.17	482.68	624.98	725.16	354.01	471.96	206.40	310.83		
7/16/2020	224.06	445.65	423.28	589.35	297.08	552.93	329.40	550.84	109.37	340.30		
7/17/2020	110.56	405.41	353.75	510.63	69.33	468.90	182.59	491.35	45.81	358.16		
7/18/2020	162.20	359.15	344.02	444.20	114.19	382.45	204.97	450.00	120.33	309.75		
7/19/2020	217.08	431.26	288.95	381.41	203.74	483.26	224.78	525.16	234.67	430.91	160.16	471.03
7/20/2020	245.55	541.96	209.18	328.60	181.64	590.08	252.68	668.08	225.57	520.28	45.94	491.78
7/21/2020	96.42	568.70	20.89	214.70	50.92	652.51	153.34	676.73	189.07	605.14		
7/22/2020	249.03	928.46	14.69	403.65	229.13	1006.65	248.62	923.24	440.50	972.53	249.05	1031.76
7/23/2020									173.07	863.87		
7/24/2020	197.41	703.07			46.97	591.19			245.76	594.14	103.86	739.50
7/25/2020	178.16	592.36			95.31	607.29			297.36	614.31	59.28	621.43
7/26/2020	190.22	539.02			236.20	652.49			385.45	618.99	48.20	485.07
7/27/2020	338.40	763.08	322.33	792.75	375.77	754.69			378.67	589.33	136.54	584.10
7/28/2020	199.08	757.79	139.86	595.32	210.95	702.27			213.87	497.99		
7/29/2020	215.61	655.18	357.67	790.17	256.32	673.73	109.41	615.88	243.77	498.63	86.02	617.33
7/30/2020	71.67	672.44	508.71	1023.40	217.83	792.08	0.77	592.12	226.91	626.85	52.20	778.26
7/31/2020	115.30	743.77	676.08	1100.33	257.91	885.66			271.37	706.30	161.16	887.00
8/1/2020	3.10	549.87	554.63	619.26	54.38	632.41			148.38	503.30		
8/2/2020	150.11	383.18	449.86	503.69	198.50	434.47	19.40	238.67	259.32	413.99	130.48	355.59
8/3/2020	180.06	497.92	423.23	615.53	212.61	533.17	32.15	343.99	263.84	476.64	81.97	421.92
8/4/2020	150.08	565.20	444.07	606.89	171.98	579.30	5.58	414.15	200.90	485.36	33.62	501.56
8/5/2020	91.81	502.50	382.87	455.59	185.03	584.70	37.05	458.10	215.90	500.12	107.14	547.80
8/6/2020	18.73	432.43	205.28	258.02	199.21	577.77	69.47	496.62	255.49	544.60	143.09	536.63
8/7/2020	75.55	439.67	72.67	132.78	216.58	513.75	46.62	351.35	251.59	484.01	96.17	379.15
8/8/2020	179.07	475.79	83.24	145.86	263.81	506.27			222.50	415.53	48.03	281.89
8/9/2020	309.69	615.34	297.54	470.93	360.71	607.43	24.30	257.68	261.75	463.37	114.69	367.47
8/10/2020	301.54	699.28			279.90	661.87	42.84	391.28	236.24	527.21	42.80	454.91
8/11/2020	148.08	453.85			129.74	491.69			110.15	368.92		

8/12/2020	243.45	280.13			198.06	274.46	187.53	266.93	280.21	323.71	114.92	218.97
8/13/2020	246.51	372.66			121.82	298.46	304.52	447.81	296.63	400.38	230.24	424.93
8/14/2020	180.62	416.56			166.65	481.79	313.39	579.94	173.10	389.88	284.81	603.65
8/15/2020	214.21	511.05			288.11	641.97	331.04	681.34	178.06	443.91	317.36	706.15
8/16/2020	193.73	527.81			192.23	623.15	183.24	623.62	81.21	419.56	158.41	652.59
8/17/2020	205.40	469.59			199.15	569.94	144.76	541.51	118.69	386.19	255.09	742.16
8/18/2020	149.31	491.57			198.75	605.51	148.95	606.31	126.23	431.91	324.61	885.23
8/19/2020	126.53	504.20			224.81	624.90	145.78	591.41	120.90	454.98	313.69	872.05
8/20/2020	240.94	622.85			253.21	651.36	229.82	658.46	138.90	488.71	255.13	770.89
8/21/2020	344.50	809.10			145.21	625.08	330.49	837.73	180.31	606.65	126.92	667.49
8/22/2020	270.69	799.99					378.63	893.93	285.38	759.91		
8/23/2020	198.50	608.12					380.53	729.95	342.29	666.67		
8/24/2020	356.83	824.70			363.32	933.49	393.98	1007.82	257.62	697.10		
8/25/2020	160.85	754.69			271.82	1042.39	162.82	1044.57				
8/26/2020	158.64	711.27	211.82	1139.27	373.76	1221.90	285.73	1065.04	88.58	901.75		
8/27/2020							13.95	882.16				
8/28/2020			92.39	555.27			39.76	367.65				
8/29/2020	101.15	439.55	215.88	581.41	147.52	635.01	37.22	277.27				
8/30/2020	120.73	538.28	30.53	465.35	155.36	758.20	68.12	402.95				
8/31/2020	124.96	574.21	987.09	2433.41	152.49	808.51	107.97	505.34				
9/1/2020	36.27	515.11			105.55	765.13	27.98	453.51				
9/2/2020	21.38	354.47			214.49	602.35						
9/3/2020	43.53	275.72			285.28	523.30						
9/4/2020	116.80	380.77			330.07	600.35	115.55	474.25				
9/5/2020	80.58	480.71			208.80	623.08	229.45	893.56				
9/6/2020	63.39	380.39			104.41	451.51	333.89	907.33				
9/7/2020	101.56	385.45			144.20	452.17	354.85	711.58				
9/8/2020	82.71	463.83			125.02	503.41	160.97	641.59				
9/9/2020	83.31	444.68			87.83	423.86	72.39	491.81				
9/10/2020	143.16	436.85			87.97	371.89	102.26	418.74				
9/11/2020	302.97	602.53			175.47	427.82	313.05	692.91				

9/12/2020	239.93	700.03			55.33	499.96	287.63	827.15		
9/13/2020	244.57	723.62			95.31	734.74	289.27	862.12		
9/14/2020	246.74	1114.23	185.36	1191.43	234.00	1605.65	289.57	1255.76		
9/15/2020										
9/16/2020			11.77	124.91	98.89	167.67				
9/17/2020	103.13	514.08	52.44	486.03	156.41	589.46				
9/18/2020	565.76	1163.39			40.48	719.06				
9/19/2020	949.91	1594.70	74.16	637.14	70.64	745.68				
9/20/2020	815.15	1618.30								
9/21/2020	997.24	1652.49	11.45	424.13	60.17	792.96				
9/22/2020	1117.04	1824.36	98.90	529.46	322.23	1292.86				
9/23/2020	726.33	1478.53	111.87	607.46	515.52	2098.29	257.51	1538.60		
9/24/2020					25.30	1420.59				
9/25/2020					277.40	589.81	212.25	475.09		
9/26/2020	156.75	741.33			105.51	612.14	279.17	740.62		
9/27/2020	187.78	782.75					70.42	609.16		
9/28/2020	481.11	794.76			201.36	805.94	376.23	774.77		
9/29/2020										
9/30/2020	211.84	291.77			7.97	279.07	13.93	134.84		
10/1/2020	185.55	388.52			92.85	680.16				
10/2/2020	46.82	369.03			0.20	780.72				
10/3/2020					111.27	642.90				
10/4/2020					304.50	890.01	20.16	681.43	62.67	274.24
10/5/2020					516.11	1067.60	73.13	651.57	108.01	272.39
10/6/2020					418.48	758.92	50.74	396.30	201.28	314.15
10/7/2020					227.21	430.38	13.44	213.67	286.73	405.39
10/8/2020					307.08	924.59	193.02	730.58	395.18	622.87
10/9/2020					498.50	2131.03	381.86	1764.95	423.56	939.00
10/10/2020									97.51	620.88
10/11/2020					49.63	740.31	129.12	668.17	172.00	387.25
10/12/2020					162.48	717.47	150.32	490.29	215.53	426.02

10/13/2020	30.25	615.35	22.28	366.96	169.50	334.31
10/14/2020	68.43	346.30			144.16	237.50
10/15/2020	243.36	553.35	51.96	333.65	216.28	359.80
10/16/2020					114.15	318.22
10/17/2020					156.92	261.27
10/18/2020					173.87	277.49
10/19/2020					176.76	302.95
10/20/2020					179.09	276.48
10/21/2020	23.44	352.42			177.16	240.08
10/22/2020	53.81	379.51			154.09	210.56
10/23/2020					118.40	162.19